To the Graduate Council:

I am submitting herewith a thesis written by Debasis Basak entitled "Application of Pulse Calorimetry to Metal Systems". I have examined the final copy of this thesis for form and content and recommend that it be accepted in partial fulfillment of the requirements for the degree of Doctor of Philosophy, with a major in Metallurgical Engineering.

Charlie R. Brooks

Dr. Charlie R. Brooks, Major Professor

We have read this thesis and recommend its acceptance :

D. L. McElroy

C. E. Stevenson

Eric T. Allen

Accepted for the Council

Carolyn Winkel

Associate Vice Chancellor and Dean of The Graduate School

# APPLICATION OF PULSE CALORIMETRY TO METAL SYSTEMS

A Dissertation
Presented for the
Doctor of Philosophy
Degree
The University of Tennessee, Knoxville.

**Debasis Basak**
**December 1995**

This thesis is dedicated to
the many students around the world
who are working hard
by day and by night
for the quest of knowledge
to reach the doors of higher learning,
and who are trying to acquire the technical skills
to make the world a better place to live.

# ACKNOWLEDGMENTS

The author would like to express his deep gratitude to his research advisor, Dr. C.R. Brooks. The author had been under his guidance and tutelage for more than five years during the course of his master's and doctoral studies and research. The author thanks him for the guidance and advice that he has received from him all along. His help in the areas of both theoretical and practical aspects of calorimetry, and metallurgy in general, is appreciated.

The author would like to thank the doctoral committee members, Dr. E.E. Stansbury, Dr. D.L. McElroy, Dr. A. Vanhook and Dr. B.F. Oliver for their efforts in going through the thesis and for providing valuable suggestions.

Special thanks are extended to Dr. D.L. McElroy for taking deep interest in the author's research and thesis, in spite of residing out of Knoxville.

Dr. E.E. Stansbury's expert advice, from time to time, was helpful for certain areas of the research, for which the author would like to thank him.

The author thanks Dr. Alexi Lei, who helped in the development of the PID control program used to conduct isothermal experiments.

The author would like to express his appreciation for the help of the machine shop and the electronic shop staff of the Materials Science and Engineering Department for their support towards

designing various parts for the calorimeter and related instrumentation. Special thanks are due to Mr. Doug Fielden, Mr. Ted Long, Mr. Greg Jones and Mr. Ron Johnson.

The secretaries of the department, Sandy and Carla were very generous and helpful to the author during his graduate student career. The author would like to extend his special thanks to them. The personnel of the payroll office were also very cooperative.

The stores and purchases staff Mr. Frank Holliway, Ms. Aileen Cagle and Randy have been of constant help to the author for which the author thanks them.

The author thanks visiting professors Dr. Makoto Kano (Japan) and Dr. Alexi Lei (Taiwan) for their support, and finally thanks fellow graduate students for their help and companionship during the author's stay at the University of Tennessee.

# ABSTRACT

The pulse calorimeter developed as a part of the author's masters thesis was used extensively in the doctoral research to determine the electrical resistivity and specific heat of Ni, $Ni_4Mo$, Fe-Al alloys and Ni-Al. The temperature range of measurements varied with different specimens but in general were between 375 K to 1300 K.

The pulse calorimeter essentially consists of a specimen in series with a standard resistor and a programmable power supply. The specimen is inside a vacuum chamber. The programmable power supply can be triggered from the computer to send a specific current to the specimen for a specific time. As the specimen heats, its temperature rises. Three signals - current, voltage and temperature (thermoelectric voltage) are acquired into the computer program to be processed later to determine the specific heat and electrical resistivity as functions of temperature. The specimen is allowed to cool from a high temperature and the temperature-time data are acquired as a function of time. This cooling data are used later to correct for the heat losses during heating.

A knife-edge apparatus was designed to determine the separation distance between the voltage taps on a specimen. This apparatus was also used to determine the room temperature electrical resistivity of specimens.

Nickel was the first specimen tested in this research. The designed pulse-calorimeter was used to determine the specific heat of nickel. The stored data, E and I, were also used to determine the electrical resistivity of nickel. The specific heat and electrical resistivity data determined over a range of temperature were compared with those of another investigator to check the accuracy of the pulse calorimetry technique. The disagreement in the electrical resistivity is <1% across the entire temperature range of comparison, 340 to 1000 K. The disagreement in the specific heat is about 1% across most of the temperature range, except just above the Curie temperature where it is about 2%.

Next, the pulse calorimeter was used to determine the electrical resistivity and specific heat of four Fe-Al alloys and a Ni-Al alloy. The compositions of the alloys tested were Fe-21.1wt%Al, Fe-18wt%Al, Fe-16wt%Al, Fe-8.5wt.%Al and Ni-8wt%Al. The electrical resistivity and specific heat were determined in the temperature range ~380 K to ~1300 K.

For the Fe-21.2wt%Al alloy, there is a sharp change of slope around ~650 K. It is believed that this is due to the formation of constitutional vacancies, e.g., triple defects. The specific heat data shows a point of inflexion around 650 K.

Fe-18 wt%Al and Fe-16 wt%Al alloys have DO3$\Rightarrow$B2 transformations at 740 K and 775 K, respectively. The electrical resistivity curves reach a maximum at the transformation

temperature. The specific heat curves show a corresponding discontinuity.

Fe-8.5 wt%Al alloy has a ferromagnetic-paramagnetic transformation and the electrical resistivity and specific heat curves are similar to those of Ni, which undergoes the same transformation. The determined Curie temperature is 966±5 K. The curve changes from concave upward to convex upward at this temperature. The specific heat rises continuously in the ferromagnetic range up to the Curie temperature. The specific heat versus temperature curve shows a discontinuity at the Curie temperature. Above the Curie temperature the specific heat decreases sharply and then rises steadily.

For the Ni-8 wt%Al alloy, electrical resistivity increases with the increase in temperature up to the highest test temperature, ~1250 K. At 890±5 K, there is a sharp change in the slope of the curve. Below 890±5 K the curve is concave upwards, and becomes essentially linear above this temperature. The Ni-Al phase diagram does not show a phase change at this point. The reason for this break in the curve is not understood, but it could be related to the formation of vacancies. The specific heat versus temperature curve does not show any discontinuity or detectable points of inflexion.

The main goal of the thesis was to determine the electrical resistivity and specific heat of $Ni_4Mo$ for three initial conditions, 1) cold-worked short range ordered, SRO($\alpha$), 2) short range ordered, SRO($\alpha$) and 3) long-range ordered, LRO($\beta$).

For cold-worked SRO(α), the electrical resistivity curve increases with increase in temperature, at first gradually and then with an increase in slope till it reaches a maximum, at ~690 K, then the curve decreases into the alpha range. For the SRO(α) initial condition, the electrical resistivity gradually increases till it reaches a maximum at ~947 K. Above this temperature electrical resistivity decreases into the alpha range. For the LRO(β) initial condition, electrical resistivity rises sharply till it reaches 1141±2 K, the equilibrium transformation temperature for the $\beta \Rightarrow \alpha$ transformation and then merges with the curves for the other two initial conditions, above the transformation temperature.

The specific heat for $Ni_4Mo$, LRO(β) initial condition increases gradually to about 1000 K, thereafter it increases very sharply near the transformation temperature. Above the transformation temperature it comes down sharply at first and then rises again. The specific heat for $Ni_4Mo$, SRO(α) initial condition, has a similar slope as that for LRO(β) initial condition. However, at the transformation temperature, the specific heat does not rise to a value as high as that for the LRO(β) initial condition. Above the transformation temperature both curves become the same because SRO(α) is present in both cases.

A proportional-integral-derivative (PID) computer program was written. It was capable of isothermally holding a specimen at a specified temperature for a specified time. This program was used to study the isothermal kinetics of alloys. Isothermal experiments were

conducted on steel and $Ni_4Mo$ specimens. The steel specimen was held isothermally at 933 K for 30 min. The kinetics of recovery, recrystallization and precipitation were studied from the electrical resistivity versus temperature curve. Two isothermal runs were made on $Ni_4Mo$ specimen, one each at 973 K and 1023 K. The start of the $\alpha \Rightarrow \beta$ transformation were determined by noting the change in the electrical resistivity versus temperature curves.

The absolute error in the determined electrical resistivity and specific heat data were estimated to be ~0.6% and ~0.9% respectively.

Repeatability tests were done on the various specimens tested with the pulse calorimeter. Two or more identical runs were made and the electrical resistivity and specific heat data determined were compared. For $Ni_4Mo$, SRO($\alpha$) initial condition, the average deviation in the two curves determined from identical runs is about 0.05% for electrical resistivity. For specific heat, the maximum deviation of the curves from each other is 2%.

# TABLE OF CONTENTS

Page

CHAPTER I - INTRODUCTION .....1

PULSE CALORIMETRY .....1
GENERAL BACKGROUND .....1
HISTORICAL OVERVIEW .....3
CURRENT RESEARCH .....5
ELECTRICAL RESISTIVITY AND SPECIFIC HEAT
DETERMINATION .....15
ELECTRICAL RESISTIVITY .....15
SPECIFIC HEAT .....16
DISCUSSION ON ALLOYS TESTED .....17
Ni(PURE) .....18
IRON ALUMINIDE ALLOYS .....19
NICKEL ALUMINIDE .....23
$Ni_4Mo$ .....23

CHAPTER II - REVIEW OF LITERATURE .....27

DEFINITION OF SPECIFIC HEAT .....27
THEORETICAL MODELS FOR SPECIFIC HEAT .....31
Ni-Mo SYSTEM .....36

Page

ORDER-DISORDER TRANSFORMATION IN $Ni_4Mo$ .....49
KINETICS OF $\alpha \rightarrow \beta$ TRANSFORMATION IN $Ni_4Mo$ .....41
THE 'K' STATE .....42
ELECTRICAL RESISTIVITY OF $Ni_4Mo$ .....44
SPECIFIC HEAT OF $Ni_4Mo$ .....47

CHAPTER III - EXPERIMENTAL PROCEDURE .....50

SPECIMENS .....50
SPECIMEN PREPARATION .....53
NICKEL .....53
FeAl AND NiAl ALLOYS .....53
$Ni_4Mo$ .....54
SPECIMEN SPECIFICATIONS .....59
NICKEL .....59
FeAl AND NiAl ALLOYS .....59
$Ni_4Mo$ .....60
DESIGN AND USE OF THE KNIFE-EDGE APPARATUS .....62
KNIFE-EDGES .....63
KNIFE-EDGE HOLDER ASSEMBLY .....65
ELECTRICAL CIRCUITRY .....69
ANALYSIS OF DIFFERENT THERMOCOUPLE
CONFIGURATIONS .....73

Page

ONE LEAD WELDED ON TOP OF THE OTHER .....73
INTRINSIC TYPE .....75
BEADED TYPE .....78
**MEASUREMENT OF ELECTRICAL RESISTIVITY .....80**
ELECTRICAL RESISTIVITY MEASUREMENTS FROM PULSE-HEATING RUNS .....80
ELECTRICAL RESISTIVITY MEASUREMENT USING THE RESISTIVITY APPARATUS .....82
**DETERMINATION OF SPECIFIC HEAT .....83**
**ISOTHERMAL TESTS .....86**

**CHAPTER IV - DISCUSSION OF EXPERIMENTAL RESULTS ..89**

**PULSE EXPERIMENTS .....89**
PURE NICKEL .....90
ELECTRICAL RESISTIVITY .....90
SPECIFIC HEAT .....91
Fe-Al ALLOYS .....94
Fe-21.2 wt%Al alloy .....94
ELECTRICAL RESISTIVITY .....94
SPECIFIC HEAT .....97
Fe-18 wt%Al alloy .....101

Page

ELECTRICAL RESISTIVITY .....101
SPECIFIC HEAT .....103

Fe-16 wt%Al alloy .....103
ELECTRICAL RESISTIVITY .....103
SPECIFIC HEAT .....103

Fe-8.5 wt%Al alloy .....107
ELECTRICAL RESISTIVITY .....107
SPECIFIC HEAT .....107

Fe-8 wt%Al ALLOY .....110
ELECTRICAL RESISTIVITY .....110
SPECIFIC HEAT .....110

Ni-20 at%Mo ALLOY .....114
ELECTRICAL RESISTIVITY .....114
a) Initial condition : LRO(β) .....114
b) Initial condition : SRO(α) .....117
c) Initial condition : cold-worked SRO(α) .....121
Results of slow heating on SRO(α) .....123
SPECIFIC HEAT .....127
a) Initial condition : LRO(β) .....127
b) Initial condition : SRO(α) .....129

COMMENTS ON P-T AND T-t CURVES .....129

ISOTHERMAL EXPERIMENTS .....131

Page

STEEL .....131

$Ni_4Mo$ .....133

**ERROR ANALYSIS** .....140

ERROR IN MASS .....140
ERROR IN THE MEASURED EFFECTIVE LENGTH .....140
ERROR IN DIAMETER .....141
ERROR IN I, E AND T CHANNELS .....143
ERROR IN dT/dt .....144
SUMMARY OF ERRORS .....145
REPEATABILITY .....147

**CONCLUSIONS AND RECOMMENDATIONS** .....150

CONCLUSIONS .....150
RECOMMENDATIONS .....153

**REFERENCES** .....156

**APPENDICES** .....161

APPENDIX I .....162
APPENDIX II .....164
APPENDIX III .....165
APPENDIX IV .....209

**VITA** .....224

# LIST OF TABLES


| Table | | Page |
|---|---|---|
| 1.1 | List of Fe-Al specimens tested in Calorimetry Laboratory | 20 |
| 3.1 | Codes, chemical composition and chemical formula of the seven specimens tested in this project | 52 |
| 3.2 | Ten readings for the measured diameter, in the axial direction and the average value, for three specimens, Ni (pure), $Ni_4Mo$ and FeAl | 55 |
| 3.3 | Swaging and annealing schedule for $Ni_4Mo$ specimen | 57 |
| 3.4 | Type and spacing of the three knife-edges and results of the calibration performed in 1978 and 1993 | 64 |
| 4.1 | Estimated errors in the quantities that are used to determine the specific heat | 146 |

# LIST OF FIGURES


| Figure | | Page |
|---|---|---|
| 1.1 | Block diagram of pulse calorimeter and its acquisition system | 8 |
| 1.2 | Schematic diagram of the specimen holder, the specimen, the calorimeter and its instrumentation | 10 |
| 1.3 | Photograph of specimen and holder | 12 |
| 1.4 | Schematic diagram of I,E,P and T signals as functions of time | 13 |
| 1.5 | Fe-Al phase diagram [10] | 22 |
| 1.6 | Ni-Al phase diagram [11] | 24 |
| 1.7 | Ni-Mo phase diagram [10] | 26 |
| 2.1 | Comparison between the Debye specific heat, the Einstein specific heat, and the actual specific heat of aluminum [15] | 34 |
| 2.2 | Ni-Mo phase diagram [10] | 37 |
| 2.3 | Crystal structure of β ($Ni_4Mo$) [19] | 38 |
| 2.4 | Isothermal time-temperature transformation diagram for ordering reaction in $Ni_4Mo$ [19] | 43 |
| 2.5 | Electrical resistivity versus temperature relationships for $Ni_4Mo$ for three initial conditions - annealed, cooled at 60 K $min^{-1}$, quenched from 950 °C and swaged 75% reduction in area. The dashed curve represents data | |

Figure Page

taken during cooling from above the transformation temperature [26] .....45

2.6 Specific heat of $Ni_4Mo$ for the initial conditions - slowly cooled, quenched from 950 °C [36] .....48

3.1 Schematic diagram of the knife-edge apparatus holder assembly .....67

3.2 Schematic diagram of the specimen, the knife-edge and the basic electrical connections .....68

3.3 Schematic diagram of the electrical components of the resistivity apparatus .....70

3.4 Schematic representation of the three thermocouple configurations used or tested with the pulse-heating specimen, a) one lead on top of the other, b) intrinsic type, and c) beaded type .....74

3.5 Electrical resistivity data of Kollie [8] and that from current research to illustrate the reversal in the sign of the pick-up with the change in the direction of the current, for intrinsic type thermocouples .....77

3.6 Electrical resistivity data of Kollie [8] and that from current research, for current flowing in either direction, illustrating the advantage and disadvantage of beaded type configuration .....77

3.7 Simplified flow-chart of the computing steps for processing the raw data file to determine the specific heat .....84

| Figure | | Page |
|---|---|---|
| 4.1 | Electrical resistivity versus temperature plot for pure nickel as determined by the author and Kollie [8] | 92 |
| 4.2 | Specific heat versus temperature plot for pure nickel as determined by the author and Kollie [8] | 93 |
| 4.3 | Fe-Al phase diagram | 95 |
| 4.4 | Electrical resistivity versus temperature plot for Fe-21.2 wt%Al | 96 |
| 4.5 | Electrical resistivity versus temperature plot for Fe-21.2 wt%Al, for current flowing in both directions | 98 |
| 4.6 | Specific heat versus temperature plot for 21.2 wt%Al | 99 |
| 4.7 | Magnified plot for specific heat versus temperature for 21.2 wt%Al, for lower temperature range | 100 |
| 4.8 | Electrical resistivity versus temperature plot for Fe-18 wt%Al. Inset shows a schematic plot based on Hyde et al.'s data for Fe-Al specimen with a DO3⇒ B 2 transformation | 102 |
| 4.9 | Specific heat versus temperature plot for Fe-18 wt%Al | 104 |
| 4.10 | Electrical resistivity versus temperature plot for Fe-16 wt%Al. Inset shows a schematic plot based on Hyde et al.'s data for Fe-Al specimen with a DO3⇒ B 2 transformation | 105 |
| 4.11 | Specific heat versus temperature plot for Fe-16 wt%Al | 106 |

Figure Page

4.12 Electrical resistivity versus temperature plot for Fe-8.5 wt%Al .....108

4.13 Specific heat versus temperature plot for Fe-8.5 wt%Al .....109

4.14 Electrical resistivity versus temperature plot for Ni-8 wt%Al .....111

4.15 Phase diagram of Ni-Al [11] .....112

4.16 Specific heat versus temperature plot for Ni-8 wt% Al .....113

4.17 Ni-Mo phase diagram [10] .....115

4.18 Electrical resistivity versus temperature plot for $Ni_4Mo$, for three initial conditions .....116

4.19 (a) Individual contributions to the overall electrical resistivity of $Ni_4Mo$, in the SRO(α) and cold-worked SRO(α) initial conditions, curve (1), thermal contribution; curve (2), contribution from the formation of SRO destroyed by cold-work; curve (3), contribution from equilibrium SRO. (b) overall electrical resistivity of $Ni_4Mo$, in the SRO(α) and cold-worked SRO(α) initial condition .....119

4.20 Power versus temperature plot for pulse-heating, for $Ni_4Mo$, cold-worked SRO(α) initial state. Heating rates - Lei : 10 K/min, Author : 1 K/sec .....120

4.21 Comparison of author's data of the electrical resistivity for $Ni_4Mo$, SRO(α) initial condition, with that of Lei [26] .....124

Figure Page

4.22 Electrical resistivity versus thermal emf plot for $Ni_4Mo$, for slow heating (average heating rate, 1 K/sec.) .....125

4.23 Power versus temperature plot for $Ni_4Mo$, for slow heating (average heating rate, 1 K/sec.) .....126

4.24 Specific heat versus temperature plot for $Ni_4Mo$, for two initial conditions, SRO($\alpha$) and LRO($\beta$) .....128

4.25 Temperature versus time plot for pulse-heating, for $Ni_4Mo$, cold-worked SRO($\alpha$) initial state .....130

4.26 Thermal emf versus time plot for isothermal holding of steel specimen at 600 °C .....132

4.27 Electrical resistivity versus time plot for isothermal holding of steel specimen at 600 °C .....134

4.28 Electrical resistivity versus time plots for isothermal holding of $Ni_4Mo$ specimen at 700 °C and 750 °C .....135

4.29 Thermal emf versus time history for initial isothermal holding of $Ni_4Mo$ specimen at 950 °C and second isothermal holding at 750 °C .....136

4.30 Fluctuation in power during isothermal holding of $Ni_4Mo$ at 700 °C .....138

4.31 Isothermal temperature-time-transformation (TTT) diagram for the $\alpha \Rightarrow \beta$ transformation in $Ni_4Mo$ .....139

4.32 Electrical resistivity data from two runs with identical test parameters, for $Ni_4Mo$ .....148

4.33 Specific heat data from two runs with identical test parameters, for $Ni_4Mo$ .....149

# ABBREVIATIONS

Expressions are abbreviated as follows, unless otherwise indicated in the text.

t - time

T - temperature

E - voltage across effective specimen length

I - current

$E_{th}$ - thermal emf

P - power

$\rho$ - electrical resistivity

Cp - specific heat at constant pressure

Cv - specific heat at constant volume

V - volume

m - mass of effective specimen

CLC # - Calorimetry Lab Code Number

$l_K$ - length between knife-edges

$l_T$ - length between voltage taps

d - diameter

l - length

q - heat

U - internal energy

S - entropy

# CHAPTER I
# INTRODUCTION

## PULSE CALORIMETRY

### GENERAL BACKGROUND

Conventional calorimetric techniques, e.g., adiabatic calorimetry [1], require the specimen to be exposed to elevated temperatures for extended periods of time. This causes thermometry inaccuracies and appreciable heat loss. Accurate corrections for this loss become difficult. Above 1300 K, the accuracy further degrades as heat loss by radiation becomes a dominant factor. Pulse calorimetry attempts to minimize this error by reducing the time the specimen is exposed to elevated temperatures. This is done by imparting a high electrical power to the specimen and using a small diameter, e.g., 0.18 cm, specimen so that high heating rate is generated by resistive self heating of the specimen. The specimen can heat up from room temperature to elevated temperature, e.g., 1300 K, in 10 sec. This minimizes heat losses and improves the accuracy of the results. The specimen environment can be at ambient temperature during the pulse experiment. The heat lost due to this temperature difference between the specimen and the surroundings can be estimated from the slope of the temperature-time curve for the post-pulse cooling history (explained later in this chapter).

Due to the fact that pulse calorimetry is a fast process, the technique can be used to its advantage to acquire data in the metastable range for alloys undergoing a relatively slow phase change. By imparting a high electrical power to the specimen it is possible to heat the specimen from room temperature to beyond the critical temperature incredibly fast, e.g., 1 sec., so that the material does not have enough time to transform above the critical temperature. Conversely, in a pulse calorimeter, a specimen can be cooled at high speed from an elevated temperature by blowing helium on to the specimen so that data for the high temperature stable phase can be obtained below the critical temperature. Such measurements are not possible with most other calorimetric techniques. The advent of high speed computers have assisted in fast data acquisition and processing.

In addition, when thermophysical data on high melting point metals, e.g., tungsten, are required, pulse calorimetry serves as the only suitable technique. Pulse calorimetry can be successfully used to measure samples in both solid and the liquid state. The experimental set-up for the measurement in the liquid state is elaborate. One way would be to enclose the specimen in a tube which would contain the metal after liquefaction. Or, a very high current, e.g., 1000 A, is passed through the specimen to melt it in microseconds before earth's gravity can have any effect to pull the column of liquid down. A successful variation to this technique has been tried under zero

gravity by Cezairliyan [2] where the specimen can stay in its place for a longer time after melting.

In addition to measurement on electrical conductors for specific heat and electrical resistivity, pulse calorimetry can be used as an important tool to detect phase changes, e.g., magnetic change, order-disorder transformation, structural change and also to detect formation of vacancies and other defects. With a temperature control program, pulse calorimetry can be used to generate isothermal kinetic data for a transformation and to estimate the enthalpy associated with it.

## HISTORICAL OVERVIEW

The first successful attempt to use pulse calorimetry for the determination of specific heat of electrical conductors was by Worthing[3], who in 1918 used a battery operated pulse calorimeter to measure on tungsten and carbon. The specimen was in the form of a filament and the absorbed power while going from one steady-state to another was recorded. Pulse time was of the order of a second. A zero-deflection galvanometer was used to record the electrical signals. The acquisition speed was limited to the time constant of the galvanometer, which being an analog device, was quite slow. The temperature was determined from the resistance of the specimen. The resistance-temperature relation was independently established.

Considerable modifications to the above technique have been made in the last 70 years by several investigators and considerable improvements have been documented. With the availability of high speed computers and digital acquisition technology, the attributes of pulse calorimetry have been exploited. Even for pulse lengths of 1 ms, enough data can be acquired with high speed acquisition devices to derive meaningful results from them. Cezairliyan [2] has compiled a list of all investigators who have worked with pulse calorimetry and tabulated information on the substances they worked with, pulse characteristics, temperature range, etc. The list is provided in Appendix I.

The next paragraphs briefly discuss pulse calorimetry work undertaken by two investigators. Around 1965, Kollie [4] designed a pulse calorimeter and used it to determine the specific heat of pure iron from 100 °C to 1400 °C. He later used the calorimeter to measure on nickel and $Ni_3Fe$. The novel feature of his technique was the use of a Digital Voltmeter (DVM) and a memory which permitted the recording of 400 readings per second with 0.1% full-scale resolution. Relatively low heating rates (10-20 K/sec) combined with the high time resolution of the recordings made this system a very attractive one for the measurement of specific heat and transition points at moderately high temperatures. The power and temperature were the recorded quantities. He employed a Pt/Pt-10%Rh thermocouple and welded it to the specimen in the intrinsic configuration, to determine the temperature.

Cezairliyan [5] has done considerable work in the field of pulse calorimetry at the National Institute of Standards and Technology [6]. He designed the millisecond resolution technique and the microsecond resolution technique. He used these pulse techniques to measure on Mo, W, Nb, Ni and has also applied these techniques to measure on binary and ternary alloys. In the microsecond resolution technique, the specimen is connected in series to a 24 kJ capacitor bank. There is a rapid resistive self heating of the specimen from the high current, e.g., 1000 A, from the capacitative discharge system. Current, voltage and radiance temperature are recorded as functions of time. The radiance temperature of the specimen is measured with a pyrometer and recorded into an oscilloscope at a speed of 2 MHz. The digital oscilloscope is directly interfaced to a desktop computer for data analysis. This method has been used to measure the heat of fusion of metals, e.g. niobium.

## CURRENT RESEARCH

The calorimetry research group at the Department of Materials Science and Engineering of the University of Tennessee, Knoxville, consists of C.R. Brooks, professor, metallurgical engineering, D.L. McElroy, retired scientist, Oak Ridge National Laboratory [7] and the author, a Ph.D. candidate . The calorimetry laboratory was set up in 1990 and a pulse calorimeter was designed. The essential elements of the University of Tennessee pulse calorimeter are,

1) Vacuum chamber
2) Specimen holder
3) Specimen
4) Mechanical pump
5) Diffusion pump
6) Thermocouple
7) Ionization gauge
8) Thermocouple gauge
9) Water-cooling system

A typical pulse lasts for 10 sec. A high speed acquisition system was built and connected to the calorimeter. The elements of the high-speed acquisition system are

1) Personal computer
2) A/D and D/A converters
3) Amplifiers
4) Programmable direct-current power supply
5) Standard resistor
6) Acquisition software

These elements were assembled in the proper manner to obtain a computerized high-temperature pulse calorimeter. The computer program used for the acquisition of the data was written by the author. The program can interact with the programmable power supply to send a current pulse for a specific period of time. The level of current can be controlled from 0 to 90 Amps. The program acquires the E, I, t signals and stores them as functions of time as a

data file. This raw data file is later opened by the data processing program to determine the specific heat of the specimen material. The entire run can be executed from the computer's keyboard.

After the calorimeter was successfully designed, its accuracy was checked by comparing the specific heat and the electrical resistivity data for pure nickel determined at Oak Ridge National Laboratory [7], by Kollie [8]. For the electrical resistivity data the disagreement with Kollie was less than 1%. For specific heat data, this disagreement was less than 2% across most of the range, except above the Curie temperature, where the disagreement is higher than 2%. After it was established that the calorimeter can determine the electrical resistivity and the specific heat of materials with acceptable accuracy, it was used to determine the electrical resistivity and specific heat of intermetallics and alloys, e.g., $Ni_4Mo$, FeAl, NiAl.

Figure 1.1 shows the block diagram of the pulse calorimeter designed and used for the current research. The block diagram includes both the calorimeter and the acquisition system. The programmable power supply can be triggered from the computer program to send a specified current for a specified length of time, to form the pulse. The power supply is connected in series with the specimen. The specimen temperature increases as a result of Joule heat generated in the specimen. The three transient signals acquired during the pulse are I, E, and thermal emf, $E_{th}$. The current, I, is the

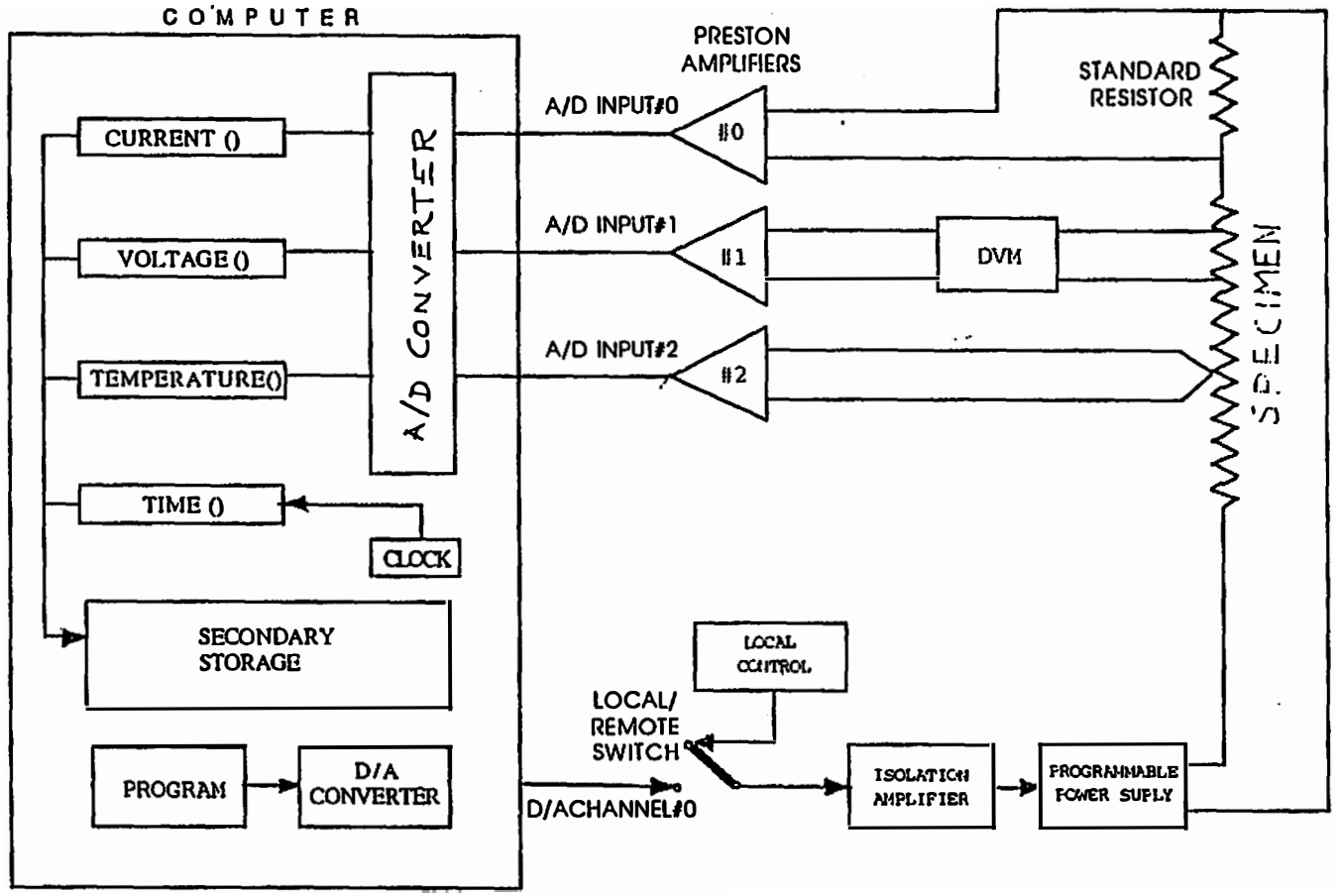


Figure 1.1 Block diagram of pulse calorimeter and its acquisition system.

current flowing through the specimen. The voltage, E, is the potential drop between the two voltage taps which are welded on to the specimen. The thermal emf, $E_{th}$, is generated from the thermocouple welded to the surface of the specimen. The thermal emf data is later converted to temperature (K) data by using $T=f(E_{th})$ equations developed at the National Institute of Standards and Technology and UTK Calorimetry Laboratory. The three signals are fed to the input of three amplifiers and then passed through a set of analog to digital converters and finally acquired into the computer program in the form of data arrays and stored into the computer's memory. For every set of data acquired the program puts a time-tag number (TT#) which is a set of integers in ascending order, using the computer's clock. These data are later accessed by the processing program to calculate specific heat data.

Figure 1.2 shows a schematic diagram of the pulse calorimeter. The specimen is held vertically inside the holder by a chuck and ferrel arrangement on both ends. When the specimen thermally expands, the limited slippage at the ferrel accommodates for the length increase. The current passes through the central rod, then through the specimen and out through the peripheral rods. A thermocouple is spot welded to the surface of the cylindrical specimen near its axial center. A 0.005 in. (0.013 cm) diameter, Pt/Pt-13%Rh thermocouple is used. Different thermocouple configurations (discussed later) were tried. Finally, the beaded configuration was selected for the pulse and the isothermal experiments. To form the

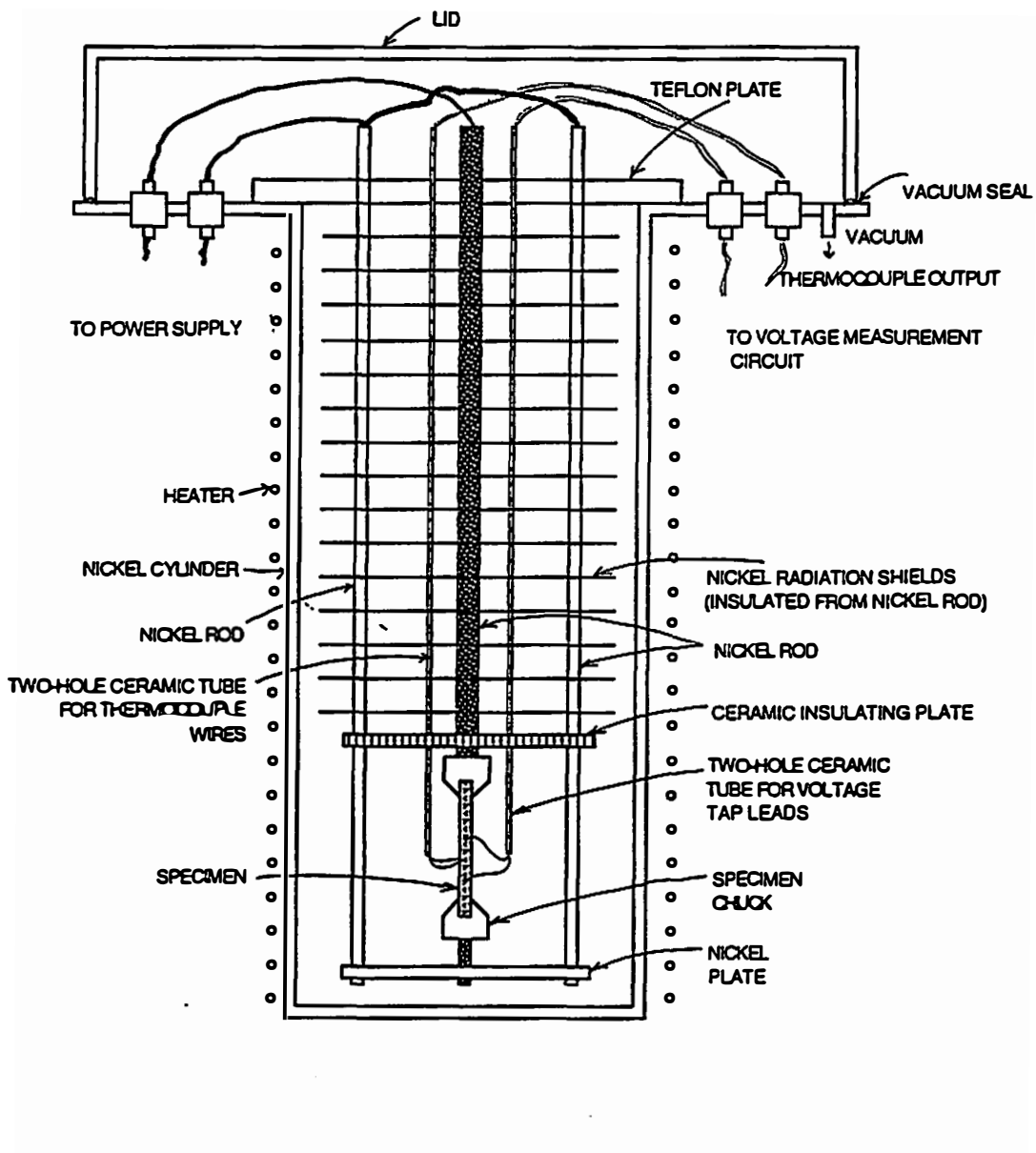


Figure 1.2 Schematic diagram of the specimen holder, the specimen, the calorimeter and its instrumentation.

bead the two leads were twisted together and melted at the end by an oxy-acetylene blowtorch. This bead was carefully spot welded to the specimen.

Two voltage taps, made out of 0.010 in. (0.025 cm) nickel wires, were spot welded to the specimen. Separations ranging from 2 to 4 cm. were used in different experiments. The separation between the taps defined the effective specimen length. All calculations are made with respect to this length of the specimen between the voltage taps. The separation between the taps is required to be known very precisely. Its accuracy affects the accuracy of the measured specific heat and electrical resistivity. This separation is electrically measured by employing a knife-edge with a resistivity apparatus. The process is detailed in Chapter III.

The thermocouple connections and the voltage taps are passed through ceramic insulators, up through the insulated top base and are taken out of the vacuum chamber to join copper wires in an ice bath reference junction. The copper wires are extended to the amplifiers. There is a set of radiation shields made out of nickel to reflect heat back to the specimen. Figure 1.3 shows photographs of the holder with the specimen in position and also the specimen with the thermocouple and voltage tap connections.

Figure 1.4 shows schematic diagrams for the signals acquired during the run. Three signals are acquired directly during pulsing: current, voltage and thermal emf. Figure 1.4a shows the current during the pulse. The programmable power supply is run in the

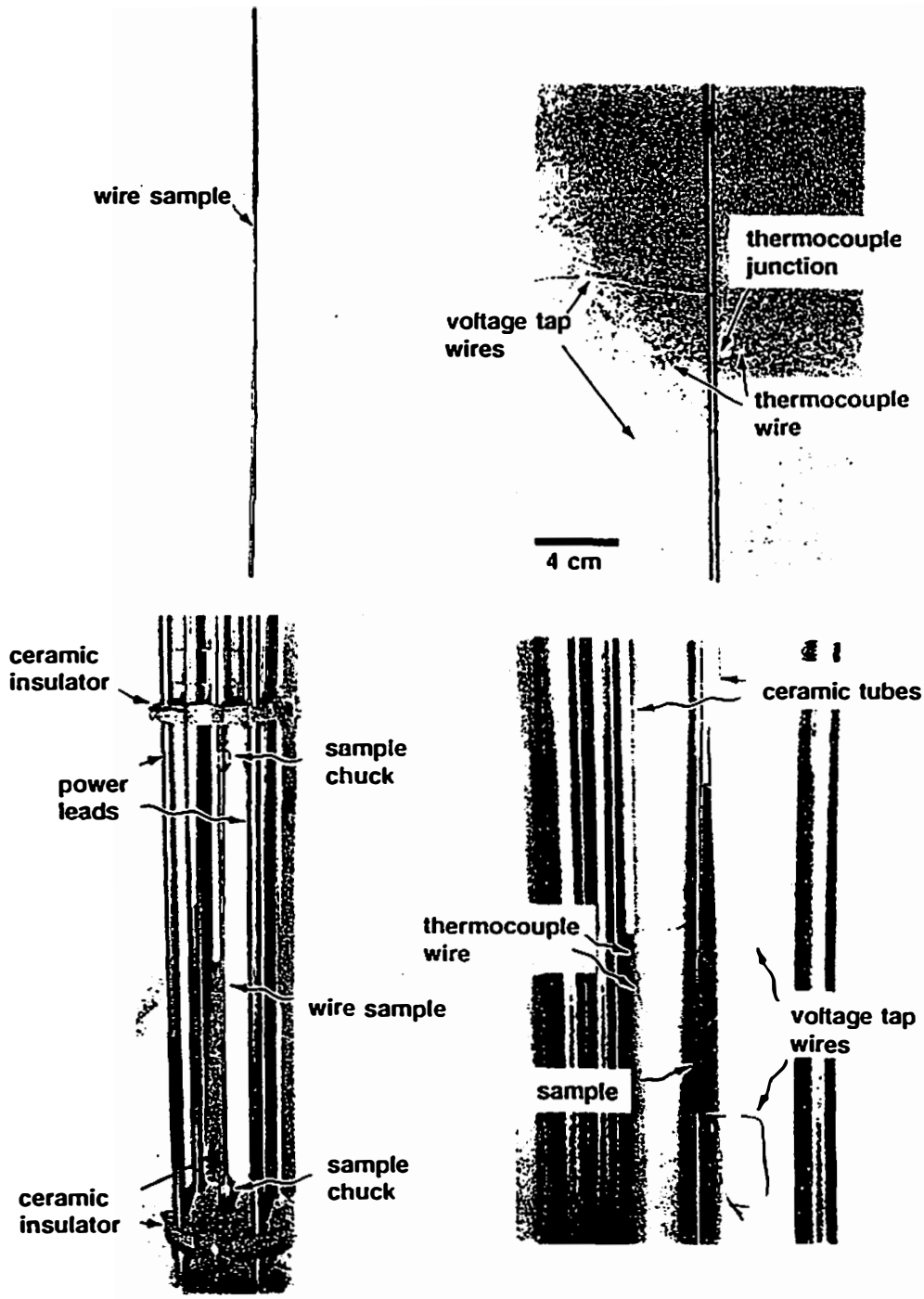


Figure 1.3 Photograph of specimen and holder.

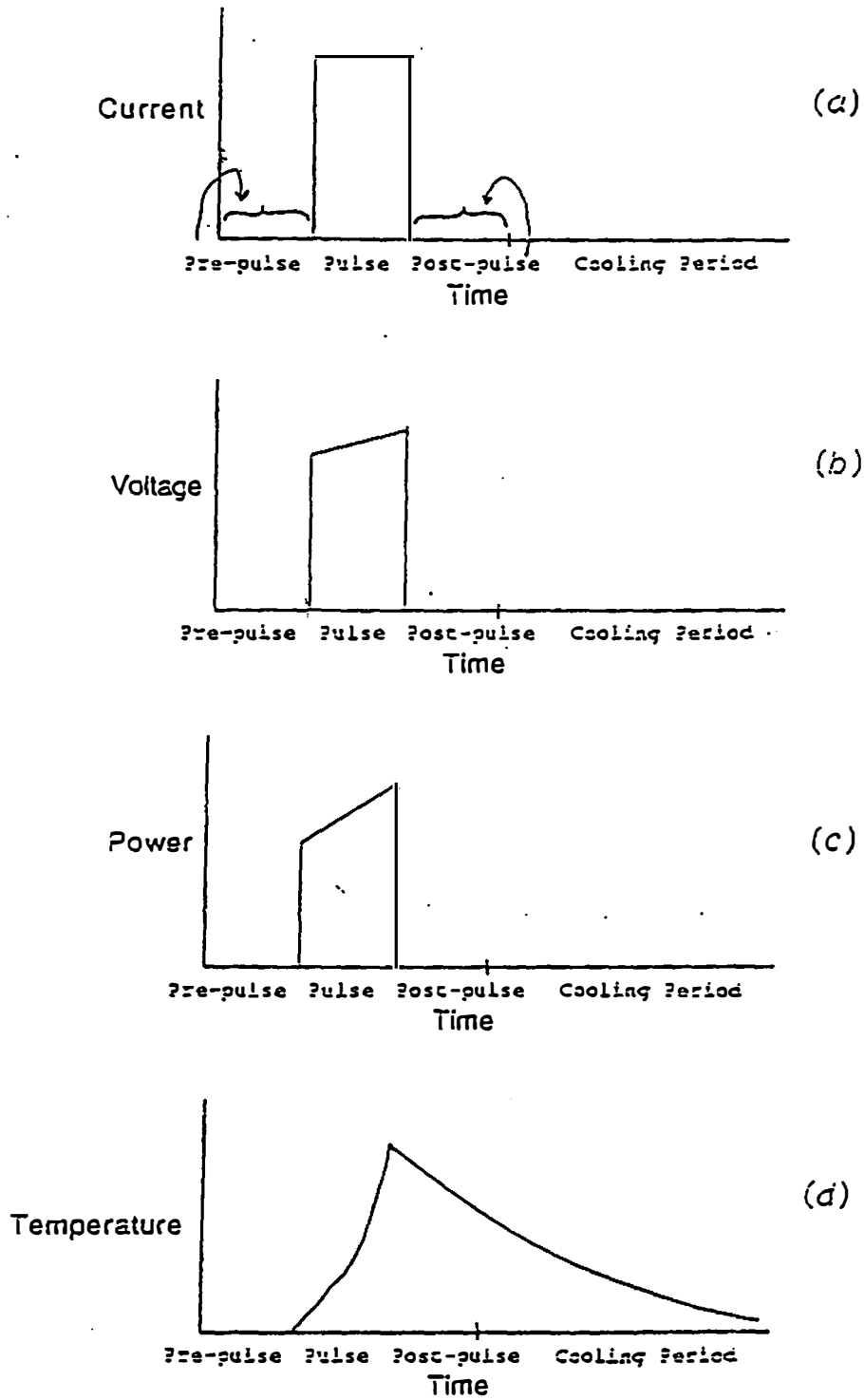


Figure 1.4 Schematic representation of (a) Current, (b) voltage, (c) power and (d) temperature profile during a specific heat experiment.

constant current mode so the current essentially remains constant during the pulse. The pulse is in the form of a square wave. During pulsing, Joule heat is generated in the specimen, proportional to $I^2R$, and hence the temperature of the specimen rises. Figure 1.4d shows this rise in temperature. After the pulse is over, the specimen cools till it reaches room temperature. The temperature signal is also recorded during cooling and is used to correct for heat losses from the specimen to its surroundings. As the specimen temperature increases its resistance changes, and the power, which is $I^2R$, changes. Voltage E, which is equal to IR, also changes because the resistance changes. The power is instantaneously computed by the acquisition program and is stored along with the I, E, T data.

For calculation of specific heat, at a certain temperature, knowledge of power, P, the slope of the temperature-time curve during heating, $dT/dt_H$, the slope of the temperature-time curve during cooling, $dT/dt_C$, at that temperature is required. While power, P, is calculated and stored in the raw data file, the slopes of the temperature-time curves are calculated by fitting the raw data. They then are substituted in the specific heat equation to calculate the specific heat.

The mass of the effective specimen is also a required quantity for the calculation of specific heat. The mass is calculated from the knowledge of the density and volume. The volume of a cylindrical specimen by, $V= (\pi/4)d^2l$. Readings of the diameter, d, are taken along the length of the specimen between the voltage taps. The

average of these readings is used in the calculation. The length of the effective specimen is the separation between the voltage taps, l, which is determined by the knife-edge apparatus. Then the mass, m, is calculated from the relationship, $m=v\rho$, where $\rho$ is the density of the specimen material. The value of the specimen mass is put in the codes of the processing program.

The program then calculates specific heat from the P, $(dT/dt)_H$, $(dT/dt)_C$ and m data. The procedure is discussed in more detail in Chapter III.

# ELECTRICAL RESISTIVITY AND SPECIFIC HEAT DETERMINATION

Electrical resistivity and specific heat can be determined using the designed pulse calorimeter.

## ELECTRICAL RESISTIVITY

Determination of electrical resistivity requires knowledge of the specimen dimensions, the potential drop across the effective specimen and the current flowing through the specimen, both of which are acquired during the pulse period. Between acquisition of two set of signals there is enough time for the computer program to compute the electrical resistivity based on the acquired voltage and current signals and the dimensions of the specimen which are in the

program code. For each set of data acquired (t, $E_{th}$, E, I), the electrical resistivity, $\rho$, is computed and recorded for the same TT#. Using the raw data file one can get a plot between electrical resistivity and thermal emf. After processing the raw data file with the MASTER program, thermal emf is converted to temperature using $T=f(E_{th})$ equations and a direct plot of electrical resistivity and temperature is obtained. The $T=f(E_{th})$ equations are the same as that used in the author's M.S. thesis [12].

## SPECIFIC HEAT

Determination of specific heat requires transient data for P and T during the pulse. Also, an estimation for the heat lost from the specimen to its surroundings is required. Figure 1.4 shows the schematic the for I, E, P, T during and after the pulse. The I and E signals are used to compute the power at each acquisition step and the values for power are written to the raw data file. The expression used for the determination of specific heat at constant pressure, Cp, is

$$Cp = \frac{EI}{m\left[\left(\frac{dT}{dt}\right)_H - \left(\frac{dT}{dt}\right)_C\right]}$$

The product of voltage drop along effective specimen, E, and the current flowing through the specimen, I, is the power, P, which appears as the numerator of the above equation.

The mass is calculated from the knowledge of the volume of the effective specimen and the density of specimen material, which is calculated (see Appendix II).

Calculation of the slope of the temperature-time curve for heating, $dT/dt_H$, and that during cooling, $dT/dt_C$, requires fitting the temperature-time data and differentiating T with respect to t to get the slope as a function of time. The slope data for cooling needs to be subtracted from that during heating to compensate for the heat lost from the specimen to the surroundings, during heating.

Experimental procedures are discussed in Chapter III.

## DISCUSSION ON ALLOYS TESTED

The accuracy and repeatability of the pulse calorimeter were determined by making measurements on nickel. Tests were conducted at different current levels, and hence at different heating rates, and their effect on the determined electrical resistivity and specific heat were observed. The direction of current was reversed and its effect on electrical resistivity and specific heat was observed. Also, tests were repeated on nickel specimens with the very same pulse parameters to determine the repeatability in the electrical resistivity and specific heat data including the repeatability in the determined Curie point. Some of the results of these tests are presented in Chapter IV.

After the accuracy and repeatability on nickel were determined, several alloys and intermetallics were tested for which the electrical resistivity and specific heat data are either not known or have not been well established. Four alloys of the Fe-Al system were tested to get electrical resistivity and specific heat data and to detect any internal change in the alloy with temperature. One alloy of the nickel-aluminum system was tested and the electrical resistivity and specific heat data were used to detect the formation of lattice defects and distinguish their types.

Finally, pulse calorimetry tests were done on $Ni_4Mo$ (Ni-20 at%Mo). The specimen was swaged down to 14% reduction in diameter. The cold worked $Ni_4Mo$ was pulsed from ~300 K to ~1400 K, and the data for electrical resistivity and specific heat were determined. Pulse tests were done on $Ni_4Mo$ in the SRO ($\alpha$) and LRO ($\beta$) initial conditions and electrical resistivity and specific heat data were determined.

A brief description of the alloys tested follows.

## Ni (PURE)

The specimen used in this research came from the stock used by Kollie [8] for his Ph.D. thesis. The stock material was acquired commercially as electrolytically pure. The composition is given on page 52.

Pure nickel is ferromagnetic below 633 K and paramagnetic above this temperature. The Curie temperature has been determined by Kollie [8] to be 633.0 K. The value determined by the author is 633 ±1 K.

Nickel was the first material to be tested on the designed pulse calorimeter. The main reasons for selecting nickel was :

1) The specific heat and electrical resistivity of nickel have been well established, so nickel would serve as a good standard.

2) Nickel does not have any complicated phase transformations which would make the measurements difficult and non-repeatable.

3) Nickel has a Curie temperature which has been well established and would serve as a benchmark for the accuracy of the measured temperature.

Touloukian [9] has compiled specific heat data for nickel of twelve investigators whose data span the temperature interval 12 K to 1584 K. One general trend in the data is agreement of about ±2% below the Curie temperature ($T_C$) but a radical diversion above $T_C$.

## IRON ALUMINIDE ALLOYS

Information about the four iron aluminide specimens tested are tabulated in Table 1.1. Fe-Al alloys have been developed to have an optimum combination of room temperature ductility and strength,

Table 1.1 List of Fe-Al specimens tested in Calorimetry Laboratory.

| CLC # | Composition | Phase |
|---|---|---|
| FAC | Fe - 21.2 wt% Al | FeAl |
| FAE | Fe - 18 wt% Al | $Fe_3Al$ |
| FAS | Fe - 16 wt% Al | $Fe_3Al$ |
| FAT | Fe - 8.5 wt% Al | α-Fe |

high temperature strength and good weldability. They have good high temperature oxidation and corrosion resistance because they can form a stable and adherent oxide film on its surface.

The specimen FAC was acquired from ORNL [7] where it was developed by the Alloy Behavior and Design Group. The material was extruded at high temperature then ground down to the required diameter, 0.07 in. (0.18 cm). It is an ordered intermetallic, FeAl ($\alpha_2$),having a B2 structure. Its composition is Fe-21.1 wt%Al (see Figure 1.5). The Fe-Al phase diagram presented in Figure 1.5 shows this alloy to be in the region of $Fe_3Al$ stability. However, according to ORNL [7] reports and the tests done in this project, the alloy is FeAl, as mentioned earlier.

The specimen FAT contains 8.5wt% Al and lies in the $\alpha$-Fe range of the phase diagram (see Figure 1.5). It is ferromagnetic at room temperature. For this composition, on heating the specimen, the only phase change noticeable is the magnetic change around 950 K (650 °C). This magnetic change affects the electrical resistivity and specific heat curves. These curves can be used as a basis to detect the occurrence of these changes.

The specimen FAS contains 16 wt% Al and is stable as $Fe_3Al$ with a $DO_3$ structure. It is mildly magnetic at room temperature. On heating this alloy it shows a transformation from $DO_3(Fe_3Al)$ to B2 ($\alpha$2) structure around 750 K (477 °C) (see Figure 1.5).

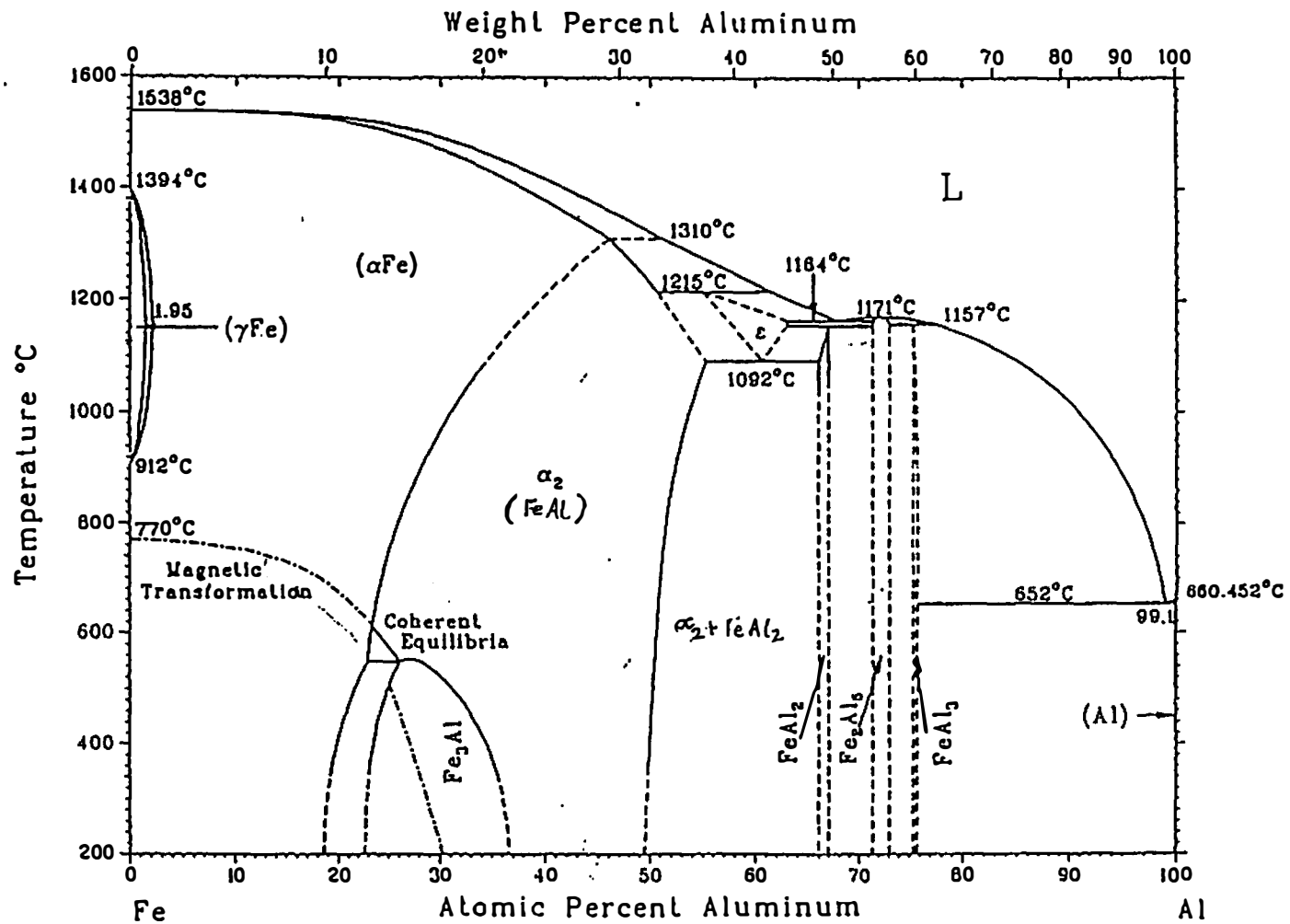


Figure 1.5 Fe-Al phase diagram[10].

The specimen FAE contains 18 wt% Al. It exists as $Fe_3Al$ phase and is non-magnetic. It has an ordered $DO_3$ structure below 740 K (467 °C) (see Figure 1.5).

It is pointed out that the tests done on Fe-Al alloys are preliminary and more tests are recommended to confirm the data and detect the phase changes present.

## NICKEL ALUMINIDE

One specimen of the Ni-Al system was tested to determine its electrical resistivity and specific heat. The specimen contained 8 wt% Al and was CLC coded as TWM. At room temperature, it lies in the two-phase region consisting of the solid-solution designated (Ni) and the intermediate phase $\alpha'$ ($AlNi_3$) which has an ordered FCC ($L1_2$) structure (see Figure 1.6). Around 1400 K it transforms to the single phase (Ni). In this experiment, data were taken up to a temperature of 1250 K (977 °C) so the phase change could not be captured in the data. Relative amounts of the phases should change as the temperature rises, according to the phase diagram. However, due to the short time involved, e.g., 10 sec., this can not happen.

## $Ni_4Mo$

The Ni-Mo system has been studied extensively. Both electron microscopy and calorimetry have been used to understand the

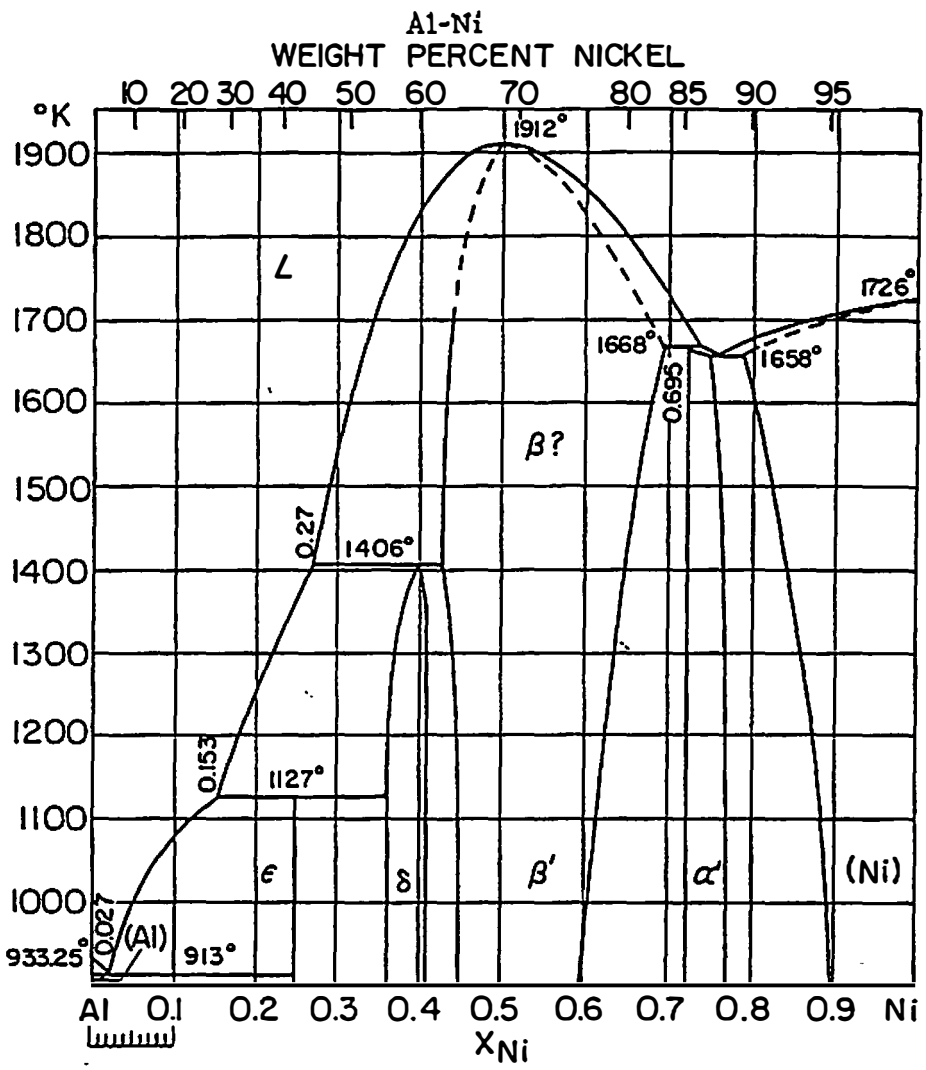


Figure 1.6 Ni-Al phase diagram [11].

order-disorder transformation, its kinetics, the effect of cold work on ordering, etc. One goal of the current research is to better understand the transformation characteristics of this alloy. $Ni_4Mo$ (Ni-20 at%Mo) was selected as the specimen (refer to Figure 1.7). At room temperature it exists as ordered $\beta$, which has a tetragonal structure. At 1141 K (868 °C) it transforms to disordered $\alpha$ which has short range order in it. Thus 1141 K (868 °C) has been determined to be the equilibrium transformation temperature for $Ni_4Mo$. However, the transformation is also dependent on the heating rate from room temperature, with the kind of heating rates (e.g., 75 °C/sec) attained with the pulse calorimeter used, in this research, it was not possible to 'beat' the transformation and take data for $\beta$(LRO) above $T_c$.

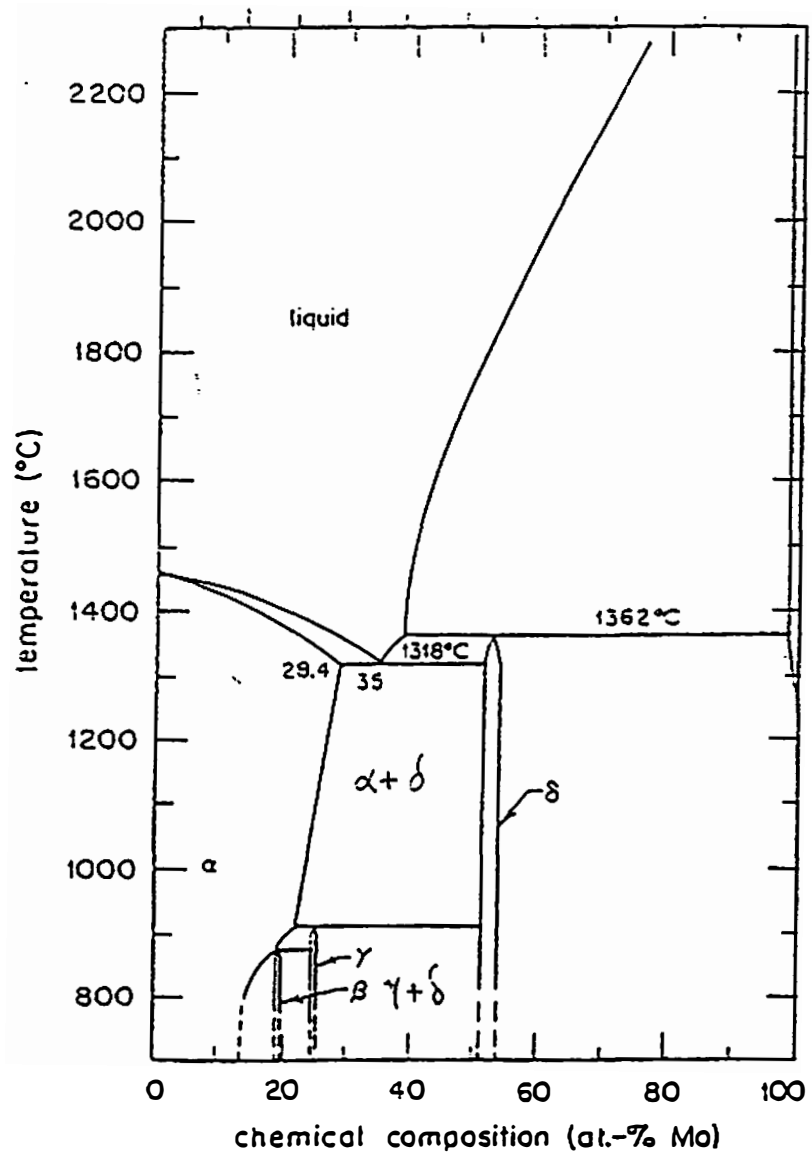


Figure 1.7 Ni-Mo phase diagram. [10].

# CHAPTER II
# REVIEW OF LITERATURE

## DEFINITION OF SPECIFIC HEAT

For a system having arbitrary mass the heat capacity, c, can be defined with the following limit

$$c = Lt\ (\Delta T \rightarrow 0)\ \frac{\Delta Q}{\Delta T} = \frac{dq}{dT} \qquad ....(1)$$

where $\Delta Q$ is the quantity of heat added to the system in order to raise its temperature by an amount $\Delta T$. Dividing the above equation by the system mass, m, yields an expression for specific heat, C.

$$C = \frac{c}{m} = \frac{dq}{dT} \qquad .... (2)$$

where dq is the quantity of heat required to raise the unit mass of the system by an amount dT. The 'd' in 'dq' refers to an infinitesimal change in 'q'. The Systeme International (SI) unit for specific heat is J-gm-mol$^{-1}$ K$^{-1}$ or J kg$^{-1}$ K$^{-1}$ (1000 J gm$^{-1}$ °C$^{-1}$).

The specific heat is path dependent so the path must be specified in order to determine its value. For any substance the equation of state will be of the form f(P,V,T) = 0, where P is hydrostatic pressure, V is volume and T is temperature. Since any two variables among the three are independent variables, only two variables can have arbitrary values at the same time. For example if T is increased only one of the two remaining variables, P or V, can be

kept constant. So two major specific heats have been defined, one at constant volume, the other at constant pressure.

$$C_p = [\frac{dq}{dT}]_p \quad ....(3) \quad \text{and} \quad C_v = [\frac{dq}{dT}]_v \quad ....(4)$$

The specific heat at constant volume, $C_v$, is an intensive property of the substance. The determination of this fundamental quantity for various metals and alloys is of great interest to physicists in interpreting the solid state. For solids it is difficult to measure $C_v$ directly. Usually the specific heat at constant pressure, $C_p$, is determined and the corresponding $C_v$ is calculated from a suitable thermodynamic relationship. This general relationship between the specific heat capacity at constant pressure and that at constant volume enables one to calculate either from the knowledge of the other. The relationship is derived as follows.

$$C_p = (dq/dT)_p \quad ....(5)$$

$$C_p = [d(U+PV)/dT]_p \quad ....(6)$$

$$C_p = (dU/dT)_p + P(dV/dT)_p \quad ....(7)$$

Internal energy U is a function of state and can be expressed as U=U(T,V)

$$dU = (\delta U/\delta T)_v \, dT + (\delta U/\delta V)_T \, dV \quad ....(8)$$

$$(\delta U/\delta T)_p=(\delta U/\delta T)_v + (\delta U/\delta V)_T(\delta V/\delta T)_p \quad ....(9)$$

$$(\delta U/\delta T)_p = C_v + (\delta U/\delta V)_T \, (\delta V/\delta T)_p \quad ....(10)$$

From equations (7) and (10),

$$C_p = C_v + [P + (\delta U/\delta V)_T] \, (\delta V/\delta T)_p \quad ....(11)$$

$$C_p = C_v + C_d \quad \text{....(12)}$$

In equation 12, $C_d$ is called the dilation correction. This contribution from the dilation of the lattice can be expressed in terms of isothermal compressibility, $\kappa$, and thermal expansion coefficient, $\alpha$. From the first and second law of thermodynamics

$$dU = TdS - PdV \quad \text{....(13)}$$

$$(\delta U/\delta V)_T = T\,(\delta S/\delta V)_T - P \quad \text{....(14)}$$

From (11) and (14)

$$C_p = C_v + T\,(\delta S/\delta V)_T\,(\delta V/\delta T)_p \quad \text{....(15)}$$

$$C_p = C_v + T\,(\delta P/\delta T)_v\,(\delta V/\delta T)_p \quad \text{....(16)}$$

But

$$(\delta P/\delta T)_v\ (\delta T/\delta V)_p\ (\delta V/\delta P)_T = -1 \quad \text{....(17)}$$

$$(\delta P/\delta T)_v = -\,(\delta V/\delta T)_p\,(\delta V/\delta P)_T = \alpha / \kappa \quad \text{....(18)}$$

where $\alpha = (1/V)\,(\delta V/\delta T)_p$ and $\kappa = -(1/V)\,(\delta V/\delta P)_T$.

From (16) and (18)

$$C_p = C_v - T\,(\delta V/\delta T)_p^2 / (\delta V/\delta P)_T = \alpha^2 VT / \kappa$$

Or $$C_p - C_v = -T\,(\delta V/\delta T)_p^2 / (\delta V/\delta P)_T = \alpha^2 VT / \kappa \quad \text{....(19)}$$

Thus $C_d = \dfrac{\alpha^2 VT}{\kappa}$ where,

$\alpha$ = volumetric coefficient of thermal expansion

$\kappa$ = coefficient of isothermal compressibility

$$C_d = C_p - C_v \quad \text{....(20)}$$

The main contributions to the specific heat capacity at constant volume, $C_v$, can be stated theoretically by considering the micro-mechanisms which lead to the changes in the internal energies of a substance. The contributions come from the following:

$C_{vt}$ = Contribution of translational motion of atoms

$C_{ve}$ = Contribution of electronic structure changes

$C_{vv}$ = Contribution of vibrational motion of atoms

$C_{vw}$ = Contribution of rearrangement of atoms

$C_{vr}$ = Contribution of rotational motion of atoms

$C_{vn}$ = Contribution of nuclear structure changes

$C_{vi}$ = Contribution from interaction of the different mechanisms. Thus, the total is the sum of the individual contributions

$$C_v = C_{vt} + C_{ve} + C_{vv} + C_{vw} + C_{vr} + C_{vn} + C_{vi} \quad ....(21)$$

In this project our interest is restricted to metals and alloys. For such solids, the translational and rotational motion contribution can be neglected. Above 10 K the nuclear contribution $C_{vn}$ also becomes negligible.

The term $C_{vw}$ takes into account configurational ordering and vacancy and divacancy formation. $C_{ve}$ also includes contributions from excitations of valence electrons and alignment of spin in magnetic effects. The contribution of $C_{vi}$ is very difficult to assess. It is assumed to be negligible. But sometimes it is necessary to make adjustments in other contributions to validate this assumption. With the aforesaid assumptions, equation (21) can be written as

$$C_v = C_{vv} + C_{ve} + C_{vw} \quad ....(22)$$

The specific heat capacity at constant pressure, $C_p$, has contributions from all the factors involved in equation (21) plus that due to dilation of the lattice, $C_d$. Thus the expression for $C_p$ will be :

$$C_p = C_d + C_{vh} + C_{va} + C_{ve} + C_{vw} \quad \text{....(23)}$$

In this equation the contribution from vibrational motion has been broken up into two components - the harmonic contribution, $C_{vh}$, and the anharmonic contribution, $C_{va}$.

The value of $C_v$ for a substance can be determined from the measured value of $C_p$ and the value of $C_d$ at the required temperature. However, little data are available for isothermal compressibility coefficient, $\kappa$, for high temperatures for most metals and alloys. For this reason approximation methods are usually employed to obtain $C_d$. For more detailed discussion on this subject, refer to Part I, Chapter 2, of Ref. 12.

## THEORETICAL MODELS FOR SPECIFIC HEAT

In 1819, an empirical rule was introduced, which stated that the molar heat capacities of all solid elements equals 3R, where R is the universal gas constant. 3R is equal to 24.94 J/K-mole. Subsequent experimental determination of values of the specific heat of various elements showed that they approximately approached 3R with increase in temperature. However, specific heat approached zero as the temperature decreased.

Calculation of the specific heat of a solid element, as a function of temperature, was one of the early triumphs of the quantum theory. The first attempt in formulating a model for the theoretical calculation of specific heat is credited to Einstein [13]. He considered the properties of a crystal comprised of n atoms, each of which, in classical terms, is considered to behave as a harmonic oscillator vibrating independently about its lattice point. The basis of all lattice dynamic theories is the harmonic approximation in which thermal vibration of the atoms about their positions are treated as a superposition of motions of harmonic oscillators, according to the laws of quantum statistics [14]. If it is assumed that each oscillator is independent, i.e., its behavior is unaffected by the behavior of its neighbors, then every oscillator would vibrate with a single fixed frequency, $\nu$. A system of such oscillators is known as Einstein crystal [15]. The mathematics of the Einstein model were worked out and after approximations and substitutions the heat capacity at constant volume, Cv, was expressed as

$$Cv \approx 3R \left(\frac{\theta_E}{T}\right)^2 \exp\left(\frac{-\theta_E}{T}\right) \qquad \text{....(24)}$$

where,

R = universal gas constant

T = absolute temperature

$\theta_E$ = Einstein characteristic temperature

The Einstein characteristic temperature, $\theta_E$, can be expressed as

$$\theta_E = h\nu/k \qquad \text{....(25)}$$

where,

h = Planck's constant
$\nu$ = frequency of vibration of atoms
k = Boltzmann's constant

The variation of Cv with $T/\theta_E$ is shown in Figure 2.1. As $T/\theta_E$ increases Cv —› 3R. $\theta_E$ and $\nu$ are obtained by fitting eq. 24 to experimental data. As can be observed from the figure for aluminum, there is a discrepancy between empirical data and the data predicted by Einstein's model. The discrepancy is more at lower temperatures. Einstein's assumption that the oscillators all vibrate with the same frequency was inadequate, however, it still predicted the classical Dulong-Petit value of 3R at high temperatures and zero at absolute zero.

The publication of Einstein's theory in 1907 provided considerable stimulus to the development of low temperature calorimetry [14]. Nernst and co-workers [16] measured the specific heat of a number of substances at low temperature, e.g., 20 K. Their results showed that the low temperature behavior predicted by Einstein model qualitatively agreed with empirical data. In 1911, Einstein [17] recognized that a more realistic model of a solid would consist of atoms vibrating collectively at many different frequencies. In spite of the inadequacy of this model, it demonstrated the need to take quantum mechanical approach to account for the dynamical model of a solid and laid the foundations for more sophisticated

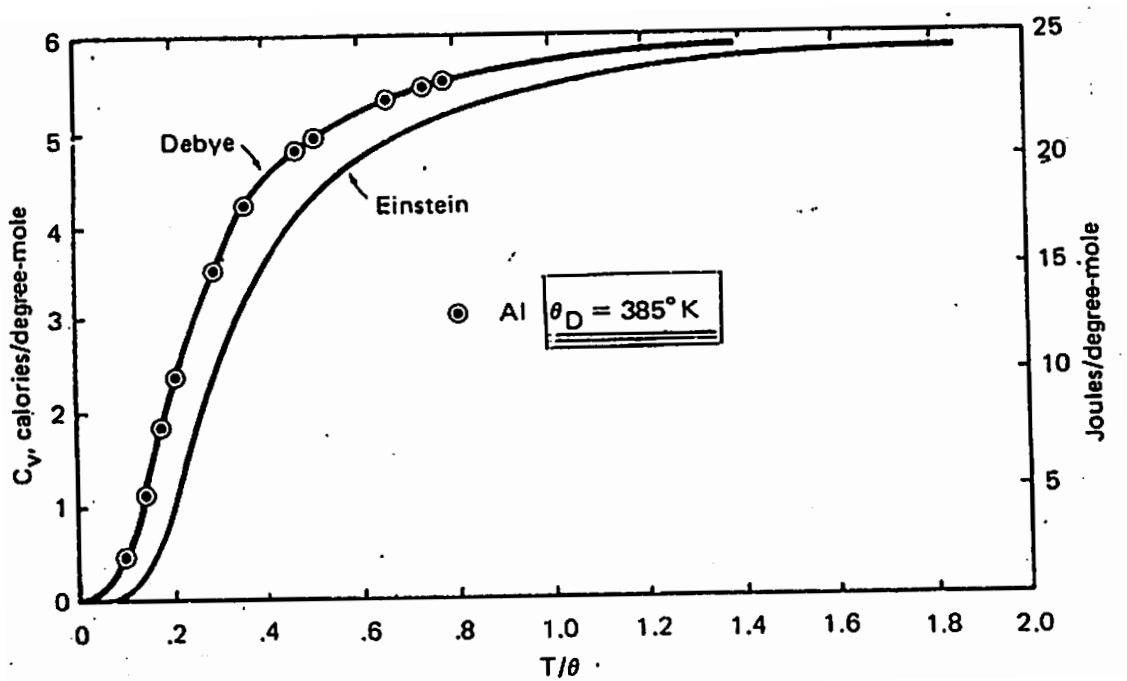


Figure 2.1 Comparison between the Debye specific heat, the Einstein specific heat, and the actual specific heat of aluminum [15].

models which were later formulated, e.g., Debye model, Born and von Karman model.

The next step in the development of the model was by Debye [18]. He assumed that the atoms vibrate with a range of frequencies, where the lower limit is fixed by the interatomic distances in the solid. Debye assumed that the number of vibrations per unit volume, per unit frequency range, increases parabolically with increasing frequency in the allowed frequency range, $0 \leq \nu \leq \nu_{max}$, where $\nu_{max}$ represents the maximum frequency of vibration and is obtained from

$$\nu_{max} = V / \lambda_{min} \qquad \text{....(26)}$$

where,

$\lambda_{min}$ = minimum wavelength of vibration

V = wave velocity in solid

In essence, Debye integrated the Einstein expression over the frequency distribution $\nu_{min}$ and $\nu_{max}$ and obtained the expression for heat capacity of solid as

$$Cv = \frac{9\eta h^3}{k^2\theta_D^3}\int_0^{\nu_D} \nu^2 \left(\frac{h\nu^2}{kT}\right)\frac{\exp(h\nu/kT)}{(1-\exp(h\nu/kT))^2}\,d\nu \qquad \text{....(27)}$$

where,

$\eta$ = Avogadro number

$\theta_D$ = Characteristic Debye temperature

$\nu_D$ = Debye frequency (which is the maximum frequency of vibration)

Figure 2.1 shows that eq. 27 gives an excellent fit to experimental data at lower temperature. Debye theory suggests that by suitable selection of a single parameter, $\theta_D$, the specific heat of any solid should fall on a universal curve as shown in the figure. However, in order to accurately fit the Debye model to the observed Cp data, suitably corrected for by the dilation constant (Cp-Cv = Cd), the value of $\nu$ required must be permitted to vary with temperature. In spite of this drawback, Debye model is still useful in describing the specific heat and other properties of solids.

## Ni-Mo SYSTEM

While Ni has poor solubility in Mo, Mo has good solubility in Ni. Refer to Figure 2.2, which shows the phase relations in the Ni-Mo system. In the current research, the Ni rich alloy $Ni_4Mo$ is of interest. There is considerable solubility of Mo in Ni in the FCC ($\alpha$) phase, but it is not stable at lower temperatures for sufficiently high Mo content. There are intermetallic compounds of which the $\beta$ phase has received considerable attention [19]. It has a long-range ordered (LRO), BCT structure (Figure 2.3), and hence its formation from $\alpha$ is referred to as disorder-order transformation. The $\beta$ phase forms from a disordered $\alpha$ phase by the rearrangement of Ni and Mo atoms on the FCC lattice sites, and hence the $\beta$ phase retains the

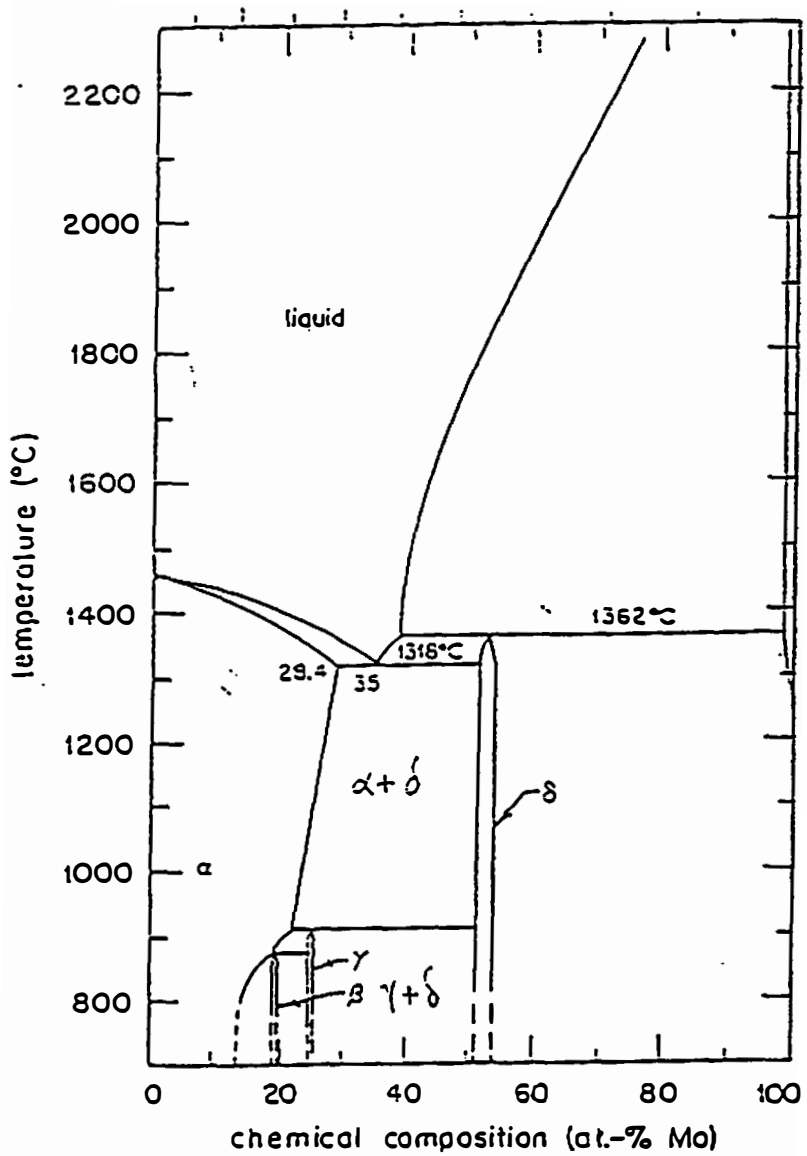


Figure 2.2 Ni-Mo phase diagram [10]

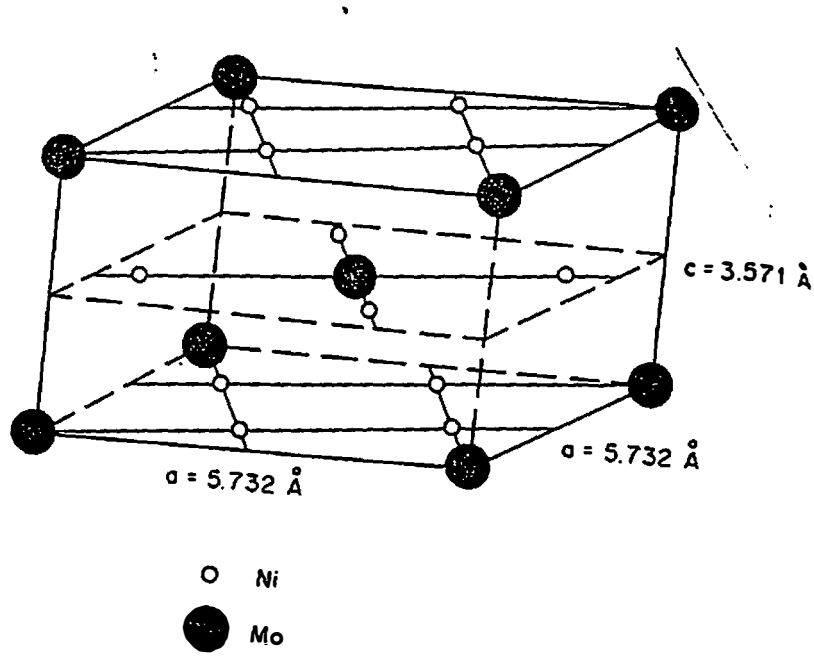


Figure 2.3 Crystal structure of β (Ni4Mo) [19].

crystallographic orientation of its parent phase. The numerous ways in which a β-domain may form from the single α phase grain lead to the three different types of domain interfaces. They were first studied by Ruedl et al. [20], who used Transmission Electron Microscopy to show that the interfaces could be anti-phase boundaries (APBs), antiparallel twins (APTs) or perpendicular twins (PTs). The equilibrium transformation temperature for α to β is 1141 K (868 °C).

Studies on Ni-Mo alloys are of interest and importance because of several reasons [19]. The phase transformations which occur in them generate spectacular microstructures, the study of which leads to a better understanding of principles governing all alloy systems. These structures significantly affect properties. Some of the compositions act as bases for commercial alloys, such as Hastalloy B2.

Thus, there is a need to get thermophysical and electrical property data, both for their own sake and for evaluating the kinetics of the disorder-order reaction from the α phase. Use can also be made of the variation in the power-time data to evaluate the heat effect for such reactions. This will lead to a better understanding of the order-disorder reaction in $Ni_4Mo$ and the concept of order-disorder in general. Electrical resistivity tests have been performed on cold-worked $Ni_4Mo$ which has SRO(α) as the starting microstructure. From studying the change in the electrical resistivity and comparing with the data without cold-work,

information can be derived on the effect of cold-work on the state of order.

Casselton and Hume-Rothery [21] made a detailed study of the entire Ni-Mo system from 800 °C to the liquidus temperature. Guthrie and Stansbury [22] made a detailed study of the system from about 12 to 48% Mo in the range 700-1000 °C. They employed x-ray diffraction and microstructural observations in their studies. A different approach was taken by Heijwegen and Rieck [23] who employed diffusion couples to study the system from 800 to 1295 °C. This technique, however, did not have sufficient accuracy to locate phase boundaries with a compositional uncertainty of $\leq \pm$ 5% Mo. Kozlov and Kushnarenko [24] determined the LRO parameter as a function of temperature for 20.7% Mo alloy.

## ORDER-DISORDER TRANSFORMATION IN $Ni_4Mo$

At solution treatment temperature in the range 900-1250 °C, $Ni_4Mo$ (Ni-20 at%Mo) is short range ordered (SRO), single phase FCC solid-solution[21]. At temperatures below 868 °C (1141 K), $Ni_4Mo$ transforms to the LRO ($\beta$) phase. The crystal structure of $\beta$ is shown in Figure 2.3. It is tetragonal with a c/a ratio of 0.623. It has been observed that the transformation occurs most rapidly around 775 °C but becomes quite sluggish below 550 °C [25]. During the transformation, the electrical resistivity decreases and the hardness

increases [26]. In the current research, use is made of the electrical resistivity data to detect the temperature ranges where transformations are taking place.

The ordering transformations can also be detected by optical microscopy. The growth of the β regions within the α matrix has been observed and reported by Saburi et al. [27]. In addition, X-ray diffraction, electron diffraction and transmission electron microscopy have been used to detect the order-disorder transformation. Electrical resistivity measurements made by Thomas [28] provided early evidence that there is structural variance within the α-phase region. He also observed that the electrical resistivity of quenched or cold-worked (disordered) alloys was higher than for slowly cooled (ordered) alloys.

It has been established that order-disorder transformation in $Ni_4Mo$ occurs by nucleation and growth, at least at temperatures above 700 °C [27,29]. However, at lower aging temperatures the possibility of a continuous transformation cannot be ruled out [30].

## KINETICS OF α—›β TRANSFORMATION IN $NI_4MO$

Considerable efforts have been made using electron microscopy to study the mechanisms and kinetics of the order-disorder transformation in $Ni_4Mo$. Use has also been made of micro-hardness and electrical resistivity measurements for this study.

The ordering reaction shows the familiar C-shaped curve, as shown in Figure 2.4. The curve was determined from resistivity measurements made after rapidly cooling from 1000 °C to the transformation temperature. The curve for the finish of the reaction is based on the time needed for the resistivity to remain constant for at least one hour [19]. The start curve is consistent with that determined by Lei [26] from resistivity measurement and that determined by Block [31] from hardness measurements of specimens quenched from α region and held isothermally at the transformation and the effects of transformations were noted.

## THE 'K – STATE'

The electrical resistivity of most Ni base solid-solution alloys is characterized by the existence of an equilibrium structural feature called the K-state [28]. The K-state was first proposed by Thomas [28] who studied several alloy systems. He found that upon cold-working specimens of certain alloys, their electrical resistivity decreased. He also suggested that one of the elements of the alloy must be a transition element. Since Thomas' work, the electrical resistivity behavior has been analyzed in terms of the K-state by several investigators [32,33]. It is generally recognized that the K-state is a state of SRO [34]. SRO clusters form in the microstructure which act as sites for the scattering of electrons. SRO clusters are non-random atom configurations which provide more effective

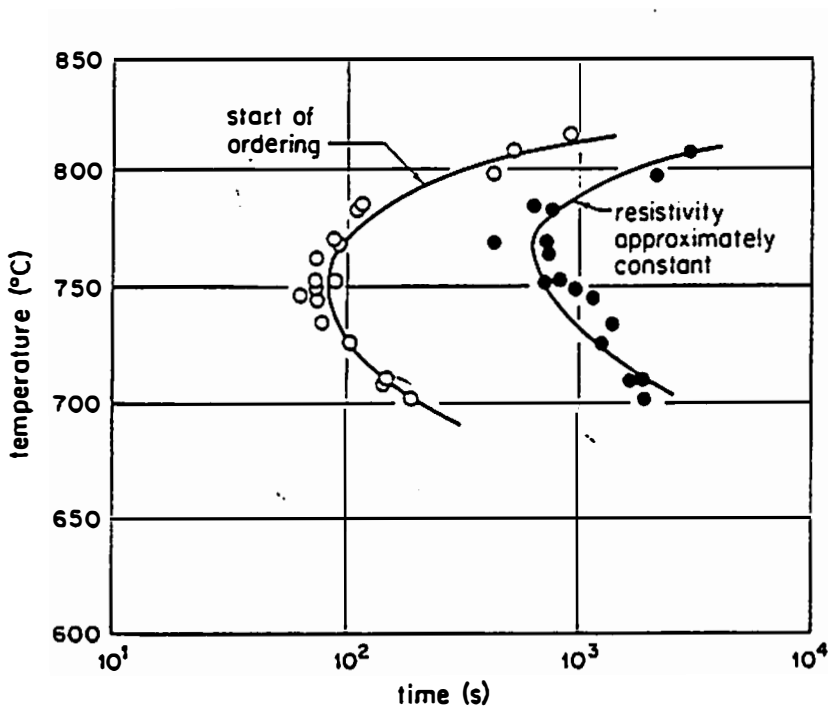


Figure 2.4 Isothermal time-temperature transformation diagram for ordering reaction in $Ni_4Mo$ [19]

electron scattering as compared to a random solid-solution [35]. In $Ni_4Mo$ the decrease in electrical resistivity with cold-work is due to the decrease in the degree of SRO. However, it is pointed out here that although SRO increases the electrical resistivity in many systems, e.g., $Ni_4Mo$, it decreases it in other systems, e.g., α-brass.

## ELECTRICAL RESISTIVITY OF $Ni_4Mo$

Electrical resistivity of $Ni_4Mo$ in various initial states, e.g., α, β and cold-worked α, has been determined by Norem [36], Vasudevan [37] and Lei [26]. The electrical resistivity of $Ni_4Mo$ determined by Lei [26] is reproduced in Figure 2.5. Curve 1 represents the electrical resistivity of $Ni_4Mo$ which has LRO(β) in the initial state. This specimen has been cooled slowly from an elevated temperature. The electrical resistivity at 25 °C is 45 μΩ-cm but increases drastically to a peak value of 135 μΩ-cm at the β—›α equilibrium transformation temperature, 868 °C (1141 K). Above this temperature the electrical resistivity continuously decreases with temperature to 1000 °C. Curve 2 represents the electrical resistivity of $Ni_4Mo$ in SRO(α) initial state. This specimen was cooled rapidly from above 950 °C. The room temperature resistivity of the SRO(α) state is 145 μΩ-cm and is higher by a factor of 3 than that of the LRO(β) initial state. The slope of curve 2 is considerably less than that of curve 1. Above about 600 °C, curve 2 decreases with increase in temperature. This is the result of progressive transformation from

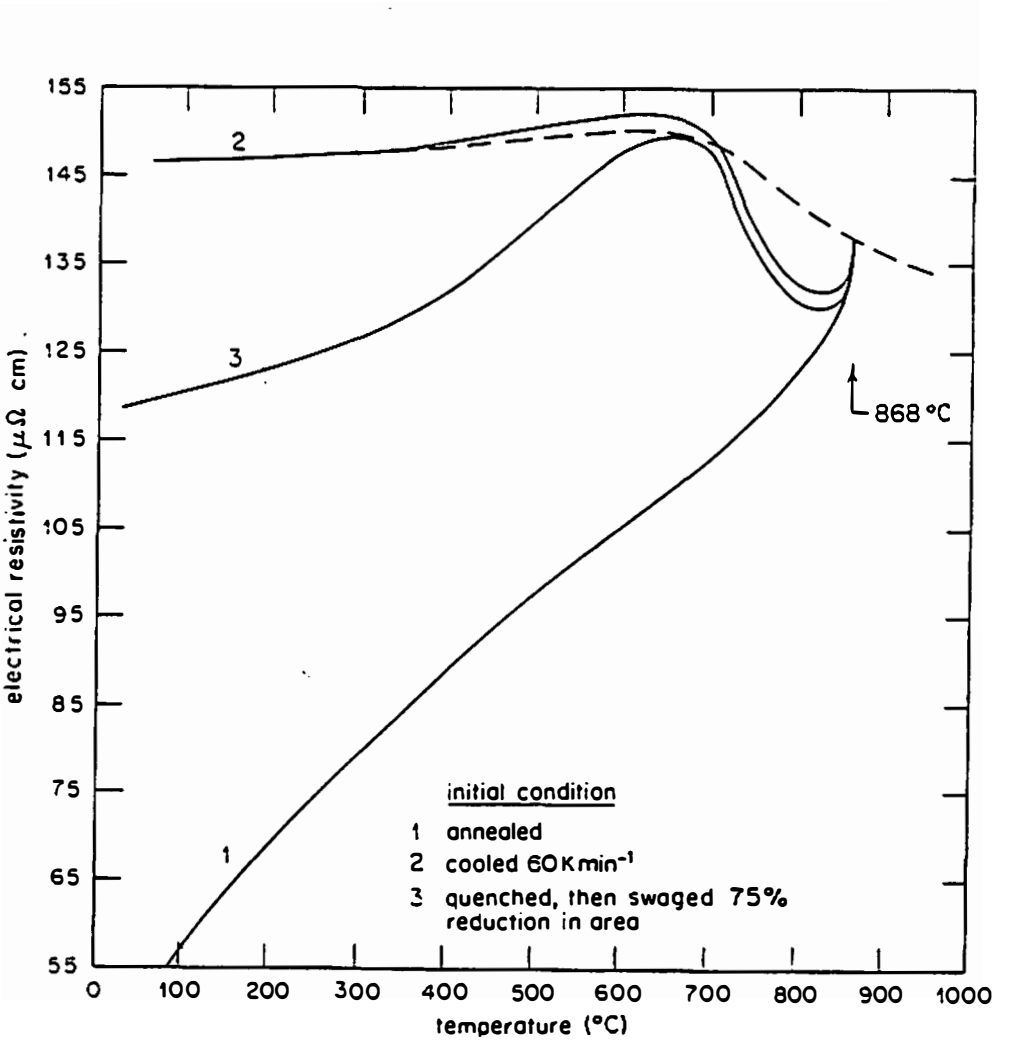


Figure 2.5 Electrical resistivity versus temperature relationships for $Ni_4Mo$ for three initial conditions - annealed, cooled at 60 K $min^{-1}$, quenched from 950 °C and swaged 75% reduction in area. The dashed curve represents data taken during cooling from above the transformation temperature [26].

SRO to LRO ($\alpha \rightarrow \beta$). The curve shown is for a heating rate of 10 K/min.

Curve 3 represents the resistivity for an initial condition of SRO($\alpha$) swaged to 75% reduction in area at 25 °C. Upon cold working, there are two ways the structure is affected - 1) introduction of defects, e.g., dislocations, and 2) destruction of SRO($\alpha$) clusters. The decrease in SRO introduced by cold-working more than compensates for the increase in electrical resistivity due to the scattering of electrons from the defects. So, there is an overall decrease in electrical resistivity [19].

On heating from an initial state of cold-worked $\alpha$, the electrical resistivity increases to 600 °C. The contributions to this increase come from the increasing thermal scattering of atoms and from a progressive return of SRO destroyed by cold-working. At the recrystallization temperature, there will be a contribution from the removal of defects, to decrease the electrical resistivity. There is also the possibility of the formation of new SRO in the recrystallized grains, if it is kinetically favorable. If new SRO forms it will contribute to an increase in the electrical resistivity. If the process of recrystallization is distributed over a considerable period of time (and hence over a large temperature span) then it might not have an observable effect in the electrical resistivity versus temperature curve. It is believed that in the curve being discussed, the effect of recrystallization has been 'masked' by the other effects.

Beyond 600 °C the curve comes down with increase in temperature because the α—›β transformation starts and dominates the change in resistivity in this region. The electrical resistivity during rapid cooling from above 868 °C (1141 K) follows the dashed curve. The cooling rate was 60 K/min. The curve goes through a maximum, similar to the curves on heating.

## SPECIFIC HEAT OF $Ni_4Mo$

The specific heat data for $Ni_4Mo$ have not been well established yet. The only known data was determined by Norem [36], who around 1965, used the adiabatic calorimeter that he designed for this purpose. He determined the specific heat for two initial conditions - 1) slowly cooled, LRO(β) and 2) quenched, SRO(α). The data is presented in Figure 2.6.

The specimen slowly cooled from the α region, has an all β structure. The data presented in Figure 2.6 is for the LRO(β) condition and has been obtained upon heating at about 20 °C/min. It is observed that as the transformation temperature is approached there is a sharp increase in the slope of the Cp curve. This is associated with the decrease of the degree of LRO as the transformation temperature is approached.

The other curve is for an initial condition of all α, which was attained by quenching from 1000 °C. This curve is more complex in nature and indicates two heat effects associated with the two minima

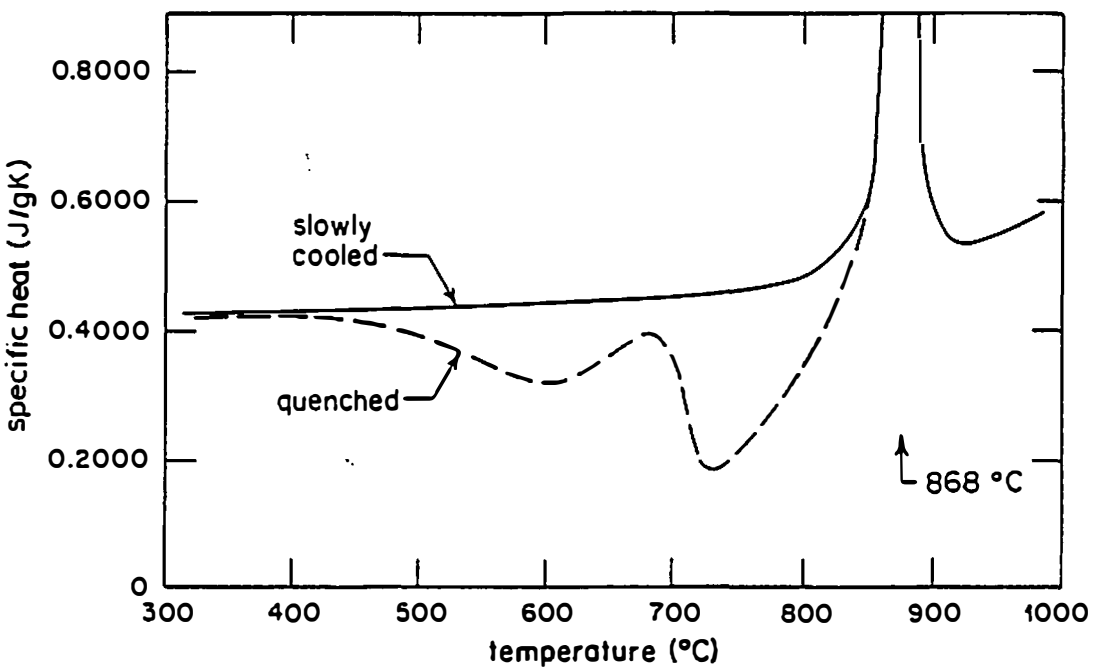


Figure 2.6 Specific heat of Ni4Mo for the initial conditions - slowly cooled, quenched from 950 °C [36]

in the curve. It is believed [19] that the first minima is associated with the intensification of SRO over that of the quenched structure and the second minima is associated with the $\alpha \rightarrow \beta$ transformation both of which release energy. Then the curve rises very sharply as it approaches Tc, as the degree of LRO in $\beta$ decreases. Above Tc, the curve comes down sharply and then rises more gradually with the increase in temperature.

# CHAPTER III
# EXPERIMENTAL PROCEDURE

## SPECIMENS

The main goal of this research was to determine the electrical resistivity and specific heat of $Ni_4Mo$ (Ni-20 at%Mo) for three initial conditions - 1) cold-worked SRO(α) state, 2) SRO(α) state and 3) LRO(β) state. Proper steps were followed to achieve these initial conditions.

1) To obtain cold-worked SRO(α) initial state, the specimen was quenched from 950 °C (1223 K) to room temperature and swaged.

2) To obtain SRO(α) initial state, the specimen was naturally cooled (1 K/sec.) from 950 °C, inside the calorimeter. SRO(α) was retained upon cooling to room temperature.

3) To obtain LRO(β) initial state, the specimen was held at 750 °C (1023 K) for 20 min. and naturally cooled (1 K/sec.) to room temperature.

From these three initial conditions the specimen was pulse-heated from room temperature to a high temperature, e.g., 1500 K. The raw data acquired was processed to determine the electrical resistivity and specific heat.

In addition to the main goal, which was the measurement on $Ni_4Mo$, tests were conducted on pure nickel, four Fe-Al specimens of

different composition and one Ni-Al specimen. Altogether seven specimens, each of a different alloy, were tested. All specimens tested, prepared and/or used in the calorimetry lab were given a code which the author named as CLC (Calorimetry Laboratory Code). This coding replaced an older coding system and facilitates identification of the specimens in the laboratory and the identification of the data file-names pertaining to each specimen. The CLC is a three letter code which is unique to each specimen prepared or used in the laboratory. The seven specimens tested in the calorimetry laboratory as a part of the Ph.D. project are tabulated in Table 3.1.

The second column shows the CLC for the specimen. The third column shows any other codes that the specimen or its stock might have had prior to ascribing the CLC. Some of the specimens have been acquired from external sources, e.g., national laboratory, private companies, and they had their own coding which is also tabulated. Column 4 shows the composition of the alloy and for the pure nickel it shows the level of impurity elements. The next column tabulates the chemical formula of the specimen material, based on the phase diagram. Column 6 shows the phase transformations, if any, for these alloys in the working temperature range. For most specimens the working temperature is 300 K to 1300 K. For some alloys, the transformation temperature was determined in the current investigation.

Table 3.1 Codes, chemical composition and chemical formula of the seven specimens tested in this project.

| No. | CLC | Other Codes | Chemical Composition | Chemical Formula | Transformations* |
|---|---|---|---|---|---|
| 1 | NIC | UTK#1 | Ni, Fe-40ppm, C-70ppm, Co-30ppm, SiC-150ppm | Ni | Magnetic |
| 2 | FAT | #23 | Fe - 8.5wt% Al | $\alpha$ | Magnetic |
| 3 | FAS | FAS-II | Fe - 16wt% Al | Fe(3)Al | DO3 -> B2 |
| 4 | FAE | #28 | Fe - 18wt% Al | Fe(3)Al | DO3 -> B2 |
| 5 | FAC | FA385M1 | Fe, 21.2 wt% Al, 0.42wt% Mo, 0.1wt% Zr, 0.03wt% C, 0.0025wt% B | FeAl | - |
| 6 | TWM | #20M | Ni - 8wt% Al | (Ni) + $\alpha'$ | - |
| 7 | NMQ | - | Ni, 29.51 wt% Mo, <0.01 wt% Al, 0.003 wt% O | Ni(4)Mo | LRO($\beta$) -> SRO($\alpha$) |

* Indicates tranformations, if any, in the working temperature range.

## SPECIMEN PREPARATION

### NICKEL

The nickel specimen used in this research was prepared from the stock used by Kollie [8] from which he prepared a specimen that he used for his Ph.D. thesis around 1969.

After an earlier specimen (UTKA#1) was found to have voids in its cross-section, a small piece from Kollie's stock was cut out, mounted, polished and examined under the optical microscope. After it was observed that the cross-section was free of voids and defects, a part of Kollie's stock was cut into three pieces. Piece 1 was 12 in. long and was used as the calorimeter specimen. Piece 2 was 3 in. long and was intended to be used in the resistivity apparatus. This specimen was given to the machine shop for cutting the ends perpendicular to the longitudinal axis. It got stuck in the jig and was destroyed. Piece 3 was about 1 in. long and was used for metallography. Piece 1, coded as NIC, was used as the pulse-calorimeter specimen. The main aim was to determine the electrical resistivity and specific heat of nickel and compare the values with those determined by earlier investigators. Thus the accuracy of the apparatus was established.

### FeAl AND NiAl ALLOYS

One of the four FeAl specimens used for calorimetric measurements was acquired from the Metals and Ceramics Division

of Oak Ridge National Laboratory [7]. The CLC of the specimen is FAC and the code given at ORNL is FA-385M1. The specimen was extruded at a 3:1 ratio at 1000°C and then at the same ratio at 900 °C. The specimen was originally 2 in. long and had a double clad of steel, as received at the Calorimetry Laboratory. The diameter, with the clad, was about 0.4 in. The clad was removed by cutting and machining. Thereafter the specimen was ground down to about 3 mm in diameter. Ten diameter readings were taken along the length of the specimen at roughly uniform separation. The values of the ten readings are tabulated in Table 3.2. The average of the six central readings was 0.1171 in. (0.2974 cm). This value was used in calculations because this is the region between the voltage taps, which forms the effective specimen.

The three other FeAl specimens and the NiAl specimen which were used in this project were acquired from 21st Century Environmental Systems [40] and were developed at the Oak Ridge National Laboratory [7].

$Ni_4Mo$

The $Ni_4Mo$ (CLC code NMQ) specimen was processed from a forged rod. Forging was discontinued at a certain point due to the formation of surface cracks. A cylindrical portion was machined out of this rod, which was about 6 in. (15 cm.) in length and 0.618 in. (1.56 cm.) in diameter. Thereafter, the specimen was annealed and swaged alternately till it was swaged down to 0.143 in. (0.363 cm.)

Table 3.2 Ten readings for the measured diameter, in the axial direction and the average value, for three specimens, Ni (pure), $Ni_4Mo$ and FeAl.

| Diameter Reading # | Ni (pure) | Ni4Mo | FeAl |
|---|---|---|---|
| | (inch) | (inch) | (inch) |
| | | | |
| 1 | 0.0702 | 0.0700 | 0.1176 |
| 2 | 0.0703 | 0.0700 | 0.1170 |
| 3 | 0.0702 | 0.0701 | 0.0069 |
| 4 | 0.0702 | 0.0700 | 0.1170 |
| 5 | 0.0699 | 0.0701 | 0.1171 |
| 6 | 0.0698 | 0.0701 | 0.1173 |
| 7 | 0.0699 | 0.0700 | 0.1172 |
| 8 | 0.0698 | 0.0700 | 0.1170 |
| 9 | 0.0697 | 0.0701 | 0.1162 |
| 10 | 0.0699 | 0.0700 | 0.1168 |
| | | | |
| Average = | 0.0699 | 0.0701* | 0.1171* |

* Average of six central readings.

An annealing furnace was set at 950 °C. This furnace was a cylindrical furnace which had facility for purging with argon. The furnace was purged for 1/2 hour and the specimen was introduced. The specimen rested on a piece of ceramic. Argon was continuously blown into the furnace. The specimen was annealed for one hour in the furnace at 950 °C, thereafter it was taken out and quenched in water. The as-quenched state consists of SRO($\alpha$) in the microstructure. This is the disordered state and is less brittle than the $\beta$-phase. Hence, it is easier to cold-work the specimen in this state.

For swaging, a set of 13 dies were used. The first die used had a diameter of 0.562 in. The specimen was swaged through this die and in the process was work-hardened. Hence, it had to be heated again, in the $\alpha$ range to relieve the stress. The measured diameter after the first stage of swaging was 0.571 in. It was heated again at 950 °C in argon for one hour and water quenched. Then it was swaged with a die size of 0.500 in. The alternate annealing and swaging continued till the specimen swaged down to 0.123 in. in diameter. The swaging schedule is given in Table 3.3. After the fifth stage of swaging the specimen became long enough to cause a practical problem during water-quenching. So, it was cut into two pieces and only one of the two pieces was worked with. In the last step, the specimen was swaged down from 0.143 in. to 0.123 in., and hence a percentage reduction in diameter due to swaging, of 14% was obtained. At this stage some cracks were observed, both on the

Table 3.3 Swaging and annealing schedule for $Ni_4Mo$ specimen.

| Step # | Procedure | Comments |
|---|---|---|
| | | |
| 1 | Purge furnace with argon | temperature = 950 °C |
| 2 | Anneal specimen for 1 hour | temperature = 950 °C |
| 3 | Quench in water | alpha phase retained |
| 4 | Swage specimen | Die size = 0.562 in. |
| 5 | Anneal specimen for 1 hour | temperature = 950 °C |
| 6 | Quench in water | alpha phase retained |
| 7 | Swage specimen | Die size = 0.500 in. |
| 8 | Anneal specimen for 1 hour | temperature = 950 °C |
| 9 | Quench in water | alpha phase retained |
| 10 | Swage specimen | Die size = 0.437 in. |
| 11 | Anneal specimen for 1 hour | temperature = 950 °C |
| 12 | Quench in water | alpha phase retained |
| 13 | Swage specimen | Die size = 0.406 in. |
| 14 | Anneal specimen for 1 hour | temperature = 950 °C |
| 15 | Quench in water | alpha phase retained |
| 16 | Swage specimen | Die size = 0.375 in. |
| 17 | Anneal specimen for 1 hour | temperature = 950 °C |
| 18 | Quench in water | alpha phase retained |
| 19 | Swage specimen | Die size = 0.312 in. |
| 20 | Anneal specimen for 1 hour | temperature = 950 °C |
| 21 | Quench in water | alpha phase retained |
| 22 | Swage specimen | Die size = 0.281 in. |
| 23 | Anneal specimen for 1 hour | temperature = 950 °C |
| 24 | Quench in water | alpha phase retained |
| 25 | Swage specimen | Die size = 0.218 in. |
| 26 | Anneal specimen for 1 hour | temperature = 950 °C |
| 27 | Quench in water | alpha phase retained |
| 28 | Swage specimen | Die size =0.187 in. |
| 29 | Anneal specimen for 1 hour | temperature = 950 °C |
| 30 | Quench in water | alpha phase retained |
| 31 | Swage specimen | Die size = 0.183 in. |
| 32 | Anneal specimen for 1 hour | temperature = 950 °C |
| 33 | Quench in water | alpha phase retained |
| 34 | Swage specimen | Die size = 0.163 in. |
| 35 | Anneal specimen for 1 hour | temperature = 950 °C |
| 36 | Quench in water | alpha phase retained |
| 37 | Swage specimen | Die size = 0.143 in. |
| 38 | Anneal specimen for 1 hour | temperature = 950 °C |
| 39 | Quench in water | alpha phase retained |
| 40 | Swage specimen | Die size = 0.123 in. |

surface of the specimen and at the cross-section. These cracks were running axially from one end of the specimen to roughly the middle of the specimen. When the cross-section was observed under the stereo optical microscope, the cracks appeared to be on the surface only. No sub-surface cracks could be observed.

After obtaining the specimen in a 14% swaged condition, it was sent to Wylie Precision Instruments [38] where it was centerlessly ground to a specific diameter. A calculation was made to check the required diameter to generate the same amount of heat generated by the nickel specimen, NIC. The calculation was based on the dimensions and the resistivity of the two materials. According to the calculation, a diameter of about 0.2 in. (0.5 cm) was required. A smaller diameter than this was also suitable. Wylie [38] was instructed to grind the specimen to about 0.07 in. (0.18 cm). The measured specimen diameter readings are presented in Table 3.2.

After grinding to a diameter of 0.07 in. (0.18 cm.) no cracks were observed on the surface or at the cross-section. Also, a small piece was cut from one end then mounted, polished and etched to observe under the microscope. The specimen was observed at magnification up to 400X. No cracks or flaws were found and the decision was made to use this specimen for current research.

## SPECIMEN SPECIFICATIONS

### NICKEL

The nickel specimen stock was purchased as electrolytically pure. A chemical analysis is shown in Table 3.1. The total contaminants present in the stock was less than 500 ppm. Analyses indicate that the nickel stock was at least 99.89% pure [9]. Piece 1 of the specimen UTK#1 was named NIC to make it consistent with the three letter CLC codes. This specimen was 11.602 in. (29.469 cm) long. Ten readings of the diameter were taken in the axial direction. They have been presented in Table 3.2. The average of the ten readings is 0.0699 in. (0.1775 cm). Also, five readings were taken along the circumference at three different positions along the length of the specimen to check for the uniformity in cross-section. The maximum difference from mean diameter in the circumferencial direction at the three points is 0.0001 in. ($2 \times 10^{-4}$ cm.), 0.0002 in. ($5 \times 10^{-4}$ cm.) and 0.0004 in. ($1 \times 10^{-3}$ cm.). The maximum percentage deviation from mean diameter is 0.5 %.

The specimen was weighed with a precision balance and was found to weigh 6.521 gm.

### FeAl AND NiAl ALLOYS

The FeAl specimen, FAC, was developed at ORNL [8] by Liu, Maziasz and Goodwin [39] under the sponsorship of the Advanced Industrial Materials Program, which is part of the Office of Industrial

Technologies, US DOE - Assistant Secretary for Energy Efficiency and Renewable Energy.

The specimen is 21.2 wt%Al with impurity elements and additions of Mo, Zr, C and B. The chemical composition is given in Table 3.1. The specimen was 2 in. long. Ten measurements of the diameter were taken which are presented in Table 3.2. The arithmetic average or mean of the six central readings for diameter is 0.1171 (0.2974). The maximum deviation from mean diameter is 0.0002 in. which is a percentage deviation of 0.17%.

The other FeAl specimens and the NiAl specimen were acquired from 21st Century Environmental Systems, Inc. [40]. The tests done on these specimens were proprietary work. Information on specimen preparation, chemical composition and details on specimen dimensions will not be provided.

$Ni_4Mo$

The specimen is coded as NMQ and contains Ni-29.51 wt%Mo. The impurity elements are given in Table 3.1. The thesis goal consisted of measuring on $Ni_4Mo$ for three initial conditions - 1) SRO($\alpha$), 2) LRO($\beta$) and 3) cold-worked SRO($\alpha$). The swaging of the specimen served a dual purpose - it reduced the diameter of the specimen and in the last step also induced a certain degree of cold-work.

The penultimate step consisted of heating the specimen in the tube furnace at 950 °C for one hour in an atmosphere of argon and

then rapidly quenching it in water. The as-quenched state consisted of SRO(α) in the microstructure. The swaging of the specimen in the last step resulted in a cold-worked SRO(α) microstructure. Due to the practical difficulties involved in swaging a specimen from an initial diameter of 0.618 in. to a final diameter of around 0.070 in. in several steps, only one specimen was prepared. Since, cold-work is an irreversible process, there was, virtually, only one chance to heat the specimen to a high temperature, e.g., 1300 K, in the pulse calorimeter and get the data as a function of temperature into the α range because the heat from the first run will anneal out the cold work. A calculation was made, based on the electrical resistivity of the specimen, to estimate the pulse time to render the specimen into the α range without going near the solidus temperature. A run was made with this estimated pulse time and the raw data for cold-worked $Ni_4Mo$, SRO(α), was recorded. Later, electrical resistivity and specific heat data were computed from the raw data. These data are presented in Chapter IV.

To obtain the data for SRO(α), several runs were made from room temperature to a high temperature, e.g. 1300 K, and the specimen naturally cooled (1 K/sec) to room temperature. When the effect of cold-work was no longer observed in the power-temperature data, the specimen was pulsed into the α range once again and this run was used to determine electrical resistivity and specific heat of the specimen for the SRO(α) initial state. It is pointed out here that the indication that the cold-work is there in the

specimen is the two dips in the power-temperature curve, pertaining to recovery and recrystallization (see Chapter IV).

To obtain the LRO(β) initial state, the specimen was held isothermally at 950 °C for 10 min., cooled down to 750 °C and held at this temperature for 20 min. The α —› β transformation was almost complete as most of the decrease in resistivity was over. After the specimen was cooled to room temperature, the microstructure was LRO(β) (predominantly).

The $Ni_4Mo$ specimen, NMQ, was about 8 in. (~20 cm) in length. Ten readings of the diameter were taken in the central ground region, which are presented in Table 3.1. The maximum deviation from mean diameter is 0.0001 in. which is a percentage deviation of 0.14%. The average of six central readings was used in the calculations. This average is 0.7000 in. (0.1778 cm). Five readings of the diameter were taken along the circumference at two locations along the length of the specimen. The maximum circumferencial deviation from the mean is 0.0001 in. for both locations.

## DESIGN AND USE OF THE KNIFE-EDGE APPARATUS

The knife-edge apparatus was designed to serve a dual-purpose. The knife-edge technique is an electrical technique to measure the separation between the voltage taps. Voltage taps used in this research are 0.01 in. (0.02 cm) nickel wires. In previous work

(M.S. thesis), a pair of vernier calipers were used to measure the separation between the voltage taps. It is a practical problem to determine whether to take the center or the side of the tap wires as the point of contact. This problem can be circumvented by measuring the distance with an electrical method - the knife-edge technique, which is a more accurate technique.

The second use of the knife-edge apparatus is the measurement of electrical resistivity of specimens independent of the pulse-heating calorimeter. This helps in determining the electrical resistivity at room temperature for comparing with the data determined by the pulse calorimeter.

## KNIFE-EDGES

Knife-edges are two sharp metal pieces glued to the cut ends of a quartz cylinder. The separation between the edge pieces was determined by using a traversing optical microscope. This microscope was calibrated using gauge blocks. These gauge blocks are metal blocks, the edge-to-edge distance of which has been determined to a high accuracy (+0.000004 in/in to - 0.000002 in/in).

In 1993, an evaluation was made of sets of knife-edges in the calorimetry laboratory. They are of different sizes and cater to different lengths of the specimen. Table 3.4 shows the results of the

Table 3.4 Type and spacing of the three knife-edges and results of the calibration performed in 1978 and 1993.

| Type of Knife Edge | Spacing (inch) March 1978 | Spacing (inch) February 1993 |
|---|---|---|
| Small | 0.1515 in. for two tests | 0.1514 to 0.1516 in. in six tests |
| Medium | 1.0015 in. for two tests | 1.0050 to 1.0060 in. in six tests |
| Large | - | 3.0324 to 3.0335 in. in six tests |

specimen calibration done in 1993, and compares them with those done in 1978. (One of the edges of the large knife-edge got detached in 1994 and was re-fixed. So, the 1978 and 1993 measurements have not been reported in Table 3.4, for the large knife-edge. Instead its current dimensions, as measured in 1994 have been reported.) A maximum difference of 0.0001 in. (0.07%) was observed for the small (0.1515 in. ) knife-edge and 0.0045 in. (0.45%) in the medium (1.0015 in.) knife-edge. The calibrated values of 1993 were used in the calculations for electrical resistivity and voltage tap separation.

## KNIFE-EDGE HOLDER ASSEMBLY

The proper contact of the two edges of knife-edge with the specimen is important. Hence a knife-edge apparatus was built to seat the knife-edge firmly with the specimen by a applying a heavy and consistent weight on the knife-edge to keep it in good contact with the specimen.

Two basic tests were performed on the knife-edge set-up to check for the stability of measurements. In one test, the knife-edge was moved from one location to another on the specimen, in the axial direction, and the measurements of the voltage drop across the taps recorded. The maximum variation in the readings, from this test, was 0.3%. In another test, voltage drop measurements were taken with no load on top of the knife-edge and then measurements

repeated with a pressure-plate on the knife-edge, then with the pressure plate plus additional load. There were no difference in the recorded readings.

The holder-assembly consists of a base plate made out of metal and a V-notch on epoxy running through its center (refer to Figure 3.1). The cylindrical specimen rests in this groove. On top of the base is a pressure-plate which has a alignment block made out of epoxy fitted to its bottom. The semi-circular groove cut out in the alignment block holds the cylindrical quartz tube parallel to the specimen. Parallelism is an important requirement for the accurate measurement of the separation. The pressure-plate has been designed to give consistent and optimum pressure on the knife-edge and specimen. The pressure-plate can slide up or down through the guiding rods at each corner of the base-plate. The base-plate has two terminals at each end to supply current to the specimen.

A schematic diagram (Figure 3.2) of the specimen with the knife-edge shows the configuration and the different electrical connections coming out from the knife-edge and the specimen. The knife-edge contacts with the specimen only at two points, i.e., at the two edges. The electrical connections from the knife-edge go to the DVM to measure the voltage drop across the knife-edge. The voltage taps spot welded to the specimen are also fed to the DVM. Current leads are connected to both end of the specimen.

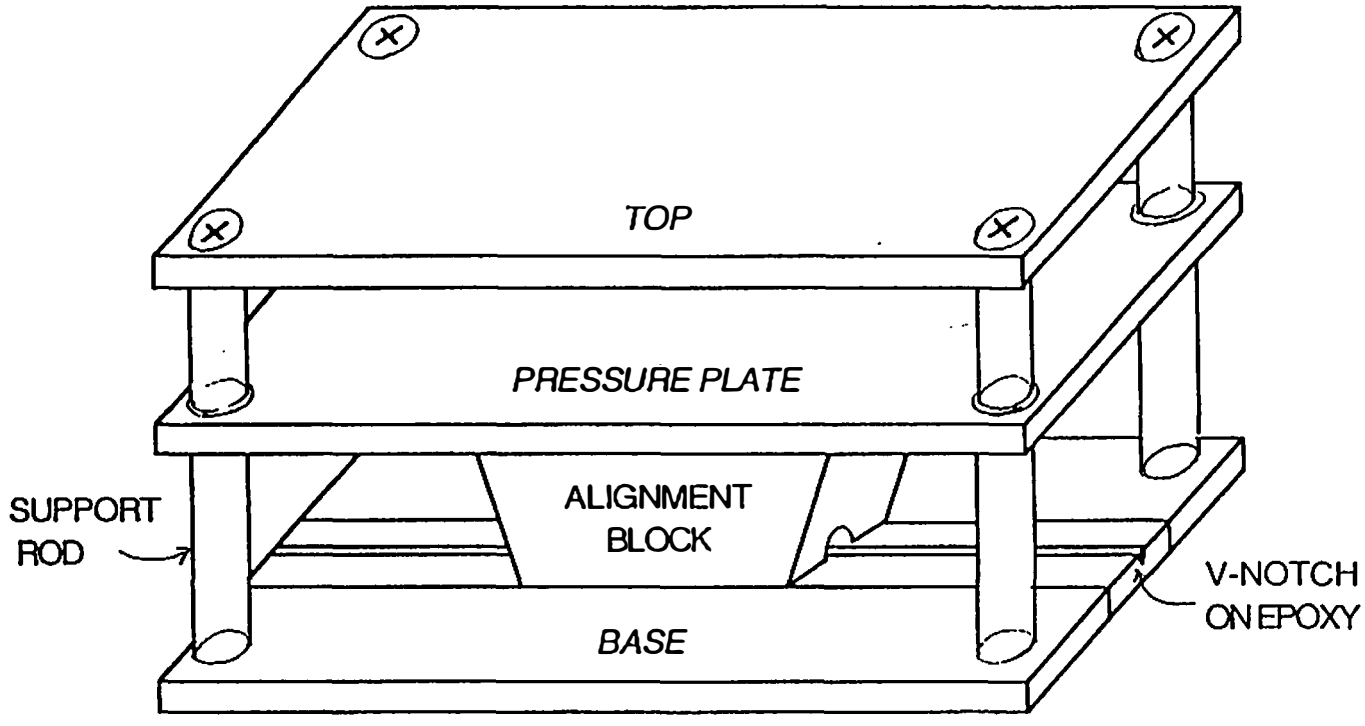


Figure 3.1 Schematic diagram of the knife-edge apparatus holder assembly.

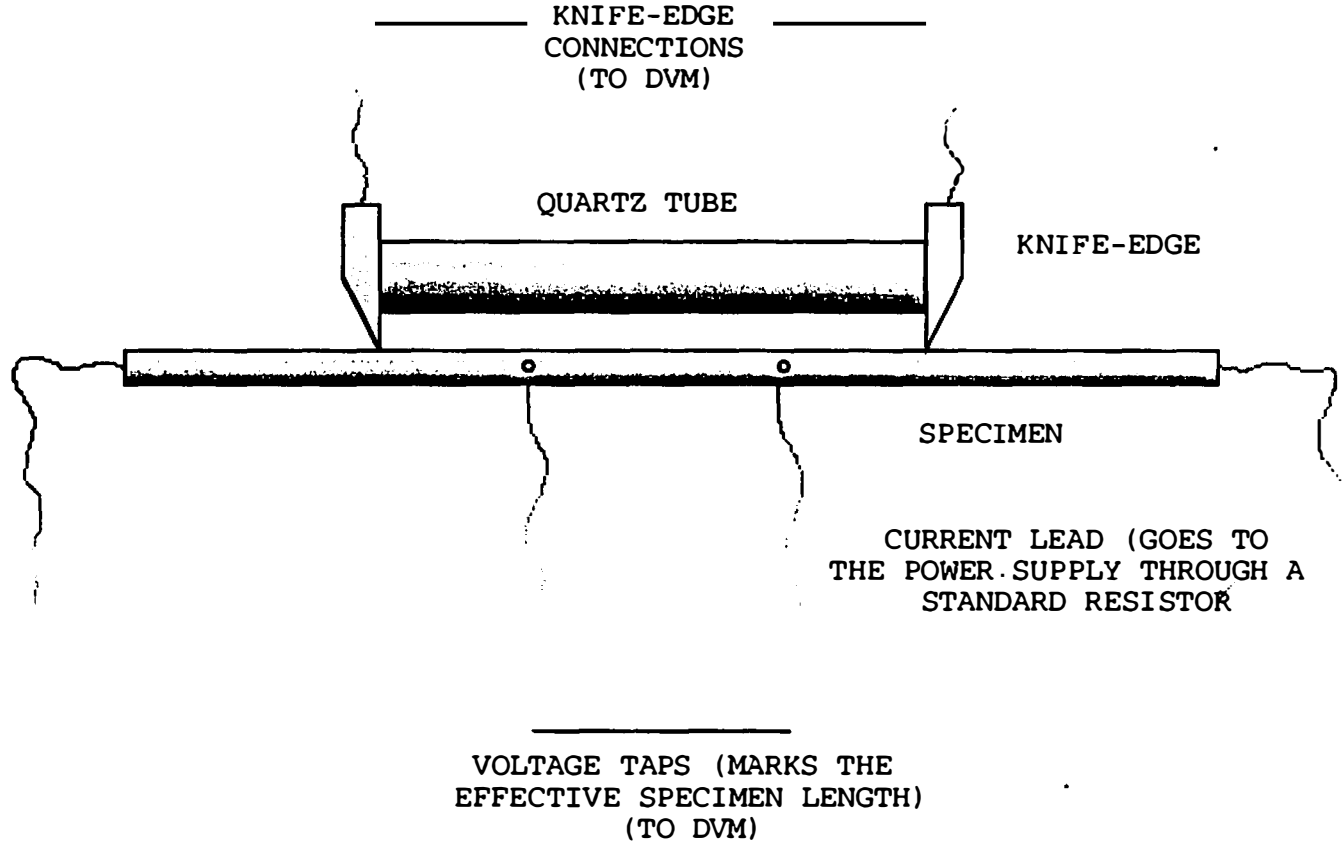


Figure 3.2 Schematic diagram of the specimen, the knife-edge and the basic electrical connections.

## ELECTRICAL CIRCUITRY

The knife-edge is used in conjunction with the resistivity apparatus which was designed to measure the electrical resistivity of the specimens at room temperature, independent of the pulse calorimeter. A schematic diagram of the electrical components and connections are shown in Figure 3.3. The knife-edge is not shown in this diagram but rests above the specimen, as shown in Figure 3.2.

The specimen is in series with a standard resistor, other resistors and the power supply. A small current, e.g., 0.1 A, is passed through the specimen. There is a switch for reversing the direction of current. A thermocouple read-out was available to indicate the temperature of the specimen. There is a rotary switch which connects the voltage taps, knife-edge leads and the standard resistor taps into a DVM. At least three voltage measurements are taken, each for voltage drop across tap, $E_T$, voltage drop across knife-edge, $E_K$, and the voltage drop across standard resistor, $E_{std}$. The measurements are repeated for current flowing in the opposite direction. The average values of $E_T$, $E_K$ and $E_{std}$, for both directions, are used in the final calculation. The values determined for $E_T$, $E_K$, and $E_{std}$ are used to determine the electrical resistivity of the specimen material and the voltage tap separation. The voltage tap separation is determined from the ratio of the voltage drop between the voltage taps and the knife-edges and the knowledge of the

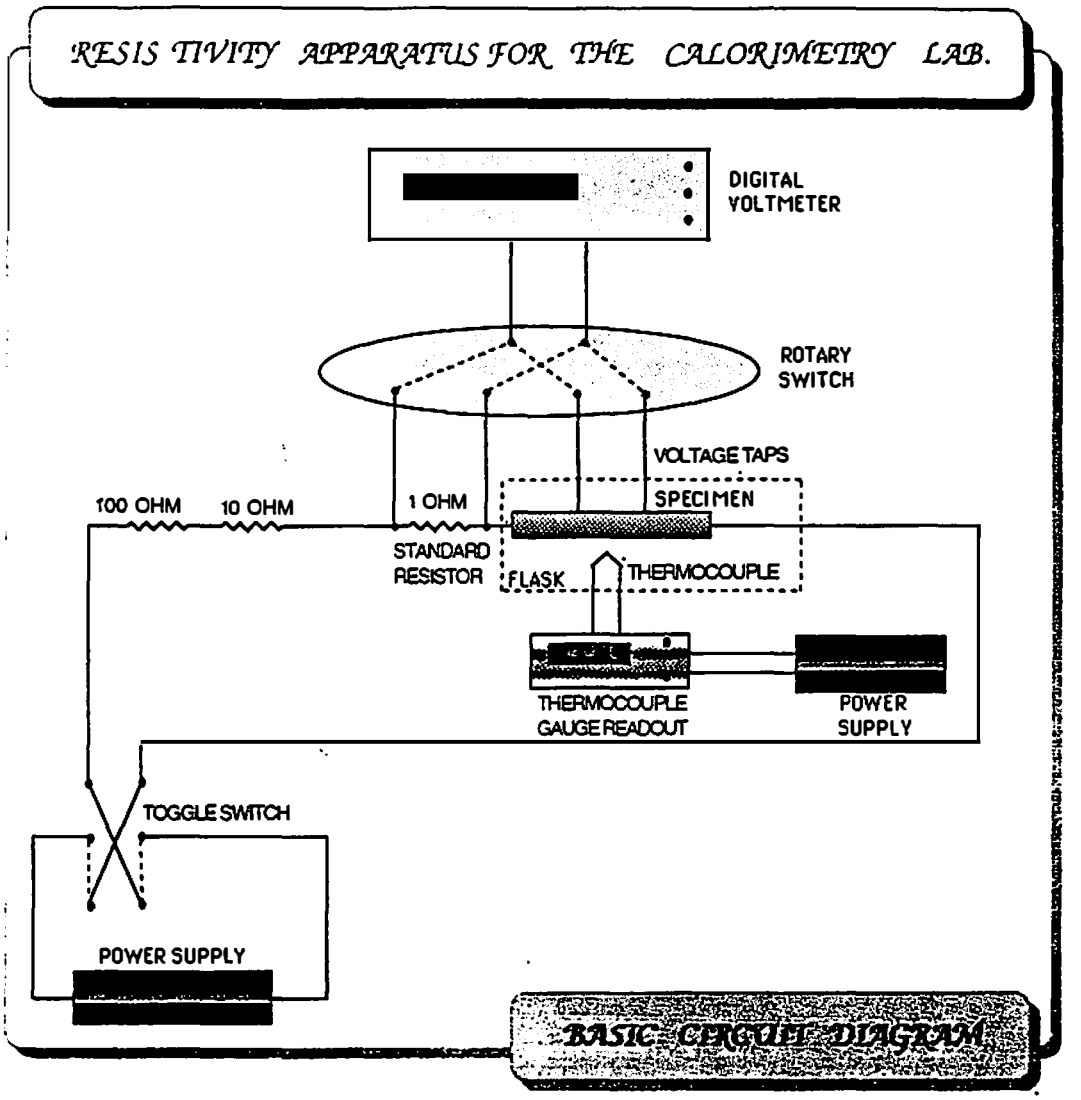


Figure 3.3 Schematic diagram of the electrical components of the resistivity apparatus.

knife-edge spacing. The electrical resistivity is determined from the knowledge of the specimen dimensions and the measured resistance.

Some sample calculations are shown below. They are for the specimen at room temperature in the LRO(β) state.

Specimen : $Ni_4Mo$

CLC# : NMQ

Average value of potential drops as measured by the DVM,

$E_T = 0.00264$ V

$E_K = 0.00526$ V

$E_{std} = 0.1357$ V

a) Determination of voltage tap spacing

$$d_T = \frac{E_T}{E_K} d_K$$

$d_K$ is the dimension of the large knife-edge, which was used with the specimen.

$d_K = 7.7198$ cm

$$d_T = \frac{0.00264}{0.00526} \times 7.7198$$

$= 3.8746$ cm

This is the voltage tap separation used in the electrical resistivity and specific heat calculations.

b) Determination of electrical resistivity

$$\rho = \frac{E_T}{I} \frac{\pi}{4} \frac{d^2}{l_T}$$

The current flowing through the standard resistor is determined from the value of its potential drop and its resistance. The current flowing through the specimen is the same as that through the standard resistor because they are in series.

The standard resistor was calibrated by the Building Materials Group at ORNL [7]. They used a knife-edge apparatus for this purpose. The resistance of the standard resistor as calibrated in February 1993 was 0.999938 Ω. A calibration done in November 1968 indicated a value of 0.99995 Ω. This is a change of 0.000011 Ω or a percentage change of 0.00115%.

Thus, $R_{std} = 0.999938\ \Omega$.

$$I_{std} = \frac{E_{std}}{R_{std}} = \frac{0.1357}{0.999938} = 0.1357\ A$$

$d = 0.17792$ cm

$l_T = 7.7198$ cm

$$\rho_{Ni_4Mo} = \frac{0.00265}{0.1357} \frac{\pi}{4} \frac{0.17792^2}{7.7198}$$

$$= 62.8\ \mu\Omega\text{–cm}$$

# ANALYSIS OF DIFFERENT THERMOCOUPLE CONFIGURATIONS

Three different thermocouple configurations were tested : 1) one lead on top of the other, 2) intrinsic type and 3) the beaded type. The primary objective of this analysis was to see which thermocouple configuration was most suitable for the type of experiments being conducted.

## ONE LEAD WELDED ON TOP OF THE OTHER

This is the first configuration that was tried. In this configuration, one thermocouple lead is spot welded on the specimen. Then the second lead is welded on top of the first lead. The exaggerated version is shown in Figure 3.4 (a). The contact point of the two leads is shown somewhat removed from the contact point of the first lead and the specimen. It has been shown in this way to illustrate the point that in this configuration the thermocouple junction could be a finite distance away from the specimen. This will result in a thermal lag, especially in a high heating rate experiment.

Experiments show that, with this configuration, the higher the heating rate, the more the measured temperature varied from the true temperature. Kollie's [8] data on electrical resistivity of nickel was used as the basis for the comparison. There are two important observations. 1) Author's data, with this thermocouple

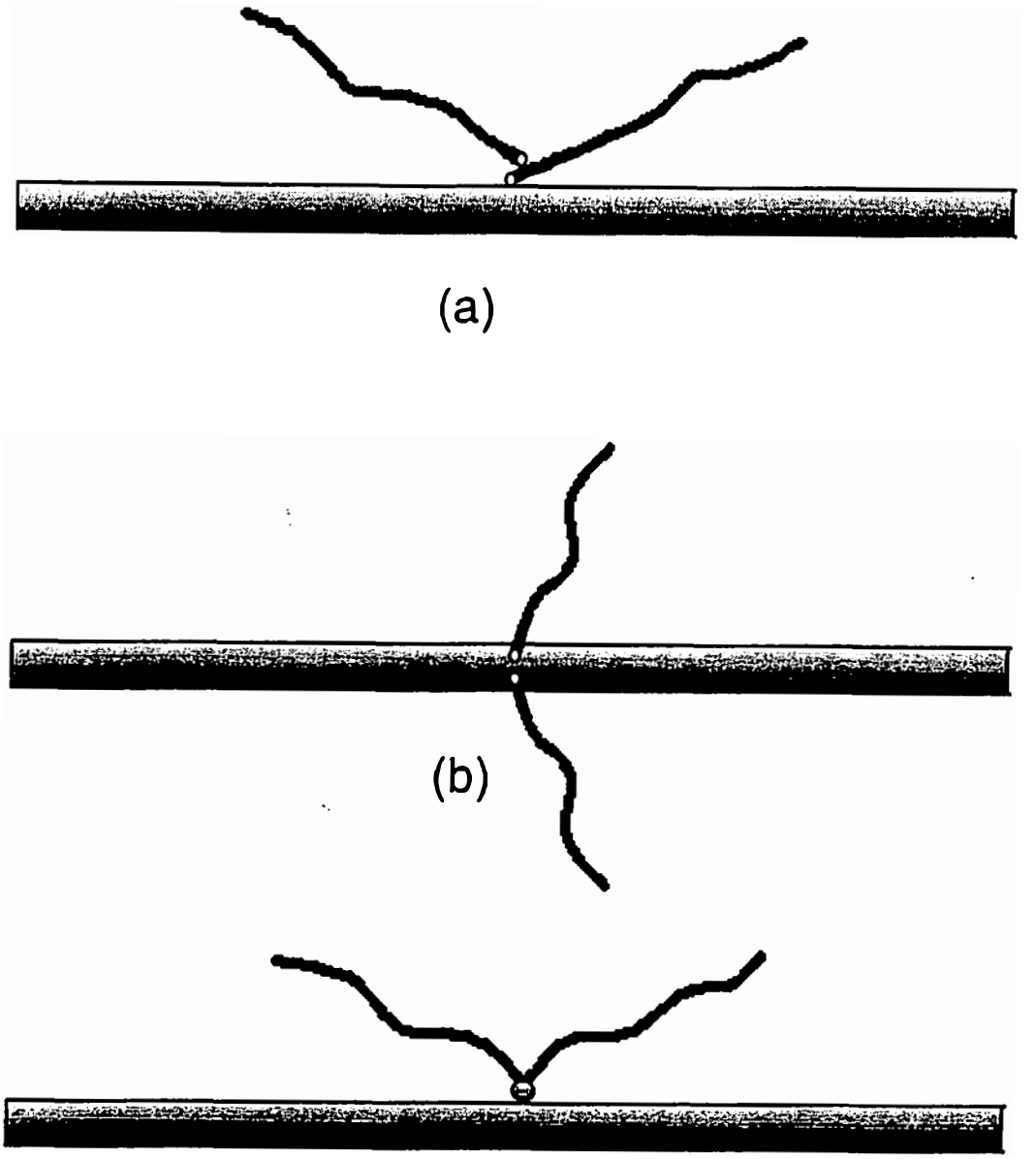


Figure 3.4 Schematic representation of the three thermocouple configurations used or tested with the pulse-heating specimen, a) one lead on top of the other, b) intrinsic type, and c) beaded type.

configuration, was shifted to the left of Kollie's data. Thus, for a given value of electrical resistivity, the corresponding temperature value with this configuration is less than that of Kollie's. This indicates that the junction of the thermocouple leads are somewhat removed from the surface of the specimen, so it requires a longer response time to reach the 'true' temperature. 2) Upon reversal of the direction of current, there is no change in the electrical resistivity curve. This means that there is no pick-up due to misalignment of the thermocouple leads on the surface of the specimen. This observation supports the fact that the junction of the thermocouple leads are away from the specimen.

It has been concluded that this configuration should be avoided with pulse experiments with high current, e.g., 80 A, flowing through the specimen. It can be used with isothermal tests where a higher response time is not detrimental to the criticality of the experiment. In general, it should be used with caution in any continuous heating processes.

## INTRINSIC TYPE

The next configuration that was tested was the intrinsic type where the two leads are welded with a lateral alignment with a small separation (Figure 3.4(b)). This configuration has been used by earlier investigators and in the current research. The first lead is welded on the surface of the specimen. The second lead is carefully

welded, preferably under the microscope, to be in lateral alignment with the first lead.

The main problem with this configuration is that even with very careful welding, there will almost always be a misalignment. Due to the lateral misalignment of the wires, there will be a voltage pick-up arising from the part of the specimen between the thermocouple leads. On reversing the direction of current, the pick-up will reverse in sign and the electrical resistivity versus temperature curve will shift to the other side. Figure 3.5 illustrates this point. Author's data from two separate runs have been superimposed, each with current flowing in opposite directions. If Kollie's [8] data is taken to be the 'true' value of electrical resistivity, then the curve is observed to shift to the left or right of the 'true' value depending on the direction of the current. If arithmetic averages of the two curves are taken at each value of electrical resistivity, then a curve with the average values can be plotted. If the deviation is large, there is a chance that the average value will not be equal to the true value. However, for practical purposes, the average of the electrical resistivity, with current flowing in either direction, will give values very close to the values without pick-up. The main advantage of this configuration is that there is no thermal lag because the hot junction is on the surface of the specimen.

This configuration maybe suitable for high heating rate temperature measurements where other configurations (Figure 3.6)

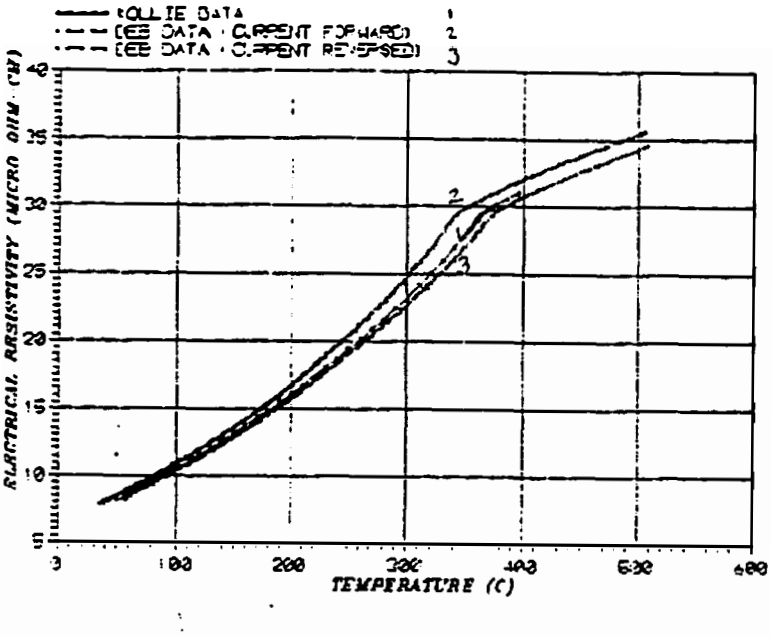


Figure 3.5 Electrical resistivity data of Kollie [8] and that from current research to illustrate the reversal in the sign of the pick-up with the change in the direction of the current, for intrinsic type thermocouples.

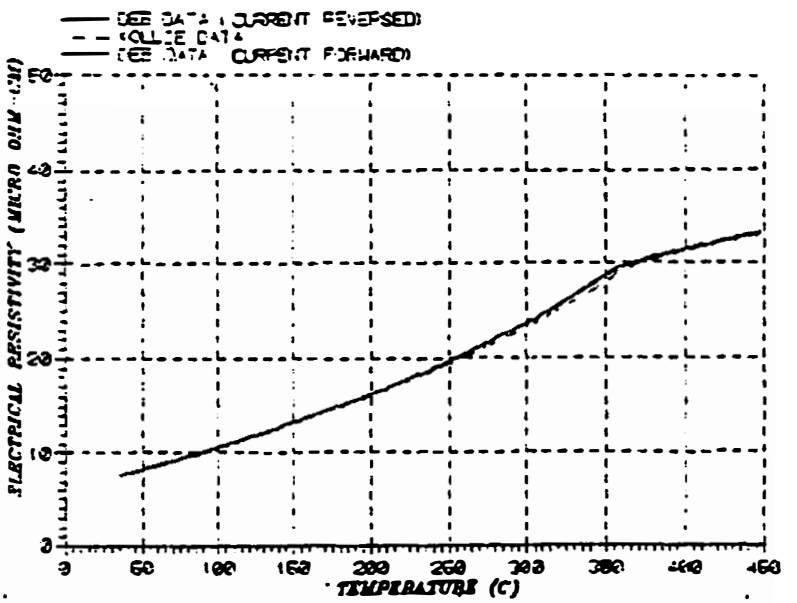


Figure 3.6 Electrical resistivity data of Kollie [8] and that from current research, for current flowing in either direction, illustrating the advantage and disadvantage of beaded type configuration.

prove disadvantageous. However, this configuration has been found to be unsuitable for several cases:

Case I : For specimens with irreversible initial condition, e.g., cold-worked specimen where there is no scope for reversing the direction of current and making another run.

Case II : In use with temperature control programs, e.g., PID. It has been found in the current research, in a series of experiments, that even a small value of thermoelectric pick-up gets amplified in the control equations sufficiently, to generate an improper output to the programmable power supply which finally results in disturbed control.

Case III : For high current pulse calorimetry, Cezairliyan [41] reports that he finds intrinsic type thermocouples unsuitable for measuring the temperature of the specimen holders, because the high current, e.g., 1000 A, that he uses results in a high pick-up which causes a huge error in the measured temperature.

## BEADED TYPE

Finally, a third configuration was tried. The leads of the thermocouple are carefully twisted near one of the ends and held in oxy-acetylene flame for about 10 seconds. The wires locally melt to form a small bead. This bead is spot welded to the specimen. Only the bead is in contact with the specimen and the leads come out of the bead. Refer to Figure 3.4 (c) for this configuration. Figure 3.6

presents author's electrical resistivity data obtained using a beaded configuration along with Kollie's data. The two runs are for current flowing in opposite directions. There are two important observations. First, the voltage pick-up is negligible as can be concluded from the fact that the two curves for author's data fall right on top of each other. This virtually eliminates the need for making two runs and taking the average of the two values. The disadvantage of this method, however, is that for high heating rates some thermal lag is likely to be there. In Figure 3.6, there is a negligible thermal lag up to about 250 °C and above 360 °C. However, between 250 and 360 °C, the solid curve 'lags behind' the dashed curve, the average lag in this range being 5 °C. Thus, beaded method can result in thermal lag for high heating rates. However, it needs to be pointed out that the data being discussed were acquired with 80 amps flowing through the specimen, which results in a relatively high heating rates. Also, a relatively larger bead size was used for this comparison test. For future electrical resistivity experiments, 40 amps current and a smaller bead size (< 1 mm in diameter) was used, to minimize this lag.

This configuration should be used with caution too. 5 mil diameter or smaller thermocouple wires should be used so that the size of the bead will be small. A small value of current should be used, wherever possible. Only a small amount of metal should be melted, so that the bead is small. In the current research beaded

configuration has been used extensively and for certain situations been found to be more suitable than the other two configurations.

## MEASUREMENT OF ELECTRICAL RESISTIVITY

In the calorimetry laboratory, there are two different methods of measuring the electrical resistivity of materials. To obtain continuous heating data on electrical resistivity as functions of temperature and time, the pulse-heating calorimeter can be used. The data file generated by the acquisition program can be used and processed to get data on electrical resistivity versus temperature. The second method is to use the resistivity apparatus, which has been designed in the calorimetry lab as a part of this research. Both methods are described below.

### ELECTRICAL RESISTIVITY MEASUREMENTS FROM PULSE-HEATING RUNS

The pulse calorimeter, which was primarily designed to determine the specific heat of the specimen, can be used without any alteration, either in the system or in the computer programs, to determine the electrical resistivity as a function of temperature. The specimen is in series with a 0.01 Ω standard resistor and the programmable power supply (refer to Figure 1.1). Electrical

resistivity is determined from the knowledge of the electrical resistance and the dimensions of the specimen. The three signals that are acquired from the specimen are the voltage drop along the effective specimen, E, (the reader is reminded that the effective specimen is the specimen between the voltage taps), the current flowing through the specimen, I, and the thermal emf, $E_{emf}$. E and I signals are already acquired into the acquisition program and written to the raw data file, from which the power is computed. So, the raw data file can be used to compute electrical resistivity. For a cylindrical specimen of diameter, d, and length, l, the expression for electrical resistivity is as given below.

$$\rho = \frac{E}{I}\frac{\pi}{4}\frac{d^2}{l}$$

The resistance is calculated from the ratio of E and I. The constant is calculated from the diameter of the specimen and the length of the effective specimen. Their product is the electrical resistivity of the specimen material, which is a material property. The voltage, E, is acquired directly from the voltage tap. The current, I, is calculated by the computer from the acquired voltage drop across the standard resistor and the value of the resistance of the standard resistor. The dimensions of the specimen are measured at room temperature and then entered into the computer program code, before the run. No correction was made for the specimen thermal expansion.

For each set of data acquired by the computer, the computer utilizes the time lag between two data points to compute the

electrical resistivity in real time and print the data on the screen for electrical resistivity along with the acquired raw data. Next the acquired raw data file is opened with the processing program, MASTER, and the thermal emf data is transferred into the CONVERT program, which has the equations for conversion of thermal emf to temperature (°C). The converted temperature data (K) is returned to the MASTER and are saved as a semi-processed data file. At this point, the file has the electrical resistivity data and the corresponding temperature data, which can be conveniently plotted.

## ELECTRICAL RESISTIVITY MEASUREMENT USING THE RESISTIVITY APPARATUS

This apparatus have been described in the section titled "Design and use of the knife-edge apparatus'. The electrical circuit is schematically represented in Figure 3.3 Sample calculations are included in the section, too. The potential drops across the voltage taps and the standard resistor are measured by the DVM and noted down. Then in the equation for electrical resistivity, the voltage, current, specimen diameter and distance between voltage taps are substituted. A manual calculation for electrical resistivity is made. This apparatus has been used to measure electrical resistivity at room temperature only.

# DETERMINATION OF SPECIFIC HEAT

The technique used for the determination of specific heat of electrical conductors by pulse-heating technique has been discussed in detail in the author's M.S. thesis titled 'Design and Development of a Computerized High Temperature Pulse Calorimeter [12]. The reader is advised to read Chapter 5 of Part III. The thesis describes the general technique and the details of the computer programs that have been developed for this specific purpose, including complete source codes of such programs.

This technique is reviewed in this section and is explained with a simplified block diagram. Figure 3.7 is a simplified flowchart which shows the computing steps to process the raw data file to determine the values of the calculated specific heat.

The raw data file has data columns for time (TT#), thermal emf (mV) and power (watt). The raw data file is created by the acquisition program, CALPUL, and opened for processing by the MASTER program. The thermal emf data are transferred into another program developed by the author, called CONVERT. CONVERT has three sets of conversion equations for converting thermal emf (mV) to temperature (°C); each equation is valid for a particular temperature range. Next the temperature (°C) data is converted to temperature (K) data and transferred back to the MASTER program. The MASTER program, next, converts the time in TT# to time in seconds, from the knowledge of the time lag

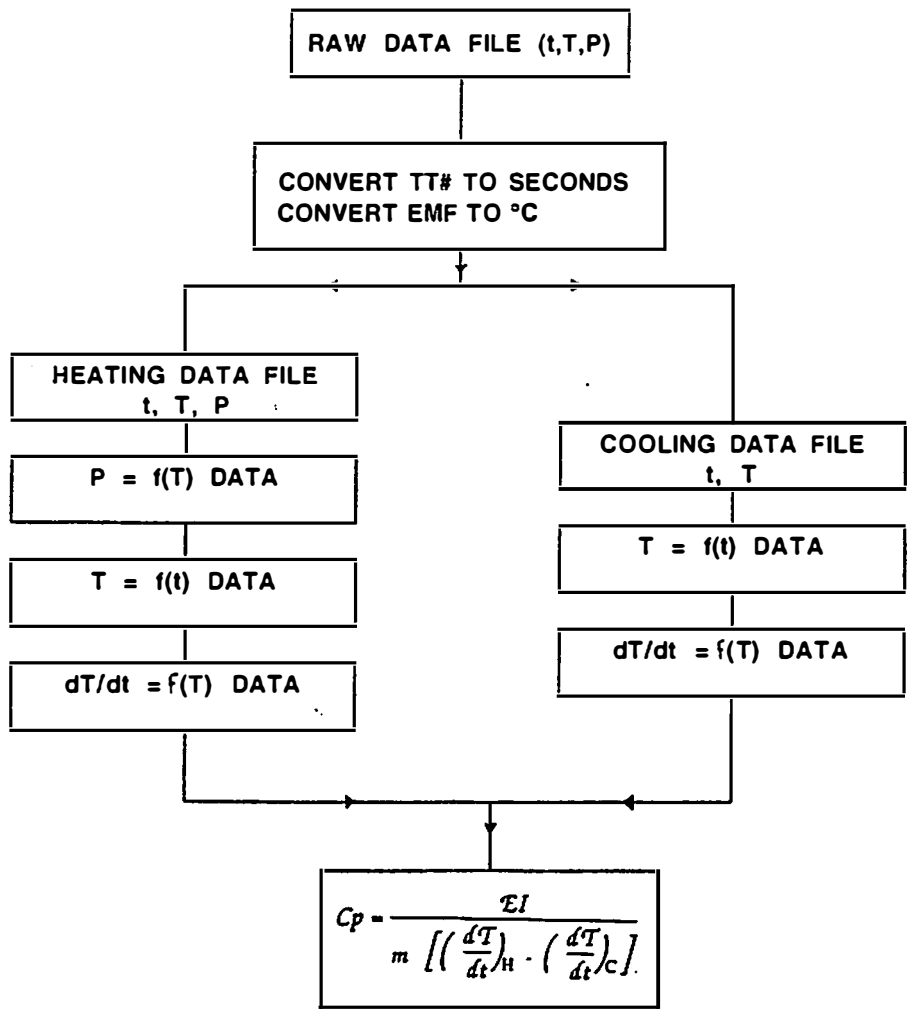


Figure 3.7 Simplified flow-chart of the computing steps for processing the raw data file to determine the specific heat.

between two subsequent data points. For determining the specific heat, several equations had to be curve-fitted and mathematically processed. To facilitate such fitting the data for heating and cooling are separated and saved in two different files. The cooling data are used to correct for the heat losses during heating. Refer to the section titled 'Electrical resistivity and specific heat determination in Part III, Chapter 1 of the author's M.S. thesis for more details on this technique. The 'heat' file is first accessed and opened and with the help of a commercial curve fitting program the power data is fitted versus temperature data with a polynomial of the form, $P = a+bT+cT^2+dT^3+\ldots\ldots$ . The coefficients of this function are stored in this program to be accessed later. Next, the temperature is fitted versus time and the fitting equations generated. The fitting equation, $T = f(t)_H$ is differentiated once with respect to time, t, and an equation for $dT/dt = f(t)_H$ is generated. For every value of t, a value for dT/dt is computed. Next, the dT/dt values are fitted versus temperature, T, and an equation for $dT/dt = f(T)_H$ is generated and the coefficients are stored in the program. Next the 'cool' file is accessed and a similar procedure is adopted to fit $T = f(t)_C$ and finally $dT/dt = f(T)_C$. The coefficients are stored in the program. As the last step, the temperature at which specific heat is to be determined is asked for, to the user, who inputs the desired temperature. From $P = f(t)_H$, $dT/dt = f(T)_H$ and $dT/dt = f(T)_C$ coefficients, the power and the slopes are calculated and substituted in the specific heat equation, as shown overleaf.

$$Cp = \frac{EI}{m[(\frac{dT}{dt})_H - (\frac{dT}{dt})_C]}$$

The mass is calculated from the knowledge of the volume of the effective specimen and the density of the specimen material. Part III, Chapter 5 of the author's M.S. thesis [12] has a detailed description on how each of these quantities are determined. The value of the mass is entered into the program code in advance. The program calculates the specific heat for each entered value of temperature. A new file is created, which contains the specific heat versus temperature data. These data can be plotted or tabulated conveniently, using this file. Refer to the section titled 'Calculations' in Part III, Chapter 5 of the author's M.S. thesis for the details of the fitting process.

## ISOTHERMAL TESTS

One of the secondary goals of this research was to develop a computer program to hold the temperature of the specimen inside the calorimeter at a constant value and noting the change in electrical resistivity and power of the specimen as functions of time. It received a boost when one of the groups at ORNL [7] wanted to do some isothermal tests on their alloy to study its recrystallization kinetics.

A proportional-integral-derivative (PID) program was written. In essence, it consists of equations which compare the set-point temperature with the measured temperature as acquired from the thermocouple, and calculates an error value at any time. The error value is used to determine the level of current for the next loop to eliminate the error and maintain the temperature at the set-point. The P, I and D parameters need to be tuned before the program can be used effectively to control the temperature. A trial-and-error procedure was used and a series of runs were made on dummy specimens to study the effects of P, I, D constants on the temperature control. These constants depend on specimen dimensions, isothermal temperature, current level, etc. The 'best' set of constants, as determined from this study, was entered into the PID program.

The PID program was used with tuned constants on several steel specimens. Due to the proprietary nature of the work, the details of the specimen and the testing cannot be discussed, however, an example of the results is presented in Chapter IV.

The PID program was also used with the $Ni_4Mo$ specimen. One advantage of the system set-up is that the experimental arrangement is the same for both continuous heating and isothermal heating, only different computer programs are activated for the two heating modes. Isothermal tests were conducted on $Ni_4Mo$ at different temperatures. For this, the isothermal program, CALISO, is activated and the control temperature is entered. The program has

the capability to hold the temperature constant for two different set-points for two different steps. For example, in an isothermal run with $Ni_4Mo$ specimen, in step I, the temperature was held constant at 950 °C for 10 min. to form all $\alpha$ in the microstructure and then naturally cooled to 750 °C, in step II, and held for 20 min. to isothermally transform $\alpha$ to $\beta$. This served a two-fold purpose - 1) studying the isothermal kinetics of this alloy by studying the change in electrical resistivity as a function of time and 2) transforming SRO($\alpha$) to LRO($\beta$) and retain it by naturally cooling it to room temperature, thus constituting a convenient way to achieve LRO($\beta$) structure in the specimen as the initial microstructure for the next pulse test.

In general, the designed isothermal technique was successfully used to study the kinetics of transformation in steel and $Ni_4Mo$. The best temperature control achieved was ± 1/4 °C . Use of intrinsic type thermocouple gave very poor results for temperature control, because of the 'pick-up' contribution of the thermal emf which got amplified in the control algorithm and caused massive jump in the current, thus rendering the temperature out of control. The beaded type thermocouple worked well and was consistently used with isothermal tests. Appendix III gives the source code of the PID program used in these experiments.

# CHAPTER IV
# DISCUSSION OF EXPERIMENTAL RESULTS

## PULSE EXPERIMENTS

As declared in the abstract, the main goal of this research was the implementation of the pulse-heating technique to determine the electrical resistivity and specific heat of $Ni_4Mo$. The same specimen was used in three initial states, 1) SRO(α), 2) cold-worked SRO(α) and 3) LRO(β). Fast heating, e.g., 50 °C/sec, was utilized in most experiments but the effect of slow heating, e.g., 1 °C/sec, on the electrical resistivity of $Ni_4Mo$, SRO(α), specimen was also studied. As a secondary goal, isothermal experiments were done on $Ni_4Mo$. The efforts to this end were three-fold: 1) develop a computer program to hold the temperature of the specimen constant inside the calorimeter chamber; 2) test the PID program with different specimens and determine proportional (P), integral (I) and derivative (D) constants and other test parameters which are best suited for the specimen in use; 3) run the isothermal program on the specimen with the 'best' PID constants and study the change in the electrical resistivity and power, to study phase transformations in the material.

The secondary goals for continuous heating were to determine the electrical resistivity and specific heat of Ni(pure), four Fe-Al

alloys and a Ni-Al alloy. Many of these alloys undergo phase transformations. Electrical resistivity and specific heat were used as the basis to identify phase transformations, e.g., magnetic, DO3 —› B2.

Chronologically, the foremost goal of the research was to determine the electrical resistivity and specific heat data for nickel and compare it with the data determined previously by other investigators, in order to establish the accuracy of the measuring technique. Once this was assessed, a series of experiments followed. This section presents the data from the experiments and discusses the results

## PURE NICKEL

### ELECTRICAL RESISTIVITY

Several tests were done on the pure nickel specimen, NIC. Initially, tests were done on the specimen with three different thermocouple configurations and the merits and demerits of each type were studied. Chapter III discussed this study along with some sample data. Several runs were also made to check the repeatability of the measurements. The results are discussed later in this chapter.

Next, electrical resistivity test results from this research were compared with the results of a previous investigator, Kollie [8], to determine the relative accuracy of the technique. This was the most important initial goal. Author's data was smoothed by a FFT filtering

technique, done using a commercial software. The scatter in the unsmoothed data was about ±0.5% from the smoothed curve. The author's smoothed data and Kollie's data are presented in Figure 4.1 on the same plot for comparison. The disagreement is less than 1% across the entire temperature range of comparison, i.e., 340 to 1000 K. The Curie temperature was determined by Kollie to be 633.0 K, and by the author, to be 633±1 K. At this temperature the curve changes from being concave upwards to convex upwards. The electrical resistivity rises with temperature in a non-linear manner till it reaches the Curie temperature where it changes in the sign of $d^2\rho/dT^2$.

SPECIFIC HEAT

Author's data on specific heat is presented in Figure 4.2, along with Kollie's [8] data. The specific heat curve follows the same trend for both data. The discontinuity at the Curie temperature is also consistent with each other. The specific heat increases with temperature as it approaches Curie temperature. In the paramagnetic range the specific heat decreases first and then, rises more gradually to the highest test temperature, i.e., 1200 K. The general disagreement of author's data with that of Kollie is about 1% across most of the temperature range, except just above the Curie temperature, where it is about 2%.

It is pointed out that the classical value of specific heat of solid elements equal 3R (= 5.9616 cal/mol-K). For a compound containing

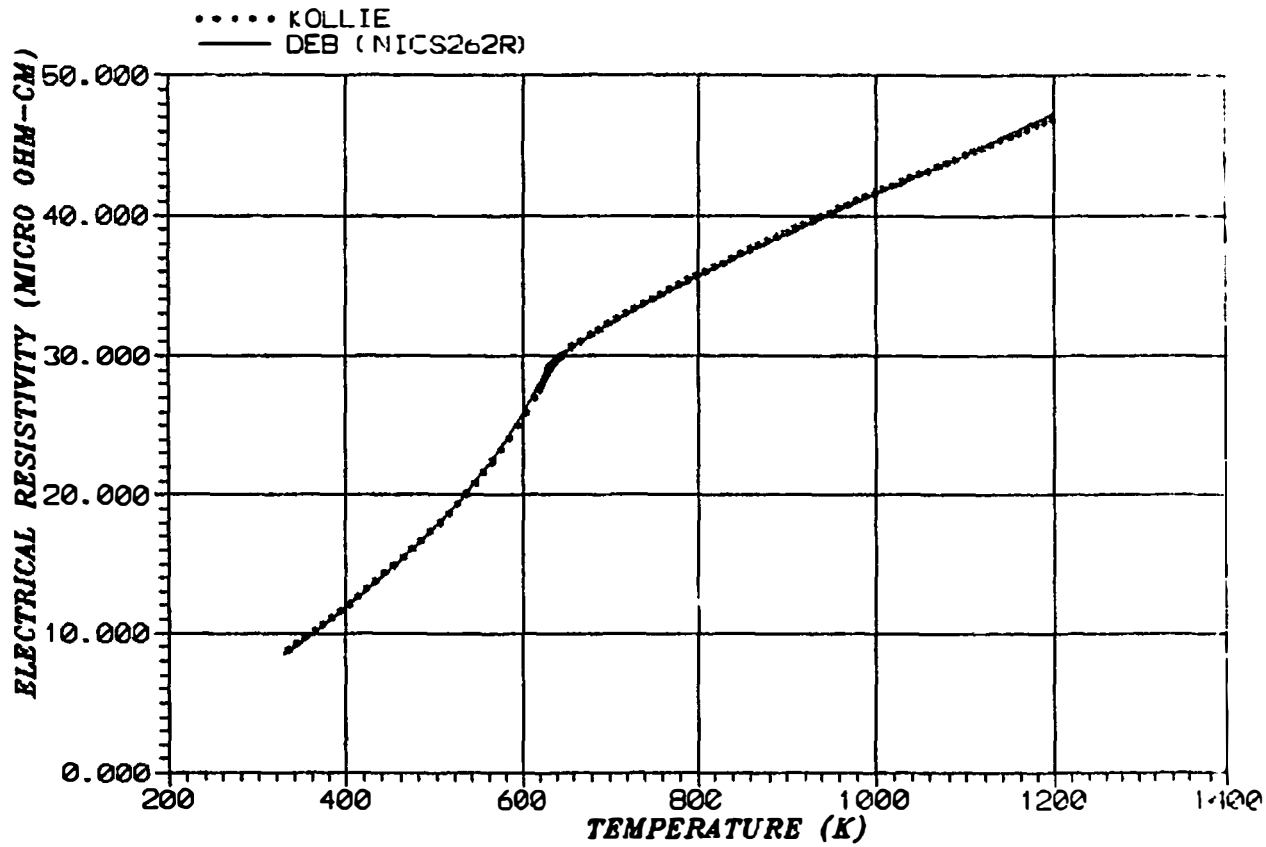


Figure 4.1 Electrical resistivity versus temperature plot for pure nickel as determined by the author and Kollie [8].

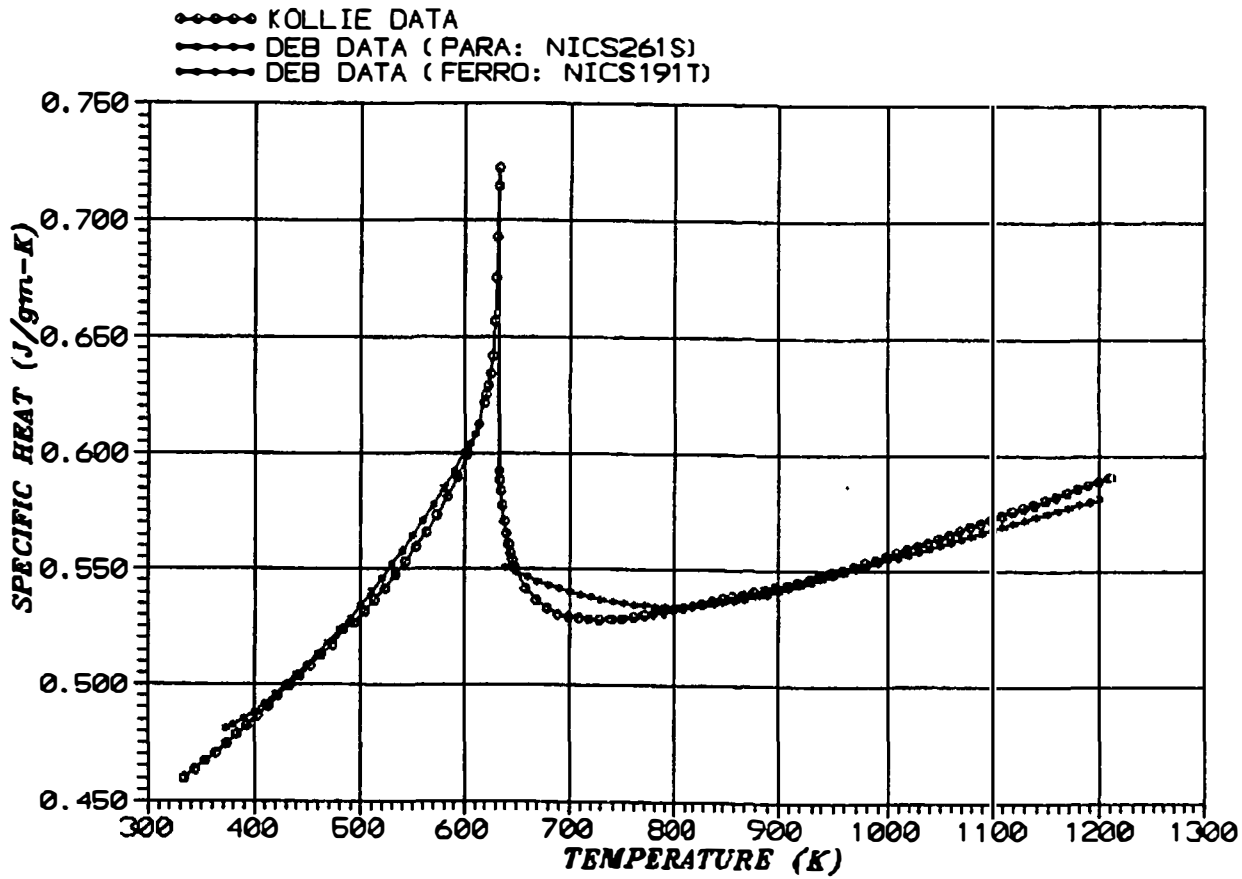


Figure 4.2 Specific heat versus temperature plot for pure nickel as determined by the author and Kollie [8].

n atoms per molecule, the specific heat would equal 3nR. The experimental values of Cp determined for metals and alloys in this research lie about 5-10% above the classical value.

## Fe-Al ALLOYS

### a) Fe-21.2 wt% Al alloy

#### ELECTRICAL RESISTIVITY

This specimen was made at the Metals and Ceramics Division of Oak Ridge National Laboratory [7]. The alloy is $\alpha_2$ with a B2 structure (See phase diagram, Figure 4.3. The electrical resistivity increases steadily from room temperature to ~650 K (377 °C), where there is a sharp change in slope (refer to Figure 4.4). Above ~650 K (377 °C) the increase in electrical resistivity is gradual. It is believed that this change in slope might be associated with the formation of constitutional vacancies [42], but more experiments need to be done before this hypothesis can be confirmed. The vacancies for this B2 phase has been postulated, on energy grounds, to be asymmetrical triple defects consisting of two vacancies on A sites and an antistructure atom on B site, 2 $p_A A_B$[43]. Around 1400 K (1127 °C), the sign of $d\rho/dT$ changes. There is a phase change at this point, $\alpha_2(FeAl) \Rightarrow \alpha(Fe)$, as indicated by the phase diagram (Figure 4.3).

An unusual and interesting observation is that upon reversing the direction of current to the specimen, the electrical resistivity data

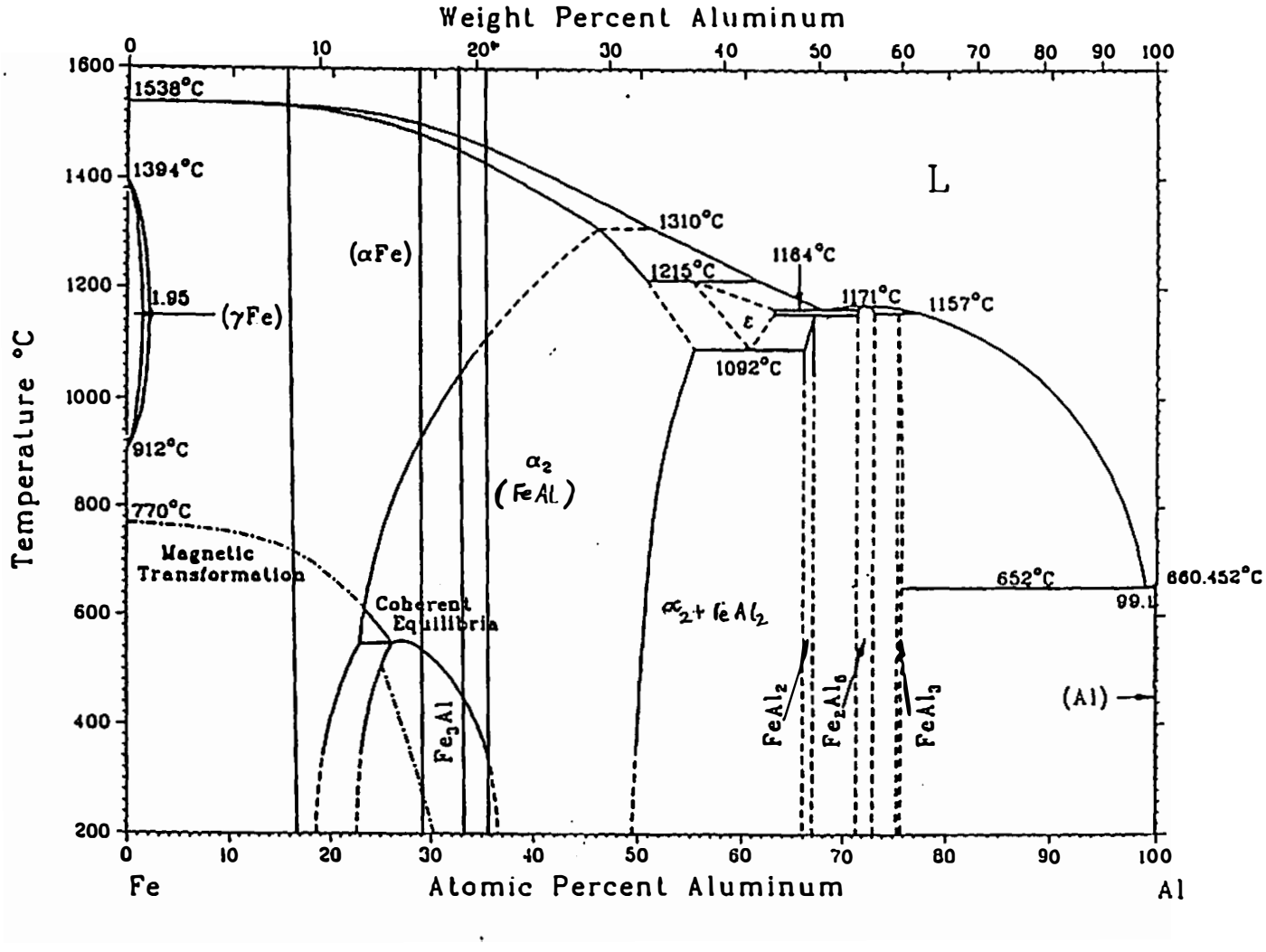


Figure 4.3 Fe-Al phase diagram [10].

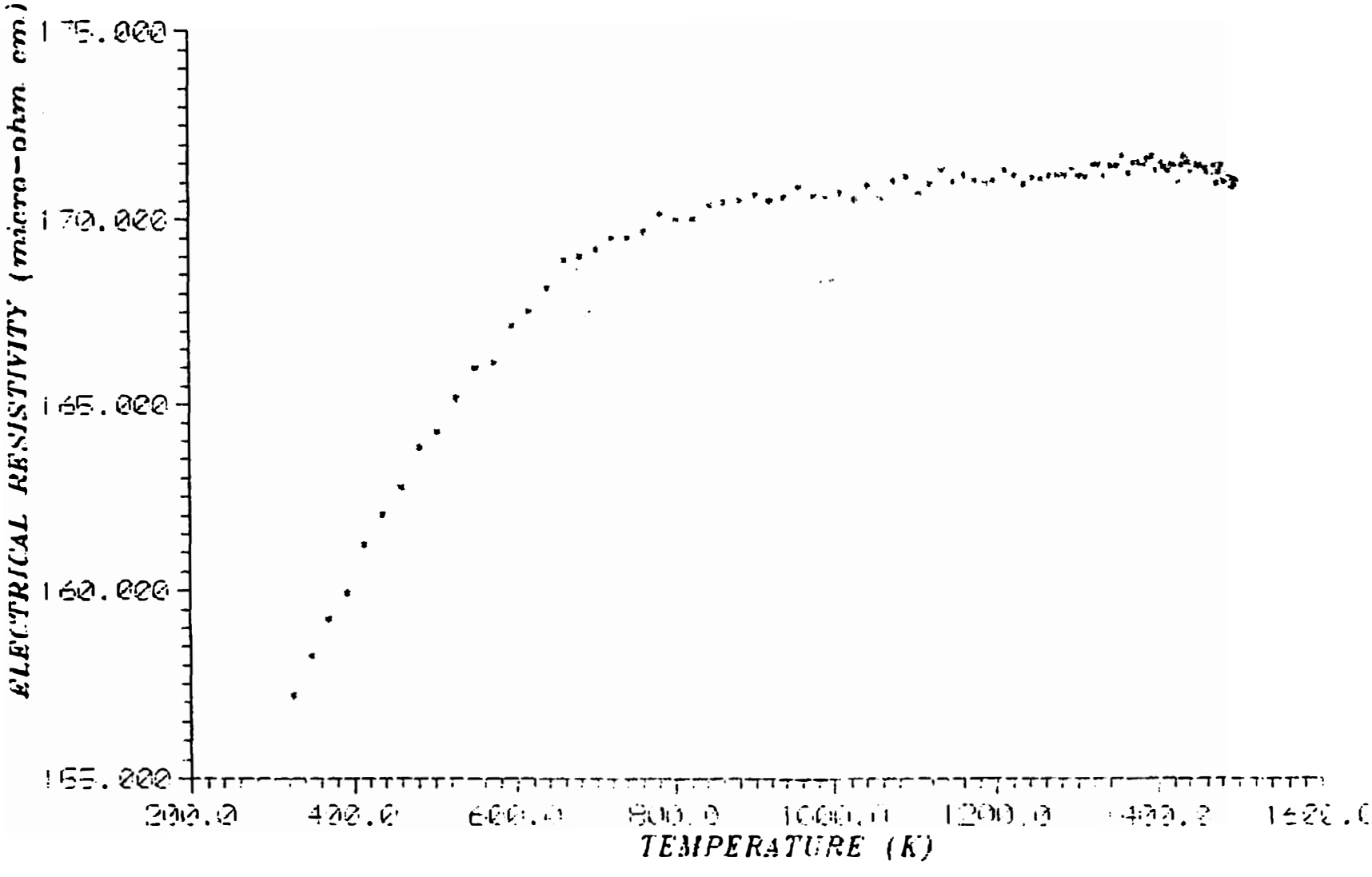


Figure 4.4 Electrical resistivity versus temperature plot for Fe-21.2 wt%Al.

was not repeatable and diverge from each other near the point where the constitutional defects are believed to form, e.g., 650 K. Figure 4.5 shows this effect. No conclusion has been drawn yet about this anomaly, and more experimentation needs to be done to explore the cause of this behavior. The deviation around 1200 K is 2.8 %. Other alloys tested in this way have shown no indication of such behavior.

SPECIFIC HEAT

Figure 4.6 shows the specific heat versus temperature. There are two aspects to be noted. Above 950 K there is a sharp rise in the slope of the curve due to the formation of thermal vacancies. The other effect may not be so evident in the Figure 4.6, so Figure 4.7 shows the data magnified from 370 K to 900 K. From this figure, the point of inflection at ~650 K can be easily identified. It is expected to be due to the same effect that causes a sharp change in slope of electrical resistivity around 650 K, namely, constitutional vacancies. It is believed that the formation of constitutional vacancies has a contribution to raise the specific heat above that of the 'regular' specific heat curve, in the temperature range they form, in this case at ~650 K. This results in the point of inflection.

The specific heat values for this alloy and some other alloys, e.g., Fe-18wt%Al, Fe-16wt%Al, Ni-8wt%Al, show a sharp upswing at a temperature much lower than melting point and ultimately rise to a value considerably higher than the classical value. This is

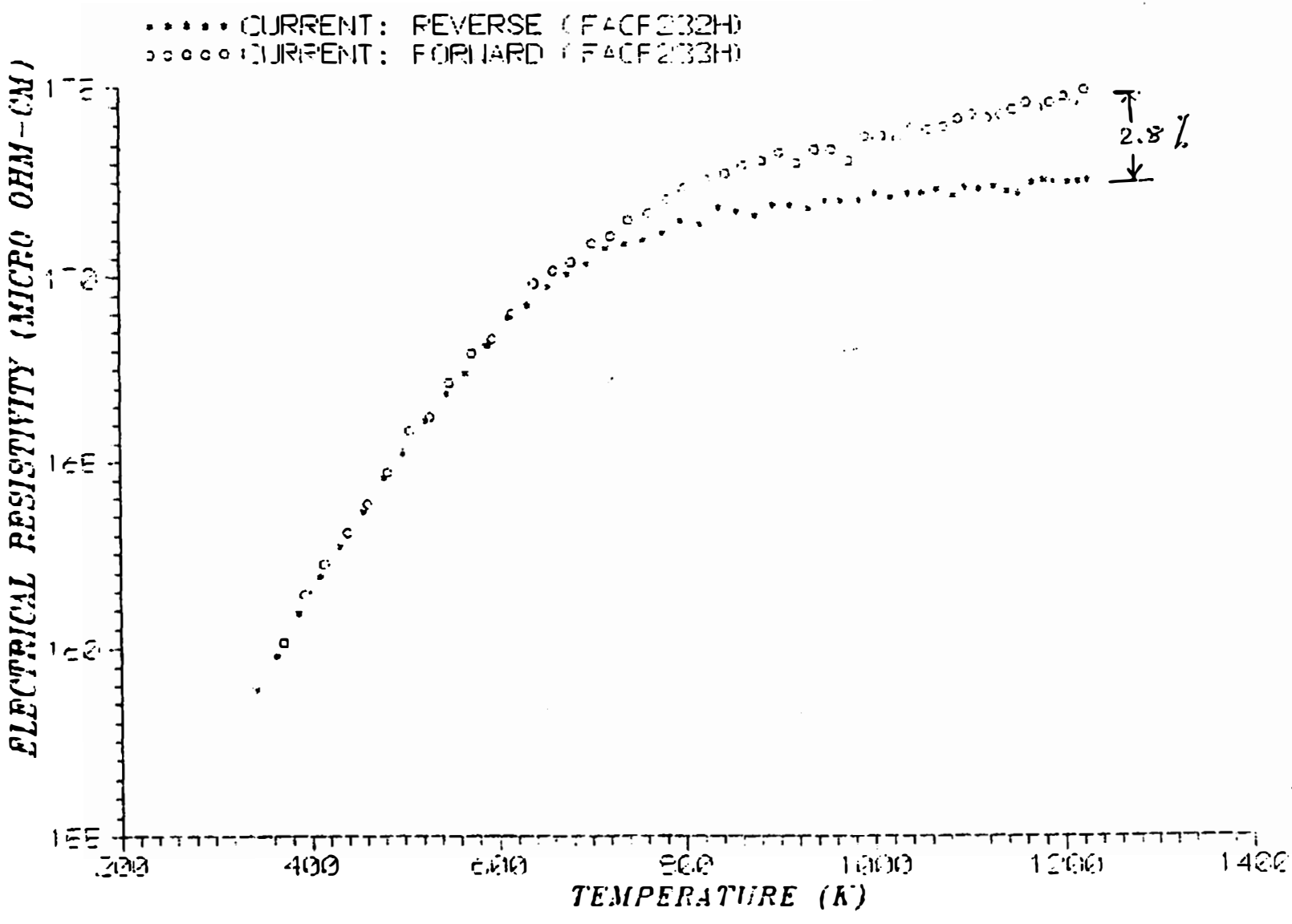


Figure 4.5 Electrical resistivity versus temperature plot for Fe-21.2 wt%Al, for current flowing in both directions.

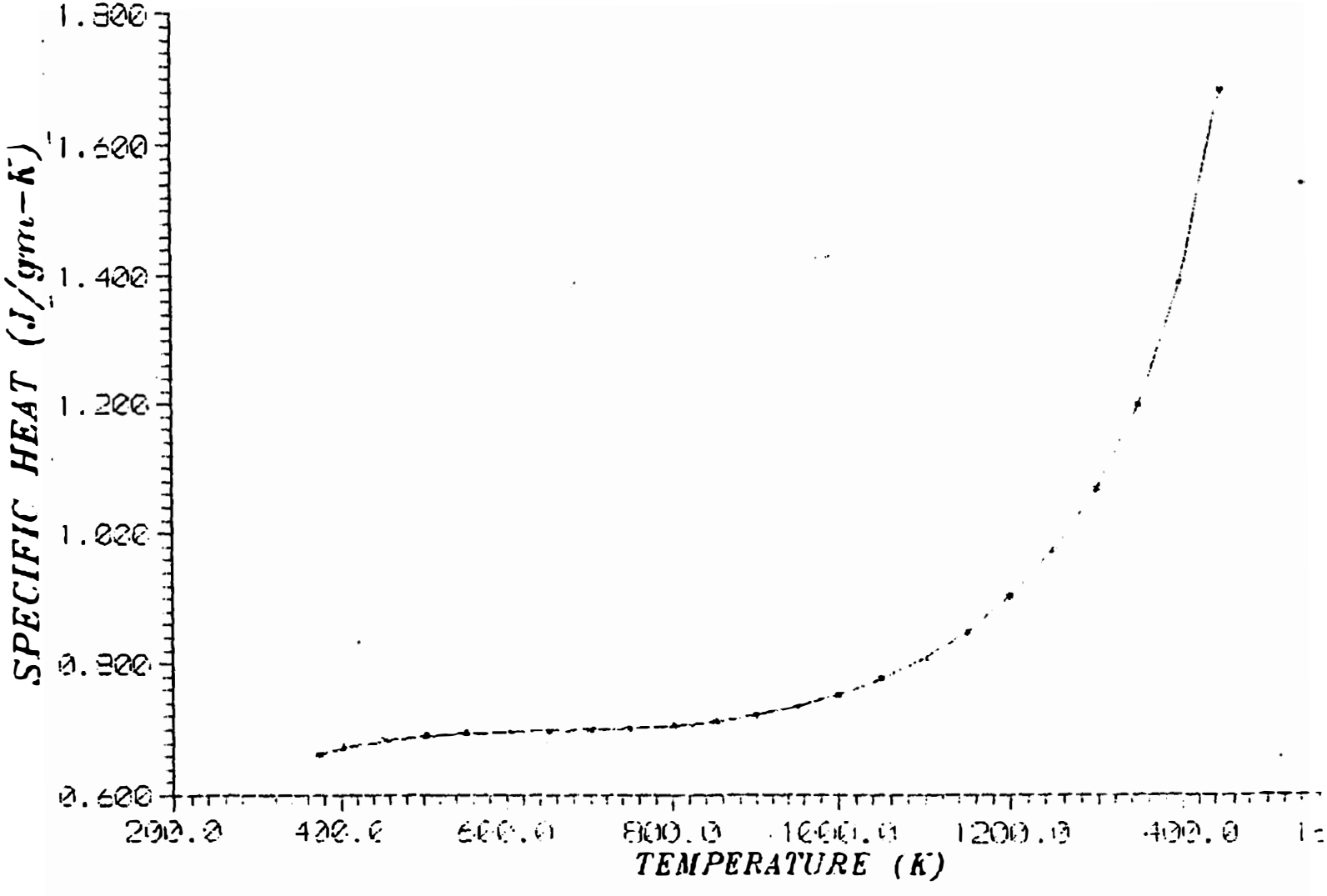


Figure 4.6 Specific heat versus temperature plot for 21.2 wt%Al.

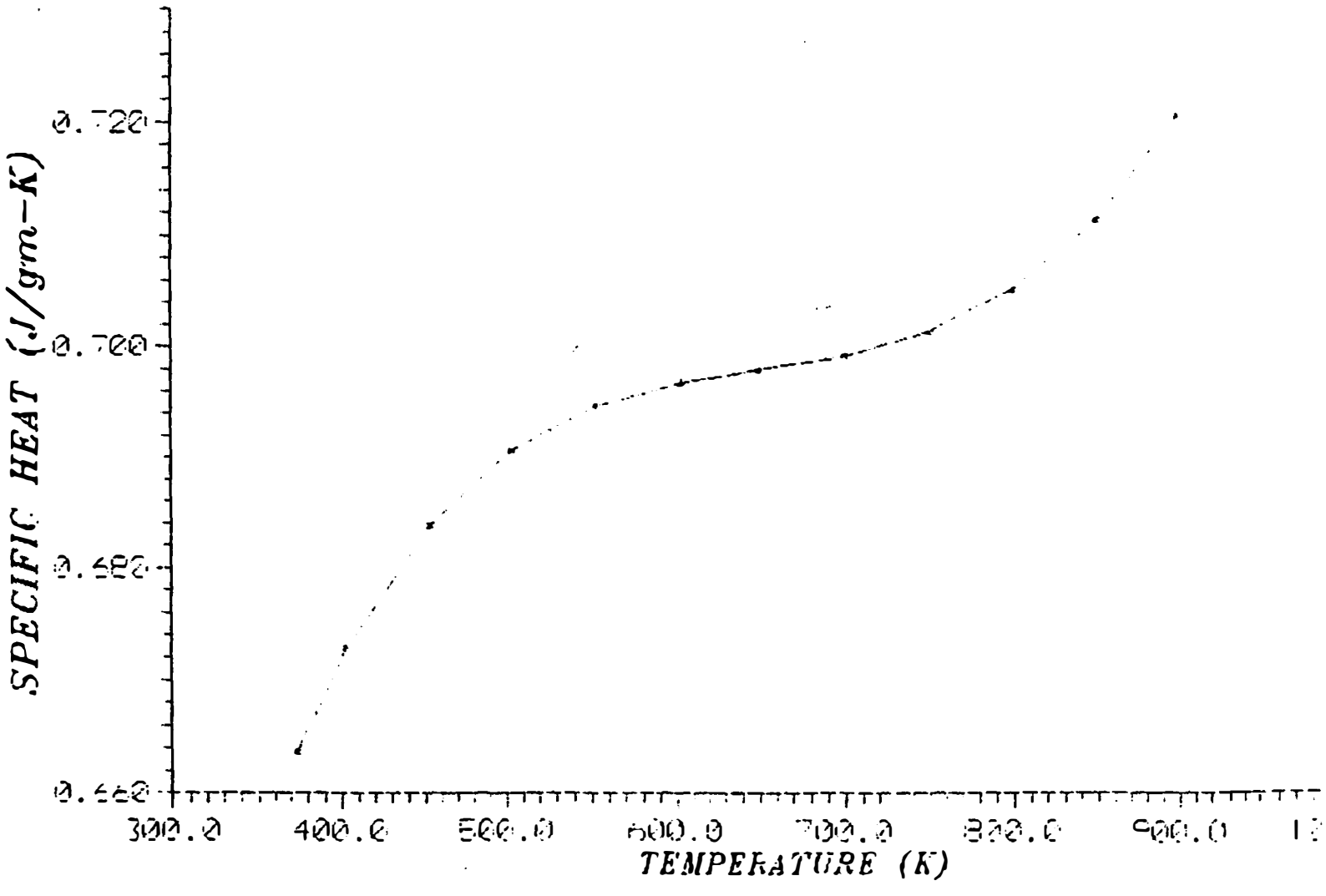


Figure 4.7 Magnified plot for specific heat versus temperature for 21.2 wt%Al, for lower temperature range.

believed to be due to vacancy formation, both thermal and constitutional types.

## Fe-18 wt%Al

### ELECTRICAL RESISTIVITY

Electrical resistivity data are presented in Figure 4.8 for this alloy. For the 18wt%Al alloy, as the specimen increases in temperature the electrical resistivity increases till it reaches a maximum at 740 K (467 °C). Thereafter, it decreases gradually up to the highest test temperature, e.g., 1440 K (1167 °C). The transformation temperature as shown by the phase diagram (Figure 4.3), is ~713 K (440 °C). In the temperature-time plot for heating, there is a change in slope at 740 K. It is believed that at this temperature, there is a major rearrangement of atoms leading to the decrease in the degree of DO3 order [44].

Hyde et al. [44], categorizes electrical resistivity versus temperature curve, for this alloy, into three distinct regions (see inset of Figure 4.8) : 1) low temperature steady increase portion, where phonon scattering dominates and the structure is highly ordered DO3 (FeAl); 2) the cusp region, which is associated with a deteriorating DO3 order; and 3) the decreasing electrical resistivity region, where the material is in the less ordered B2 ($\alpha_2$) state [44]. The transformation temperature is at the bottom of the cusp.

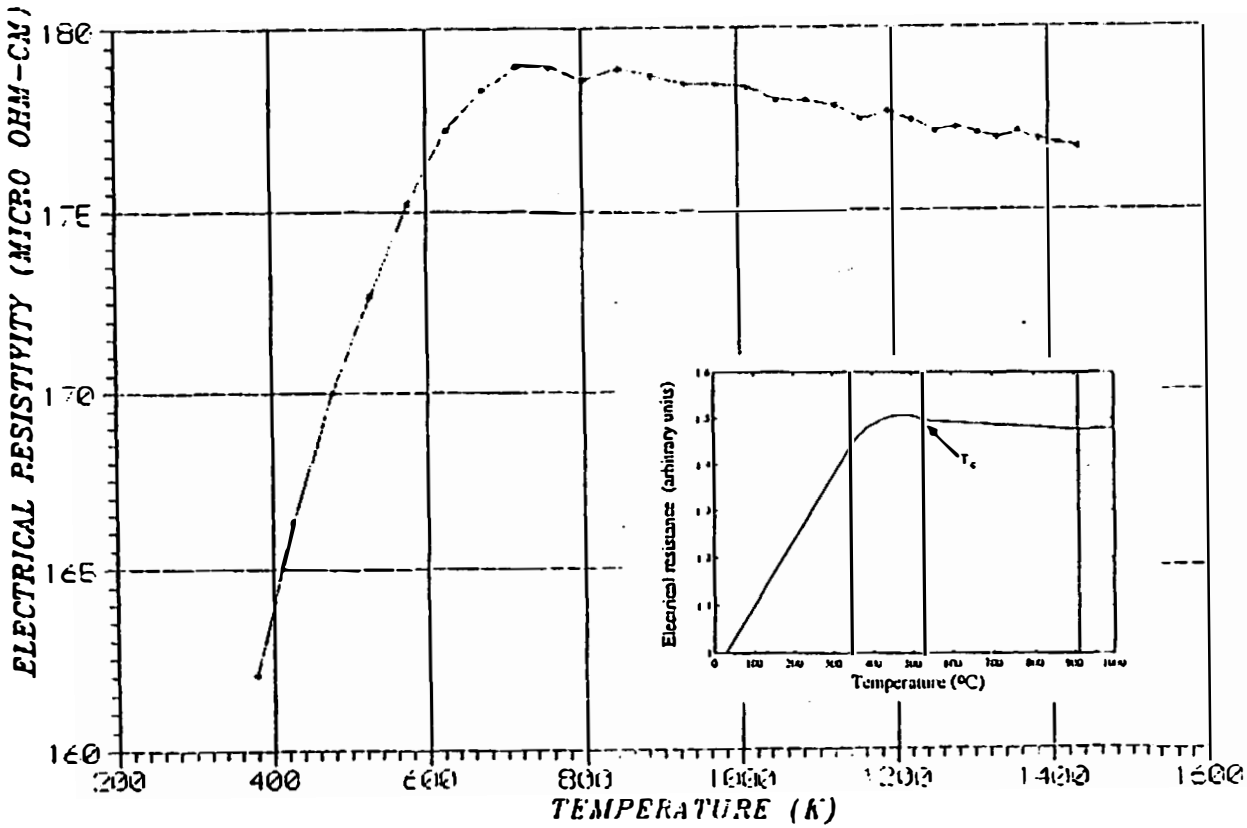


Figure 4.8 Electrical resistivity versus temperature plot for Fe-18 wt%Al. Inset shows a schematic plot based on Hyde et al.'s data for Fe-Al specimen with a DO3⇒B2 transformation.

SPECIFIC HEAT

Figure 4.9 shows the specific heat data for the same alloy. Specific heat goes up steadily with temperature. There is a discontinuity at 780 K which corresponds to the maximum in the electrical resistivity curve. It is believed that at this point there is a rearrangement of atoms in the crystal from a highly ordered state to a less ordered state. The phase diagram (Figure 4.3) shows the transformation to occur at 713 K (440 °C).

## Fe-16 wt%Al alloy

ELECTRICAL RESISTIVITY

16wt%Al alloy shows the same behavior as the 18 wt%Al alloy (Figure 4.10). For this alloy, the electrical resistivity versus temperature curve increases with increase in temperature up to a maximum which occurs at a temperature of 775 K (502 °C). Thereafter, it decreases gradually to the highest test temperature, e.g., 1370 K. The transformation temperature as shown by the phase diagram (Figure 4.3), is 793 K (520 °C). In the temperature-time plot for heating, there is a change in slope at 775 K (502 °C). This corresponds to the maximum point in the electrical resistivity plot.

SPECIFIC HEAT

Specific heat shows the same trend as that of the Fe-18 wt%Al alloy, with a discontinuity at 775 K (502 K) (Figure 4.11). This

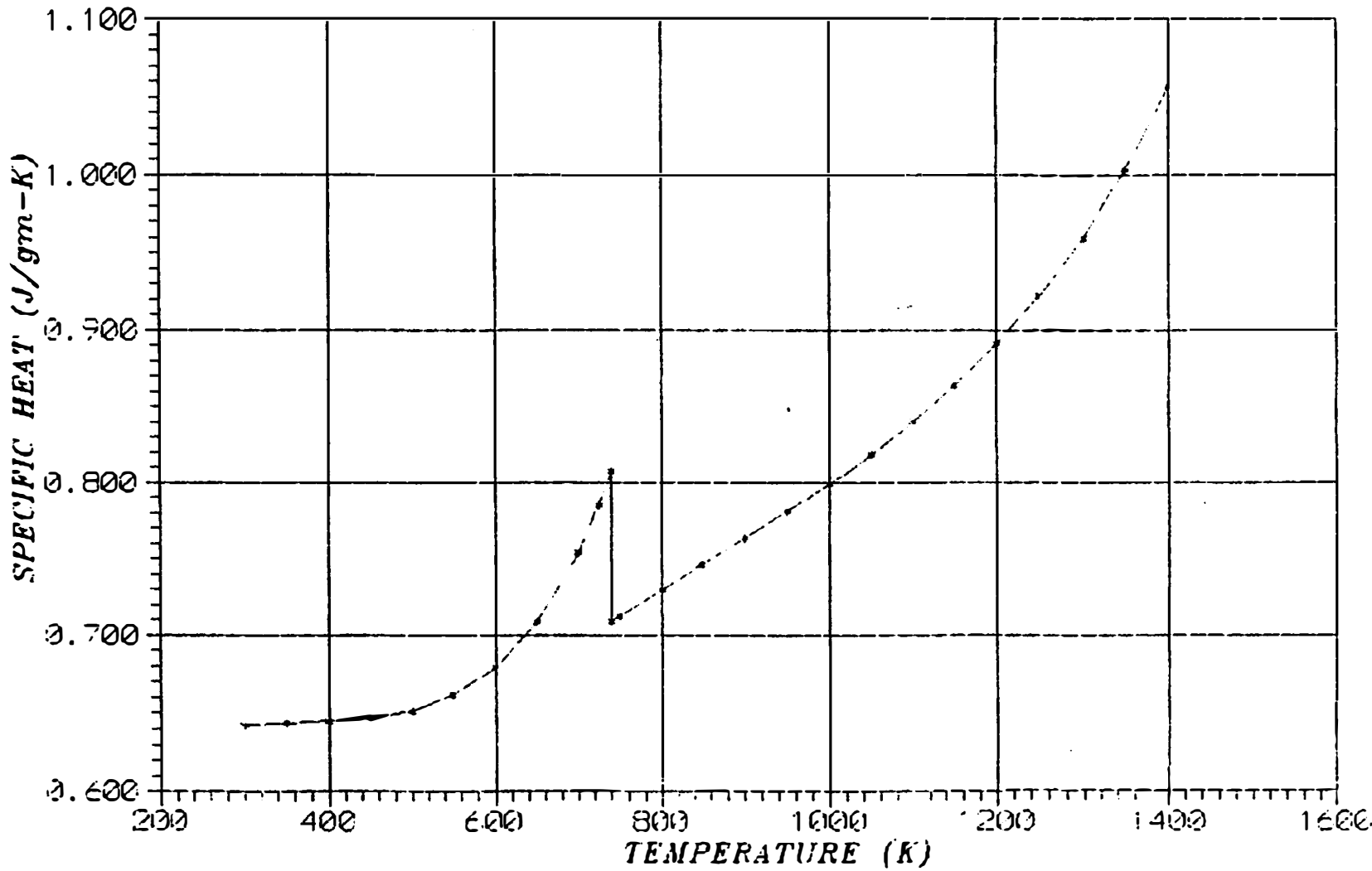


Figure 4.9 Specific heat versus temperature plot for Fe-18 wt%Al.

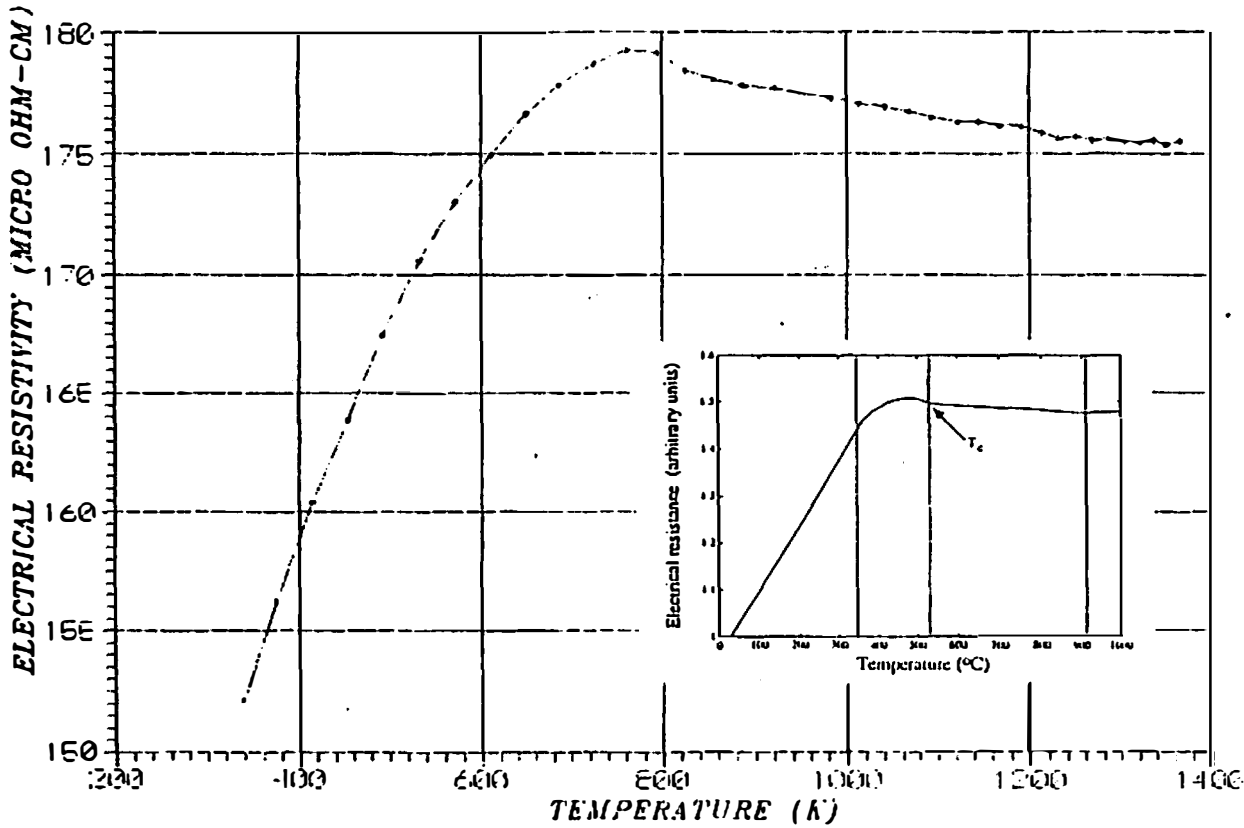


Figure 4.10 Electrical resistivity versus temperature plot for Fe-16 wt%Al. Inset shows a schematic plot based on Hyde et al.'s data for Fe-Al specimen with a DO3⇒B2 transformation.

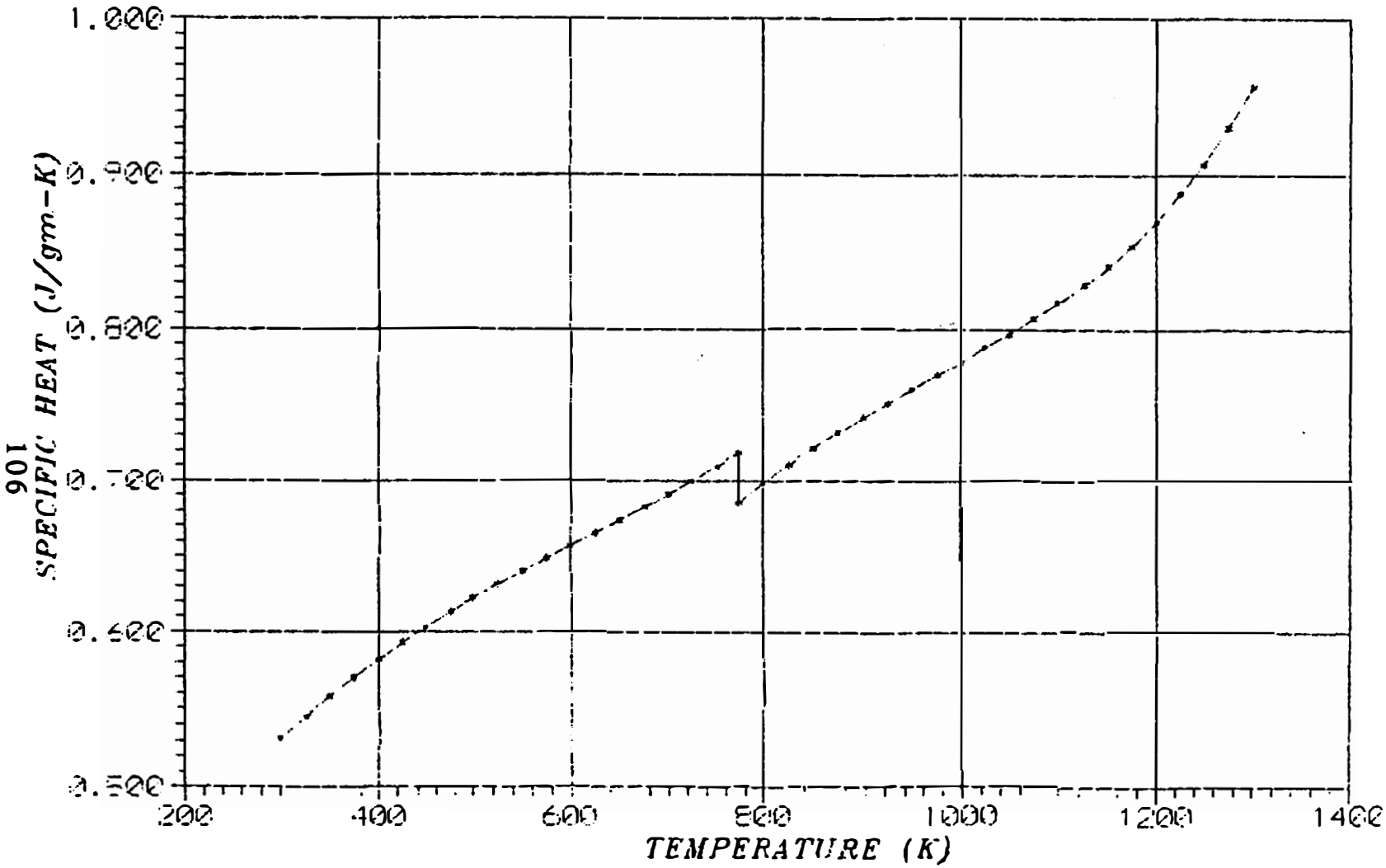


Figure 4.11 Specific heat versus temperature plot for Fe-16 wt%Al.

discontinuity corresponds to the maximum point of the electrical resistivity versus temperature curve.

## Fe-8.5 wt%Al alloy

### ELECTRICAL RESISTIVITY

This alloy is ferromagnetic at room temperature. The electrical resistivity versus temperature data is similar but much greater in value than that of nickel (Figure 4.12). Below Tc, the curve is concave upward and above Tc, the curve is concave downward. The determined Curie temperature is 966 K (693 °C). This is the point at which $d^2\rho/dT^2$ changes in sign. The phase diagram, however, shows the Curie temperature to be 983 K (710 °C).

### SPECIFIC HEAT

Specific heat data increases steadily till it reaches the Curie temperature, 966±5 K, whereafter in the paramagnetic range, it initially decreases and then increases with increase in temperature (Figure 4.13). There is a discontinuity in the specific heat data at Curie temperature. The curve is similar in nature to the curve for nickel (Figure 4.1).

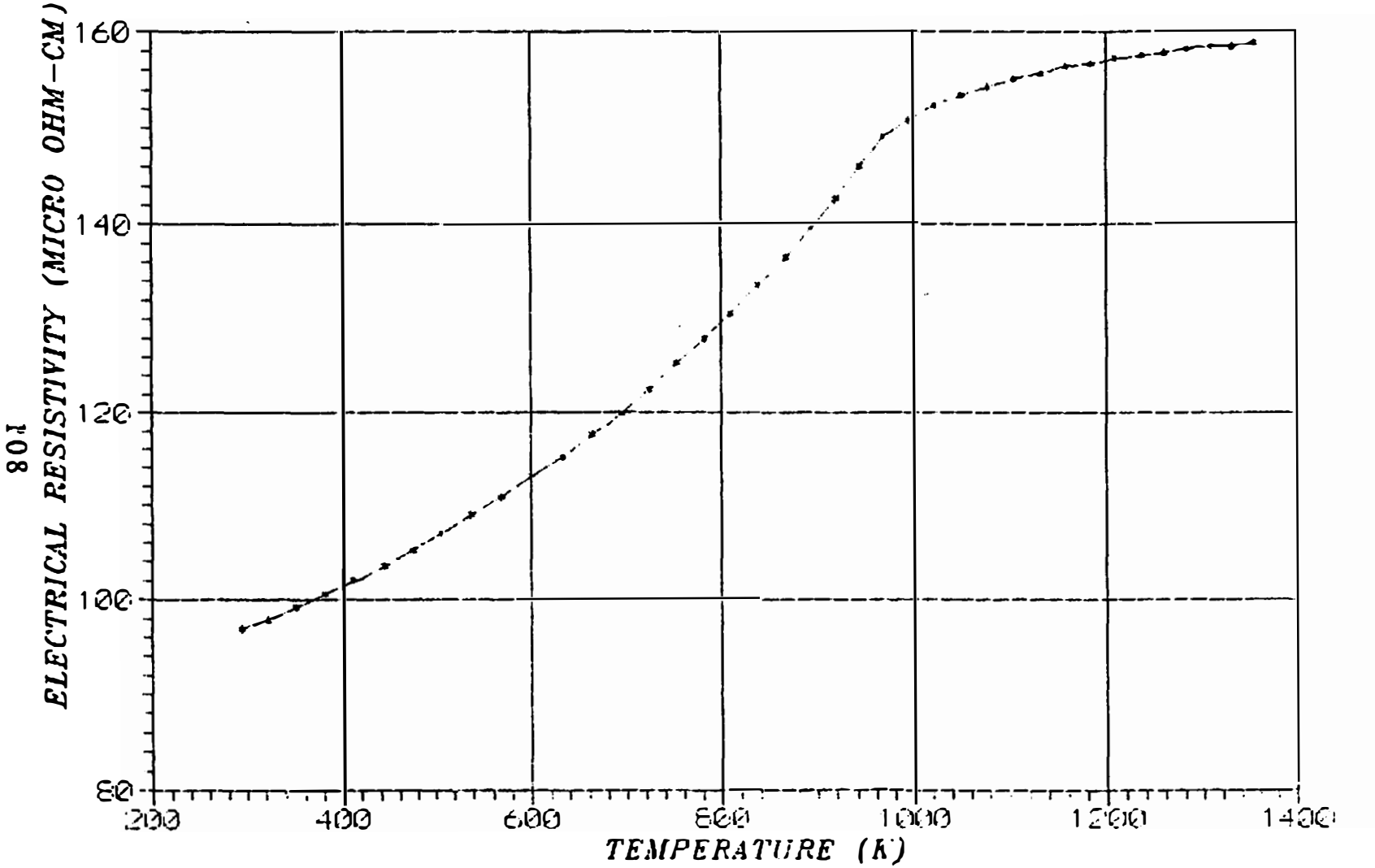


Figure 4.12 Electrical resistivity versus temperature plot for Fe-8.5 wt%Al.

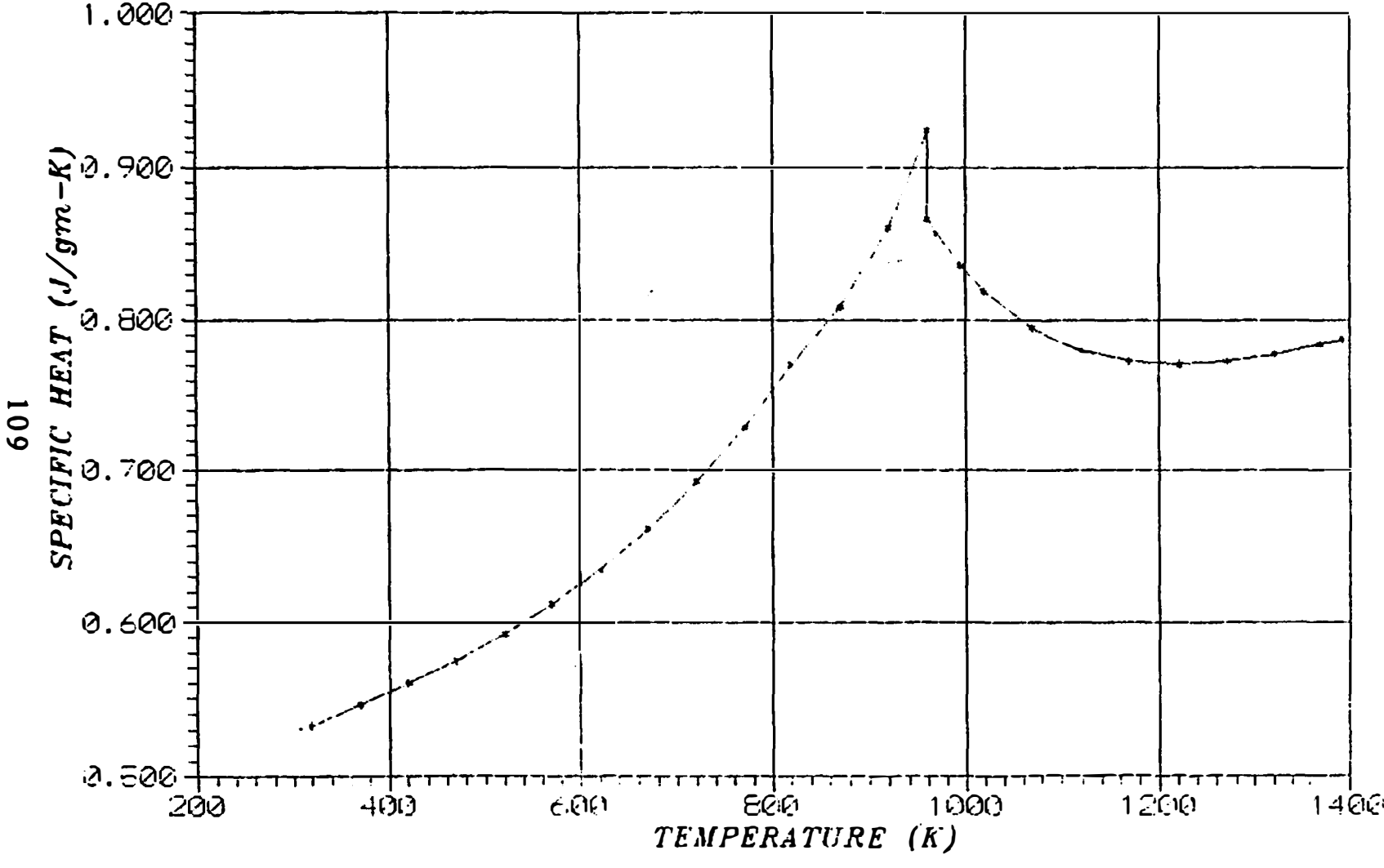


Figure 4.13 Specific heat versus temperature plot for Fe-8.5 wt%Al.

## Ni-8 wt%Al alloy

### ELECTRICAL RESISTIVITY

Electrical resistivity increases steadily to 890±5 K (Figure 4.14). Below 890 K, the curve is convex upward. Above 890 K, the curve becomes approximately linear. There is also a considerable change of slope at this point. The reason for this is not clearly understood. The phase diagram (Figure 4.15) does not show any phase change at this temperature. However, it has been observed that this curve is similar to the curve for Fe-21.2 wt%Al (Figure 4.4). In the Fe-21.2 wt%Al alloy, the slope change is believed to be due to the formation of constitutional vacancies. Also, it has been suggested by Neuman et al. [45] that certain NiAl alloys would form constitutional triple defects due to the presence of excess of Group III component. However, no definite conclusion is drawn in this thesis, about this possibility. More research needs to be done to understand this.

Electrical resistivity data is reported in Appendix IV.

### SPECIFIC HEAT

Since, there are no phase changes in the working temperature range, for this alloy, the specific heat does not show any discontinuity or detectable points of inflection (refer to Figure 4.16). The specific heat rises sharply at higher temperatures, as expected, due to the thermal vacancies.

Specific heat data is reported in Appendix IV.

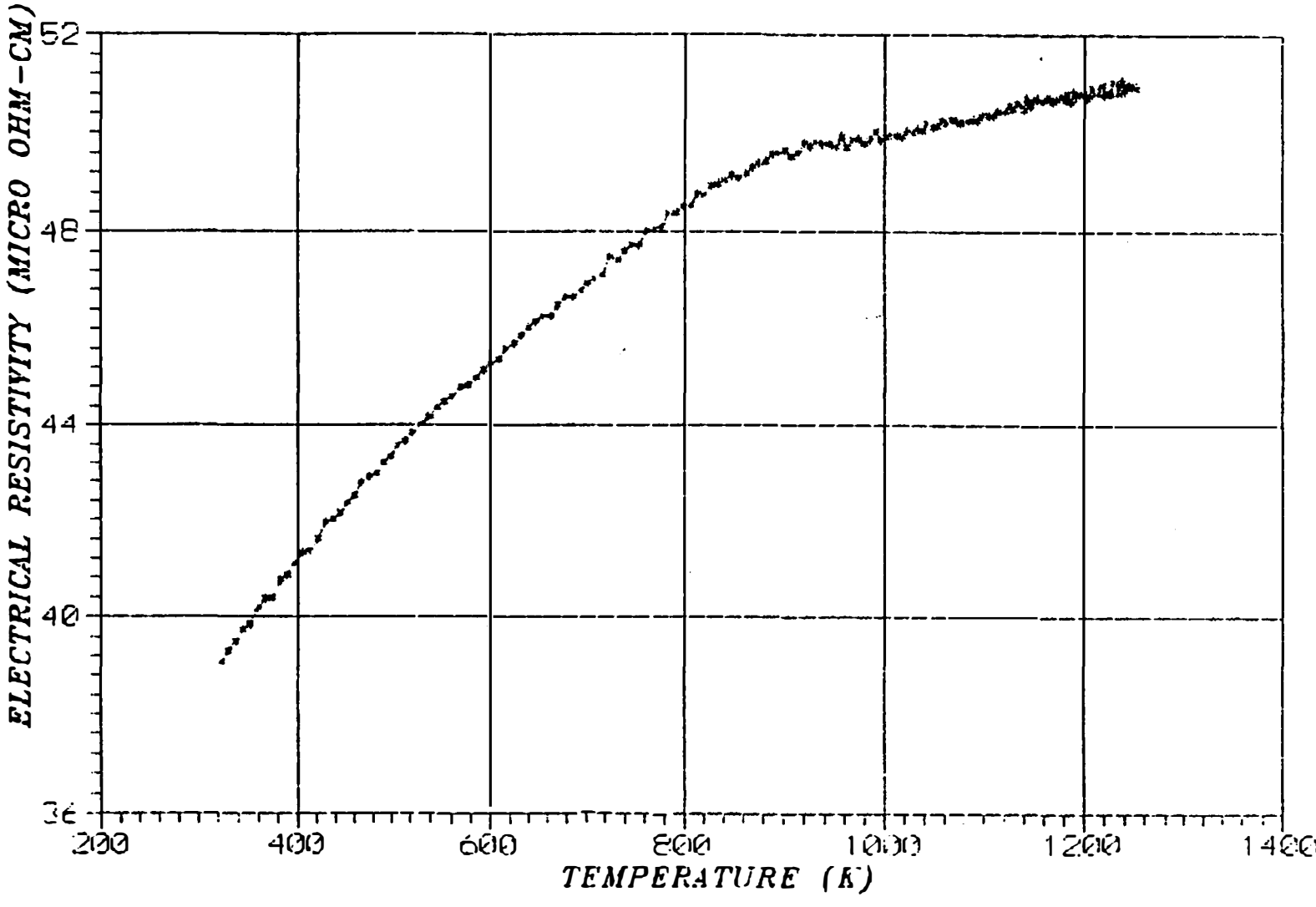


Figure 4.14 Electrical resistivity versus temperature plot for Ni-8 wt%Al.

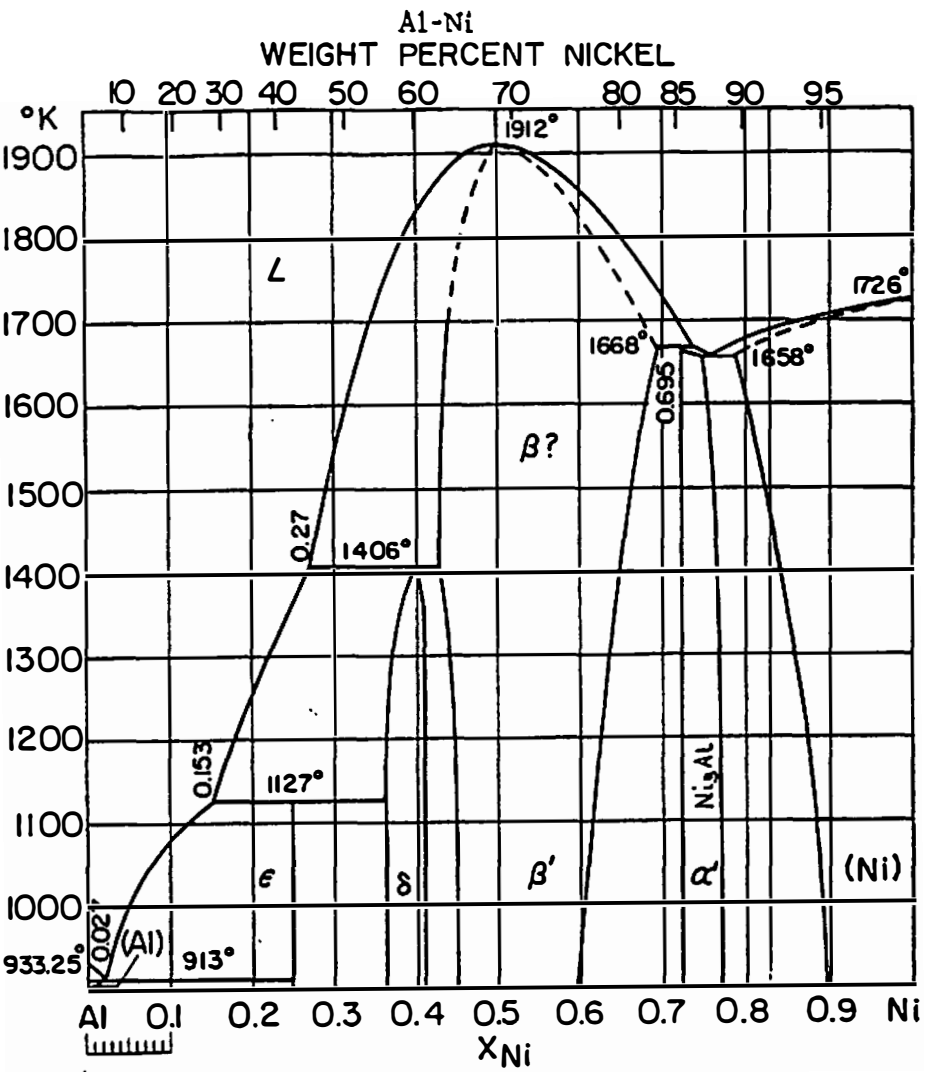


Figure 4.15 Phase diagram of Ni-Al [11].

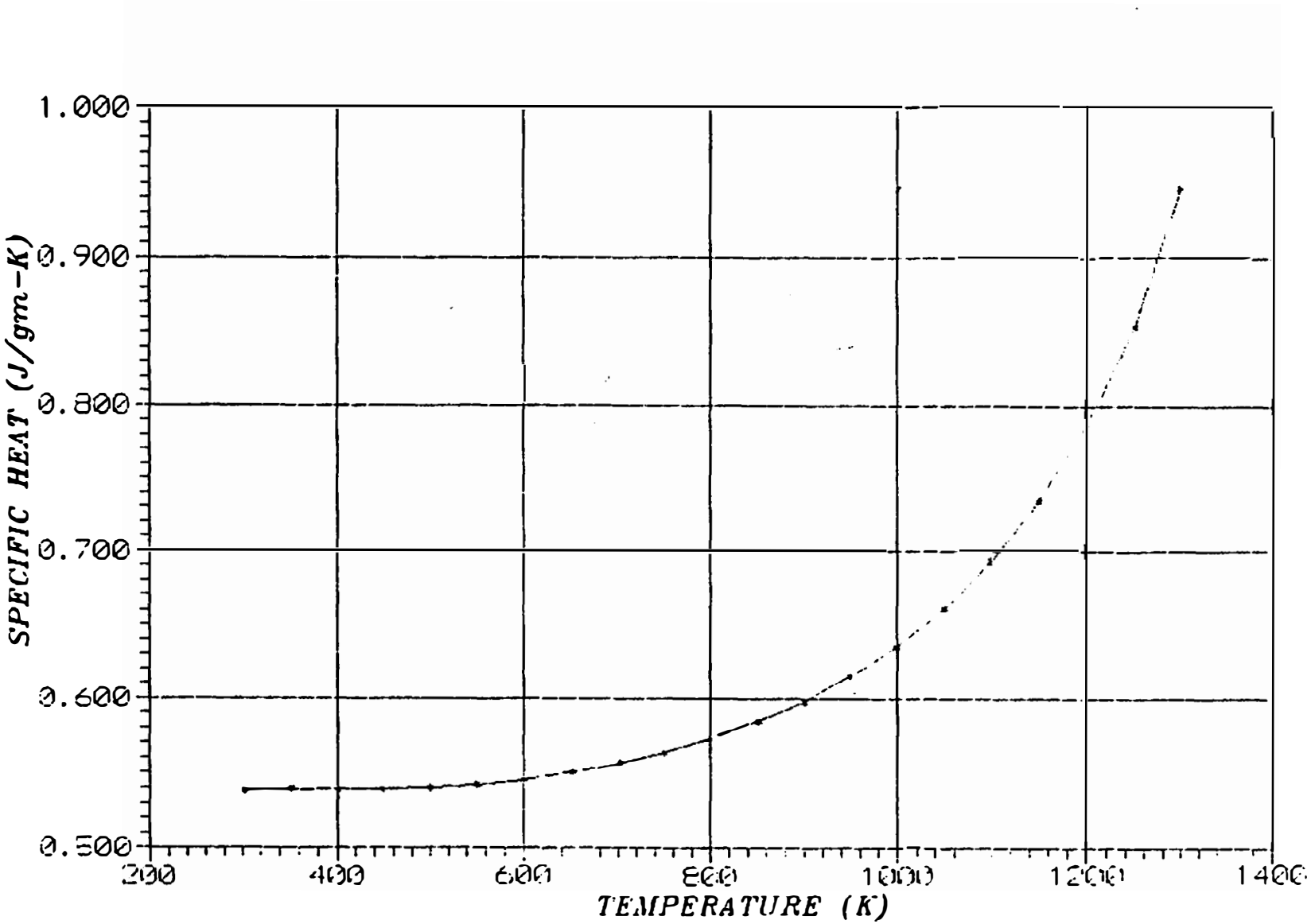


Figure 4.16 Specific heat versus temperature plot for Ni-8 wt% Al.

## Ni-20 at% Mo alloy

As pointed out, the main goal of this thesis was to determine the electrical resistivity and specific heat of $Ni_4Mo$ for three initial conditions, 1) cold-worked SRO($\alpha$), 2) SRO($\alpha$) and 3) LRO($\beta$). Pulse-heating was utilized to heat the specimen from room temperature to a high temperature, 1300 K, and the electrical resistivity determined as a function of temperature. Typical heating rates attained in these experiments were 50-75 K/sec. A run was also made with a much slower heating-rate, e.g., 1 K/sec, by an improvised technique using the isothermal program, CALISO.

The electrical resistivity and specific heat for $Ni_4Mo$ are presented and discussed in this section. The phase diagram for Ni-Mo is presented in Figure 4.17.

## ELECTRICAL RESISTIVITY

### a) Initial condition : LRO($\beta$)

Curve 1 of Figure 4.18 shows the electrical resistivity data for the LRO($\beta$) initial condition. At room temperature, the electrical resistivity for LRO($\beta$) condition is the lowest of those of the three conditions and is represented by curve 1. The electrical resistivity at 376 K is 75.6 $\mu\Omega$-cm. Electrical resistivity rises rather sharply with temperature till it reaches 1141±2 K, which has been determined to be the equilibrium transformation temperature for the $\beta \Rightarrow \alpha$

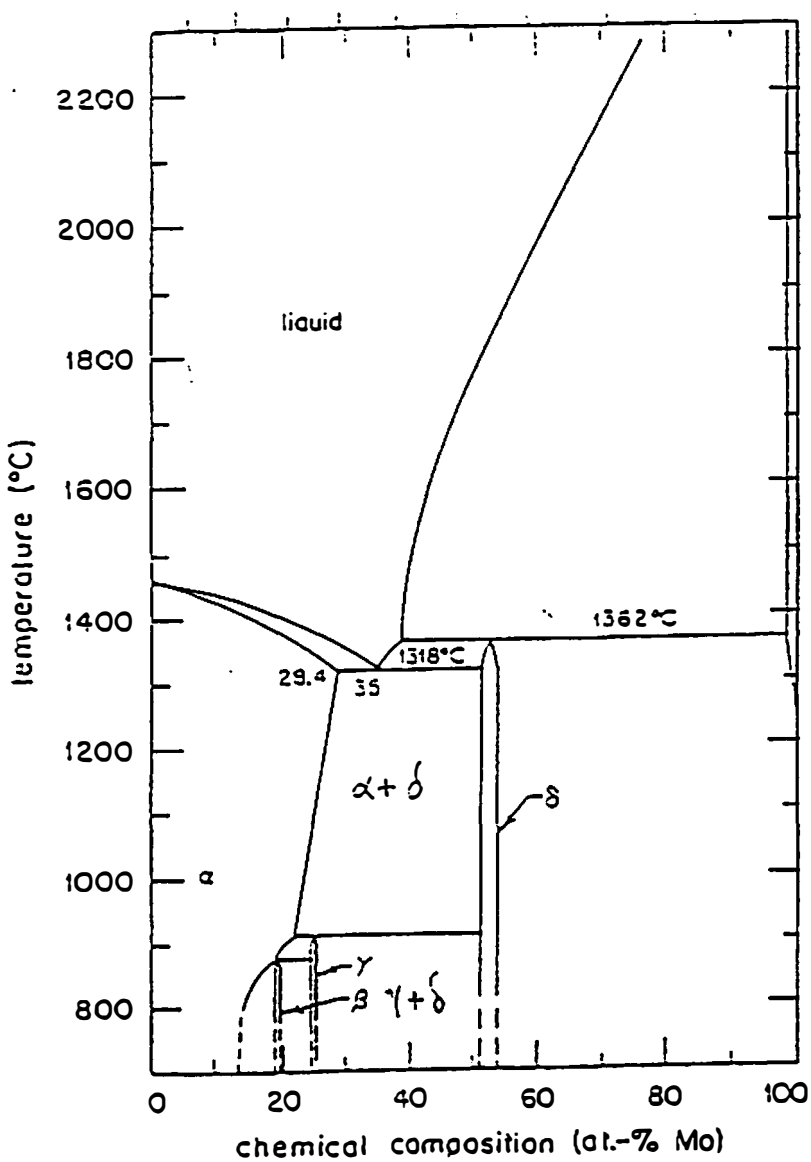


Figure 4.17Ni-Mo phase diagram [10]

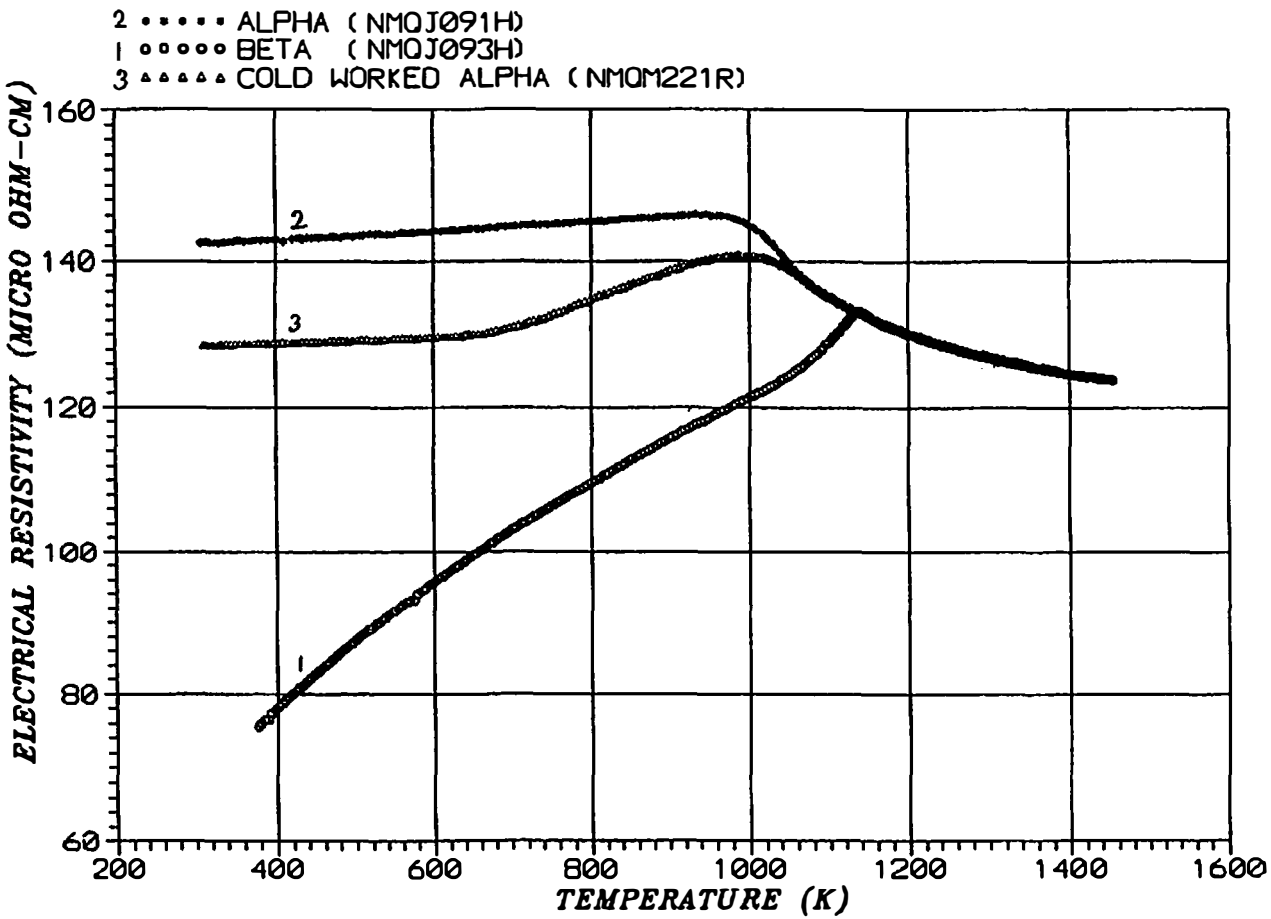


Figure 4.18 Electrical resistivity versus temperature plot for $Ni_4Mo$, for three initial conditions.

transformation. The electrical resistivity passes through a maximum at the transformation temperature, its value being 133.2 μΩ-cm. Thereafter, the electrical resistivity decreases all the way to 1453 K. Below 1141 K, the increase in electrical resistivity with temperature is mainly attributed to thermal scattering. Just below the transformation temperature, Tc, 1141 K, the increase in electrical resistivity is sharper. This increase is due to the decrease in the LRO parameter, just below Tc. At 1141 K, β transforms to α. Above Tc, no LRO is present. SRO still exists but its amount decreases with the increase in temperature. Thus, with increase in temperature, above Tc, less SRO scattering sites are present, hence electrical resistivity decreases. It is pointed out that the thermal contribution would still contribute to the increase in electrical resistivity, but the SRO contribution more than compensates for the thermal contribution, so an overall decrease in the electrical resistivity is realized, above Tc.

b) Initial condition : SRO(α)

Curve 2, Figure 4.18, gives the electrical resistivity for the SRO(α) initial condition, as a function of temperature. Electrical resistivity at 376 K is 142.7 μΩ-cm. This is about 1.9 times the electrical resistivity of LRO(β) at this temperature. Electrical resistivity for SRO(α) condition is higher than that of LRO(β) condition because the SRO clusters serve as sites for scattering of electrons.

As the temperature increases, the electrical resistivity gradually increases till it reaches a maximum at ~947 K. Above this temperature, there is a decrease in the electrical resistivity. This decrease continues beyond Tc. For the explanation of this curve refer to the schematic of the contributions presented in Figure 4.19(a) and the net resistivity presented in Figure 4.19(b). There are two different contributions to electrical resistivity, for this curve. One contribution comes from the thermal scattering. This contribution goes up with temperature. The SRO contribution remains constant up to a certain temperature, but about ~100 K below Tc the contribution causes the electrical resistivity to go down due to the decrease in SRO. The net curve is a result of a superimposition of these two contributions. From room temperature to ~947 K, the thermal contribution dominates and causes the electrical resistivity to rise. Above ~947 K the SRO contribution dominates and causes a decrease in electrical resistivity.

It is pointed out that the electrical resistivity curve is similar across most of the temperature range, as compared to Lei's [26] data (refer to Figure 4.20). For Lei's data, there is an additional decrease in electrical resistivity around ~970 K, and a subsequent sharp increase in electrical resistivity just below 1141 K. This occurs due to the $\alpha \Rightarrow \beta$ transformation. Also, Lei's data shows a higher resistivity above transformation temperature, as compared to author's data. Lei's data has been taken with a heating rate of 10 K/min. Author's data was acquired for a heating rate of 50-75 K/sec. The time

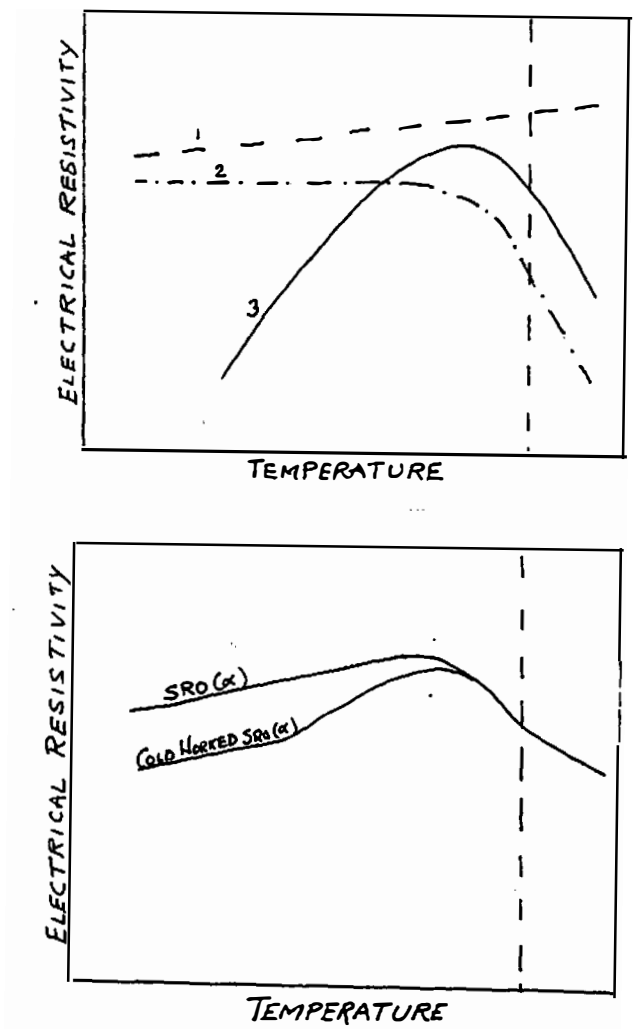


Figure 4.19 (a) Individual contributions to the overall electrical resistivity of $Ni_4Mo$, in the SRO(α) and cold-worked SRO(α) initial conditions, curve (1), thermal contribution; curve (2), contribution from the formation of SRO destroyed by cold-work; curve (3), contribution from equilibrium SRO formation. (b) Overall electrical resistivity of $Ni_4Mo$, in the SRO(α) and cold-worked SRO(α) initial conditions.

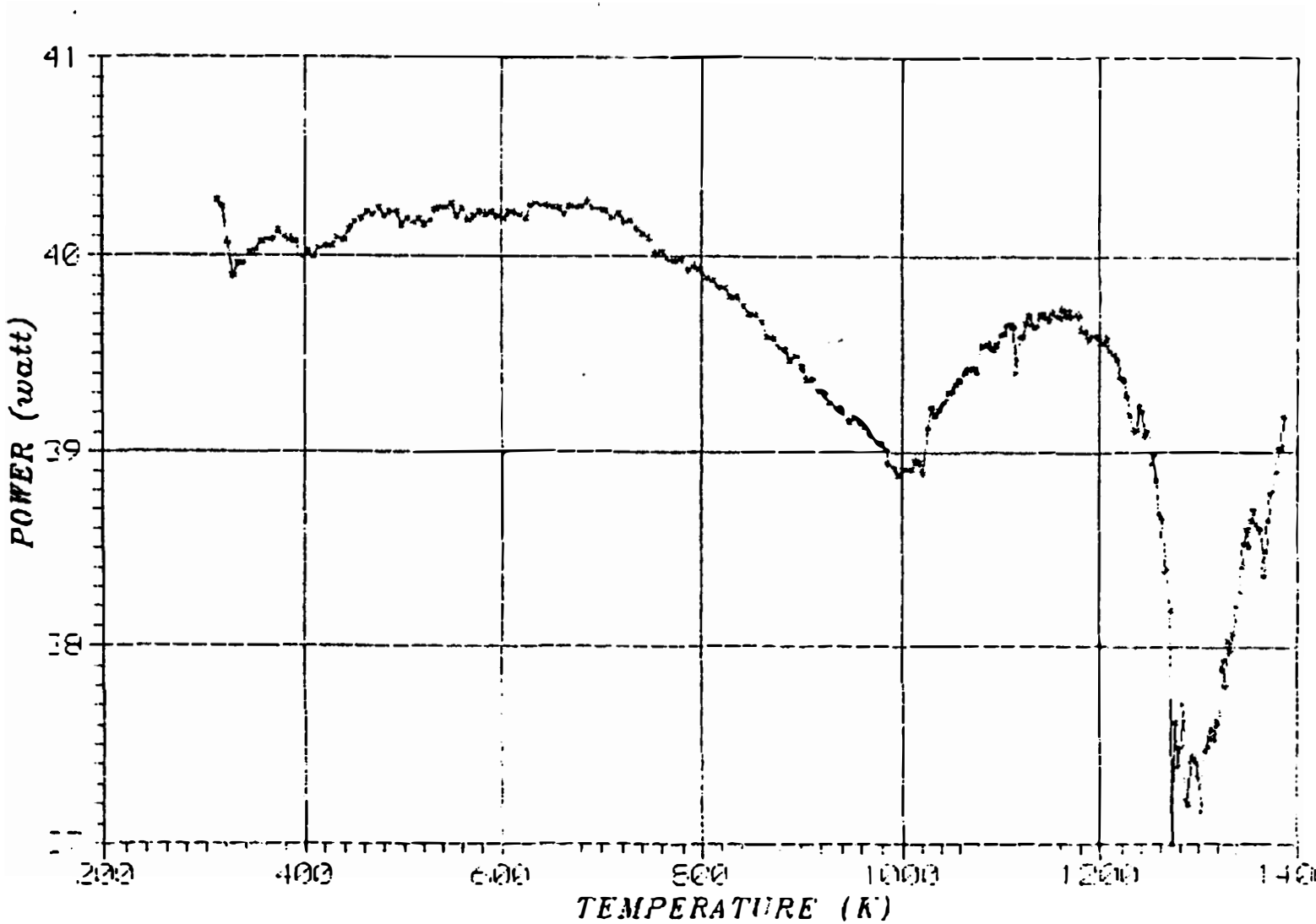


Figure 4.20 Power versus temperature plot for pulse-heating, for $Ni_4Mo$, cold-worked SRO(α) initial state. Heating rates - Lei : 10 K/min, Author : 1 K/sec.

available at this speed was not enough for the $\alpha \Rightarrow \beta$ transformation to occur. Hence its effect has not been observed in the electrical resistivity data.

c) Initial condition : cold-worked SRO($\alpha$)

Curve 3, Figure 4.18, gives the electrical resistivity for 14% cold-worked SRO($\alpha$) initial condition. The electrical resistivity at 376 K is 128.7 $\mu\Omega$-cm. This is a decrease of 14 $\mu\Omega$-cm (9.8%) in comparison to the non-cold-worked SRO($\alpha$) initial condition. This is attributed to the breakdown of the SRO clusters which more than compensates for the increase in electrical resistivity due to electron scattering from defects.

As the temperature rises, the electrical resistivity increases. The rise is gradual at first, up to ~690 K, thereafter there is an increase in the slope until it reaches a maximum, and then decreases and the curve merges with curves 1 and 2. It is believed that at least three different contributions play a role in determining the nature of the curve. These contributions are presented as schematic curves in Figure 4.19(a) and the net resistivity is plotted in Figure 4.19(b). Up to about ~690K, thermal scattering dominates and there is a gradual increase in electrical resistivity with temperature. Between ~690 K and ~1000 K, there is a further increase in electrical resistivity due to the increase in SRO over the initially cold-worked structure [19]. Beyond ~1000 K, the dominance is from the decrease in the degree of SRO with the increase in temperature. The decrease in SRO causes

the electrical resistivity to come down smoothly and join curve 2 (in Figure 4.18) below Tc and then curve 1, at Tc. Above transformation temperature, the structure is SRO(α), irrespective of the initial condition. So, curves 1, 2 and 3 become the same curve.

The effect of recovery and recrystallization on electrical resistivity also needs to be addressed. For the 14% cold-worked SRO(α) alloy, recovery and recrystallization would contribute to the decrease in electrical resistivity due to the removal of defects. Once the recrystallized grains form, there is a potential for SRO to form in the recrystallized grains, since it is thermodynamically stable at this temperature. It will actually form at the temperature where it is kinetically favorable. The formation of SRO clusters will have an effect in increasing the electrical resistivity.

By observing the curve (Figure 4.18) for cold-worked SRO(α) initial condition, the occurrence of recovery or recrystallization is not evident. It is pointed out here that the amount of cold-work was only 14%. However, from the power versus temperature plot (Figure 4.20), it is clear that recovery and recrystallization do occur. The two dips in the power versus temperature curve indicates that there is a release of heat associated with these processes. The fact that these dips disappear on annealing from subsequent runs show that these dips are indeed due to recovery and recrystallization. Several different effects contribute to the electrical resistivity at the same time and it is concluded that the effect of the other

contributions at least partially masks the effect of recovery and recrystallization.

Results of slow heating on SRO(α)

The electrical resistivity data presented thus far are for heating rates of approximately 50-75 K/sec. This speed is too high to get data for equilibrium resistivity. Lei's [26] data were taken using a heating rate of 10 K/min. A comparison of author's data and Lei's [26] data is presented in Figure 4.21. In the current research an experiment was designed to check whether a relatively slow heating rate, as compared to the heating rates for pulse heating, could 'capture' the minima in the electrical resistivity curve. The result of this experiment is shown in Figure 4.22 and 4.23. Figure 4.22 shows the electrical resistivity as a function of thermal emf. The slow heating, 1 K/sec, was slow enough to allow the curve to come nearer to its equilibrium value. The minima occurs around 1090 K, which is consistent with Lei's [26] data. The corresponding power versus temperature curve is plotted in Figure 4.23. This curve shows a dip near the transformation temperature, which indicates that energy is released in the $\alpha \Rightarrow \beta$ transformation. If the power losses can be estimated, then the energy released during the transformation can be calculated from this curve.

Coming back to Figure 4.21, author's data for electrical resistivity for SRO(α) initial condition lies below that of Lei's [26] data because author's specimen was air-cooled from the α-region to

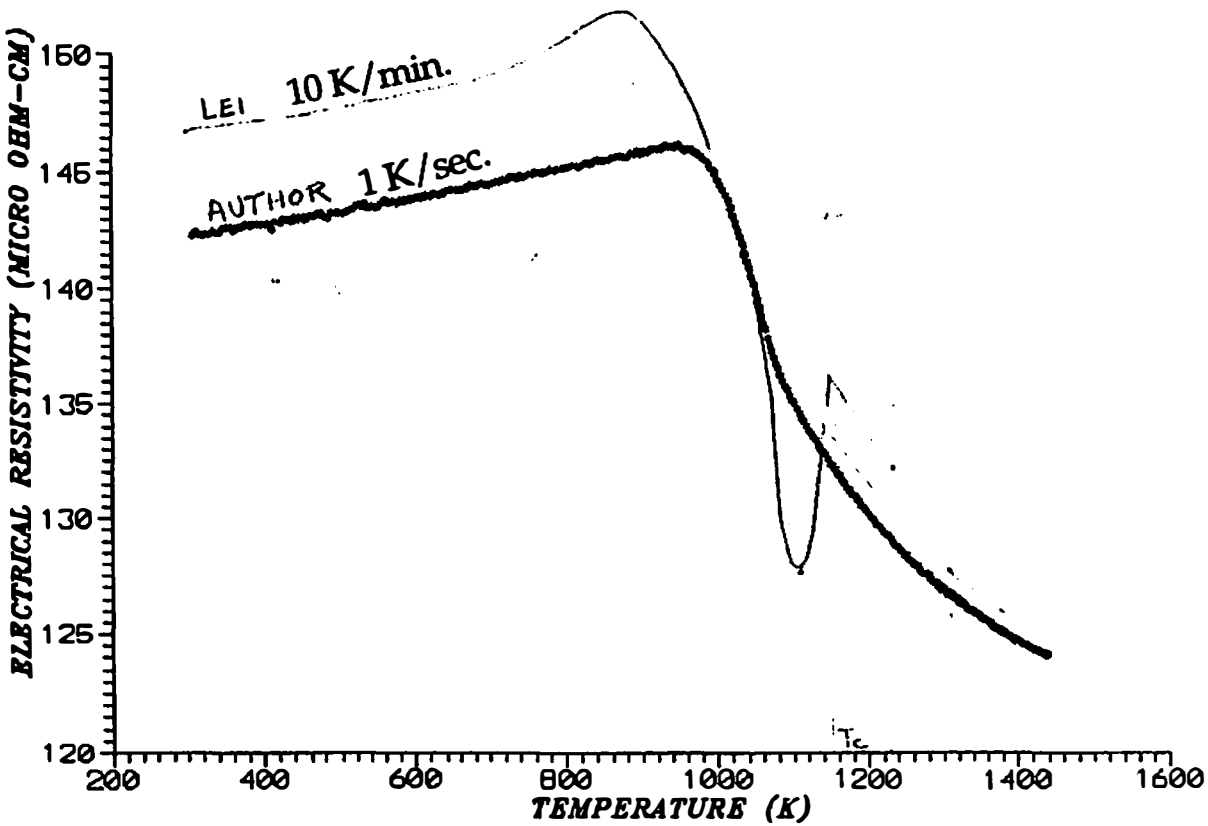


Figure 4.21 Comparison of author's data for the electrical resistivity of $Ni_4Mo$, SRO($\alpha$) initial condition, with that of Lei [26].

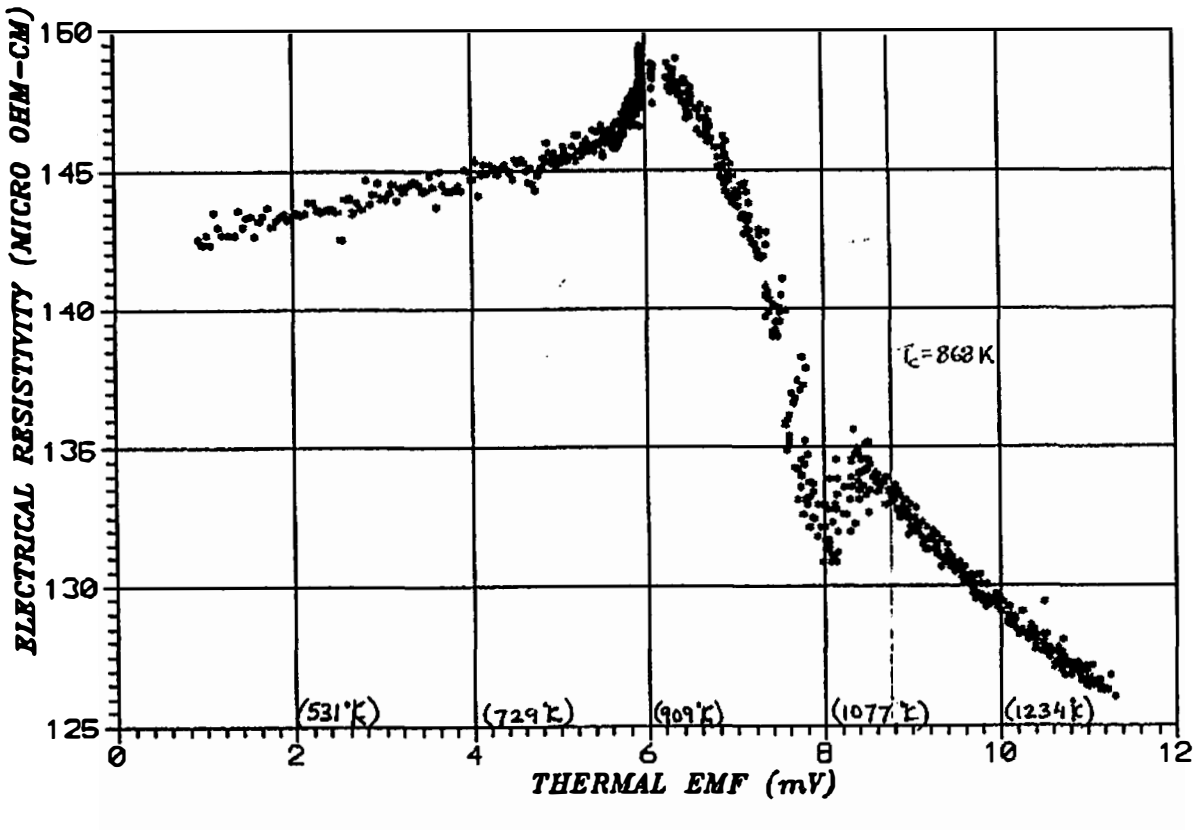


Figure 4.22 Electrical resistivity versus temperature plot for $Ni_4Mo$, for slow heating (average heating rate, 1 K/sec.).

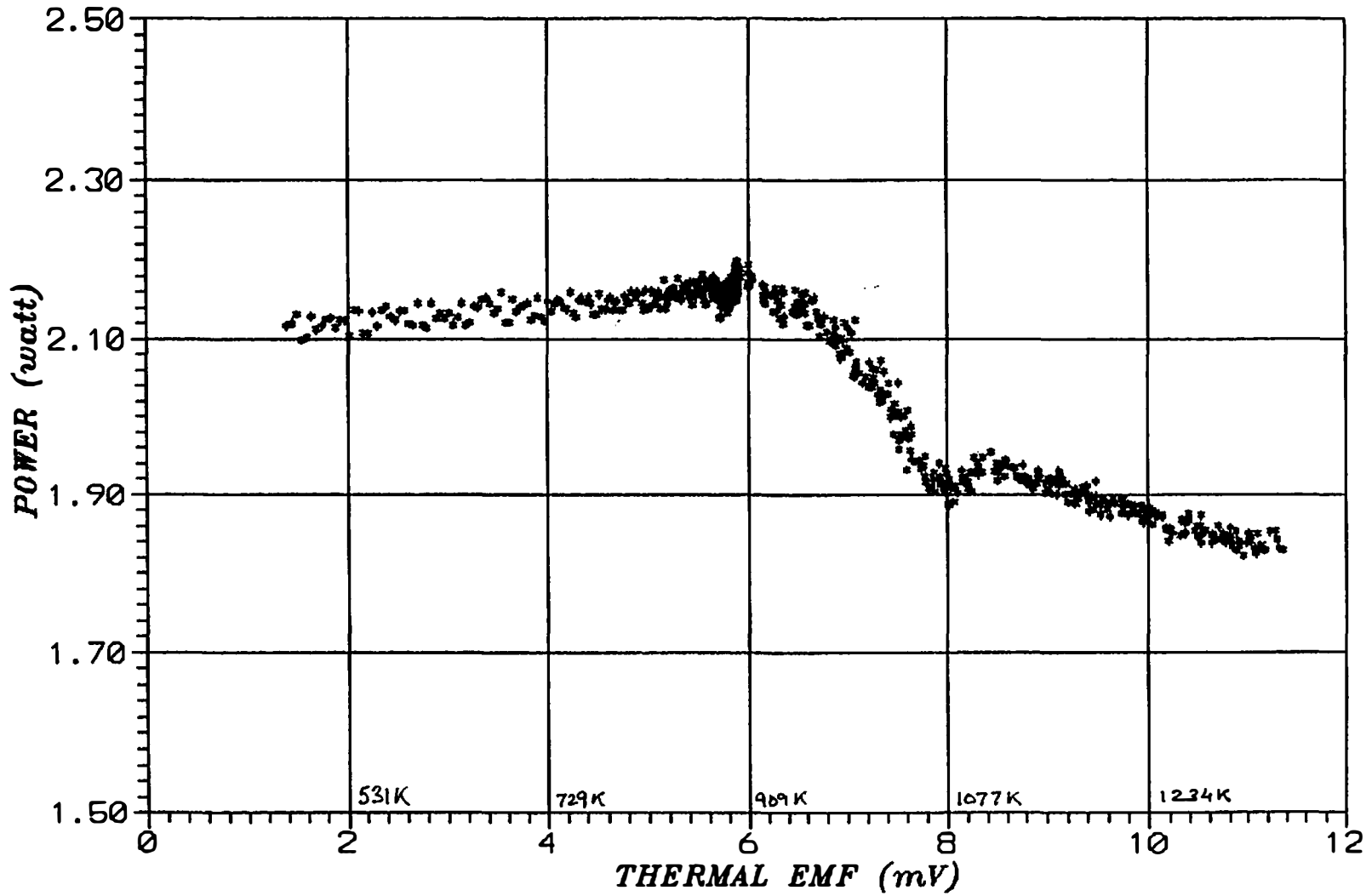


Figure 4.23 Power versus temperature plot for $Ni_4Mo$, for slow heating (average heating rate, 1 K/sec.).

room temperature while Lei's [26] specimen was quenched from the α-region. Thus, Lei's [26] specimen retained more SRO(α) at room temperature and had a higher electrical resistivity up to about 1000 K. Above Tc, Lei's [26] data is higher than the author's data. Due to the fast heating, author's specimen did not reach the equilibrium condition in the short heating time, e.g., 15 sec., hence the discrepancy. It is also pointed out that the electrical resistivity obtained by the author by using a relatively slow technique (1 K/sec.) lies between Lei's [26] data and the author's pulse data. This shows that with slower heating the data tends towards equilibrium values.

## SPECIFIC HEAT

### a) Initial condition : LRO(β)

The specific heat of $Ni_4Mo$, LRO(β), as a function of temperature, is presented in Figure 4.24 along with the data for the SRO(α) initial state. On heating from room temperature, the specific heat rises gradually to about 1000 K, thereafter it rises very sharply, due to LRO(β)⇒SRO(α) transformation. Above the critical temperature, the curve comes down sharply at first and then rises again, merging with the specific heat curve for SRO(α) initial condition, which will be discussed next. This is as expected, because, above Tc, the structure is all α, for both cases.

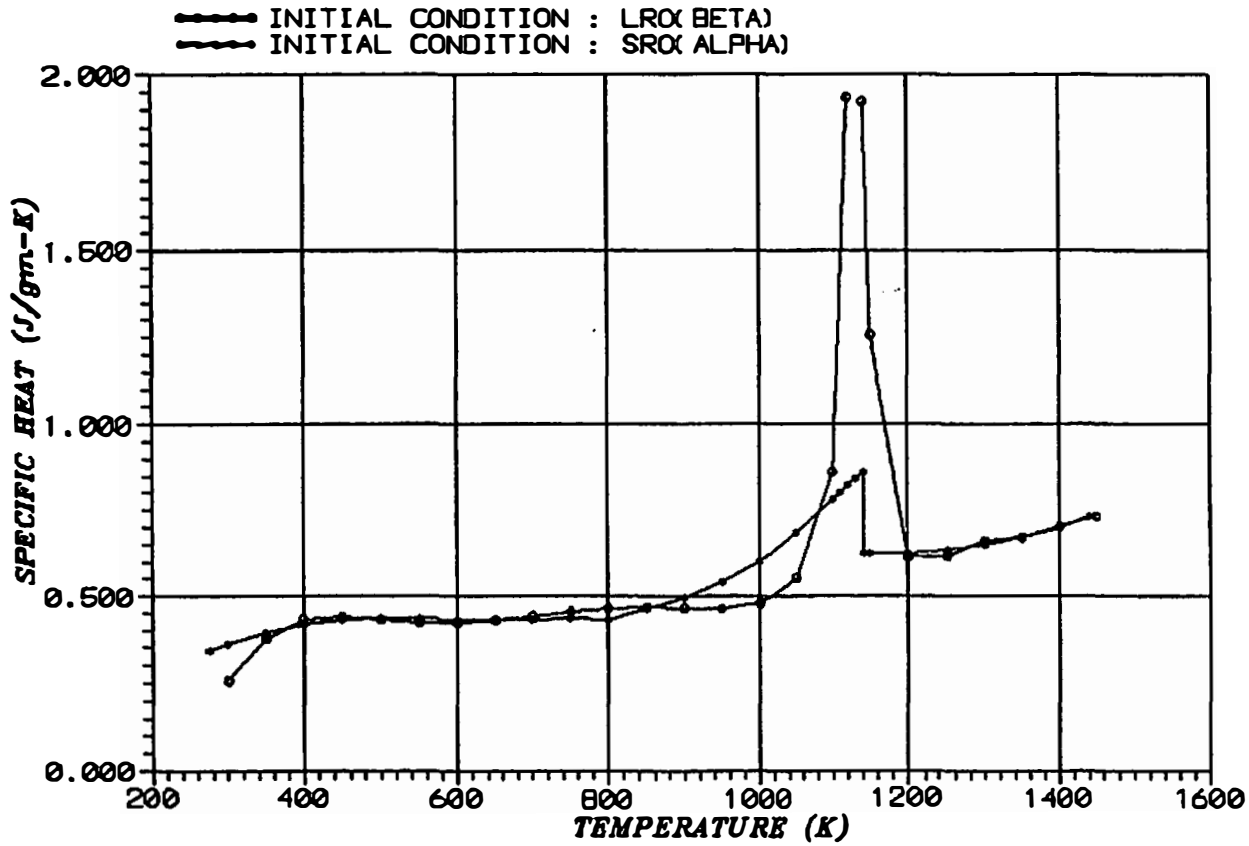


Figure 4.24 Specific heat versus temperature plot for $Ni_4Mo$, for two initial conditions, SRO($\alpha$) and LRO($\beta$).

b) Initial condition : SRO(α)

The specific heat for the SRO(α) initial condition has similar slope as that for LRO(β) up to about 850 K, whereafter there is an increase in the slope. However, the specific heat does not rise to a value as high as that for the LRO(β) initial condition, at Tc. The magnitude of the discontinuity is less. Above Tc, both curves become the same because the specimen consists of all SRO(α) for both cases.

COMMENT ON P-T AND T-t CURVES.

Electrical resistivity and specific heat data were presented in the preceding section as a part of the final results. To arrive at the determined value of specific heat, P versus T and T versus t are two data plots which are utilized. To give an idea to the reader about the nature of these plots, the P versus T and T versus t plots are presented for the cold-worked SRO(α) initial condition, in Figures 4.20 and 4.25 respectively. The two minima in the power versus temperature curve are very pronounced. It is believed that the first minima is associated with recovery and the second with recrystallization of the cold-worked matrix. It can be confirmed from this figure that energy is released upon annealing, in two distinct stages. From the corresponding P versus t plot, the magnitude of the energy released can be calculated. However, a baseline for the calculation of area under the curve is required. Also, estimation of heat loss during the processes poses a problem. However, the

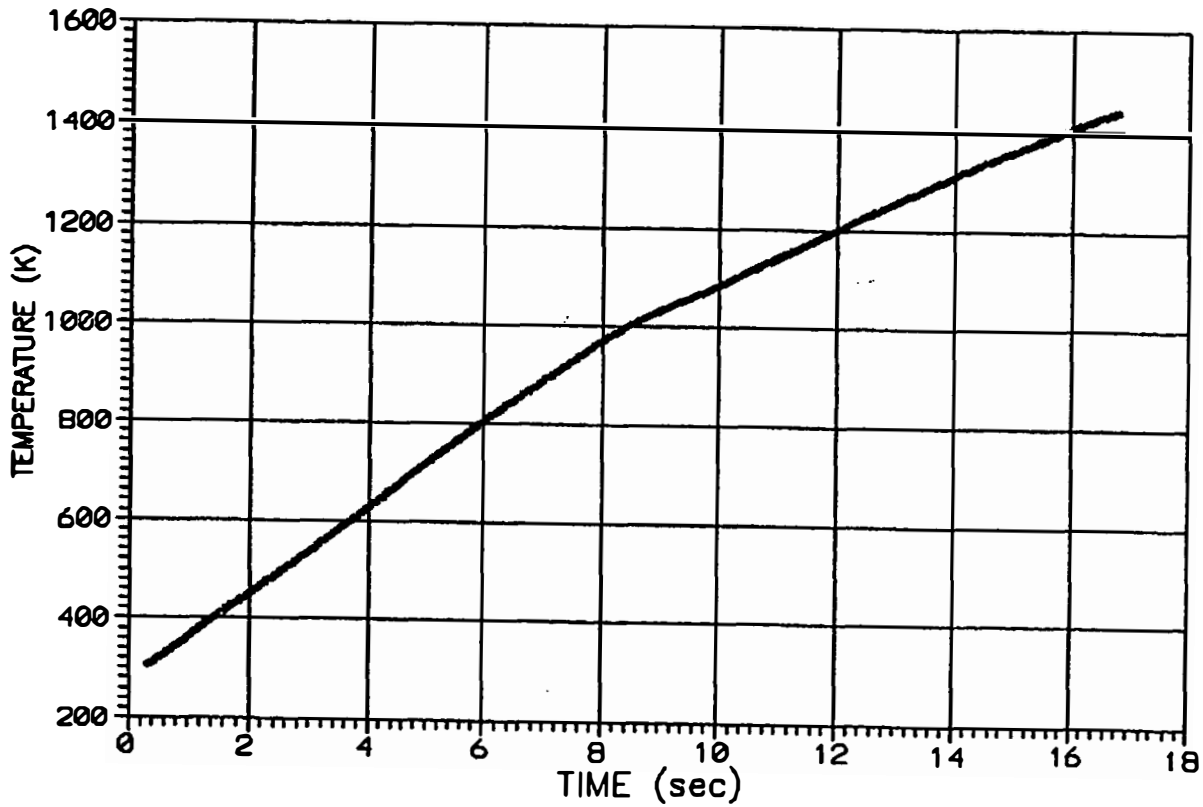


Figure 4.25 Temperature versus time plot for pulse-heating, for $Ni_4Mo$, cold-worked SRO($\alpha$) initial state.

relative magnitude of the energy released has been estimated. It is found out from the ratio of the area measurement that the energy released during recrystallization is about 1.6 times the energy released during recovery.

Figure 4.25 shows the temperature versus time data for cold-worked SRO(α) initial condition. The temperature of the specimen increases steadily with time. Though difficult to notice at this resolution, there are two points where there are breaks in this curve, one at ~1000 K and the other at ~1040 K. It is believed that the change in the degree of SRO causes this slight change in the rate of heating.

## ISOTHERMAL EXPERIMENTS

Isothermal tests were conducted on steel specimen and on the $Ni_4Mo$ specimen. The steel specimen was used initially to design and test the PID computer program. A brief discussion of the results with the steel specimen is included followed by the isothermal test results with the $Ni_4Mo$ specimen.

### STEEL

Figure 4.26 shows the thermal emf as a function of time for an isothermal run. The steel specimen was held isothermally at 660 °C for more than 30 min. The temperature control obtained was better

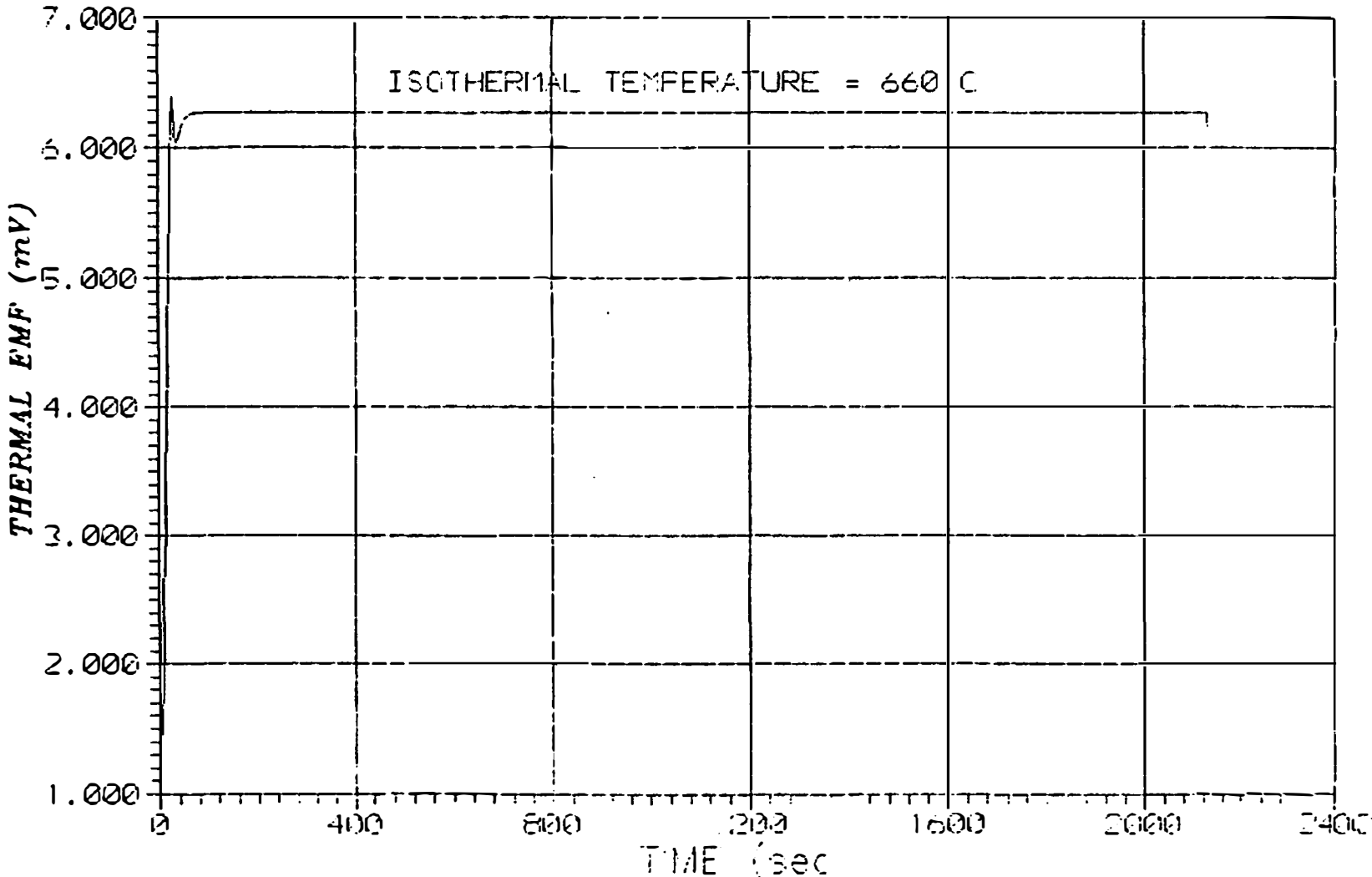


Figure 4.26 Thermal emf versus time plot for isothermal holding of steel specimen at 600 °C.

than ±0.5 °C. It can be seen from Figure 4.27 that the electrical resistivity decreases at first. This is believed to be due to the recovery process and partly due to the recrystallization of the cold-worked matrix. It is also observed that the electrical resistivity increases subsequently and remains more or less constant. This is believed to be due to the formation of precipitates. The decrease in electrical resistivity associated with recrystallization has been partially masked by the precipitation.

## $Ni_4Mo$

In addition to the numerous continuous heating experiments done on $Ni_4Mo$, a few isothermal experiments were conducted. Figure 4.28 shows the electrical resistivity versus time data for isothermal runs, one at 700 °C and the other at 750 °C. The specimen was first held at 950 °C, in the α range, for 10 min. This results in α in the microstructure. Then it was naturally cooled (5 K/sec) to a lower temperature, i.e., 750 °C, and held there for 20 min. During the isothermal holding, α transforms to β. An example of the heating scheme is shown in Figure 4.29. Coming back to Figure 4.28, in the first 10 min. the electrical resistivity remains constant at 950 °C (near 129 μΩ-cm). On cooling to the lower temperature, the electrical resistivity sharply increases . This is because the degree of SRO is more around 700-750 °C than at 950 °C. On isothermal holding, the electrical resistivity starts decreasing at a certain time. This is the

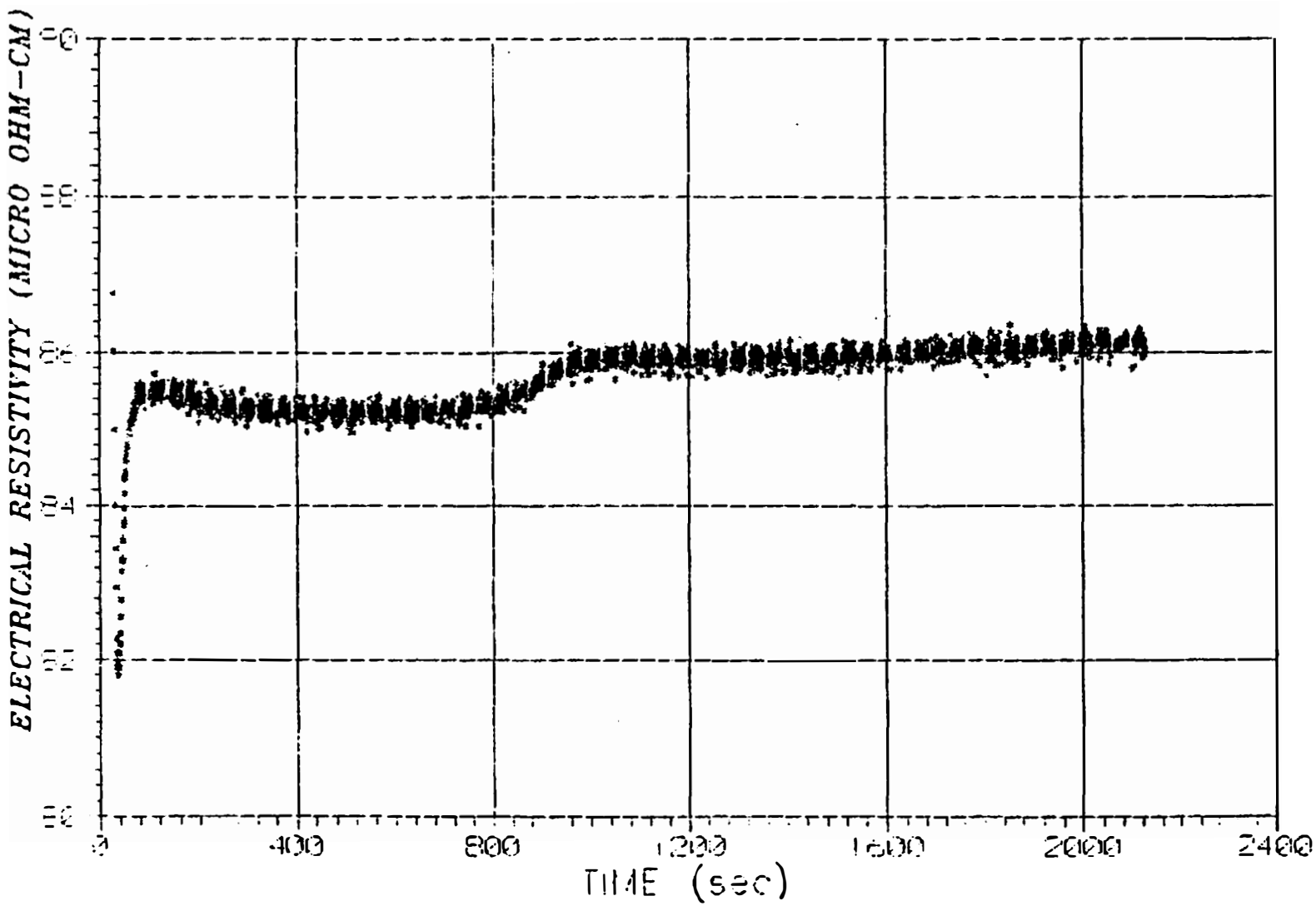


Figure 4.27 Electrical resistivity versus time plot for isothermal holding of steel specimen at 600 °C.

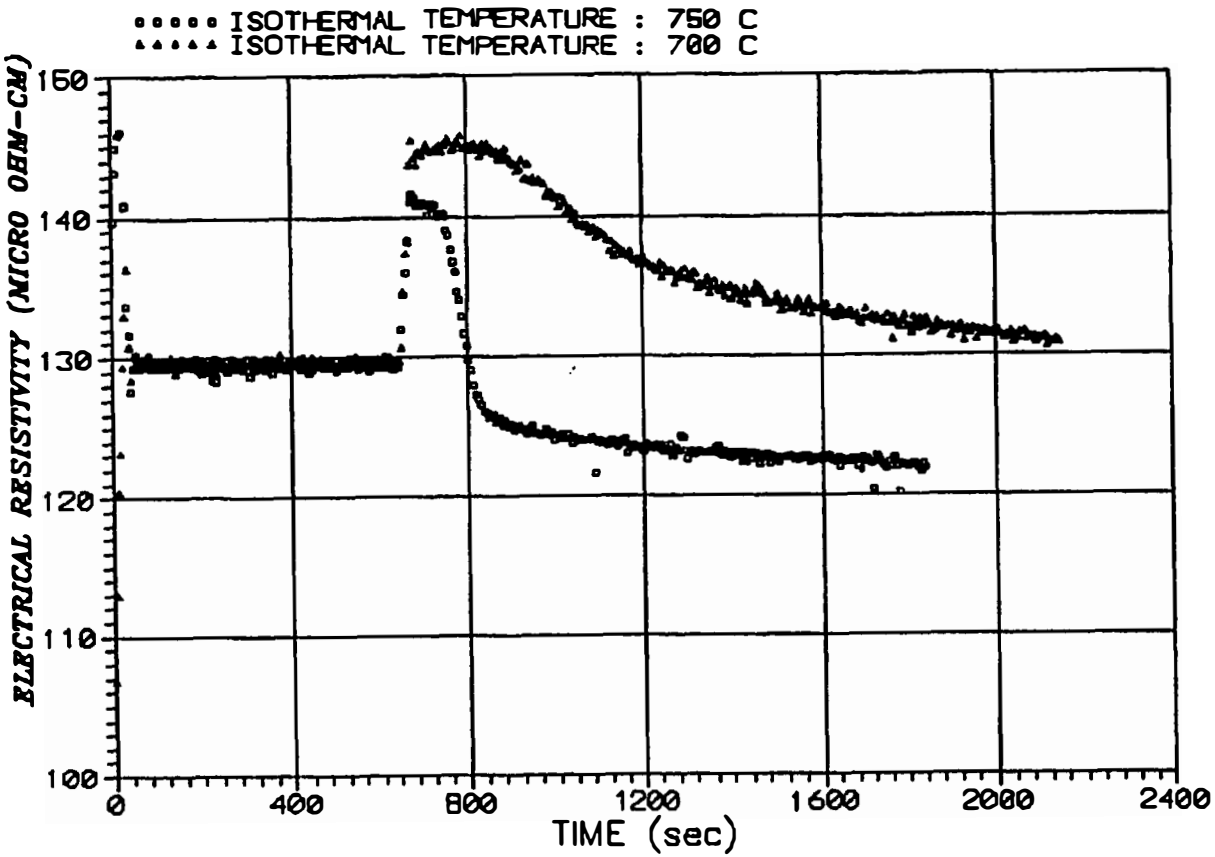


Figure 4.28 Electrical resistivity versus time plots for isothermal holding of $Ni_4Mo$ specimen at 700 °C and 750 °C.

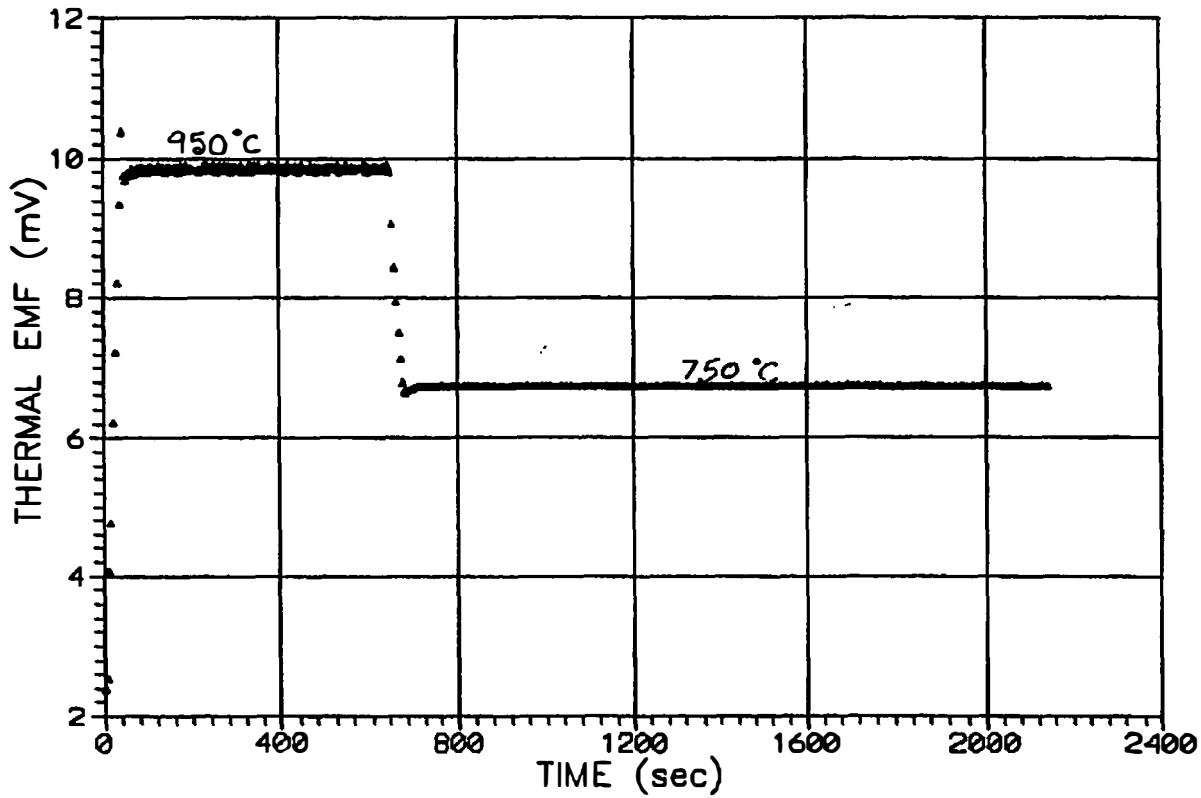


Figure 4.29 Thermal emf versus time history for initial isothermal holding of $Ni_4Mo$ specimen at 950 °C and second isothermal holding at 750 °C.

start time of $\alpha \Rightarrow \beta$ transformation. The decrease in electrical resistivity corresponds to the disappearance of SRO with progressive $\alpha \Rightarrow \beta$ transformation. The end time of $\alpha \Rightarrow \beta$ transformation corresponds to the time at which the electrical resistivity becomes more or less constant.

Due to the fluctuation in power during the isothermal experiment, the power versus time profile could not be generated, during the transformation. So, the heat released could not be estimated. The fluctuation in the power is shown in Figure 4.30.

It can be observed from the figure that both start time and end time for holding at 700 °C (973 K) is longer than those for holding at 750 °C (1023 K). This is consistent with the TTT diagram for $\alpha \Rightarrow \beta$ transformation. The start time determined from the electrical resistivity data is 290 sec for 700 °C and 120 sec. for 750 °C. The start times predicted by the TTT diagram, presented in Figure 4.31, are 300 sec. for 700 °C and 90 sec. for 750 °C. The end times could not be determined from the resistivity curves as the resistivity values had not become constant at the end of the experiment. So, the end times have not been compared.

If isothermal experiments are repeated at several different temperatures, the TTT diagram for the $\alpha \rightarrow \beta$ reaction can be constructed.

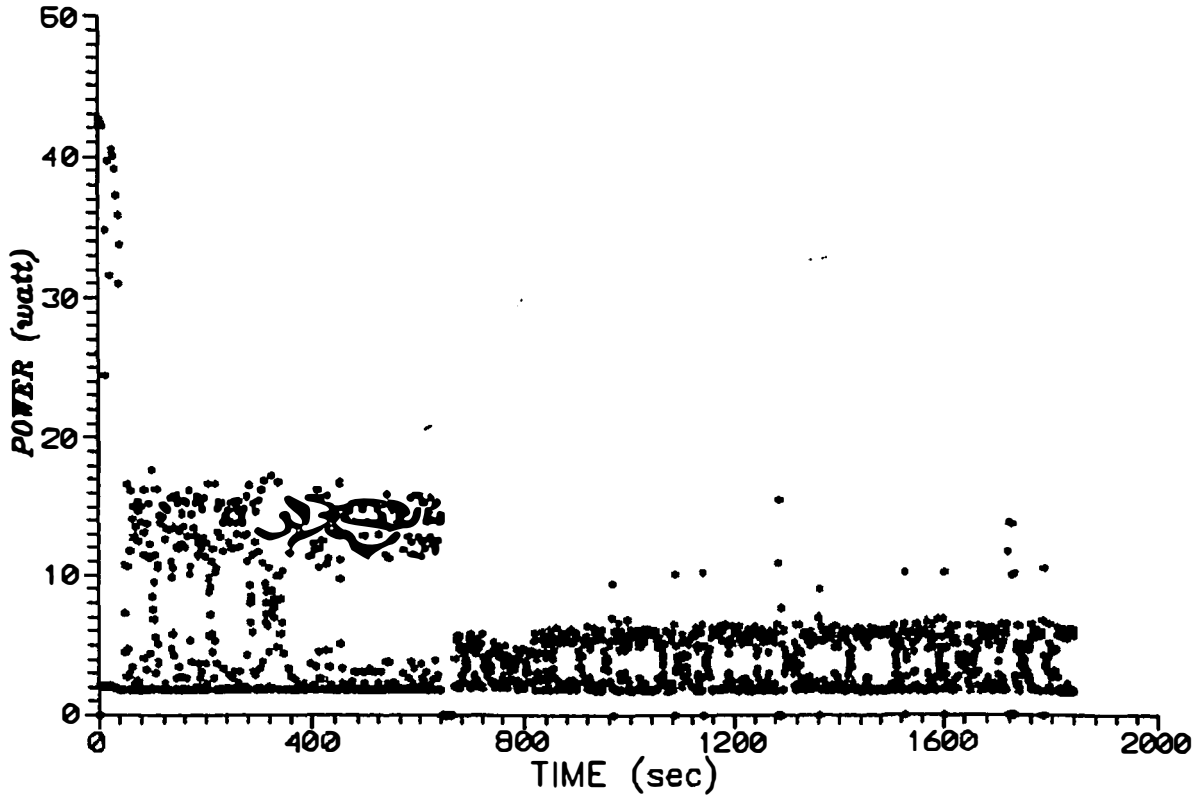


Figure 4.30 Power versus time data during isothermal holding of $Ni_4Mo$ at 700 °C.

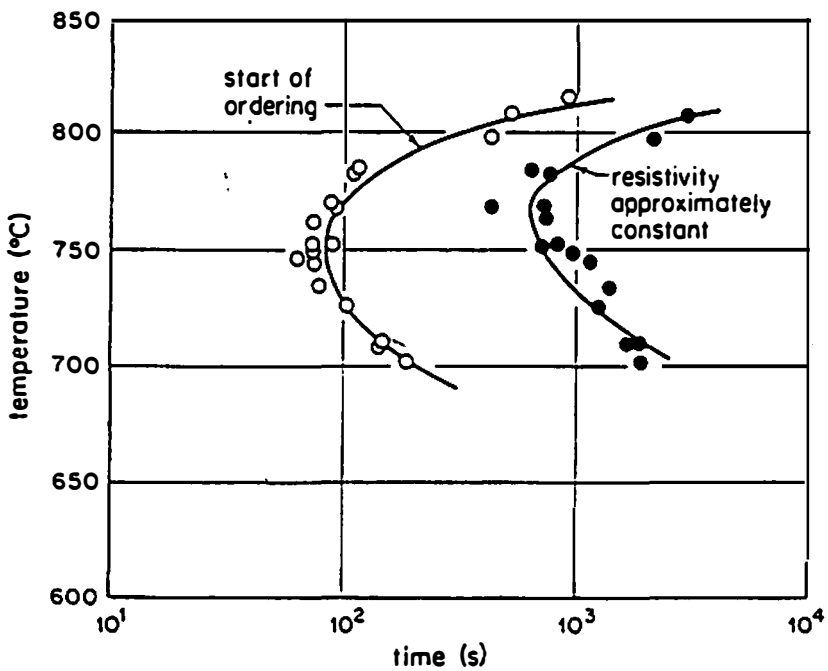


Figure 4.31 Isothermal temperature-time-transformation (TTT) diagram for the $\alpha \Rightarrow \beta$ transformation in $Ni_4Mo$.

# ERROR ANALYSIS

The total error in the calculated specific heat at any temperature is due to the combined effects of errors accruing from experimental and physical factors. Some of the important factors which can significantly affect the accuracy of the calculated specific heat are discussed in the next few paragraphs.

## ERROR IN MASS

Mass of the specimen, m, can be expressed as $m=\rho \pi d^2 l/4$. To find out the total error in mass, the errors in l, $d^2$, and $\rho$ need to be estimated and summed up. The $Ni_4Mo$ specimen, NIC, will be taken as a specific example.

## ERROR IN THE MEASURED EFFECTIVE LENGTH

The maximum error in measured effective length is estimated below. The effective length is measured with the knife-edge apparatus described in Chapter III. A Leeds and Northrup DVM was used for this measurement. The maximum error in the measured voltage signal, at 25 °C, has been specified by the manufacturer to be 0.004%.

The accuracy of measurement of the knife-edge separation distance is estimated to be 0.04%, as described below. A Scherr-Tumico traversing optical microscope, in the Mechanical Engineering

Department of the University of Tennessee, Knoxville, was used to measure the separation between the two edges of the knife-edge. Gauge blocks were used to calibrate the traversing optical microscope. The accuracy in the measured edge-to-edge distance of the gauge blocks lies between +0.000004 in/in and - 0.000002 in/in.

Six readings for knife-edge #3 (large) were taken. The values ranged from 3.0324 in. to 3.0335 in. Maximum scatter in the measurement was $= \frac{3.0335-3.0324}{3.0324} X100$

$= 0.04\%$

Delta ($\Delta$) of a certain quantity, in the equation below, represents the error in that quantity. The error in the measured length, $\Delta l_t$, is estimated as follows,

$$\frac{l_t}{l_k} = \frac{E_t}{E_k}$$

$$\Delta l_t = \Delta E_t + \Delta E_k + \Delta l_k$$

$$= 0.004\% + 0.004\% + 0.04\%$$

$$= 0.048\% \cong 0.05\%$$

ERROR IN DIAMETER

The ten individual measurements of diameter are tabulated in Table 3.2. The arithmetic mean of the measured diameter is 0.0700 in. Variance can be calculated from the formula v= , where v is variance, $y_{var}$ is dependent variable, y is arithmetic mean and n is the number of data points.

$$v = = \frac{4(0.0701-0.0700)^2}{10-1}$$

$$= 4.44 \times 10^{-9}$$

If the error in the measured diameter is random, then 95.45 % of the data will fall between $2\sigma$, where $\sigma$ is the standard deviation. This can be inferred from the standard normal curve [46]. The standard deviation can be calculated from the relation

$\sigma = = = 9.52 \times 10^{-4}$

Therefore, $\sigma \times 100\% = 0.09\%$. So, $2\sigma \times 100\% = 0.18\%$. Since, the d term arrears as a square in the mass equation, the error in $d^2$ will be $4\sigma \times 100\% = 0.36\% \cong 0.4\%$. This is the error in mass due to the scatter in the diameter.

The density has been calculated from the knowledge of the crystal structure and lattice parameters of the $Ni_4Mo$ unit cell. The calculation is provided in Appendix II. The density has not been corrected for either temperature or for the change in crystal structure. The maximum error in the calculated density is estimated to be 0.15%.

If the error in length (0.05 %), the error in diameter (0.4 %) and the error in the density (0.15%) add up in the same direction, the calculated mass can be in error by about = 0.6%.

## ERROR IN I, E AND T CHANNELS

The accuracy in the signals for I, E and T channels is limited by the resolution of the A/D converter. For the current channel the voltage drop across the standard resistor is measured, for the voltage channel, the voltage drop across the voltage taps is measured, and for the temperature channel the thermal emf from the thermocouple is measured.

These signals are then sent to the amplifiers, where they are amplified by a certain gain, e.g., 20, 500. Thereafter, they are sent to the A/D converter, which converts the analog signals to digital counts. The digital signals are then acquired into the computer program. The accuracy of these signals depend on the accuracy of the specified gain of the amplifier and the resolution of the A/D converters. The A/D converters used were 12 bit converters. A full scale reading of 10 V corresponds to $2^{12} = 4096$ digital counts. 4096 counts corresponds to 10 V, hence 1 count corresponds to 2.44 mV.

Let's take a typical example. A typical voltage coming into the amplifier, for the voltage channel, is 0.2 V. The gain setting for the voltage channel is 10. Thus, 2 V (0.2 V x 10) signal would be coming at the input of the A/D converter. The percentage error due to the resolution limitation would be $(2.44 \times 10^{-3} / 2) \times 100 \cong 0.1\%$.

The amplifiers have been calibrated several times. A calibration result shows the percentage error in the gains to be 0.01%, 0.02%, 0.01%, in the current, voltage and temperature channels respectively.

These values are lower than the error accruing from the resolution of the A/D converters. Thus the maximum error in the current and voltage channel would be ~0.1%.

For the temperature channel, in addition to the ~0.1% error accruing from the A/D converter resolution, there will be an error due to the usage of uncalibrated thermocouples. An error in temperature reading of about 2 K is expected [47], due to this. This would result in an error of about 0.4% at 500 K. The total error in temperature is thus 0.1% + 0.4% = 0.5%.

Error in dT/dt

The accuracy of dT/dt is most elusive [4]. The factors which can affect the determined slope can be grouped into the following categories.

1) Error in temperature measurement.

2) Error in time measurement.

3) Statistical error associated with fitting dT/dt = f(T) data.

The previous section discussed the factors which affect the error in determined temperature. The error in determined temperature causes the T=f(t) curve to shift higher or lower. Due to this shift the slope at a slightly different temperature (e.g., 2 K) will be calculated. From a practical standpoint, however, this error in slope will be small because the error in temperature will not change the curvature of the T=f(t) curve to any appreciable extent. Typical

dT/dt versus T curves show that a typical error in slope due to an error in temperature of ±2 K is about 0.08%.

The computer clock is very accurate and the data points for time are not affected to the extent that an error in time can affect the accuracy in dT/dt significantly.

There is a statistical error associated with fitting dT/dt data. The reader is reminded here that the T data have first been fitted versus time to obtain the T=f(t) relation. Then, the dT/dt=f(t) function has been determined by differentiating the T=f(t) function. However, finally the dT/dt=f(T) function is required. So, the dT/dt data have been fitted against smoothed T data. Since both T and dT/dt data have been smoothed by polynomials first, the data points for dT/dt=f(T) should lie on a smooth curve. But, depending on the nature of fitting the dT/dt=f(T) data, there may be small statistical error. Based on a mean temperature of 500 K, the percentage error due to this is 0.01 %. This value has been arrived at by dividing the square root of Sum of the Residuals of fit for the function by the slope at 500 K.

## Summary of Errors

The errors are now summarized and are finally used to estimate the error in electrical resistivity and specific heat.

Error in Mass: 0.05%+0.4%+0.15%= 0.6%

Error in Current: 0.1%

Error in Voltage: 0.1%

Error in Temperature: 0.1%+0.4% = 0.5%

Error in dT/dt : 0.08%+0.01% = 0.09% ≅ 0.10%

Table 4.1 Estimated errors in the quantities that are used to determine the specific heat.

| Quantities | Percentage Error |
|---|---|
| Mass (m) | 0.45% |
| Current (I) | 0.1 % |
| Voltage (E) | 0.1% |
| Temperature (T) | 0.5 % |
| Slope (dT/dt) | 0.1% |

From Table 4.1, the errors in the measured specific heat and electrical resistivity is calculated, as given below. The error in the slope during cooling will be neglected in this estimation because typically the slope during heating, e.g., 75 K/sec., is much higher than the slope during cooling, e.g., 0.2 K/sec., or $\Delta(dT/dt)_H >> \Delta(dT/dt)_C$

$$C_p = \frac{4 E I}{\rho \pi d^2 l \left[\frac{dT}{dt_H} - \frac{dT}{dt_C}\right]}$$

$$\Delta Cp = \Delta E+\Delta I+\Delta m+\Delta(dT/dt)$$

$$= 0.1\%+0.1\%+0.6\%+0.1\%$$

$$\cong 0.9\% \text{ (error in the determined specific heat)}$$

$$\rho = \frac{E}{I}\frac{\pi}{4}\frac{d^2}{l}$$

$$\Delta\rho = 2\Delta d+\Delta l+\Delta E+\Delta I$$

$$= 2 \times 0.18\%+0.05\%+0.1\%+0.1\%$$

$$\cong 0.6\% \text{ (error in the determined electrical resistivity)}$$

## REPEATABILITY

In this section, the repeatability of the specific heat and the electrical resistivity data is shown. Figure 4.32 shows the agreement in the electrical resistivity data for $Ni_4Mo$, for the SRO($\alpha$) initial condition, for two identical runs. These runs have been made with the same experimental parameters. The runs also had the same heating rates. The agreement is good throughout the entire testing range, the average deviation from each other being 0.05%.

The specific heat data determined from the same two runs have been presented in Figure 4.33. As pointed out, these runs were made with identical experimental parameters. Again, the agreement in general is good. The maximum deviation is at lower temperatures and just above Tc. The maximum deviation in the data for the two runs is 2%.

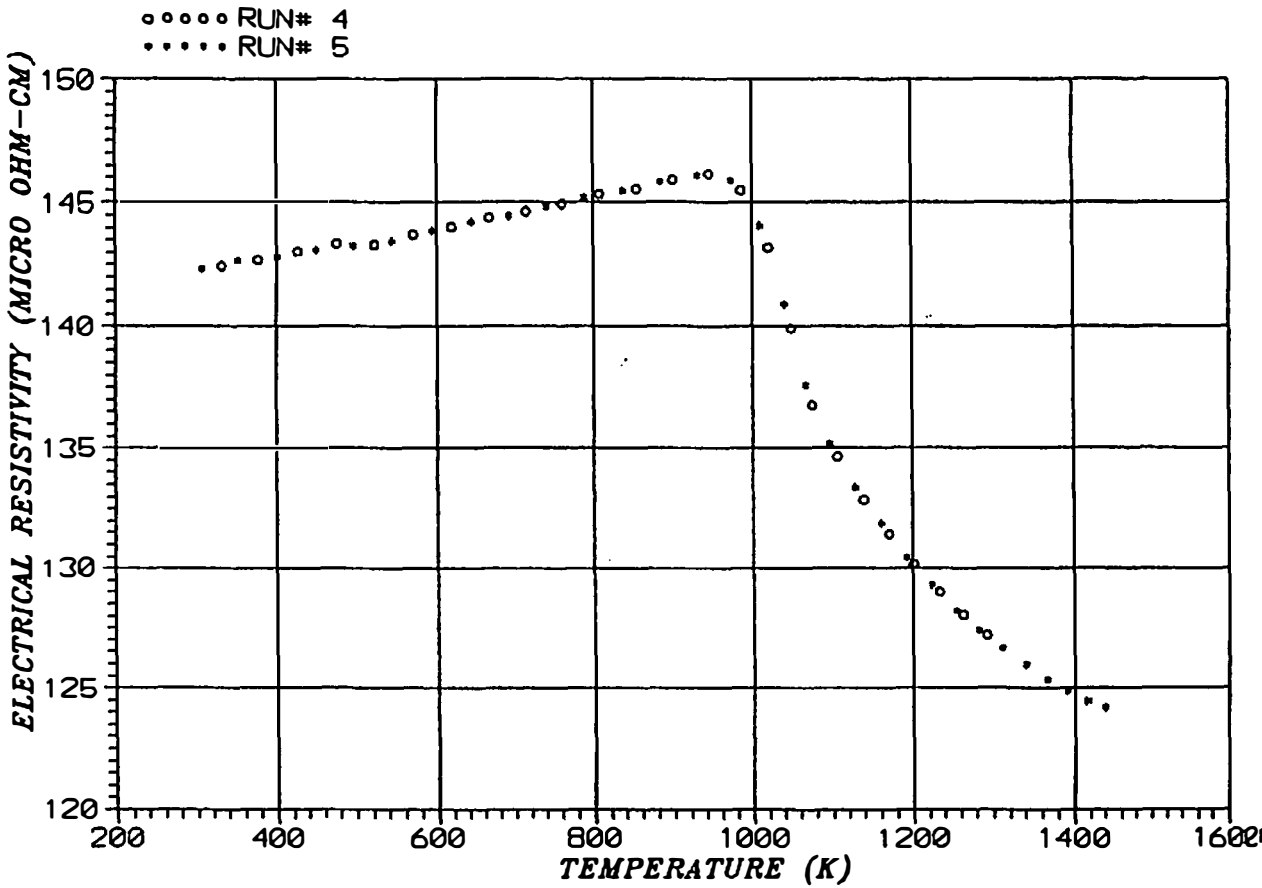


Figure 4.32 Electrical resistivity data from two runs with identical test parameters.

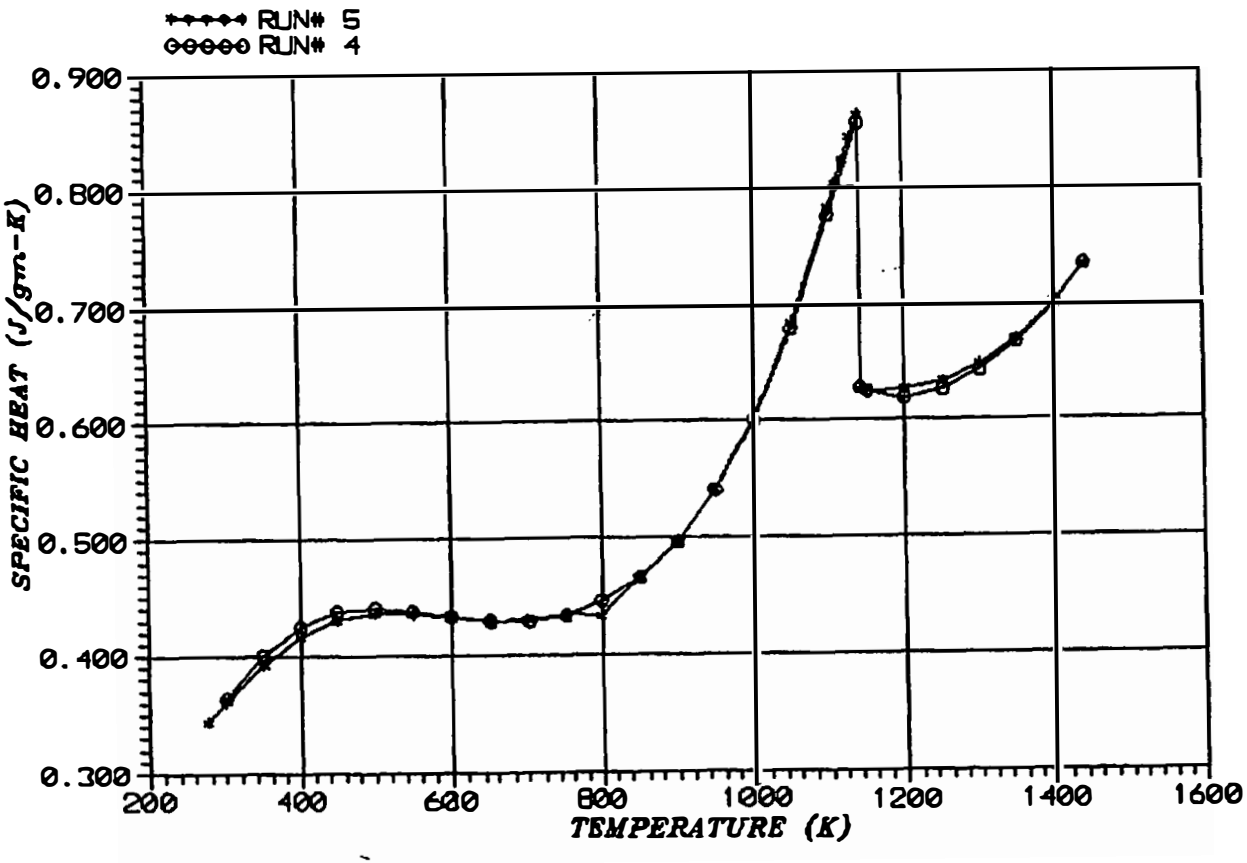


Figure 4.33 Specific heat data from two runs with identical test parameters.

# CONCLUSIONS AND RECOMMENDATIONS

## CONCLUSIONS

1) Pulse calorimetry is an effective technique to determine the specific heat of electrical conductors, e.g., metals and alloys, for a wide range of temperatures. The main advantage of this technique is the relatively fast heating, e.g., 75 K/sec., of the specimen, which keeps the specimen from being exposed to elevated temperatures for an extended period of time. The raw data acquired for specific heat can also be used to calculate the electrical resistivity.

2) Pulse calorimetry has been used as an instrument to detect phase changes in materials, e.g., magnetic change, B2⇒DO3 and order-disorder. By studying the electrical resistivity versus temperature and power versus temperature curves, the temperature range of occurrence of these changes can be determined. In addition changes in specific heat can also serve as a tool to locate certain phase changes.

3) Pulse calorimetry has been used as an instrument to detect the formation of certain types of defects, e.g., constitutional defects, which occur in certain alloys, e.g., FeAl. The presence of these defects affects the electrical resistivity and specific heat versus temperature curve. By studying the change in electrical resistivity

and specific heat, the temperature of formation of these defects can be identified.

4) The pulse-calorimeter used in this research was tested initially with pure nickel as the specimen. The electrical resistivity and specific heat data were compared to those of an earlier investigator. Average disagreement in electrical resistivity was <1% and in specific heat was <2%.

5) Four different Fe-Al specimens were studied. They had compositions ranging from 8.5wt%Al to 21.2wt%Al. For the 21.2wt%Al alloy, the electrical resistivity shows a sharp change in slope at ~650 K. The specific heat shows a point of inflexion at the same temperature. It is believed that these changes are due to the formation of constitutional vacancies, e.g., triple defects. Another interesting observation for this alloy is that above ~650 K, the slope of electrical resistivity data are different for tests done with current flowing in one direction and in the reverse direction. The reason for this behavior have not been established.

The 18wt%Al alloy transforms from DO3 to B2 at ~740 K. The electrical resistivity has a peak at this temperature, while specific heat shows a discontinuity. The 16wt%Al alloy transforms from DO3 to B2 at ~830 K. Similar changes are observed in the electrical resistivity and specific heat data.

The 8.5wt%Al alloy has a ferromagnetic to paramagnetic transformation at ~966 K. There is a sharp change in slope in the

electrical resistivity curve at this temperature. The specific heat curve shows a corresponding discontinuity.

6) The electrical resistivity of a Ni-8wt%Al alloy shows a sharp change in slope at ~890 K. The specific heat, however, does not show any distinct change at this temperature.

7) The electrical resistivity and specific heat of $Ni_4Mo$ is dependent on its initial state. The electrical resistivity and specific heat data extracted from these experiments, as functions of temperature, show that the nature of the curve depends on the degree of SRO present in the structure. SRO clusters act as scattering centers for the flow of electrons and hence contributes to increasing electrical resistivity of the material. Fast heating (75 K/sec.) was employed to avoid the $\alpha \Rightarrow \beta$ transformation. Hence data in the metastable state were taken, below Tc.

8) Isothermal heating is useful in getting kinetic data for phase changes. By repeating isothermal tests at different temperatures, a TTT diagram for the alloy can be constructed. In this research a PID temperature control program was written for this purpose. This program was used on $Ni_4Mo$ to study the kinetics of the $\alpha \Rightarrow \beta$ transformation at 700 °C and 750 °C. This program was also used on a steel specimen to study the kinetics of recrystallization and precipitation.

9) Three different thermocouple configurations were studied and their relative merits and demerits were discussed.

10) An error analysis was conducted on the specific heat and electrical resistivity data determined by the designed pulse calorimeter. The estimated maximum error in the specific heat was 0.75% and in the electrical resistivity was 0.61%.

11) Both pulse heating and isothermal heating can provide information leading to a better understanding of the properties of the alloy and can help in alloy design.

## RECOMMENDATIONS

1) Specimen should always be centerless ground before use in the calorimeter. Centerless grinding resulted in a maximum scatter from the average diameter of 0.14%, which is a significant improvement from the scatter in the diameter measurement of a non-centerlessly ground specimen, e.g., 0.5%.

2) A programmable power supply of a higher current rating should be used . For the specimen dimensions used in this research, a maximum heating rate of 75 K/sec. could be realized. The current power supply has a rating of 90 A at 6V. A higher current power supply could be utilized to heat the specimen faster. This would minimize heat losses and acquire data in metastable states.

3) It is recommended that an additional amplifier be used in conjunction with a thermocouple which can be attached at a location slightly removed from the center of the specimen. By noting the

thermal emf from both thermocouples, the longitudinal variation in temperature can be estimated.

4) Tests should be done on Fe-21.2 wt%Al alloy developed at ORNL [7], which showed an anomaly in the electrical resistivity upon reversing the direction of current. Experiment should be designed to measure the Seebeck coefficient of the alloy, to see whether this alloy has an unusually high value for this coefficient.

5) The knife-edge apparatus should be used to determine the effective length of the specimen. It has been shown that error in the measurement of length, by the knife-edge apparatus, is 0.05%.

6) The slowest heating achieved for this study, for $Ni_4Mo$ specimen, was 1 K/sec. A PID temperature control program, by the name CALISO, was developed and used for this purpose. By further fine-tuning the PID parameters, a smoother control over the current can be achieved, which can result in slower heating than that cited above. It is recommended that an experiment be done with a heating rate of 0.1 K/sec. or less to get data closer to equilibrium values.

7) A second specimen holder was designed. It is identical to the original one, except it has a spring loading arrangement at the top. The next researcher is advised to attach the spring in tension, so that any thermal stresses in the specimen will be accommodated by the contraction of the spring.

8) For $Ni_4Mo$, isothermal runs have been made at two different holding temperatures, 700 °C and 750 °C. The change in the

electrical resistivity served as an index to determine the start and the finish of the $\alpha \Rightarrow \beta$ transformation. It is recommended that the isothermal tests be repeated at several different temperatures in the range 675 °C to 825 °C, and the TTT diagram be constructed.

# REFERENCES

# REFERENCES


1) Brooks, C.R., Stansbury, E.E., High Temperatures-High Pressures, 1, 289-307, 1969.

2) Cezairliyan, A., 'Pulse calorimetry', Specific Heat of Solids, Hemispherical Publishing Corporation, New York, 1988.

3) Worthing, A.G., Phys. Rev., 12, 199-225, 1918.

4) Kollie, T.G., M.S. Thesis, University of Tennessee, Knoxville, 1965.

5) Cezairliyan, A., McLure, J.L., International Journal of Thermophysics, 8, 577, 1987.

6) National Institute of Standards and Technology, Gaithersburg, Maryland.

7) Oak Ridge National Laboratory, Oak Ridge, Tennessee.

8) Kollie, T.G., Ph.D. Thesis, University of Tennessee, Knoxville, 1969.

9) Touloukian, Y.S., (Editor), Thermophysical Properties Research Center, TPRC Report, 16, 323, 1966.

10) Elliot, R.P., Constitution of Binary Alloys, First Supplement, McGraw Hill, New York, 1965.

11) Hultgren, K., Desai, P.D., Hawkins, D.T., Gleiser, M., Kelly, K.K., 'Selected Values of Thermophysical Properties of Binary Alloys', American Society for Metals, Metals Park, Ohio, 1973.

12) Basak, D., M.S. Thesis, University of Tennessee, Knoxville, 1992.

13) Einstein, A., Ann. Physik, 22, 180-190, 1907.

14) Miiller, A.P.,'Theory of specific heat of solids', Specific Heat of Solids', Hemisphere Publishing Corporation, New York, 1988.

15) Gaskell, D.R., 'Introduction to metallurgical thermodynamics', Hemisphere Publishing Corporation, 1981.

16) Nernst, W. Lindemann, F.A., Z. Electrochem, 17, 817-827, 1911.

17) Einstein, A., Ann. Physik, 35, 679-694,1911.

18) Debye, P., Ann Physik, 39, 789-839, 1912.

19) Brooks, C.R., Spruiell, J.E., Stansbury, E.E., International Metals Reviews, 29, 210, 1984.

20) Ruedl, E., Delavignette, P., Amelinckx, S., Phys. Status Solidi., 28, 305, 1968.

21) Casselton, R.E.W., Hume-Rothery, W., J. Less Common Met., 7, 212, 1964.

22) Stansbury, E.E., Guthrie, P.V., ORNL Report 3078, ORNL, Oak Ridge, Tennessee, 1961.

23) Heijwegen, C.P., Rieck, G.D., Z. Metallkd., 64, 450, 1973.

24) Kozlov, E.V., Kushnarenko, V.M., Phys. Met. Metallogr., 46(2), 75, 1978.

25) Spruiell, J.E., Ph.D., Thesis, University of Tennessee, Knoxville, 1963.

26) Lei, T.S., Ph.D. Thesis, University of Tennessee, Knoxville, 1979.

27) Saburi, T., Kanai, E., Nenno, S., J. Less-common Met., 37, 59,1974.

28) Thomas, H., Z. Phys., 129, 219, 1951.

29) Kear, B.H., Sims, C.T., Stoloff, N.S., Westbrook, J.H., (eds.), 'Ordered alloys', Claitor's Publishing Division, Baton Rouge, Louisiana, 275, 1970.

30) Cook, H.E., Mater. Sci. Eng., 25, 127, 1976.

31) Block, S.J., M.S. Thesis, University of Tennessee, Knoxville, 1976.

32) Baer, H.G., Z. Metallkde, 56, 79, 1965.

33) Guy, A.G., Trans. Am. Soc. Metals, 55, 737, 1962.

34) Chang, T.P., M.S. Thesis, University of Tennessee, Knoxville, 1965.

35) Lei, T.S., Vasudevan, K., Stansbury, E.E., Materials Research Society, 39, 163,1985.

36) Norem, W.E., Ph.D. Thesis,University of Tennessee, Knoxville, 1965.

37) Vasudevan, K., M.S. Thesis, University of Tennessee, Knoxville, 1982.

38) Wylie Precision Instruments, Cincinnati, Ohio.

39) Liu, C.T., Maziasz, P.J., and Goodwin, G., Alloy Behavior and Design Group, ORNL, Oak Ridge, Tennessee.

40) 21st Century Environmental Systems, Knoxville, Tennessee.

41) Cezairliyan, A., personal communications, 1995.

42) Ho, K., Dodd, R.A., Scripta Meta., 12, 1055, 1978.

43) Wasilewski, R.J., J. Phys. Chem. Solids, 29, 39, 1968.

44) Hyde, T.A., Sellers, C.H., Wright, J.K., Wright, R.N., Scripta Meta., 30, 113, 1994.

45) Neumann, J.P., Chang, Y.A., Lee, C.M., Acta. Meta., 24, 593, 1976.

46) Spiegel, M.R., 'Theory and Problems of Probability and Statistics', Schaum's Outline Series, McGraw Hill, Inc., New York, 1991.

47) Seybolt, A.U., Burke, J.E., 'Experimental Metallurgy', John Wiley and Sons, Inc., New York, 1953.

# APPENDICES

# APPENDIX I

Summary of Pulse Experiments for the Measurement of Specific Heat of Electrical Conductors* [2]

| No. | Investigator | Ref. | Year | Category | Power Source | Pulse Length s | Heating Rate $K \cdot s^{-1}$ | Substance | Temp. Range K | Spec. Geom. | Power Meas. | Temp. Meas. | Recording | Uncertainty |
|---|---|---|---|---|---|---|---|---|---|---|---|---|---|---|
| 1 | Worthing | 1 | 1918 | Ia | B | 1 | | W,C | 1200-2400 | W | EI | R | V | |
| 2 | Lapp | 2 | 1929 | Ib | B | | | Ni | 100-730 | R | W | TC | V | 2 |
| 3 | Grew | 3 | 1934 | Ib | B | | | Ni | 90-720 | R | EI | TC | V | 2 |
| 4 | Avramescu | 4 | 1939 | II | B | 1-2 | | Al,Cu | 400-1300 | R | EI | R | G | 2 |
| 5 | Néel and Persoz | 5 | 1939 | Ib | B | 0.1 | | Cu,Ni,Pt | 300-1300 | W | W | R | V | 2 |
| 6 | Kurrelmeyer et al. | 6 | 1943 | Ib | C | 0.002-0.05 | | Pt | 300 | W | B | R | V | 0.5 |
| 7 | Baxter | 7 | 1944 | II | | 0.05 | | | | W | EI | R | G | |
| 8 | Pallister | 8 | 1949 | Ib | B | | 1 | Fe | 273-1500 | R | EI | TC | V | 2 |
| 9 | Nathan | 9 | 1951 | II | B | | 15-1000 | Steel | 770 | R | EI | TC | S | |
| 10 | Khotkovich and Bagrov | 10 | 1951 | II | B | 0.01 | $10^4$-$5\times10^4$ | Cu,W,Mo,Cd | | W | EI | R | G | 3 |
| 11 | Pochapsky | 11 | 1953 | Ib | C | 0.001 | | Al,Pb | 273-920 | W | B | R | V | 5 |
| 12 | Pochapsky | 12 | 1954 | Ib | C | 0.001 | | Pt | 273-900 | W | B | R | V | 5 |
| 13 | Strittmater et al. | 13 | 1957 | II | B | 0.05-0.15 | 3000-9000 | Pt,Ni | 300-720 | W | EI | R | S | 5-10 |
| 14 | Rasor and McClelland | 14 | 1960 | Ib | B | | 50 | Mo,Ta,C | 1300-3920 | R | EI | O | G | 5 |
| 15 | Wallace et al. | 15 | 1960 | Ib | B | 0.04 | | Fe | 300-1300 | W | B | R | S | 2 |
| 16 | Wallace | 16 | 1960 | Ib | B | 0.03 | | Th | 300-1300 | W | B | R | S | 2 |
| 17 | Pasternak et al. | 17 | 1962 | Ia | B | 1-10 | 100-1000 | Pt | 300-1100 | W | EI | R | R | |
| 18 | Pasternak et al. | 18 | 1963 | Ia | B | | 35-2000 | Pt | 400-1300 | W | EI | R | R | |
| 19 | Taylor and Finch | 19 | 1964 | II | B | | $10^3$-$6\times10^4$ | Mo,Ta | 100-3200 | W | EI | R | S | 4-7 |
| 20 | Parker | 20 | 1965 | Ia | C | $10^{-5}$ | $10^4$-$10^9$ | Ti | 300-1100 | S | C | TC | S | |
| 21 | Kollie | 21 | 1967 | Ia | R | 4-60 | 10-20 | Fe | 300-1200 | R | EI | TC | D | 1 |
| 22 | Affortit and Lallement | 22 | 1968 | II | B | 0.1-1 | | Nb,W | 300-3600 | W | EI | TC,O | S | 3-5 |
| 23 | Affortit | 23 | 1969 | II | B | <1 | | UN,UC,$UO_2$ | 700-3100 | R | EI | TC,O | S | 5 |
| 24 | Finch and Taylor | 24 | 1969 | II | B | | $7\times10^3$-$1.6\times10^5$ | $ZrU_{0.04}H_{0.3}$ | 300-800 | R | EI | R,O | S | 5 |
| 25 | Jura and Stark | 25 | 1969 | II | B | 0.1 | | Fe | 80-300 | W | EI | TC | S | 5 |
| 26 | Kollie et al. | 26 | 1969 | Ib | R | 10-35 | 20 | Fe | 300-1500 | R | EI | TC | D | 1-2 |
| 27 | Cezairliyan et al. | 27 | 1970 | II | B | 0.3-0.7 | 4000-8000 | Mo | 1900-2800 | T | EI | O | D | 2-3 |
| 28 | Dikhter and Lebedev | 28 | 1970 | II | C | $<5\times10^{-5}$ | | W | 2600-4500 | W | EI | O | S | |
| 29 | Dikhter and Lebedev | 29 | 1971 | II | C | | | Mo | 2200-3700 | W | EI | O | S | |
| 30 | Cezairliyan et al. | 30 | 1971 | II | B | 0.3-0.5 | 4000-6000 | Ta | 1900-3200 | T | EI | O | D | 2-3 |
| 31 | Cezairliyan and McClure | 31 | 1971 | II | B | 0.4-0.6 | 4000-7000 | W | 2000-3600 | T | EI | O | D | 2-3 |
| 32 | Cezairliyan | 32 | 1971 | II | B | 0.4-0.5 | 5000 | Nb | 1500-2700 | T | EI | O | D | 2 |
| 33 | Cezairliyan | 33 | 1972 | II | B | 0.4-0.5 | 4000-7000 | Ta-10W | 1500-3200 | T | EI | O | D | 3 |
| 34 | Cezairliyan | 34 | 1973 | II | B | 0.4 | 5000-7000 | Nb-1Zr | 1500-2700 | T | EI | O | D | 3 |
| 35 | Cezairliyan and McClure | 35 | 1974 | II | B | 0.5-0.9 | 2000-4000 | Fe | 1500-1800 | T | EI | O | D | 3 |
| 36 | Cezairliyan et al. | 36 | 1974 | II | B | 0.4 | 4000-5000 | V | 1500-2100 | T | EI | O | D | 3 |

Summary of Pulse Experiments for the Measurement of Specific Heat of Electrical Conductors[a] (Continued)

| No. | Investigator | Ref. | Year | Category | Power Source | Pulse Length s | Heating Rate $K \cdot s^{-1}$ | Substance | Temp. Range K | Spec. Geom. | Power Meas. | Temp. Meas. | Recording | Uncertainty |
|---|---|---|---|---|---|---|---|---|---|---|---|---|---|---|
| 37 | Cezairliyan and Righini | 37 | 1974 | II | B | 0.4-0.5 | 3000-5000 | Zr | 1500-2100 | T | EI | O | D | 3 |
| 38 | Cezairliyan | 38 | 1974 | II | B | 0.4-0.5 | 4000-5000 | Nb-10Ta-10W | 1500-2800 | T | EI | O | D | 3 |
| 39 | Cezairliyan and Righini | 39 | 1975 | II | B | 0.2-0.5 | 3000-8000 | C | 1500-3000 | T | EI | O | D | 3 |
| 40 | Cezairliyan and McClure | 40 | 1975 | II | B | 0.3-0.5 | 4000-8000 | Hf-3Zr | 1500-2400 | T | EI | O | D | 3 |
| 41 | Lebedev et al. | 41 | 1976 | II | C | | $10^{8}$ | Mo,W | 1500-3700 | W | EI | O | S | |
| 42 | Gathers et al. | 42 | 1976 | II | C | $<10^{-6}$ | | Ta | 2500-8000 | W | EI | O | S | |
| 43 | Shaner et al. | 43 | 1976 | II | C | $<10^{-6}$ | | Mo,Nb,Ta,W | 2500-5000 | W | EI | O | S | |
| 44 | Shaner et al. | 44 | 1977 | II | C | $<10^{-6}$ | | Mo,Ta | 2000-7500 | W | EI | O | S | |
| 45 | Shaner et al. | 45 | 1977 | II | C | $<10^{-6}$ | | Nb,Pb | 2000-6000 | W | EI | O | S | |
| 46 | Lebedev and Mozharov | 46 | 1977 | II | C | | $10^{8}$-$10^{9}$ | Ta | 2300-3900 | T | EI | O | S | 8 |
| 47 | Cezairliyan and Miiller | 47 | 1977 | II | B | 0.5-0.6 | 3000-4000 | Ti | 1500-1900 | T | EI | O | D | 3 |
| 48 | Cezairliyan et al. | 48 | 1977 | II | B | 0.4-0.5 | 3000-4000 | Ti-6Al-4V | 1500-1900 | T | EI | O | D | 3 |
| 49 | Righini et al. | 49 | 1977 | II | B | 0.6-1.5 | 1000-3000 | Zircaloy-2 | 1300-2000 | T | EI | O | D | 4 |
| 50 | Petrova and Chekhovskoi | 50 | 1978 | Ib | B | | 300-500 | NbC,TaC,ZrC | 1600-2300 | R | EI | O | S,D | 3-4 |
| 51 | Taylor | 51 | 1978 | Ia | R | 6 | | W | 1500-2400 | R | EI | R | D | |
| 52 | Naito et al. | 52 | 1979 | Ib | | | | C,SiC | 300-1200 | R | EI | TC | | |
| 53 | Gathers et al. | 53 | 1979 | II | C | $<5\times10^{-5}$ | | Pt | 2000-7500 | W | EI | O | S | |
| 54 | Seydel et al. | 54 | 1979 | II | C | | $10^{9}$ | Mo | 2900-6000 | W | EI | O | S | 3-5 |
| 55 | Cezairliyan and Miiller | 55 | 1980 | II | B | 0.6 | 2000 | Steel | 1400-1700 | T | EI | O | D | 3 |
| 56 | Miiller and Cezairliyan | 56 | 1980 | II | B | 0.5-0.6 | 3000-4000 | Pd | 1400-1800 | T | EI | O | D | 3 |
| 57 | Cezairliyan and Miiller | 57 | 1980 | II | B | 0.4-0.8 | 4000 | C-composite | 1500-3000 | T | EI | O | D | 3 |
| 58 | Righini and Rosso | 58 | 1980 | II | B | 0.7-1.1 | 1700-3000 | Pt | 1000-2000 | T | EI | O | D | - |

[a]Abbreviations and Notes

Category: Designation of categories are described in Section 9.2.2.
Power Source: B = Battery, C = Capacitor, R = Regulated DC power supply.
Temp. Range: Range between two extreme temperatures covered by the investigator regardless of particular substance.
Spec. Geom.: R = Rod (diam. > 1 mm), S = Strip, T = Tube, W = Wire (diam. ≤ 1 mm).
Power Meas.: B = Bridge, C = Capacitor energy, EI = Voltage-current, W = Wattmeter.
Temp. Meas.: O = Optical, R = Resistive, TC = Thermocouple.
Recording: D = Digital, G = Oscillographic, R = Chart recording, S = Oscilloscopic, V = Visual-manual.
Uncertainty: Total error in specific heat as reported in the literature by the investigators. (In some instances where the measured qu enthalpy and the authors gave only the error in enthalpy the entry in this column is left blank.)

# APPENDIX II

## CALCULATION OF THEORETICAL DENSITY OF $Ni_4Mo$

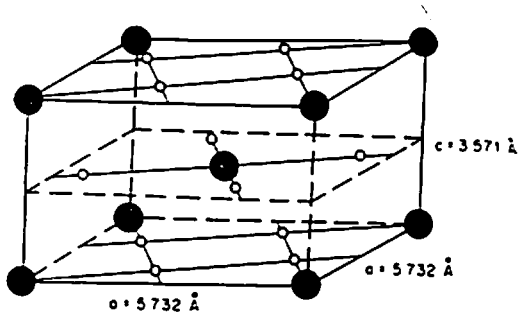


Crystal structure of β (Ni4Mo)

The figure above shows the unit cell of $Ni_4Mo$.
Effective number of nickel atoms = 4 + 8 (1/2) = 8
Effective number of molybdenum atoms = 1 + 8 (1/8) = 2

mass of unit cell =
(Atomic wt. of Ni X no. of Ni atoms in unit cell + Atomic wt. of Mo X no. of Mo atoms in unit cell) X amu
$= (58.71 \times 8 + 95.94 \times 2) \times 1.660 \times 10^{-27}$ kg
$= 1.098 \times 10^{-24}$ kg

volume of unit cell =
$a^2c$ (where a and c are unit cell dimensions)
$= (5.732)^2 \times 3.571 \times 10^{-30}$ $m^3$
$= 1.173 \times 10^{-28}$ $m^3$

$$\rho = \frac{\text{mass of atoms in the unit cell}}{\text{volume of unit cell}}$$

$$= \frac{1.098 \times 10^{-24}}{1.173 \times 10^{-28}} \text{ kg/m}^3$$

$= 9360$ kg/$m^3$
$= 9.360$ g/$cm^3$

# APPENDIX III

| Electrical resistivity of nickel (NIC) | | |
|---|---|---|
| Temperature (K) | Electrical Resistivity (micro-ohm-cm) | |
| | | |
| 328.8 | 8.509 | |
| 328.8 | 8.509 | |
| 329.3 | 8.529 | |
| 331.0 | 8.609 | |
| 331.0 | 8.609 | |
| 331.3 | 8.622 | |
| 331.3 | 8.622 | |
| 331.3 | 8.622 | |
| 331.8 | 8.642 | |
| 333.4 | 8.721 | |
| 333.4 | 8.721 | |
| 333.4 | 8.721 | |
| 333.4 | 8.721 | |
| 334.4 | 8.767 | |
| 334.8 | 8.783 | |
| 334.8 | 8.783 | |
| 335.1 | 8.794 | |
| 335.1 | 8.794 | |
| 335.6 | 8.810 | |
| 336.1 | 8.831 | |
| 336.8 | 8.857 | |
| 336.8 | 8.857 | |
| 337.3 | 8.873 | |
| 338.3 | 8.910 | |
| 338.3 | 8.910 | |
| 338.3 | 8.910 | |
| 340.0 | 8.973 | |
| 340.4 | 8.989 | |
| 341.1 | 9.016 | |
| 342.8 | 9.080 | |
| 344.4 | 9.144 | |
| 344.7 | 9.155 | |
| 345.4 | 9.182 | |
| 345.4 | 9.182 | |

| | | |
|---|---|---|
| 348.5 | 9.344 | |
| 349.2 | 9.384 | |
| 349.6 | 9.408 | |
| 349.9 | 9.424 | |
| 351.5 | 9.520 | |
| 351.5 | 9.520 | |
| 351.9 | 9.543 | |
| 351.9 | 9.543 | |
| 351.9 | 9.543 | |
| 353.9 | 9.637 | |
| 354.6 | 9.671 | |
| 354.6 | 9.671 | |
| 355.0 | 9.691 | |
| 355.0 | 9.691 | |
| 355.2 | 9.704 | |
| 356.2 | 9.751 | |
| 356.9 | 9.784 | |
| 358.0 | 9.838 | |
| 358.2 | 9.850 | |
| 358.7 | 9.868 | |
| 358.9 | 9.881 | |
| 359.9 | 9.923 | |
| 360.3 | 9.942 | |
| 360.6 | 9.954 | |
| 361.0 | 9.972 | |
| 361.0 | 9.972 | |
| 361.2 | 9.984 | |
| 361.9 | 10.015 | |
| 362.2 | 10.027 | |
| 364.5 | 10.145 | |
| 366.9 | 10.269 | |
| 366.9 | 10.269 | |
| 367.2 | 10.283 | |
| 367.2 | 10.283 | |
| 367.4 | 10.296 | |
| 368.1 | 10.331 | |
| 368.5 | 10.351 | |
| 368.5 | 10.351 | |
| 369.4 | 10.398 | |
| 369.8 | 10.417 | |
| 370.8 | 10.464 | |
| 372.4 | 10.544 | |
| 372.8 | 10.564 | |

| | | |
|---|---|---|
| 373.0 | 10.577 | |
| 374.4 | 10.642 | |
| 375.0 | 10.674 | |
| 375.9 | 10.719 | |
| 375.9 | 10.719 | |
| 377.3 | 10.783 | |
| 377.3 | 10.783 | |
| 377.5 | 10.796 | |
| 377.9 | 10.815 | |
| 378.8 | 10.860 | |
| 381.1 | 10.943 | |
| 381.3 | 10.953 | |
| 381.7 | 10.967 | |
| 383.7 | 11.040 | |
| 383.9 | 11.050 | |
| 385.5 | 11.134 | |
| 385.5 | 11.134 | |
| 385.9 | 11.154 | |
| 386.5 | 11.189 | |
| 386.5 | 11.189 | |
| 387.0 | 11.217 | |
| 388.1 | 11.273 | |
| 388.3 | 11.287 | |
| 389.0 | 11.322 | |
| 389.0 | 11.322 | |
| 389.6 | 11.356 | |
| 390.9 | 11.426 | |
| 391.5 | 11.461 | |
| 391.5 | 11.461 | |
| 391.8 | 11.475 | |
| 391.8 | 11.475 | |
| 392.7 | 11.524 | |
| 393.7 | 11.579 | |
| 394.6 | 11.628 | |
| 394.9 | 11.642 | |
| 395.3 | 11.663 | |
| 396.1 | 11.705 | |
| 396.5 | 11.724 | |
| 397.4 | 11.766 | |
| 399.3 | 11.857 | |
| 399.6 | 11.869 | |
| 400.5 | 11.911 | |
| 401.7 | 11.972 | |

| | | |
|---|---|---|
| 402.3 | 12.003 | |
| 403.0 | 12.034 | |
| 403.0 | 12.034 | |
| 403.2 | 12.046 | |
| 403.9 | 12.077 | |
| 403.9 | 12.077 | |
| 403.9 | 12.077 | |
| 404.2 | 12.095 | |
| 407.0 | 12.255 | |
| 407.2 | 12.269 | |
| 407.6 | 12.291 | |
| 409.1 | 12.377 | |
| 409.4 | 12.392 | |
| 409.7 | 12.413 | |
| 409.7 | 12.413 | |
| 410.0 | 12.428 | |
| 411.2 | 12.497 | |
| 412.1 | 12.546 | |
| 412.9 | 12.595 | |
| 413.9 | 12.650 | |
| 415.4 | 12.733 | |
| 415.4 | 12.733 | |
| 416.0 | 12.762 | |
| 416.0 | 12.762 | |
| 416.9 | 12.803 | |
| 420.8 | 12.990 | |
| 420.8 | 12.990 | |
| 421.1 | 13.002 | |
| 421.4 | 13.020 | |
| 422.3 | 13.065 | |
| 422.9 | 13.098 | |
| 423.1 | 13.111 | |
| 423.1 | 13.111 | |
| 423.1 | 13.111 | |
| 423.5 | 13.131 | |
| 424.3 | 13.177 | |
| 425.0 | 13.210 | |
| 428.0 | 13.386 | |
| 428.0 | 13.386 | |
| 428.2 | 13.400 | |
| 429.1 | 13.450 | |
| 430.0 | 13.506 | |
| 430.9 | 13.555 | |

| | | |
|---|---|---|
| 431.1 1 | 3.567 | |
| 431.1 1 | 3.567 | |
| 432.1 | 13.615 | |
| 432.7 | 13.646 | |
| 435.5 | 13.789 | |
| 436.4 | 13.831 | |
| 437.0 | 13.866 | |
| 437.6 | 13.900 | |
| 437.9 | 13.921 | |
| 439.0 | 13.983 | |
| 439.3 | 14.004 | |
| 439.6 | 14.018 | |
| 439.9 | 14.038 | |
| 440.2 | 14.052 | |
| 440.5 | 14.073 | |
| 441.6 | 14.135 | |
| 441.9 | 14.155 | |
| 446.0 | 14.375 | |
| 446.2 | 14.387 | |
| 446.8 | 14.419 | |
| 447.4 | 14.452 | |
| 448.8 | 14.544 | |
| 449.3 | 14.583 | |
| 449.7 | 14.606 | |
| 449.7 | 14.606 | |
| 450.5 | 14.660 | |
| 451.1 | 14.699 | |
| 452.3 | 14.776 | |
| 452.5 | 14.791 | |
| 453.1 | 14.829 | |
| 455.6 | 14.989 | |
| 455.9 | 15.004 | |
| 456.8 | 15.062 | |
| 456.8 | 15.062 | |
| 458.2 | 15.148 | |
| 459.3 | 15.217 | |
| 460.1 | 15.265 | |
| 461.3 | 15.334 | |
| 461.3 | 15.334 | |
| 461.9 | 15.369 | |
| 462.7 | 15.417 | |
| 465.2 | 15.582 | |
| 465.2 | 15.582 | |

| | | |
|---|---|---|
| 465.4 | 15.597 | |
| 466.0 | 15.635 | |
| 466.0 | 15.635 | |
| 469.1 | 15.826 | |
| 469.1 | 15.826 | |
| 469.6 | 15.861 | |
| 469.6 | 15.861 | |
| 470.8 | 15.932 | |
| 472.7 | 16.052 | |
| 473.5 | 16.101 | |
| 474.0 | 16.136 | |
| 475.2 | 16.206 | |
| 475.2 | 16.206 | |
| 476.5 | 16.291 | |
| 477.9 | 16.374 | |
| 478.8 | 16.430 | |
| 479.6 | 16.478 | |
| 479.8 | 16.492 | |
| 480.9 | 16.561 | |
| 481.2 | 16.582 | |
| 483.4 | 16.720 | |
| 483.7 | 16.742 | |
| 484.2 | 16.771 | |
| 484.7 | 16.807 | |
| 485.0 | 16.829 | |
| 488.0 | 17.028 | |
| 488.3 | 17.042 | |
| 488.8 | 17.079 | |
| 488.8 | 17.079 | |
| 489.9 | 17.153 | |
| 492.0 | 17.291 | |
| 492.9 | 17.349 | |
| 493.1 | 17.363 | |
| 494.2 | 17.436 | |
| 494.5 | 17.450 | |
| 496.1 | 17.560 | |
| 496.9 | 17.611 | |
| 498.2 | 17.698 | |
| 498.8 | 17.734 | |
| 499.3 1 | 7.771 | |
| 500.4 | 17.843 | |
| 500.9 | 17.881 | |
| 503.0 | 18.024 | |

| | | |
|---|---|---|
| 503.4 | 18.047 | |
| 504.3 | 18.115 | |
| 504.7 | 18.137 | |
| 505.2 | 18.175 | |
| 507.8 | 18.363 | |
| 507.8 | 18.363 | |
| 508.7 | 18.425 | |
| 508.9 | 18.441 | |
| 509.7 | 18.495 | |
| 512.0 | 18.654 | |
| 513.1 | 18.726 | |
| 513.7 | 18.762 | |
| 514.7 | 18.834 | |
| 514.7 | 18.834 | |
| 516.3 | 18.938 | |
| 517.1 | 18.997 | |
| 518.6 | 19.101 | |
| 519.5 | 19.161 | |
| 520.0 | 19.198 | |
| 521.0 | 19.268 | |
| 521.3 | 19.292 | |
| 523.7 | 19.464 | |
| 524.4 | 19.518 | |
| 524.9 | 19.558 | |
| 525.5 | 19.596 | |
| 526.0 | 19.635 | |
| 528.9 | 19.861 | |
| 529.1 | 19.877 | |
| 529.8 | 19.936 | |
| 529.8 | 19.936 | |
| 531.4 | 20.060 | |
| 533.2 | 20.200 | |
| 534.0 | 20.257 | |
| 535.0 | 20.339 | |
| 536.1 | 20.421 | |
| 536.1 | 20.421 | |
| 537.9 | 20.555 | |
| 538.9 | 20.634 | |
| 540.4 | 20.744 | |
| 541.0 | 20.784 | |
| 541.8 | 20.847 | |
| 542.7 | 20.922 | |
| 542.7 | 20.922 | |

| | | |
|---|---|---|
| 545.6 | 21.149 | |
| 546.1 | 21.191 | |
| 546.8 | 21.249 | |
| 547.7 | 21.316 | |
| 547.9 | 21.333 | |
| 551.2 | 21.597 | |
| 551.2 | 21.597 | |
| 552.3 | 21.679 | |
| 552.5 | 21.695 | |
| 553.5 | 21.777 | |
| 555.8 | 21.966 | |
| 556.5 | 22.026 | |
| 557.4 | 22.094 | |
| 558.6 | 22.197 | |
| 559.1 | 22.240 | |
| 560.9 | 22.390 | |
| 561.4 | 22.434 | |
| 563.4 | 22.602 | |
| 563.9 | 22.646 | |
| 564.6 | 22.707 | |
| 566.0 | 22.824 | |
| 566.2 | 22.842 | |
| 568.6 | 23.056 | |
| 569.5 | 23.128 | |
| 570.2 | 23.190 | |
| 570.7 | 23.235 | |
| 571.7 | 23.324 | |
| 574.7 | 23.583 | |
| 574.7 | 23.583 | |
| 575.9 | 23.690 | |
| 576.2 | 23.716 | |
| 577.2 | 23.798 | |
| 579.7 | 24.025 | |
| 580.4 | 24.089 | |
| 581.7 | 24.198 | |
| 582.2 | 24.243 | |
| 583.0 | 24.318 | |
| 585.2 | 24.525 | |
| 585.6 | 24.563 | |
| 587.7 | 24.751 | |
| 587.9 | 24.770 | |
| 588.9 | 24.867 | |
| 590.1 | 24.983 | |

| | | |
|---|---|---|
| 590.4 | 25.012 | |
| 593.2 | 25.273 | |
| 593.9 | 25.340 | |
| 594.9 | 25.439 | |
| 595.9 | 25.539 | |
| 596.3 | 25.578 | |
| 599.3 | 25.875 | |
| 599.5 | 25.895 | |
| 600.7 | 26.020 | |
| 601.0 | 26.051 | |
| 602.2 | 26.175 | |
| 604.7 | 26.423 | |
| 605.2 | 26.475 | |
| 606.9 | 26.656 | |
| 607.4 | 26.710 | |
| 608.2 | 26.795 | |
| 610.4 | 27.030 | |
| 610.8 | 27.072 | |
| 613.0 | 27.310 | |
| 613.3 | 27.342 | |
| 614.5 | 27.472 | |
| 616.0 | 27.633 | |
| 616.2 | 27.655 | |
| 618.9 | 27.939 | |
| 619.9 | 28.044 | |
| 620.6 | 28.117 | |
| 621.3 | 28.191 | |
| 622.1 | 28.275 | |
| 624.9 | 28.563 | |
| 625.4 | 28.613 | |
| 626.6 | 28.732 | |
| 626.9 | 28.761 | |
| 628.3 | 28.889 | |
| 631.5 | 29.181 | |
| 631.5 | 29.181 | |
| 633.6 | 29.581 | |
| 634.1 | 29.637 | |
| 635.3 | 29.693 | |
| 638.0 | 29.750 | |
| 638.5 | 29.806 | |
| 641.3 | 29.864 | |
| 641.3 | 29.921 | |
| 643.0 | 29.979 | |

| | | |
|---|---|---|
| 644.7 | 30.037 | |
| 645.0 | 30.096 | |
| 648.0 | 30.154 | |
| 649.3 | 30.214 | |
| 650.4 | 30.273 | |
| 651.4 | 30.332 | |
| 652.3 | 30.392 | |
| 655.7 | 30.453 | |
| 656.6 | 30.513 | |
| 657.8 | 30.573 | |
| 658.7 | 30.634 | |
| 659.9 | 30.695 | |
| 663.4 | 30.818 | |
| 663.4 | 30.756 | |
| 666.0 | 30.879 | |
| 666.2 | 30.941 | |
| 667.9 | 31.002 | |
| 670.7 | 31.126 | |
| 670.7 | 31.064 | |
| 674.1 | 31.188 | |
| 674.3 | 31.250 | |
| 675.7 | 31.312 | |
| 677.8 | 31.374 | |
| 678.5 | 31.436 | |
| 681.5 | 31.498 | |
| 682.5 | 31.560 | |
| 683.6 | 31.622 | |
| 685.1 | 31.684 | |
| 686.2 | 31.745 | |
| 689.5 | 31.807 | |
| 690.6 | 31.869 | |
| 691.9 | 31.930 | |
| 692.5 | 31.992 | |
| 694.1 | 32.053 | |
| 697.7 | 32.114 | |
| 697.7 | 32.175 | |
| 700.4 | 32.236 | |
| 700.6 | 32.297 | |
| 702.2 | 32.357 | |
| 705.3 | 32.418 | |
| 705.5 | 32.478 | |
| 708.8 | 32.538 | |
| 709.0 | 32.598 | |

| | | |
|---|---|---|
| 710.8 | 32.657 | |
| 712.6 | 32.717 | |
| 713.4 | 32.776 | |
| 716.3 | 32.835 | |
| 717.7 | 32.894 | |
| 718.9 | 32.952 | |
| 720.0 | 33.011 | |
| 721.4 | 33.069 | |
| 724.6 | 33.127 | |
| 725.7 | 33.185 | |
| 727.1 | 33.243 | |
| 728.1 | 33.300 | |
| 729.4 | 33.358 | |
| 733.1 | 33.472 | |
| 733.1 | 33.415 | |
| 736.0 | 33.529 | |
| 736.3 | 33.586 | |
| 738.1 | 33.642 | |
| 740.9 | 33.699 | |
| 741.1 | 33.755 | |
| 744.5 | 33.811 | |
| 744.7 | 33.867 | |
| 746.6 | 33.923 | |
| 748.6 | 33.979 | |
| 749.0 | 34.034 | |
| 752.4 | 34.090 | |
| 753.8 | 34.145 | |
| 754.9 | 34.201 | |
| 756.3 | 34.256 | |
| 757.4 | 34.311 | |
| 760.8 | 34.366 | |
| 762.0 | 34.421 | |
| 763.5 | 34.476 | |
| 764.2 | 34.531 | |
| 766.2 | 34.585 | |
| 769.4 | 34.695 | |
| 769.4 | 34.640 | |
| 772.8 | 34.749 | |
| 772.8 | 34.804 | |
| 774.5 | 34.858 | |
| 777.4 | 34.913 | |
| 777.4 | 34.967 | |
| 780.8 | 35.021 | |

| | | |
|---|---|---|
| 781.5 | 35.076 | |
| 783.0 | 35.130 | |
| 785.1 | 35.184 | |
| 786.0 | 35.238 | |
| 788.6 | 35.292 | |
| 790.4 | 35.346 | |
| 791.7 | 35.400 | |
| 792.9 | 35.454 | |
| 794.5 | 35.508 | |
| 797.7 | 35.562 | |
| 798.6 | 35.616 | |
| 800.6 | 35.669 | |
| 801.1 | 35.723 | |
| 802.8 | 35.776 | |
| 806.2 | 35.830 | |
| 806.2 | 35.883 | |
| 809.5 | 35.937 | |
| 809.7 | 35.990 | |
| 811.5 | 36.043 | |
| 814.1 | 36.096 | |
| 814.3 | 36.149 | |
| 817.8 | 36.202 | |
| 818.6 | 36.255 | |
| 820.3 | 36.308 | |
| 821.8 | 36.361 | |
| 822.7 | 36.413 | |
| 825.8 | 36.466 | |
| 827.3 | 36.518 | |
| 828.8 | 36.571 | |
| 830.0 | 36.623 | |
| 831.5 | 36.675 | |
| 834.7 | 36.727 | |
| 835.5 | 36.779 | |
| 838.1 | 36.831 | |
| 838.1 | 36.883 | |
| 839.8 | 36.934 | |
| 843.3 | 37.037 | |
| 843.3 | 36.986 | |
| 846.5 | 37.089 | |
| 846.8 | 37.140 | |
| 848.9 | 37.191 | |
| 851.3 | 37.242 | |
| 851.8 | 37.293 | |

| | | |
|---|---|---|
| 855.0 | 37.344 | |
| 855.9 | 37.395 | |
| 857.4 | 37.446 | |
| 859.1 | 37.496 | |
| 860.2 | 37.547 | |
| 863.0 | 37.598 | |
| 864.5 | 37.648 | |
| 866.2 | 37.698 | |
| 867.1 3 | 7.748 | |
| 868.4 | 37.799 | |
| 871.9 | 37.849 | |
| 872.7 | 37.899 | |
| 875.0 | 37.949 | |
| 875.3 | 37.998 | |
| 877.2 | 38.048 | |
| 880.7 | 38.098 | |
| 880.7 | 38.148 | |
| 883.6 | 38.197 | |
| 883.9 | 38.247 | |
| 885.8 | 38.296 | |
| 888.4 | 38.346 | |
| 888.8 | 38.395 | |
| 892.0 | 38.444 | |
| 892.8 | 38.493 | |
| 894.6 | 38.543 | |
| 896.2 | 38.592 | |
| 897.1 | 38.641 | |
| 899.9 | 38.690 | |
| 901.6 | 38.739 | |
| 903.0 | 38.788 | |
| 904.3 | 38.836 | |
| 905.6 | 38.885 | |
| 908.8 | 38.934 | |
| 909.8 | 38.983 | |
| 911.7 | 39.031 | |
| 912.4 | 39.080 | |
| 914.1 | 39.128 | |
| 917.3 | 39.177 | |
| 917.4 | 39.225 | |
| 920.6 | 39.274 | |
| 920.8 | 39.322 | |
| 922.7 | 39.370 | |
| 925.3 | 39.418 | |

| | | |
|---|---|---|
| 925.5 | 39.466 | |
| 928.8 | 39.514 | |
| 929.4 | 39.562 | |
| 931.1 | 39.610 | |
| 932.9 | 39.658 | |
| 933.6 | 39.706 | |
| 936.5 | 39.754 | |
| 938.1 | 39.801 | |
| 939.5 | 39.849 | |
| 940.6 | 39.896 | |
| 941.9 | 39.944 | |
| 945.4 | 39.991 | |
| 946.2 | 40.039 | |
| 948.3 | 40.086 | |
| 948.7 | 40.133 | |
| 950.6 | 40.180 | |
| 953.7 | 40.274 | |
| 953.7 | 40.227 | |
| 956.8 | 40.321 | |
| 957.2 | 40.368 | |
| 958.9 | 40.414 | |
| 961.4 | 40.461 | |
| 961.8 | 40.508 | |
| 965.1 | 40.554 | |
| 965.5 | 40.601 | |
| 967.4 | 40.647 | |
| 968.8 | 40.693 | |
| 969.7 | 40.739 | |
| 972.6 | 40.785 | |
| 974.2 | 40.831 | |
| 975.3 | 40.877 | |
| 976.7 | 40.923 | |
| 977.9 | 40.969 | |
| 981.2 | 41.014 | |
| 982.0 | 41.060 | |
| 984.1 4 | 1.105 | |
| 984.3 | 41.151 | |
| 986.3 | 41.196 | |
| 989.4 | 41.241 | |
| 989.4 | 41.286 | |
| 992.5 | 41.331 | |
| 992.7 | 41.376 | |
| 994.3 | 41.421 | |

| | | |
|---|---|---|
| 996.9 | 41.466 | |
| 997.2 | 41.510 | |
| 1000.5 | 41.555 | |
| 1001.3 | 41.599 | |
| 1002.7 | 41.644 | |
| 1004.1 | 41.688 | |
| 1005.0 | 41.732 | |
| 1007.5 | 41.776 | |
| 1009.2 | 41.820 | |
| 1010.6 | 41.864 | |
| 1011.6 | 41.907 | |
| 1012.9 | 41.951 | |
| 1016.1 | 41.995 | |
| 1017.1 | 42.038 | |
| 1018.9 | 42.081 | |
| 1019.3 | 42.124 | |
| 1020.9 | 42.167 | |
| 1024.0 | 42.253 | |
| 1024.0 | 42.210 | |
| 1027.1 | 42.296 | |
| 1027.2 | 42.338 | |
| 1029.0 | 42.381 | |
| 1031.3 | 42.423 | |
| 1031.7 | 42.465 | |
| 1034.6 | 42.508 | |
| 1035.5 | 42.550 | |
| 1036.5 | 42.592 | |
| 1038.5 | 42.633 | |
| 1039.1 | 42.675 | |
| 1041.7 | 42.717 | |
| 1043.3 | 42.758 | |
| 1044.4 | 42.800 | |
| 1045.3 | 42.841 | |
| 1046.7 | 42.882 | |
| 1049.8 | 42.923 | |
| 1050.5 | 42.964 | |
| 1052.6 | 43.005 | |
| 1052.7 | 43.046 | |
| 1054.4 | 43.087 | |
| 1057.1 | 43.168 | |
| 1057.1 | 43.128 | |
| 1059.9 | 43.249 | |
| 1059.9 | 43.209 | |

| | | |
|---|---|---|
| 1061.7 | 43.290 | |
| 1063.9 | 43.330 | |
| 1064.3 | 43.370 | |
| 1067.1 | 43.410 | |
| 1067.9 | 43.451 | |
| 1069.3 | 43.491 | |
| 1070.7 | 43.531 | |
| 1071.5 | 43.571 | |
| 1073.8 | 43.611 | |
| 1075.2 | 43.651 | |
| 1076.4 | 43.691 | |
| 1077.4 | 43.731 | |
| 1078.6 | 43.771 | |
| 1081.5 | 43.811 | |
| 1082.3 | 43.851 | |
| 1084.1 | 43.891 | |
| 1084.3 | 43.931 | |
| 1086.1 | 43.971 | |
| 1088.7 | 44.011 | |
| 1088.9 | 44.051 | |
| 1091.6 | 44.091 | |
| 1091.6 | 44.131 | |
| 1093.2 | 44.171 | |
| 1095.7 | 44.212 | |
| 1095.7 | 44.252 | |
| 1098.5 | 44.292 | |
| 1099.0 | 44.332 | |
| 1100.5 | 44.372 | |
| 1101.9 | 44.413 | |
| 1102.6 | 44.453 | |
| 1105.0 | 44.494 | |
| 1106.1 | 44.534 | |
| 1107.5 | 44.575 | |
| 1108.3 | 44.615 | |
| 1109.5 | 44.656 | |
| 1112.4 | 44.696 | |
| 1113 44 | 0.737 | |
| 1114.8 | 44.777 | |
| 1114.9 | 44.818 | |
| 1116.7 | 44.859 | |
| 1119.2 | 44.899 | |
| 1119.4 | 44.940 | |
| 1121.9 | 44.980 | |

| | | |
|---|---|---|
| 1121.9 | 45.021 | |
| 1123.5 | 45.062 | |
| 1125.7 | 45.143 | |
| 1125.7 | 45.102 | |
| 1128.8 | 45.183 | |
| 1129.0 | 45.224 | |
| 1130.3 | 45.264 | |
| 1131.9 | 45.305 | |
| 1132.3 | 45.345 | |
| 1134.8 | 45.385 | |
| 1135.9 | 45.425 | |
| 1136.9 | 45.465 | |
| 1137.9 | 45.505 | |
| 1138.9 | 45.545 | |
| 1141.7 | 45.584 | |
| 1142.5 | 45.624 | |
| 1144.0 | 45.703 | |
| 1144.0 | 45.663 | |
| 1145.6 | 45.742 | |
| 1148.3 | 45.781 | |
| 1148.5 | 45.819 | |
| 1150.8 | 45.858 | |
| 1151.0 | 45.896 | |
| 1152.2 | 45.935 | |
| 1154.4 | 45.973 | |
| 1154.7 | 46.010 | |
| 1157.1 | 46.048 | |
| 1157.8 | 46.085 | |
| 1158.9 | 46.123 | |
| 1160.3 | 46.160 | |
| 1160.6 | 46.196 | |
| 1162.9 | 46.233 | |
| 1164.0 | 46.269 | |
| 1165.1 | 46.305 | |
| 1165.8 | 46.341 | |
| 1166.8 | 46.377 | |
| 1169.6 | 46.412 | |
| 1170 46 | 0.447 | |
| 1171.6 | 46.482 | |
| 1171.7 | 46.517 | |
| 1173.1 | 46.551 | |
| 1175.6 | 46.586 | |
| 1175.7 | 46.620 | |

| | | |
|---|---|---|
| 1177.8 | 46.654 | |
| 1178.1 | 46.687 | |
| 1179.2 | 46.721 | |
| 1181.3 | 46.788 | |
| 1181.3 | 46.754 | |
| 1183.9 | 46.821 | |
| 1184.3 | 46.854 | |
| 1185.2 | 46.886 | |
| 1186.6 | 46.919 | |
| 1187.0 | 46.952 | |
| 1189.3 | 46.984 | |
| 1190.4 | 47.016 | |
| 1191.3 | 47.049 | |
| 1191.9 | 47.081 | |
| 1192.9 | 47.113 | |
| 1195.7 | 47.145 | |
| 1195.9 | 47.178 | |
| 1197.6 | 47.210 | |
| 1197.8 | 47.242 | |
| 1198.8 | 47.274 | |
| 1201.0 | 47.306 | |
| 1201.4 | 47.339 | |
| 1203.1 | 47.371 | |
| 1203.7 | 47.404 | |
| 1204.6 | 47.436 | |
| 1206.3 | 47.469 | |
| 1206.5 | 47.502 | |
| 1209.0 | 47.535 | |
| 1209.3 | 47.568 | |
| 1210.3 | 47.601 | |
| 1211.4 | 47.635 | |
| 1211.8 | 47.669 | |
| 1213.9 | 47.702 | |
| 1215.4 | 47.737 | |
| 1215.7 | 47.771 | |
| 1216.3 | 47.806 | |
| 1217.3 | 47.841 | |
| 1219.5 | 47.876 | |
| 1220.1 | 47.911 | |
| 1221.4 | 47.947 | |
| 1221.8 | 47.983 | |
| 1222.7 | 48.019 | |
| 1224.6 | 48.056 | |

| | | |
|---|---|---|
| 1225.1 | 48.093 | |
| 1226.8 | 48.130 | |
| 1227.2 | 48.167 | |
| 1227.9 | 48.205 | |
| 1229.9 | 48.282 | |
| 1229.9 | 48.243 | |
| 1232.2 | 48.321 | |
| 1232.5 | 48.360 | |
| 1233.2 | 48.399 | |

| SPECIFIC HEAT OF NICKEL (NIC) | |
|---|---|
| | |
| TEMPERATURE (K) | SPECIFIC HEAT (J/gm-K) |
| 373 | 0.4962 |
| 380 | 0.4977 |
| 390 | 0.5003 |
| 400 | 0.5035 |
| 410 | 0.5070 |
| 420 | 0.5109 |
| 430 | 0.5152 |
| 440 | 0.5196 |
| 450 | 0.5244 |
| 460 | 0.5293 |
| 470 | 0.5344 |
| 480 | 0.5397 |
| 490 | 0.5452 |
| 500 | 0.5509 |
| 510 | 0.5567 |
| 520 | 0.5627 |
| 530 | 0.5689 |
| 540 | 0.5753 |
| 550 | 0.5819 |
| 560 | 0.5888 |
| 570 | 0.5959 |
| 580 | 0.6033 |
| 590 | 0.6111 |
| 600 | 0.6191 |
| 605 | 0.6233 |
| 610 | 0.6276 |
| 615 | 0.6319 |
| | |
| | |
| | |
| 640 | 0.5509 |
| 650 | 0.5487 |
| 660 | 0.5466 |
| 670 | 0.5448 |
| 680 | 0.5431 |
| 690 | 0.5416 |
| 700 | 0.5402 |
| 710 | 0.5390 |
| 720 | 0.5380 |

| | | |
|---|---|---|
| 730 | 0.5370 | |
| 740 | 0.5362 | |
| 750 | 0.5356 | |
| 760 | 0.5351 | |
| 770 | 0.5347 | |
| 780 | 0.5344 | |
| 790 | 0.5342 | |
| 800 | 0.5342 | |
| 810 | 0.5343 | |
| 820 | 0.5346 | |
| 830 | 0.5349 | |
| 840 | 0.5354 | |
| 850 | 0.5361 | |
| 860 | 0.5368 | |
| 870 | 0.5377 | |
| 880 | 0.5387 | |
| 890 | 0.5398 | |
| 900 | 0.5411 | |
| 910 | 0.5425 | |
| 920 | 0.5441 | |
| 930 | 0.5458 | |
| 940 | 0.5476 | |
| 950 | 0.5496 | |
| 960 | 0.5518 | |
| 970 | 0.5541 | |
| 980 | 0.5566 | |
| 990 | 0.5592 | |
| 100 | 0 0.5619 | |
| 101 | 0 0.5648 | |
| 102 | 0 0.5679 | |
| 103 | 0 0.5711 | |
| 104 | 0 0.5745 | |
| 105 | 0 0.578 | |
| 106 | 0 0.5817 | |
| 107 | 0 0.5855 | |
| 108 | 0 0.5895 | |
| 109 | 0 0.5936 | |
| 110 | 0 0.5979 | |
| 111 | 0 0.6023 | |
| 112 | 0 0.6069 | |
| 113 | 0 0.6116 | |
| 114 | 0 0.6165 | |
| 115 | 0 0.6215 | |

| | | |
|---|---|---|
| 116 | 0 0.6266 | |
| 117 | 0 0.632 | |
| 118 | 0 0.6374 | |
| 119 | 0 0.6431 | |
| 120 | 0 0.6488 | |
| 121 | 0 0.6547 | |
| 122 | 0 0.6608 | |
| 123 | 0 0.667 | |
| 124 | 0 0.6734 | |
| 125 | 0 0.6799 | |
| 126 | 0 0.6866 | |
| 127 | 0 0.6934 | |
| 128 | 0 0.7004 | |
| 129 | 0 0.7075 | |
| 130 | 0 0.7148 | |

| ELECTRICAL RESISTIVITY OF Ni(4)Mo | | |
|---|---|---|
| INITIAL CONDITION : SRO (ALPHA) | | |
| | | |
| TEMPERATURE | FLECTRICAL RESISTIVITY | |
| (K) | (micro-ohm-cm) | |
| 306.60 | 142.34 | |
| 310.94 | 142.43 | |
| 314.51 | 142.41 | |
| 319.67 | 142.33 | |
| 323.18 | 142.39 | |
| 328.11 | 142.35 | |
| 332.99 | 142.47 | |
| 337.26 | 142.47 | |
| 342.06 | 142.46 | |
| 346.81 | 142.55 | |
| 351.52 | 142.66 | |
| 356.19 | 142.68 | |
| 360.96 | 142.54 | |
| 366.22 | 142.64 | |
| 370.77 | 142.63 | |
| 375.93 | 142.78 | |
| 381.05 | 142.73 | |
| 386.13 | 142.80 | |
| 390.51 | 142.78 | |
| 395.50 | 142.81 | |
| 401.08 | 142.80 | |
| 405.35 | 142.82 | |
| 410.34 | 142.56 | |
| 415.66 | 140.35 | |
| 420.56 | 142.87 | |
| 425.31 | 142.99 | |
| 430.02 | 143.03 | |
| 434.69 | 142.91 | |
| 439.93 | 143.05 | |
| 444.53 | 143.04 | |
| 449.69 | 143.09 | |
| 454.24 | 143.03 | |
| 458.75 | 143.13 | |
| 463.80 | 143.16 | |
| 468.26 | 143.19 | |
| 473.25 | 143.25 | |
| 477.65 | 143.17 | |
| 482.58 | 143.07 | |

| | | |
|---|---|---|
| 488.04 | 143.30 | |
| 492.37 | 143.30 | |
| 497.21 | 143.26 | |
| 502.04 | 143.30 | |
| 506.73 | 143.38 | |
| 511.50 | 143.40 | |
| 516.79 | 143.48 | |
| 521.51 | 143.65 | |
| 526.22 | 143.59 | |
| 530.90 | 143.67 | |
| 535.56 | 143.46 | |
| 540.74 | 143.57 | |
| 545.36 | 143.46 | |
| 550.49 | 143.57 | |
| 555.49 | 143.68 | |
| 565.13 | 143.69 | |
| 570.18 | 143.76 | |
| 575.22 | 143.71 | |
| 580.23 | 143.80 | |
| 585.23 | 143.80 | |
| 589.60 | 143.85 | |
| 595.08 | 143.87 | |
| 609.88 | 143.94 | |
| 614.78 | 144.02 | |
| 619.57 | 144.01 | |
| 629.30 | 144.06 | |
| 634.63 | 144.08 | |
| 638.96 | 144.16 | |
| 644.17 | 144.23 | |
| 648.96 | 144.26 | |
| 654.22 | 144.25 | |
| 658.98 | 144.28 | |
| 663.72 | 144.28 | |
| 668.82 | 144.36 | |
| 673.57 | 144.43 | |
| 678.28 | 144.38 | |
| 683.45 | 144.46 | |
| 688.52 | 144.54 | |
| 693.19 | 144.46 | |
| 698.33 | 144.49 | |
| 702.98 | 144.52 | |
| 707.63 | 144.62 | |
| 712.64 | 144.62 | |

| | | |
|---|---|---|
| 717.73 | 144.70 | |
| 722.35 | 144.69 | |
| 727.33 | 144.78 | |
| 731.92 | 144.82 | |
| 736.97 | 144.77 | |
| 741.55 | 144.85 | |
| 746.58 | 144.79 | |
| 751.50 | 144.85 | |
| 756.05 | 144.93 | |
| 761.05 | 145.00 | |
| 766.03 | 144.95 | |
| 770.92 | 145.04 | |
| 775.42 | 145.00 | |
| 780.38 | 145.16 | |
| 784.87 | 145.12 | |
| 789.71 | 145.18 | |
| 794.64 | 145.13 | |
| 799.55 | 145.21 | |
| 808.80 | 145.28 | |
| 813.69 | 145.27 | |
| 818.56 | 145.23 | |
| 822.98 | 145.39 | |
| 832.59 | 145.47 | |
| 837.42 | 145.55 | |
| 841.71 | 145.54 | |
| 846.52 | 145.54 | |
| 851.33 | 145.58 | |
| 856.12 | 145.64 | |
| 860.82 | 145.71 | |
| 865.16 | 145.66 | |
| 869.92 | 145.66 | |
| 874.68 | 145.81 | |
| 879.34 | 145.81 | |
| 884.08 | 145.89 | |
| 888.81 | 145.81 | |
| 893.44 | 145.84 | |
| 897.72 | 146.01 | |
| 907.11 | 146.10 | |
| 911.71 | 146.15 | |
| 915.95 | 146.09 | |
| 925.28 | 146.17 | |
| 929.84 | 146.04 | |
| 934.05 | 145.95 | |

| | | |
|---|---|---|
| 939.11 | 145.98 | |
| 943.30 | 146.02 | |
| 947.41 | 145.88 | |
| 952.01 | 145.88 | |
| 964.93 | 145.51 | |
| 969.42 | 145.33 | |
| 973.14 | 145.16 | |
| 977.28 | 144.98 | |
| 985.11 | 144.50 | |
| 989.23 | 144.28 | |
| 992.92 | 144.07 | |
| 996.52 | 143.81 | |
| 1000.20 | 143.53 | |
| 1003.45 | 143.12 | |
| 1007.12 | 142.83 | |
| 1010.46 | 142.50 | |
| 1013.70 | 142.26 | |
| 1016.94 | 141.94 | |
| 1019.76 | 141.46 | |
| 1022.99 | 141.21 | |
| 1026.22 | 140.90 | |
| 1029.03 | 140.49 | |
| 1031.84 | 140.25 | |
| 1035.06 | 139.78 | |
| 1037.94 | 139.54 | |
| 1040.74 | 139.23 | |
| 1043.12 | 138.80 | |
| 1048.70 | 138.25 | |
| 1051.57 | 137.87 | |
| 1054.35 | 137.60 | |
| 1057.13 | 137.32 | |
| 1062.28 | 136.74 | |
| 1065.13 | 136.55 | |
| 1067.90 | 136.25 | |
| 1070.66 | 135.98 | |
| 1073.42 | 135.75 | |
| 1076.18 | 135.64 | |
| 1078.94 | 135.37 | |
| 1081.78 | 135.18 | |
| 1084.93 | 134.99 | |
| 1088.08 | 134.81 | |
| 1091.23 | 134.62 | |
| 1094.37 | 134.39 | |

| | | |
|---|---|---|
| 1097.51 | 134.24 | |
| 1100.65 | 134.05 | |
| 1103.78 | 133.83 | |
| 1107.31 | 133.68 | |
| 1110.04 | 133.53 | |
| 1116.68 | 133.16 | |
| 1122.90 | 132.91 | |
| 1126.01 | 132.76 | |
| 1132.61 | 132.39 | |
| 1135.70 | 132.28 | |
| 1138.88 | 132.17 | |
| 1142.28 | 131.95 | |
| 1148.53 | 131.70 | |
| 1151.60 | 131.51 | |
| 1155.07 | 131.33 | |
| 1158.14 | 131.23 | |
| 1164.67 | 131.01 | |
| 1167.73 | 130.90 | |
| 1170.78 | 130.76 | |
| 1173.84 | 130.58 | |
| 1177.28 | 130.47 | |
| 1180.32 | 130.36 | |
| 1183.76 | 130.25 | |
| 1186.41 | 130.07 | |
| 1189.83 | 130.00 | |
| 1192.87 | 129.89 | |
| 1195.90 | 129.75 | |
| 1198.92 | 129.68 | |
| 1202.33 | 129.54 | |
| 1205.35 | 129.36 | |
| 1208.37 | 129.29 | |
| 1211.38 | 129.22 | |
| 1214.78 | 129.08 | |
| 1217.79 | 128.97 | |
| 1220.79 | 128.83 | |
| 1223.79 | 128.76 | |
| 1226.79 | 128.62 | |
| 1229.86 | 128.55 | |
| 1236.22 | 128.37 | |
| 1238.82 | 128.20 | |
| 1242.19 | 128.13 | |
| 1245.17 | 128.02 | |
| 1251.12 | 127.92 | |

| | | |
|---|---|---|
| 1257.06 | 127.68 | |
| 1260.02 | 127.61 | |
| 1262.98 | 127.61 | |
| 1265.94 | 127.50 | |
| 1271.47 | 127.26 | |
| 1277.74 | 127.05 | |
| 1280.39 | 127.09 | |
| 1283.33 | 126.91 | |
| 1286.27 | 126.95 | |
| 1292.14 | 126.71 | |
| 1297.62 | 126.64 | |
| 1300.55 | 126.54 | |
| 1303.47 | 126.50 | |
| 1306.39 | 126.33 | |
| 1311.92 | 126.26 | |
| 1314.84 | 126.23 | |
| 1317.75 | 126.13 | |
| 1320.28 | 126.06 | |
| 1323.19 | 126.02 | |
| 1326.09 | 125.95 | |
| 1334.04 | 125.82 | |
| 1336.93 | 125.68 | |
| 1339.52 | 125.62 | |
| 1347.44 | 125.51 | |
| 1350.32 | 125.48 | |
| 1353.20 | 125.34 | |
| 1355.70 | 125.31 | |
| 1358.28 | 125.28 | |
| 1361.15 | 125.24 | |
| 1363.66 | 125.14 | |
| 1366.16 | 125.11 | |
| 1368.65 | 125.08 | |
| 1371.15 | 125.01 | |
| 1373.76 | 125.01 | |
| 1376.33 | 124.94 | |
| 1378.82 | 124.87 | |
| 1381.31 | 124.84 | |
| 1383.80 | 124.74 | |
| 1386.65 | 124.81 | |
| 1388.77 | 124.71 | |
| 1393.81 | 124.61 | |
| 1396.29 | 124.57 | |
| 1398.77 | 124.54 | |

| | | |
|---|---|---|
| 1401.25 | 124.51 | |
| 1403.80 | 124.44 | |
| 1406.27 | 124.41 | |
| 1408.38 | 124.41 | |
| 1411.22 | 124.38 | |
| 1413.33 | 124.34 | |
| 1415.87 | 124.28 | |
| 1418.34 | 124.24 | |
| 1420.81 | 124.24 | |
| 1422.91 | 124.18 | |
| 1425.38 | 124.11 | |
| 1427.91 | 124.18 | |
| 1430.01 | | |
| 1432.47 | | |
| 1434.57 | | |
| 1437.03 | | |
| 1439.20 | | |

| ELECTRICAL RESISTIVITY OF Ni(4)Mo | | |
|---|---|---|
| INITIAL CONDITION : LRO (BETA) | | |
| | | |
| TEMPERATURE | ELECTRICAL RESISTIVITY | |
| (K) | (micro-ohm-cm) | |
| 372.8 | 75.14 | |
| 376.6 | 75.59 | |
| 379.7 | 76.01 | |
| 384.2 | 76.47 | |
| 388.7 | 76.55 | |
| 392.4 | 77.38 | |
| 396.8 | 77.83 | |
| 401.1 | 78.24 | |
| 405.4 | 78.65 | |
| 409.7 | 79.12 | |
| 413.9 | 79.53 | |
| 418.7 | 79.95 | |
| 422.9 | 80.40 | |
| 427.0 | 80.85 | |
| 432.3 | 81.32 | |
| 436.3 | 81.70 | |
| 440.9 | 82.10 | |
| 445.5 | 82.64 | |
| 450.7 | 83.00 | |
| 455.2 | 83.50 | |
| 460.3 | 83.99 | |
| 464.8 | 84.40 | |
| 469.8 | 84.87 | |
| 474.8 | 85.30 | |
| 479.7 | 85.80 | |
| 484.7 | 86.22 | |
| 489.5 | 86.60 | |
| 495.0 | 87.10 | |
| 500.3 | 87.60 | |
| 505.2 | 88.10 | |
| 510.5 | 88.50 | |
| 515.7 | 88.90 | |
| 520.9 | 89.40 | |
| 526.2 | 89.88 | |
| 531.9 | 90.30 | |
| 537.1 | 90.79 | |
| 542.2 | 91.23 | |
| 547.8 | 91.62 | |

| | | |
|---|---|---|
| 553.5 | 92.05 | |
| 558.6 | 92.53 | |
| 564.0 | 92.80 | |
| 569.1 | 93.10 | |
| 574.1 | 93.10 | |
| 578.6 | 94.00 | |
| 584.2 | 94.40 | |
| 589.1 | 94.87 | |
| 594.1 | 95.34 | |
| 599.5 | 95.60 | |
| 604.4 | 96.10 | |
| 609.8 | 96.40 | |
| 614.8 | 96.88 | |
| 620.0 | 97.20 | |
| 625.4 | 97.70 | |
| 630.7 | 98.08 | |
| 636.0 | 98.44 | |
| 641.3 | 98.86 | |
| 646.6 | 99.20 | |
| 652.2 | 99.66 | |
| 657.5 | 100.00 | |
| 663.2 | 100.40 | |
| 668.3 | 100.00 | |
| 674.0 | 101.00 | |
| 684.3 | 102.00 | |
| 695.0 | 102.00 | |
| 700.6 | 103.00 | |
| 705.7 | 103.00 | |
| 711.3 | 103.00 | |
| 716.3 | 104.10 | |
| 721.8 | 104.00 | |
| 727.3 | 104.00 | |
| 732.8 | 105.20 | |
| 737.9 | 105.00 | |
| 743.3 | 105.90 | |
| 748.3 | 106.00 | |
| 753.8 | 106.00 | |
| 759.1 | 107.00 | |
| 764.6 | 107.00 | |
| 769.6 | 107.00 | |
| 774.9 | 108.00 | |
| 780.3 | 108.00 | |
| 785.6 | 108.60 | |

| | | |
|---|---|---|
| 791.0 | 109.00 | |
| 796.0 | 109.00 | |
| 801.2 | 109.00 | |
| 806.6 | 110.00 | |
| 811.8 | 110.30 | |
| 817.2 | 110.00 | |
| 822.5 | 110.00 | |
| 827.2 | 111.00 | |
| 832.5 | 111.00 | |
| 837.8 | 111.00 | |
| 843.0 | 112.00 | |
| 848.3 | 112.00 | |
| 853.4 | 112.00 | |
| 858.2 | 113.00 | |
| 863.4 | 113.00 | |
| 873.8 | 114.00 | |
| 878.9 | 114.00 | |
| 884.0 | 114.00 | |
| 889.2 | 115.00 | |
| 894.3 | 115.00 | |
| 904.5 | 115.00 | |
| 909.6 | 116.00 | |
| 914.3 | 116.50 | |
| 919.3 | 116.00 | |
| 924.4 | 117.00 | |
| 929.4 | 117.00 | |
| 934.4 | 117.00 | |
| 939.5 | 117.00 | |
| 944.5 | 118.10 | |
| 949.1 | 118.00 | |
| 954.1 | 118.00 | |
| 959.0 | 119.00 | |
| 964.1 | 119.40 | |
| 968.9 | 119.00 | |
| 973.5 | 119.00 | |
| 978.5 | 120.00 | |
| 987.9 | 120.00 | |
| 992.9 | 120.00 | |
| 997.7 | 121.00 | |
| 1007.0 | 121.00 | |
| 1011.0 | 122.00 | |
| 1016.0 | 122.00 | |
| 1025.0 | 122.00 | |

| | | |
|---|---|---|
| 1029.0 | 123.00 | |
| 1034.0 | 123.00 | |
| 1038.0 | 123.00 | |
| 1043.0 | 124.00 | |
| 1047.0 | 124.00 | |
| 1051.0 | 124.00 | |
| 1055.0 | 124.90 | |
| 1059.0 | 125.00 | |
| 1063.0 | 125.00 | |
| 1071.0 | 126.00 | |
| 1075.0 | 126.50 | |
| 1078.0 | 126.00 | |
| 1082.0 | 127.00 | |
| 1086.0 | 127.00 | |
| 1090.0 | 127.00 | |
| 1092.0 | 128.00 | |
| 1096.0 | 128.00 | |
| 1099.0 | 128.00 | |
| 1102.0 | 129.00 | |
| 1105.0 | 129.00 | |
| 1108.0 | 130.00 | |
| 1111.0 | 130.00 | |
| 1113.0 | 130.00 | |
| 1115.0 | 130.00 | |
| 1118.0 | 131.00 | |
| 1120.0 | 131.40 | |
| 1122.0 | 131.00 | |
| 1125.0 | 132.00 | |
| 1129.0 | 132.40 | |
| 1129.0 | 132.00 | |
| 1131.0 | 132.80 | |
| 1131.0 | 132.00 | |
| 1132.0 | 132.00 | |
| 1133.4 | 133.02 | |
| 1133.0 | 133.06 | |
| 1134.0 | 133.00 | |
| 1135.0 | 133.20 | |
| 1136.0 | 133.20 | |
| 1136.0 | 133.00 | |
| 1137.0 | 133.00 | |
| 1138.4 | 133.26 | |
| 1139.0 | 133.20 | |
| 1139.0 | 133.20 | |

| | | |
|---|---|---|
| 1141.0 | 133.20 | |
| 1141.0 | 133.10 | |
| 1142.0 | 133.00 | |
| 1143.0 | 133.00 | |
| 1145.0 | 132.99 | |
| 1146.0 | 132.80 | |
| 1147.0 | 132.70 | |
| 1149.0 | 132.60 | |
| 1151.0 | 132.53 | |
| 1153.0 | 132.39 | |
| 1155.0 | 132.20 | |
| 1157.0 | 132.00 | |
| 1159.0 | 131.90 | |
| 1162.0 | 131.79 | |
| 1165.0 | 131.61 | |
| 1168.0 | 131.40 | |
| 1171.0 | 131.20 | |
| 1178.0 | 130.90 | |
| 1181.0 | 130.84 | |
| 1185.0 | 130.70 | |
| 1188.0 | 130.60 | |
| 1192.0 | 130.40 | |
| 1195.0 | 130.29 | |
| 1198.0 | 130.10 | |
| 1201.0 | 130.00 | |
| 1204.0 | 130.01 | |
| 1208.0 | 129.80 | |
| 1211.0 | 129.50 | |
| 1215.0 | 129.40 | |
| 1218.5 | 129.39 | |
| 1221.5 | 129.32 | |
| 1224.0 | 129.10 | |
| 1227.0 | 129.00 | |
| 1231.0 | 128.91 | |
| 1234.0 | 128.80 | |
| 1238.0 | 128.70 | |
| 1241.0 | 128.50 | |
| 1244.0 | 128.40 | |
| 1247.0 | 128.40 | |
| 1254.0 | 128.20 | |
| 1257.0 | 128.00 | |
| 1260.0 | 127.99 | |
| 1263.7 | 127.85 | |

| | | |
|---|---|---|
| 1267.0 | 127.75 | |
| 1270.0 | 127.60 | |
| 1272.0 | 127.50 | |
| 1276.0 | 127.48 | |
| 1279.0 | 127.40 | |
| 1282.0 | 127.20 | |
| 1285.0 | 127.21 | |
| 1288.0 | 127.10 | |
| 1291.0 | 127.10 | |
| 1294.0 | 127.00 | |
| 1300.0 | 126.80 | |
| 1303.8 | 126.71 | |
| 1307.1 | 126.68 | |
| 1310.0 | 126.57 | |
| 1313.0 | 126.44 | |
| 1316.0 | 126.40 | |
| 1319.0 | 126.30 | |
| 1322.0 | 126.20 | |
| 1324.0 | 126.10 | |
| 1327.0 | 126.10 | |
| 1331.0 | 126.00 | |
| 1334.0 | 125.90 | |
| 1336.0 | 125.90 | |
| 1339.0 | 125.80 | |
| 1342.7 | 125.82 | |
| 1345.6 | 125.71 | |
| 1348.0 | 125.60 | |
| 1351.0 | 125.58 | |
| 1354.0 | 125.52 | |
| 1357.0 | 125.40 | |
| 1360.0 | 125.40 | |
| 1362.0 | 125.30 | |
| 1365.0 | 125.20 | |
| 1368.0 | 125.21 | |
| 1371.0 | 125.20 | |
| 1373.0 | 125.10 | |
| 1376.0 | 125.10 | |
| 1379.0 | 124.90 | |
| 382.0 | 125.12 | |
| 1384.0 | 124.80 | |
| 1387.0 | 124.90 | |
| 1390.0 | 124.70 | |
| 1392.0 | 124.70 | |

| | | |
|---|---|---|
| 1395.0 | 124.60 | |
| 1398.0 | 124.60 | |
| 1400.0 | 124.62 | |
| 1403.0 | 124.60 | |
| 1406.0 | 124.40 | |
| 1408.0 | 124.40 | |
| 1411.0 | 124.30 | |
| 1414.0 | 124.40 | |
| 1416.5 | 124.40 | |
| 1418.9 | 124.33 | |
| 1421.0 | 124.20 | |
| 1424.0 | 124.20 | |
| 1426.0 | 124.26 | |
| 1429.0 | 124.20 | |
| 1431.0 | 124.10 | |
| 1434.0 | 124.04 | |
| 1436.0 | 124.00 | |
| 1439.0 | 124.00 | |
| 1441.0 | 124.00 | |
| 1444.0 | 123.90 | |
| 1446.0 | 123.90 | |
| 1449.0 | 123.90 | |
| 1451.5 | 123.84 | |
| 1453.0 | 123.70 | |

| ELECTRICAL RESISTIVITY OF Ni(4)Mo | | |
|---|---|---|
| INITIAL CONDITION : COLD-WORKED SRO (ALPHA) | | |
| | | |
| TEMPERATURE | ELECTRICAL RESISTIVITY | |
| (K) | (micro-ohm-cm) | |
| 311.7 | 128.51 | |
| 316.7 | 128.55 | |
| 322.4 | 128.51 | |
| 328.1 | 128.55 | |
| 333.0 | 128.62 | |
| 339.2 | 128.62 | |
| 344.7 | 128.66 | |
| 350.3 | 128.69 | |
| 356.2 | 128.69 | |
| 362.2 | 128.72 | |
| 368.1 | 128.72 | |
| 374.0 | 128.72 | |
| 379.7 | 128.76 | |
| 386.1 | 128.87 | |
| 391.8 | 128.83 | |
| 397.4 | 128.87 | |
| 403.6 | 128.83 | |
| 409.7 | 129.01 | |
| 415.2 | 128.87 | |
| 421.7 | 128.90 | |
| 427.6 | 128.90 | |
| 432.9 | 129.04 | |
| 439.3 | 129.01 | |
| 445.1 | 129.04 | |
| 450.7 | 129.00 | |
| 456.4 | 129.08 | |
| 462.7 | 129.04 | |
| 468.8 | 129.15 | |
| 474.3 | 129.11 | |
| 480.3 | 129.11 | |
| 486.4 | 129.18 | |
| 491.8 | 129.18 | |
| 497.7 | 129.25 | |
| 503.6 | 129.22 | |
| 509.4 | 129.29 | |
| 515.3 | 129.36 | |
| 521.0 | 129.25 | |
| 526.8 | 129.32 | |

| | | |
|---|---|---|
| 532.5 | 129.36 | |
| 544.3 | 129.39 | |
| 550.0 | 129.46 | |
| 555.5 | 129.53 | |
| 561.6 | 129.53 | |
| 566.7 | 129.46 | |
| 572.7 | 129.53 | |
| 578.7 | 129.46 | |
| 584.2 | 129.57 | |
| 590.1 | 129.60 | |
| 595.6 | 129.67 | |
| 601.5 | 129.64 | |
| 606.9 | 129.74 | |
| 612.8 | 129.74 | |
| 618.7 | 129.71 | |
| 623.9 | 129.78 | |
| 629.3 | 129.85 | |
| 635.5 | 129.88 | |
| 640.8 | 129.99 | |
| 646.6 | 129.99 | |
| 651.8 | 130.10 | |
| 658.0 | 130.10 | |
| 663.7 | 130.13 | |
| 669.3 | 130.27 | |
| 675.0 | 130.38 | |
| 681.1 | 130.56 | |
| 686.7 | 130.63 | |
| 692.7 | 130.81 | |
| 698.8 | 130.95 | |
| 704.3 | 131.06 | |
| 710.4 | 131.24 | |
| 716.8 | 131.45 | |
| 722.8 | 131.74 | |
| 729.2 | 131.92 | |
| 735.2 | 132.06 | |
| 741.5 | 132.28 | |
| 747.9 | 132.64 | |
| 754.3 | 132.97 | |
| 760.6 | 133.16 | |
| 766.9 | 133.45 | |
| 773.2 | 133.74 | |
| 779.9 | 134.07 | |
| 786.1 | 134.33 | |

| | | |
|---|---|---|
| 792.9 | 134.55 | |
| 799.1 | 134.81 | |
| 805.3 | 135.11 | |
| 811.5 | 135.37 | |
| 817.7 | 135.56 | |
| 823.8 | 135.85 | |
| 830.0 | 136.15 | |
| 836.1 | 136.30 | |
| 842.2 | 136.46 | |
| 848.3 | 136.76 | |
| 853.9 | 137.06 | |
| 860.4 | 137.25 | |
| 866.5 | 137.45 | |
| 872.0 | 137.75 | |
| 878.1 | 137.91 | |
| 884.1 | 138.03 | |
| 889.6 | 138.30 | |
| 895.6 | 138.56 | |
| 901.6 | 138.80 | |
| 907.1 | 138.88 | |
| 913.0 | 139.07 | |
| 918.5 | 139.35 | |
| 924.4 | 139.47 | |
| 929.4 | 139.63 | |
| 935.3 | 139.86 | |
| 940.7 | 139.98 | |
| 946.2 | 140.07 | |
| 951.6 | 140.30 | |
| 957.0 | 140.38 | |
| 962.0 | 140.46 | |
| 967.4 | 140.47 | |
| 972.3 | 140.67 | |
| 977.3 | 140.63 | |
| 982.2 | 140.67 | |
| 986.7 | 140.76 | |
| 991.7 | 140.69 | |
| 996.2 | 140.70 | |
| 1000.6 | 140.65 | |
| 1005.5 | 140.65 | |
| 1009.6 | 140.50 | |
| 1013.7 | 140.49 | |
| 1018.1 | 140.45 | |
| 1022.2 | 140.27 | |

| | | |
|---|---|---|
| 1026.2 | 140.11 | |
| 1029.9 | 140.02 | |
| 1033.9 | 139.87 | |
| 1037.9 | 139.63 | |
| 1041.5 | 139.44 | |
| 1045.1 | 139.32 | |
| 1048.7 | 139.16 | |
| 1051.9 | 138.85 | |
| 1055.5 | 138.66 | |
| 1059.1 | 138.43 | |
| 1062.3 | 138.09 | |
| 1065.5 | 137.93 | |
| 1069.0 | 137.66 | |
| 1072.2 | 137.51 | |
| 1075.1 | 137.21 | |
| 1078.6 | 136.98 | |
| 1081.8 | 136.67 | |
| 1084.9 | 136.37 | |
| 1088.1 | 136.25 | |
| 1091.2 | 136.03 | |
| 1094.4 | 135.85 | |
| 1097.5 | 135.62 | |
| 1101.1 | 135.36 | |
| 1104.2 | 135.21 | |
| 1107.3 | 135.05 | |
| 1110.8 | 134.76 | |
| 1114.0 | 134.57 | |
| 1117.1 | 134.37 | |
| 1120.6 | 134.25 | |
| 1123.7 | 133.95 | |
| 1126.8 | 133.87 | |
| 1129.9 | 133.72 | |
| 1133.4 | 133.40 | |
| 1136.5 | 133.36 | |
| 1140.0 | 133.25 | |
| 1143.1 | 132.99 | |
| 1146.6 | 132.81 | |
| 1149.6 | 132.74 | |
| 1153.1 | 132.59 | |
| 1156.2 | 132.41 | |
| 1159.6 | 132.20 | |
| 1162.7 | 132.19 | |
| 1166.2 | 131.94 | |

| | | |
|---|---|---|
| 1169.2 | 131.72 | |
| 1172.3 | 131.62 | |
| 1175.3 | 131.54 | |
| 1178.8 | 131.36 | |
| 1181.8 | 131.26 | |
| 1185.2 | 131.08 | |
| 1188.3 | 130.94 | |
| 1191.7 | 130.87 | |
| 1194.4 | 130.72 | |
| 1197.8 | 130.58 | |
| 1201.2 | 130.47 | |
| 1204.2 | 130.29 | |
| 1206.9 | 130.11 | |
| 1210.3 | 130.05 | |
| 1213.3 | 129.97 | |
| 1216.3 | 129.90 | |
| 1219.7 | 129.69 | |
| 1222.7 | 129.51 | |
| 1225.3 | 129.55 | |
| 1228.7 | 129.37 | |
| 1231.7 | 129.23 | |
| 1234.7 | 129.13 | |
| 1237.7 | 129.09 | |
| 1241.0 | 128.98 | |
| 1244.0 | 128.88 | |
| 1249.6 | 128.70 | |
| 1253.0 | 128.56 | |
| 1255.5 | 128.42 | |
| 1258.6 | 128.38 | |
| 1261.5 | 128.31 | |
| 1264.5 | 128.24 | |
| 1267.5 | 128.17 | |
| 1270.4 | 128.02 | |
| 1273.4 | 127.92 | |
| 1275.9 | 127.84 | |
| 1278.9 | 127.81 | |
| 1281.4 | 127.70 | |
| 1284.4 | 127.59 | |
| 1287.0 | 127.52 | |
| 1289.6 | 127.45 | |
| 1292.5 | 127.48 | |
| 1295.1 | 127.41 | |
| 1300.6 | 127.19 | |

| | | |
|---|---|---|
| 1303.5 | 127.16 | |
| 1305.7 | 127.05 | |
| 1308.6 | 126.98 | |
| 1311.2 | 127.02 | |
| 1313.7 | 126.88 | |
| 1316.3 | 126.84 | |
| 1319.2 | 126.70 | |
| 1321.3 | 126.66 | |
| 1324.3 | 126.60 | |
| 1326.8 | 126.49 | |
| 1329.4 | 126.35 | |
| 1331.9 | 126.39 | |
| 1334.4 | 126.35 | |
| 1336.9 | 126.35 | |
| 1339.5 | 126.25 | |
| 1342.0 | 126.22 | |
| 1344.6 | 126.08 | |
| 1347.1 | 126.05 | |
| 1349.6 | 126.01 | |
| 1352.2 | 125.87 | |
| 1354.7 | 125.87 | |
| 1357.2 | 125.81 | |
| 1360.1 | 125.70 | |
| 1362.2 | 125.63 | |
| 1364.7 | 125.59 | |
| 1367.3 | 125.66 | |
| 1369.8 | 125.52 | |
| 1372.3 | 125.49 | |
| 1374.5 | 125.49 | |
| 1377.0 | 125.43 | |
| 1379.5 | 125.32 | |
| 1382.0 | 125.29 | |
| 1384.5 | 125.19 | |
| 1386.7 | 125.13 | |

| SPECIFIC HEAT OF Ni(4)Mo | |
|---|---|
| INITIAL CONDITION : SRO (ALPHA) | |
| | |
| TEMPERATURE | SPECIFIC HEAT |
| (K) | (J/gm-K) |
| 275 | 0.3441 |
| 300 | 0.3616 |
| 350 | 0.3929 |
| 400 | 0.4164 |
| 450 | 0.4304 |
| 500 | 0.4359 |
| 550 | 0.4356 |
| 600 | 0.4327 |
| 650 | 0.4300 |
| 700 | 0.4301 |
| 750 | 0.4349 |
| 800 | 0.4330 |
| 850 | 0.4658 |
| 900 | 0.4963 |
| 950 | 0.5408 |
| 1000 | 0.6027 |
| 1050 | 0.6845 |
| 1100 | 0.7828 |
| 1110 | 0.8030 |
| 1120 | 0.8231 |
| 1130 | 0.8427 |
| 1141 | 0.8628 |
| 1141 | 0.6264 |
| 1150 | 0.6258 |
| 1200 | 0.6266 |
| 1250 | 0.6339 |
| 1300 | 0.6481 |
| 1350 | 0.6700 |
| 1400 | 0.7009 |
| 1440 | 0.7335 |
| | |

| SPECIFIC HEAT OF Ni(4)Mo | |
|---|---|
| INITIAL CONDITION : LRO (BETA) | |
| | |
| TEMPERATURE | SPECIFIC HEAT |
| (K) | (J/gm-K) |
| 300 | 0.2580 |
| 350 | 0.3778 |
| 400 | 0.4332 |
| 450 | 0.4401 |
| 500 | 0.4307 |
| 550 | 0.4226 |
| 600 | 0.4219 |
| 650 | 0.4289 |
| 700 | 0.4412 |
| 750 | 0.4547 |
| 800 | 0.4646 |
| 850 | 0.4675 |
| 900 | 0.4644 |
| 950 | 0.4630 |
| 100 | 0.4796 |
| 105 | 0.5528 |
| 110 | 0.8620 |
| 1120 | 1.9349 |
| 1141 | 4.9563 |
| 1141 | 1.9234 |
| 1150 | 1.2579 |
| 1200 | 0.6155 |
| 1250 | 0.6182 |
| 1300 | 0.6621 |
| 1350 | 0.6712 |
| 1400 | 0.7025 |
| 1450 | 0.7322 |
| | |

# APPENDIX IV

## SOURCE CODE FOR PID TEMPERATURE CONTROL PROGRAM

```
C****          10-14-94     ********************************ALEXI*DEB*

       PROGRAM CALORIMETER ISOTHERMAL

C****          CALORIMETER ISOTHERMAL WAS WRITTEN TO TAKE THREE A/D
INPUTS ON
C****          CHANNELS 0-3 AND TO OUTPUT A CONTROL SIGNAL WITH THE
D/A ON
C****          CHANNEL 0 FOR THE CONTROL OF TEMPERATURE.
C****          CALORIMETER ISOTHERMAL HAS FILE CAPABILITY.

C****          DEFINE VARIABLES ***************************

       INTEGER*2 STIM,JTIM,HTIM,ITIC
       INTEGER*4 TEMP1
       INTEGER*2 VOLT1,VOLT2
       INTEGER*2 IWS1(22),IWS2(22),IWS3(22),IREG(8),IVAL
       INTEGER*2 TIME(5000),IN
       INTEGER*2 IEXIT,ILOAD
       INTEGER*2 KEY,INKEY,WAITKY
       INTEGER*2 INTERVAL1 INTERVAL2,INTERVAL3
       INTEGER*2 IEMF1,IEMF2,IEMF3,IEMFR
C      INTEGER*2 INTCOOL,ITICOOL,INTEND

       REAL*8 DATAR0(5000),DATAR1(5000),DATAR2(5000),POWER(5000)
       REAL*8 RHO(5000)
       REAL*8
STIME,JTIME,HTIME,XSAVE,XPRINT,XEND,XRETURN,XRUN,XQUIT
       REAL*8 CURTOT
       CHARACTER*12 FNAME

       EXTERNAL ISR1,ISR2,ISR3

C****          ESTABLISH COMMON LOCATIONS *****************

       COMMON/TIME/STIM,JTIM,HTIM,ITIC
       COMMON/ID/STIME,JTIME,HTIME,XSAVE,XPRINT,XEND,XRETURN,XR
UN,X QUIT
       COMMON/TEMP/TEMP1
       COMMON/VOLT/VOLT1,VOLT2
       COMMON/FLAG/IEXIT,IVAL,ILOAD
       COMMON/INPUTS/TIME,IN
       COMMON/FILE/FNAME
       COMMON/EMF/IEMF1,IEMF2,IEMF3,IEMFR
```

```
      COMMON/INTERVAL/INTERVAL1,INTERVAL2,INTERVAL3
      COMMON/DATAR/DATAR0,DATAR1,DATAR2,POWER,RHO
C     COMMON/COOL/INTCOOL,ITICOOL,INTEND
      COMMON/PIDVAR1/PIDPG,PIDIT,PIDDT
      COMMON/PIDVAR2/TEMSET,ERPRE,CURIMO,CURTOT,TIMDER


C****       PRE MAIN LOOP ******************************

      CALL ALDV(0,0)      ! SET D/A TO 0
5     WRITE(*,10)
10    FORMAT(1X,/,/,/,/,/,/,/,/,/)
      WRITE(*,20)
20    FORMAT(9X,'** PROGRAM - CALISO VERSION 1.0 ** ',/,/)
      WRITE(*,30)
30    FORMAT(13X,'CAPS LOCK MUST BE ON',/,/,/)
      WRITE(*,70)
70    FORMAT(9X,'TEMPERATURE INPUT 1  ON A/D CH0')
      WRITE(*,75)
75    FORMAT(9X,'SAMPLE VOLTAGE INPUT 2  ON A/D CH1')
      WRITE(*,80)
80    FORMAT(9X,'SHUNT CURRENT INPUT 3  ON A/D CH2')
      WRITE(*,82)
82    FORMAT(9X,'KEPCO CURRENT OUTPUT 1 ON D/A CH0',/,/)
      WRITE(*,85)
85    FORMAT(9X,'**** SPACE TO PROCEED ****')
      KEY=WAITKY()
      IF (KEY.NE.32)GO TO 5

C****       MAIN LOOP **********************************

115   CALL PREINFO
      IVAL=0
      ITIC=STIM           ! SET LOOP FOR SAMPLE RATE
C     CALL WTIME(0,0,0,0)      ! SET CLOCK (THIS LINE HAS NO UTILITY)
      CALL ISRSET(28,ISR1,IWS1)  ! INITIALIZE ISR1
      CALL ISRSET(27,ISR2,IWS2)  ! SET UP ^BREAK ISR
      CALL ISRSET(35,ISR3,IWS3)  ! SET UP ^C ISR

C     ICO1=(ICURRENT1*2.29)+2048   ! CALCULATE OUTPUT TO MATCH
RANGE
C     ICO2=(ICURRENT2*2.29)+2048
C     ICO3=(ICURRENT3*2.29)+2048

C     ICO1=ICURRENT1*(4096/100)    ! CONVERT ANALOG TO DIGITAL
C     ICO2=ICURRENT2*(4096/100)    ! BEFORE SENDING TO KEPCO
C     ICO3=ICURRENT3*(4096/100)
C120  KEY=INKEY()
120   IF(ILOAD.EQ.0)GO TO 125    ! DEB CHANGE(120 ON)
      CALL LOAD
```

```
C****  CALCULATION MODULE ************************************

       POWER(IVAL)=DATAR0(IVAL)*DATAR1(IVAL)
       IF (DATAR0(IVAL).NE.0) THEN
       RHO(IVAL)=((0.0443/6.067)*
     1 (DATAR1(IVAL)/DATAR0(IVAL))*1D6
       ENDIF
       IF (IVAL.GT.INTERVAL3)ITIC=1000

C****          END CALCULATION ****

C****  CONTROL MODULE ****************************************

       CALL ALSETD(0,0)          ! SET DAC OUTPUT
       IF(IVAL.EQ.1) THEN
       TEMSET=150
       ENDIF

       IF(IVAL.LE.INTERVAL1) THEN
       TEMSET=IEMF1+TEMSET
       IF(TEMSET.GE.IEMF2) THEN
       TEMSET=IEMF2
       ENDIF
       PIDPG=0.2
       PIDIT=8.0
       PIDDT=1.0
       CALL PID
       IF (CURTOT.LT.10)CURTOT=10
       ICO1=CURTOT*(4096/100)
       CALL ALDV (0,ICO1)
       IEMFR=TEMSET
       ENDIF

       IF (IVAL.GT.INTERVAL1) THEN
       IF (IVAL.LE.INTERVAL2) THEN
       TEMSET=IEMF2
       PIDPG=0.2
       PIDIT=8.0
       PIDDT=1.0
       CALL PID
       IF (CURTOT.LT.10)CURTOT=10
       ICO2=CURTOT*(4096/100)
       CALL ALDV(0,ICO2)
       IEMFR=IEMF2
       ENDIF
       ENDIF

       IF(IVAL.GT.INTERVAL2) THEN
       IF (IVAL.LE.INTERVAL3) THEN
       TEMSET=IEMF3
       PIDPG=0.2
```

```
      PIDIT=8.0
      PIDDT=1.0
    CALL PID
      IF(((DATAR2(IVAL)*1000)-(IEMF3+25)).GT.0)CURTOT=1
      IF(((DATAR2(IVAL)*1000)-(IEMF3+25)).LE.0)THEN
      IF(CURTOT.LT.10)CURTOT=10
      ENDIF

      ICO3=CURTOT*(4096/100)
      CALL ALDV(0,ICO3)
      WRITE(*,2)ICO3
2     FORMAT(9X,'ICO3=',I5)
      IEMFR=IEMF3
      ENDIF
      ENDIF

      IF(IVAL.GT.INTERVAL3) THEN
      CALL ALDV(0,0)
      IEMF=0
      ENDIF

      IF(IVAL.GT.INTERVAL3) THEN
      DO 410, I=1,5
      CALL BEEP(700,25)
      DO 420, J=1,100
420   CONTINUE
      CALL BEEP(900,50)
410   CONTINUE
      WRITE(*,450)
450   FORMAT(24X,'END OF RUN')
      WRITE(*,500)INTERVAL3
500   FORMAT(/,/,12X,'PAST  TIME  TAG#',I5,8X,' END  OF  RUN')
      WRITE(*,600)
600   FORMAT(9X,'HIT SPACEBAR TO CALL THE SAVE MODULE',/)
      WRITE(*,700)
700   FORMAT(9X,'ANY OTHER KEY TO EXIT')
      KEY=WAITKY()          ! DEB CHANGE(KEY 2:VIEW ENABLE)
      IF (KEY.EQ.32) CALL DISK
      IF (KEY.NE.0) GO TO 140   ! DEB REM(LINE# 140 EXIT COMMON POINT)
      ENDIF


C****         END CONTROL ****
      IF (IVAL.EQ.INTERVAL3+1) THEN
      WRITE(*,100)
100   FORMAT(24X,'COOLING PERIOD BEGINS')
      CALL BEEP(500,10)
      ENDIF
      WRITE(*,121)TIME(IVAL),DATAR0(IVAL),DATAR1(IVAL),DATAR2(IVAL)
  1  ,POWER(IVAL),RHO(IVAL),IEMFR !  SCREEN OUTPUT
121     FORMAT(3X,I5,6X,F9.6,7X,F8.6,2X,F8.3,1X,F8.3,2X,F7.3,2X,I5)
```

```
C125  IF (KEY.EQ.32)GO TO 140    ! DEB CHANGE (STOP FLAG OFF)
125   IF (IEXIT.NE.0)GO TO 140   ! IF ON ^C OR ^BREAK:DEB CH(125 ON)
130   IF (IVAL.NE.10000)GO TO 120 ! IF ON MAX ARRAY SIZE
140   CALL ALDV(0,0)              ! SET D/A TO 0
      CALL ISRCLR(IWS1)          ! TERMINATES ISR1
      CALL ISRCLR(IWS2)          ! TERMINATES ISR2
      CALL ISRCLR(IWS3)          ! TERMINATES ISR3
      CALL EXIT                  ! EXIT
      GO TO 5        ! FLOW RETURNS TO THIS POINT ON, RUN AGAIN

      STOP
      END

C****        PRE-EXPERIMENT INFORMATION SCREEN ******************

      SUBROUTINE PREINFO

      INTEGER*2 STIM,JTIM,HTIM,ITIC
      INTEGER*2 TEMP1
      INTEGER*2 VOLT1,VOLT2
      INTEGER*2 TIME(5000),IN
      INTEGER*2 IEXIT,IVAL,ILOAD
      INTEGER*2 KEY,WAITKY
      INTEGER*2 IEMF1,IEMF2,IEMF3
      INTEGER*2 INTERVAL1,INTERVAL2,INTERVAL3
C     INTEGER*2 INTCOOL,ITICOOL,INTEND

      REAL*8
STIME,JTIME,HTIME,XSAVE,XPRINT,XEND,XRETURN,XRUN,XQUIT
      CHARACTER*12 FNAME

      COMMON/TIME/STIM,JTIM,HTIM,ITIC
      COMMON/ID/STIME,JTIME,HTIME,XSAVE,XPRINT,XEND,XRETURN,XR
UN,X QUIT
      COMMON/TEMP/TEMP1
      COMMON/VOLT/VOLT1,VOLT2
      COMMON/FLAG/IEXIT,IVAL,ILOAD
      COMMON/INPUTS/TIME,IN
      COMMON/EMF/IEMF1,IEMF2,IEMF3
      COMMON/INTERVAL/INTERVAL1,INTERVAL2,INTERVAL3
C     COMMON/COOL/INTCOOL,ITICOOL,INTEND
      COMMON/FILE/FNAME


60    CALL PULSE  ! D/A SETUP
62    WRITE(*,70)
      WRITE(*,63)
63    FORMAT(9X,/,/,/,/,/)
      WRITE(*,65)
65    FORMAT(15X,'**** PRESS SPACEBAR TO ACTIVATE OUTPUT
****',/)
```

```
        WRITE(*,66)
66      FORMAT(24X,'AND START DATA ACQUISITION'/,/,/,/,/)
        WRITE(*,67)
67      FORMAT(15X,'THIS PROGRAM AUTOMATICALLY DEACTIVATES
OUTPUT',/)
        WRITE(*,68)INTERVAL3
68     FORMAT(15X,'AT THE END OF INTERVAL3 (TT#',I4
     1  ,' FOR THIS RUN)'/)
        WRITE(*,69)
69      FORMAT(15X,'AND STOPS DATA ACQUISITION AT THE END OF
THE',/)
        WRITE(*,691)INTEND
691     FORMAT(18X,'COOLING PERIOD (TT#',I4,' FOR THIS RUN)'/)
        WRITE(*,70)
        KEY=WAITKY()
        IF (KEY.NE.32)GO TO 62
        WRITE(*,70)
70      FORMAT(/,/,/,/)
        WRITE(*,80)
80      FORMAT(9X,'*** OUTPUT ACTIVE AND ACQUISITION IN
PROGRESS ***'/,/)
        WRITE(*,90)
90      FORMAT(10X,'--- CTRL BREAK WILL ABORT DATA ACQUISITION
---'
     1  ,/,/,/)
        WRITE(*,100)
100     FORMAT(1X,'TIME TAG#',7X,'CURRENT',5X,'VOLTAGE',5X,
     2  'TEMP',3X,'POWER',8X,'RHO',2X,'KEPCO I'/)
        RETURN
        END



C****          OPERATOR QUERY **********************************

        SUBROUTINE PULSE

        INTEGER*2 STIM,JTIM,HTIM,ITIC
        INTEGER*2 TEMP1
        INTEGER*2 VOLT1,VOLT2
        INTEGER*2 TIME(5000),IN
        INTEGER*2 IEXIT,IVAL,ILOAD
        INTEGER*2 KEY,WAITKY,CHOICE
        INTEGER*2 IEMF1,IEMF2,IEMF3
        INTEGER*2 INTERVAL1,INTERVAL2,INTERVAL3
C       INTEGER*2 INTCOOL,ITICOOL,INTEND

        REAL*8
STIME,JTIME,HTIME,XSAVE,XPRINT,XEND,XRETURN,XRUN,XQUIT
        CHARACTER*12 FNAME
```

```
      COMMON/TIME/STIM,JTIM,HTIM,ITIC
      COMMON/ID/STIME,JTIME,HTIME,XSAVE,XPRINT,XEND,XRETU
RN,X RUN,XQUIT
      COMMON/TEMP/TEMP1
      COMMON/VOLT/VOLT1,VOLT2
      COMMON/FLAG/IEXIT,IVAL,ILOAD
      COMMON/INPUTS/TIME,IN
      COMMON/FILE/FNAME
      COMMON/EMF/IEMF1,IEMF2,IEMF3
      COMMON/INTERVAL/INTERVAL1,INTERVAL2,INTERVAL3
C     COMMON/COOL/INTCOOL,ITICOOL,INTEND


      WRITE(*,200)
200   FORMAT(/,/,/,/,/,/,/,/,/,/,/,/,/,/,/,/)
      WRITE(*,210)
210   FORMAT(9X,'1) MAKE A STANDARD RUN',/)
      WRITE(*,220)
220   FORMAT(9X,'2) ENTER RUN PARAMETERS',/)
      WRITE(*,230)
230   FORMAT(12X,'ENTER CODE FOR YOUR CHOICE (1/2)',/)
      CHOICE=WAITKY()
      WRITE(*,235)CHOICE
235   FORMAT(9X,I5)
      IF (CHOICE.EQ.50) GOTO 5
      IF (CHOICE.EQ.49) THEN
      WRITE(*,240)
240   FORMAT(/,/,/,/,/,/,/,/,/,/,/,/,/,/,/)
      ENDIF

5     WRITE(*,10)
10    FORMAT(/,/,/,/,/,/,/,/,/,/,/,/,/,/,/)
      WRITE(*,15)
15    FORMAT(12X,'**ENTER ISOTHERMAL PARAMETERS**')
      WRITE(*,16)
16    FORMAT(12X,'_____',/,/)
      WRITE(*,20)
20    FORMAT(9X,'ENTER HEATING RATE FOR INTERVAL 1 IN
"µV/sec"',/)
      WRITE(*,30)
      READ(*,30)IEMF1
30    FORMAT(I5)
      WRITE(*,40)
40    FORMAT(9X,'ENTER 1st STAGE ISOTHERMAL TEMPERATURE IN
"µV"',/)
      READ(*,50)IEMF2
50    FORMAT(I5)
      WRITE(*,60)
60    FORMAT(9X,'ENTER 2nd STAGE ISOTHERMAL TEMPERATURE IN
"µV"',/)
```

```
      READ(*,70)IEMF3
70    FORMAT(I5)

      WRITE(*,140)
140   FORMAT(9X,'ENTER TEMPERATURE CONTROL SAMPLING TIME
     1 IN "TICS" ')
      WRITE(*,145)
145   FORMAT(9X,'(1 TIC IS 55 MILLISECONDS,18 TICS IS 1 SECOND)')
      READ(*,150)STIM
150   FORMAT(I5)


      WRITE(*,80)
80    FORMAT(9X,'ENTER TOTAL NUMBER OF READINGS IN
INTERVAL 1
     1 AS "TT#"',/)
      READ(*,90)INTERVAL1
90    FORMAT(I5)
      WRITE(*,100)
100   FORMAT(9X,'ENTER TOTAL NUMBER OF READINGS IN
INTERVAL 2
     1 AS "TT#"',/)
      READ(*,110)INTERVAL2
110   FORMAT(I5)
      WRITE(*,120)
120   FORMAT(9X,'ENTER TOTAL NUMBER OF READINGS IN
INTERVAL 3
     1 AS "TT#"',/)
      READ(*,130)INTERVAL3
130   FORMAT(I5)

175   INTERVAL3=INTERVAL1+INTERVAL2+INTERVAL3
      INTERVAL2=INTERVAL1+INTERVAL2
C     INTEND= INTERVAL3
      WRITE(*,180)
180   FORMAT(/,/)
      RETURN
      END


C****         LOAD ARRAYS  ******************************

      SUBROUTINE LOAD

      INTEGER*2 STIM,JTIM,HTIM,ITIC
      INTEGER*2 TEMP1
      INTEGER*2 VOLT1,VOLT2
      INTEGER*2 TIME(5000),IN
      INTEGER*2 IEXIT,IVAL,ILOAD
      INTEGER*2 IEMF1,IEMF2,IEMF3
```

```
      INTEGER*2 INTERVAL1,INTERVAL2,INTERVAL3

      REAL*8
DATAR0(5000),DATAR1(5000),DATAR2(5000),POWER(5000)
      REAL*8
STIME,JTIME,HTIME,XSAVE,XPRINT,XEND,XRETURN,XRUN,XQUIT


      COMMON/TIME/STIM,JTIM,HTIM,ITIC
      COMMON/ID/STIME,JTIME,HTIME,XSAVE,XPRINT,XEND,XRETU
RN,X RUN,XQUIT
      COMMON/TEMP/TEMP1
      COMMON/VOLT/VOLT1,VOLT2
      COMMON/FLAG/IEXIT,IVAL,ILOAD
      COMMON/INPUTS/TIME,IN
      COMMON/EMF/IEMF1,IEMF2,IEMF3
      COMMON/INTERVAL/INTERVAL1,INTERVAL2,INTERVAL3
      COMMON/DATAR/DATAR0,DATAR1,DATAR2
      IVAL=IVAL+1          ! INCREMENT SAMPLE NUMBER

      CALL ALAV(0,1,IN)          ! ADC CH0 CURRENT
      DATAR0(IVAL)=(100./4096.)*FLOAT(IN)    !  SCALE  INPUT  TO
MATCH RANGE
      DATAR0(IVAL)=DATAR0(IVAL)

      CALL ALAV(1,1,IN)          ! ADC CH1 VOLTAGE
      DATAR1(IVAL)=(10./4096.)*FLOAT(IN)
      DATAR1(IVAL)=DATAR1(IVAL)/10

      CALL ALAV(2,1,IN)          ! ADC CH2 TEMPERATURE
      DATAR2(IVAL)=(10./4096.)*FLOAT(IN)
      DATAR2(IVAL)=DATAR2(IVAL)*2

      TIME(IVAL)=IVAL    ! ARRAY FOR SAMPLE NUMBER
      ILOAD=0        ! RESET LOAD FLAG
      RETURN
      END

C****       P I D          C O N T R O L          M O D U L E
**********************************

C     THIS TEMPERATURE CONTROLLER COMBINES THREE MODES
OF FEEDBACK
C     WHICH ARE PROPORTIONAL INTEGRAL AND DERIVATIVE

      SUBROUTINE PID

      INTEGER*2 STIM,JTIM,HTIM,ITIC
      INTEGER*4 TEMP1
      INTEGER*2 VOLT1, VOLT2
      INTEGER*2 IWS1(22),IWS2(22),IWS3(22), IREG(8),IVAL
```

```
      INTEGER*2 TIME(5000),IN
      INTEGER*2 IEXIT,ILOAD
      INTEGER*2 KEY,INKEY,WAITKY
      INTEGER*2 INTERVAL1,INTERVAL2,INTERVAL3
      INTEGER*2 IEMF1,IEMF2,IEMF3,IEMFR

      REAL*8    DATAR0(5000),DATAR1(5000),DATAR2(5000),
POWER(5000)
      REAL*8 STIME,JTIME,HTIME
      REAL*8 CURTOT

      COMMON/TIME/STIM,JTIM,HTIM,ITIC
      COMMON/FLAG/IEXIT,IVAL,ILOAD
      COMMON/TEMP/TEMP1
      COMMON/EMF/IEMF1,IEMF2,IEMF3
      COMMON/INTERVAL/INTERVAL1,INTERVAL2,INTERVAL3
      COMMON/PIDVAR1/PIDPG,PIDIT,PIDDT
      COMMON/PIDVAR2/TEMSET,ERPRE,CURIMO,CURTOT,TIMDER
      COMMON/DATAR/DATAR0,DATAR1,DATAR2,POWER,RHO

      ERROR=TEMSET-(DATAR2(IVAL)*1000.)

      WRITE(*,2)PIDIT
2     FORMAT(9X,'PIDIT =',F9.2)

      CURINC=PIDPG*ERROR*STIM*0.055/PIDIT
      IF(IVAL.EQ.1)CURIMO=0
      IF(IVAL.EQ.(INTERVAL1+1))CURIMO=0
      IF(IVAL.EQ.(INTERVAL2+1))CURIMO=0
      CURIMO=CURIMO+CURINC
      IF(CURIMO.LT.0)CURIMO=0

      CURPMO=PIDPG*ERROR
      IF(IVAL.EQ.1)GOTO 5
      ERDER=ERROR-ERPRE
      GOTO 10
5     ERDER=0
10    IF(ERDER.EQ.0)GOTO 15

      WRITE(*,12)TIMDER
12    FORMAT(9X,'TIMDER=',F8.2)

      CURDMO=PIDPG*PIDDT*ERDER/(TIMDER*0.055)

      WRITE(*,13)CURDMO
13    FORMAT(9X,'CURDMO=',F8.2)

      TIMDER=STIM
      GOTO 20
15    CURDMO=0
      TIMDER=2*STIM
```

```
20      CURTOT=CURPMO+CURIMO+CURDMO
        IF(CURTOT.GT.80)CURTOT=80
        ERPRE=ERROR

        WRITE(*,21)CURTOT
21      FORMAT(9X,'CURTOT=',F8.2)

        RETURN
        END

C****       S A V E       A N D       P R I N T       M O D U L E
*******************************

        SUBROUTINE DISK

        INTEGER*2 STIM,JTIM,HTIM,ITIC
        INTEGER*2 TEMP1
        INTEGER*2 VOLT1,VOLT2
        INTEGER*2 TIME(5000),IN
        INTEGER*2 IEXIT,IVAL,ILOAD
        I



NTEGER*2 KEY,WAITKY
        REAL*8
DATAR0(5000),DATAR1(5000),DATAR2(5000),POWER(5000)
        REAL*8 RHO(5000)
        REAL*8
STIME,JTIME,HTIME,XSAVE,XPRINT,XEND,XRETURN,XRUN,XQUIT
        CHARACTER*12 FN□MF

        COMMON/TIME/STIM,JTIM,HTIM,ITIC
        COMMON/ID/STIME,JTIME,HTIME,XSAVE,XPRINT,XEND,XRETU
RN,X RUN,XQUIT
        COMMON/TEMP/TEMP1
        COMMON/VOLT/VOLT1,VOLT2
        COMMON/FLAG/IEXIT,IVAL,ILOAD
        COMMON/INPUTS/TIME,IN
        COMMON/FILE/FNAME
        COMMON/DATAR/DATAR0,DATAR1,DATAR2,POWER,RHO

4       WRITE(*,5)
5       FORMAT(/,/,/,/,/,/,/,/,/,/,/,/,/,/,/,/,/,/,/)
        WRITE(*,6)
6       FORMAT(9X,'PRESS "S" TO STORE DATA ON DISK')
        WRITE(*,7)
7       FORMAT(9X,'PRESS "P" TO PRINT DATA ON PRINTER')
        WRITE(*,8)
8       FORMAT(9X,'PRESS "B" TO BOTH STORE AND PRINT DATA')
        WRITE(*,9)
```

```
9       FORMAT(9X,'PRESS "E" TO EXIT WITHOUT STORING OR
PRINTING')

        KEY=WAITKY()
        IF (KEY.EQ.80) GOTO 45
        IF (KEY.EQ.69) GOTO 80
        IF (KEY.NE.83) THEN
        IF (KEY.NE.80) THEN
        IF (KEY.NE.66) THEN
        IF (KEY.NE.69) THEN
        CALL BEEP(200,500)
        GO TO 4
        ENDIF
        ENDIF
        ENDIF
        ENDIF


        WRITE(*,10)
10      FORMAT(9X,'ENTER FILENAME FOR DATA',/)
        WRITE(*,15)
15      FORMAT(9X,'FORMAT - XXXXXXXX.XXX',/)
        READ(*,20)FNAME
20      FORMAT(A12)

        OPEN(3,FILE=FNAME,STATUS='NEW')
        DO 1 J=1,IVAL
        WRITE(3,40)TIME(J),DATAR0(J),DATAR1(J),DATAR2(J),POWER(J)
     1  ,RHO(J),IEMFR
40       FORMAT(3X,I5,6X,F9.6,7X,F8.6,2X,F8.3,1X,F8.3,2X,F6.3,2X  ,I5)
1       CONTINUE
        CLOSE(3,STATUS='KEEP')

        IF (KEY.EQ.83)GOTO 80

45      WRITE(*,50)
50      FORMAT(/,/,/,/)
        OPEN(2,FILE='PRN ,
        WRITE(2,60)
60      FORMAT(5X,'TIME
TAG#',3X,'CURRENT',5X,'VOLTAGE',5X,'TEMPERATURE'
     2  ,2X,'POWER',/)
        DO 2 J=1,IVAL
        WRITE(2,70)TIME(J),DATAR0(J),DATAR1(J),DATAR2(J),POWER(
J),RHO(J)
     1  ,IEMFR
70       FORMAT(3X,I5,6X,F9.6,7X,F8.6,2X,F8.3,1X,F8.3,2X,F6.3,2X  ,I5)
2       CONTINUE
        CLOSE(2)
80      RETURN
        END
```

```
C****       DEB END ************

C****       INTERUPT SERVICE ROUTINES ******************

      SUBROUTINE ISR1(IREG)

      INTEGER*2 STIM,JTIM,HTIM,ITIC
      INTEGER*2 IEXIT,IVAL,ILOAD

      COMMON/TIME/STIM,JTIM,HTIM,ITIC
      COMMON/FLAG/IEXIT,IVAL,ILOAD

      ITIC=ITIC-1          ! DECREMENT LOOP VALUE
      IF (ITIC.NE.0)GO TO 10   ! LOOP FOR SAMPLE RATE
      ILOAD=1              ! SET FLAG TO ACQUIRE DATA
      ITIC=STIM            ! RESET LOOP VALUE
10    RETURN
      END


      SUBROUTINE ISR2(IREG)

      INTEGER*2 IREG(8)
      INTEGER*2 IEXIT,IVAL,ILOAD

      COMMON/FLAG/IEXIT,IVAL,ILOAD

      IEXIT=1              ! SET FLAG ON ^BREAK
      RETURN
      END

      SUBROUTINE ISR3(IREG)

      INTEGER*2 IREG(8)
      INTEGER*2 IEXIT,IVAL,ILOAD

      COMMON/FLAG/IEXIT,IVAL,ILOAD

      IEXIT=1              ! SET FLAG ON ^C
      RETURN
      END

C****       EXIT *******  ********************************

      SUBROUTINE EXIT

      REAL*8 ANS
      REAL*8
STIME,JTIME,HTIME,XSAVE,XPRINT,XEND,XRETURN,XRUN,XQUIT
```

```
      COMMON/ID/STIME,JTIME,HTIME,XSAVE,XPRINT,XEND,XRETU
RN,X RUN,XQUIT

5     WRITE(*,10)
10    FORMAT(/,/,/,/,/,/,/,/,/,/,/,/,/,/,/)
      WRITE(*,15)
15    FORMAT(9X,'ENTER OPTION',/,/)
      WRITE(*,30)
30    FORMAT(9X,'RUN    --- RUN PROGRAM AGAIN')
      WRITE(*,40)
40    FORMAT(9X,'QUIT   --- EXIT TO DOS',/)
      READ(*,50)ANS
50    FORMAT(A8)
      IF (ANS.EQ.XRUN)GO TO 80
      IF (ANS.EQ.XQUIT)GO TO 90
      GO TO 5
80    RETURN
90    STOP
      END

C****       BLOCK DATA ********************************

      BLOCKDATA

      INTEGER*2 STIM,JTIM,HTIM,ITIC
      INTEGER*2 TEMP1
      INTEGER*2 VOLT1,VOLT2
      INTEGER*2 TIME(5000),IN
      INTEGER*2 IEXIT,IVAL,ILOAD
      INTEGER*2 IEMF1,IEMF2,IEMF3
      INTEGER*2 INTERVAL1,INTERVAL2,INTERVAL3

      REAL*8
STIME,JTIME,HTIME,XSAVE,XPRINT,XEND,XRETURN,XRUN,XQUIT
      CHARACTER*12 FNAME

      COMMON/TIME/STIM,JTIM,HTIM,ITIC
      COMMON/ID/STIME,JTIME,HTIME,XSAVE,XPRINT,XEND,XRETU
RN,X RUN,XQUIT
      COMMON/TEMP/TEMP1
      COMMON/VOLT/VOLT1,VOLT2
      COMMON/FLAG/IEXIT,IVAL,ILOAD
      COMMON/INPUTS/TIME,IN
      COMMON/EMF/IEMF1,IEMF2,IEMF3
      COMMON/INTERVAL/INTERVAL1,INTERVAL2,INTERVAL3
      COMMON/FILE/FNAME
      COMMON/DATAR/DATAR0,DATAR1,DATAR2

      DATA STIME/'STIM'/,JTIME/'JTIM'/,HTIME/'HTIM'/
      DATA JTIM/18/,HTIM/5/
      DATA IEXIT/0/,IVAL/0/
```

```
DATA XSAVE/'SAVE'/,XPRINT/'PRINT'/,XEND/'END'/
DATA XRETURN/'RETURN'/,XRUN/'RUN'/,XQUIT/'QUIT'/
END
```

# VITA

Debasis Basak was born in Berhampore, a mid-size town by the Holy Ganges, in the state of West Bengal (home of the Royal Bengal Tiger) in India. He attended elementary school and high school at De Nobili School, in a coal-field town of Dhanbad, in the adjoining state of Bihar. He attended plus-two (junior college) in the same school.

He then joined the Bachelor of Science (Engineering) program in metallurgical engineering at Bihar Institute of Technology, Sindri in 1984. He got the B.Sc. (Engineering) degree in 1988.

The author, then, was offered a job with Tata Iron and Steel Co., in Jamshedpur, Bihar, where he served for several months as a Graduate Trainee Engineer. Though the hands-on engineering experience at the blast furnace, steel melting shop, etc., and the training in managerial skills were a very positive learning experience for the author, he decided to quit the job and go abroad for higher studies, to broaden his domain of experience with technology, as also with the world and its people.

In 1990, the author joined the M.S. degree program in metallurgical engineering at the University of Tennessee, Knoxville, U.S.A. He received his M.S. degree in 1992.

The author, then, decided to carry on with his higher studies in the same discipline at the same university and joined the doctoral program in metallurgical engineering. He received the Ph.D. degree in 1995.

The author plans to involve himself with research and development work in engineering for industry or national laboratories.